



**REACTIONS BETWEEN SODIUM AND SILICON
MINERALS DURING GASIFICATION
OF LOW-RANK COAL**

by

ADAM KOSMINSKI

Thesis submitted for the degree of
Doctorate of Philosophy

in

The University of Adelaide
Department of Chemical Engineering
Faculty of Engineering

September 2001

In the loving memory of my dearest wife Barbara

*...ile Cię trzeba cenić
ten tylko się dowie kto Cię stracił...*

DECLARATION

This work contains no material which has been accepted for the award of any other degree or diploma in any university or any other tertiary institution, and to the best of my knowledge and belief contains no material previously published or written by any other person, except where due references has been made in the text.

I give consent to this copy of my thesis, when deposited in the University Library, being made available for photocopying and loan.

SIGNED

DATE: 21.09.01

ACKNOWLEDGMENTS

This work has been supported by Cooperative Research Centre for Clean Power from Lignite. I wish to thank the Centre for the opportunity to carry this project and for providing me with the financial support, which enabled me to undertake this project. Particular thanks I wish to extend to the Director of the Centre Dr David Brockway, Dr Peter Jackson and to Mr Howard Mitchell for their support, understanding and compassion during that difficult period in my personal life.

I am indebted to Professor John B. Agnew for his supervision, guidance and faith throughout this project. I am also very thankful for his encouragement, understanding and personal support. I also wish to thank Dr Alan Manzoori for his support during initial stages of the project and his helpful suggestions and comments.

I would also like to extend my greatest thanks to Gary Klicke and Frank Myszka for the chemical analyses, personal support and friendship over the years. I wish to thank a number of colleagues who have been invaluable to me throughout this project, for their constructive comments, suggestions and discussions. For this I would like to thank Grant Schluter, Dr Temi Linjewile, Dr Ying-he He, Dr Hari Babu Vuthaluru and particularly Dr Sankar Bhattacharya.

I want to thank my friend Władek Niewiarowski for great personal support and help offered in caring for my wife during her long illness.

My most sincere thanks and appreciation I wish to extend to Dr Davide P. Ross for his invaluable help over the years, for his help in editing this thesis and for his great friendship and personal support.

Finally I am particularly grateful to my wife, Barbara, for her love, faith and support throughout very many years of being my best ever friend, for being my wife. Without Barbara's continuing support and encouragement and great love and sacrifice I could not have achieved what I have. Unfortunately Barbara you cannot see this thesis being finally finished. Your loss is unmeasurable. I love you forever.

SUMMARY

Fluidised bed gasification (FBG) associated with integrated gasification combine cycle (IGCC) power generation is an important way of using vast low-rank coal resources in an economic and environmentally acceptable manner. A key factor in the successful operation of coal gasification systems is the ability to control and mitigate ash-related problems. Such problems are closely tied to the abundance and association of the inorganic components in coal and the gasification conditions. Of particular importance for low-rank coals is the presence of sodium, which has been found to cause FBG operational problems such as bed agglomeration and ash deposition. However, the critical fundamental mechanisms of sodium behaviour in coal gasification systems are not fully understood.

The main objective of this study was to elucidate the role of sodium and silicon minerals in formation of liquid phases potentially responsible for fluidised bed agglomeration during gasification of a high-sulphur low-rank coal in order to identify ways of preventing formation of those phases. Experimental investigations involved the preparation of synthetic coals, or separate mineral mixtures, with known quantities of organically-bound sodium or sodium chloride and silica or kaolin either separately or in combination. The mineral mixtures were used as an aid in the interpretation of the reactions of sodium with silica or kaolin in the coal char. In addition, thermodynamic predictions were made for the possible compositions and phase distribution of sodium and silicon species formed during gasification and pyrolysis of these synthetic coals.

The synthetic coals were pyrolysed and gasified in a horizontal tubular reactor under conditions representative of a typical fluidised bed gasifier. Other than mineral composition parameters, the reaction temperatures (650°C, 750°C and 850°C), gas environment (pure atmospheres of either nitrogen, carbon dioxide or steam) and reaction times (45 seconds to 35 minutes) were varied. Mineral mixtures were exposed to the same experimental conditions. The collected coal char and post-reaction mineral mixture products were analysed by wet chemical methods, electron microscopy and mineralogical methods.

The experimental program investigated sodium transformation and extent of vaporisation in each of the individual atmospheres. The organically-bound sodium was found to be transformed into sodium carbonate, contrary to thermodynamic predictions of the formation of sodium sulphide for pyrolysis conditions. Up to half of the sodium was vaporised from the char. Volatilisation of sodium increased with temperature and time, and was highest for gasification with carbon dioxide. Sodium chloride present in coal vaporised during pyrolysis and gasification and reacted with coal partly forming sodium carbonate. The release of sodium was disproportionate to that of chlorine. Almost all of the chlorine was released at 850°C, and its release was twice as high as sodium. The release of sodium and chlorine was dependent on temperature and time, but not on the particular gas atmosphere.

Steam was found, both theoretically and experimentally, to be the most important component of the gasification environment. Steam substantially reduced the melting temperature of sodium carbonate and consequently gasification with steam resulted in the formation, in a liquid-solid state reaction, of liquid silicates at as low as 750°C, while gasification with carbon dioxide resulted in the same at 850°C. Sodium chloride and silica reacted only in steam and formed fused silicates at 750°C, with the rate of silicate formation substantially slower than for reaction between silica and sodium carbonate. Formation of silicates around silica particles and fused silicate joints between individual silica grains inside the char was established to occur uniformly throughout char particles in gasification conditions. Liquid silicates would be a cause of bed agglomeration and defluidisation during fluidised bed gasification of coal.

Qualitative agreement was found for gasification but not for pyrolysis conditions between experimental results and thermodynamic predictions for the formation of liquid silicates from organically-bound sodium and silica, but at higher than predicted temperatures. The results for mineral mixtures were in better agreement with thermodynamic calculations as the rate of formation of silicates was much higher in mixtures than in the synthetic coal. The prediction by equilibrium calculations for all of the silica to be fully dissolved in liquid silicates was not observed under any of the experimental conditions. However, partial silica dissolution was concluded for mineral mixture products. Silica solubility in the formed liquid silicates will increase the total mass of fused silicate glass formed in a FBG.

Partial agreement has been established between theoretical predictions and experimental results for gasification and pyrolysis of coal with organically-bound sodium and kaolin. Experimental results showed that kaolin and sodium had reacted upon reaching 650°C to form a solid sodium aluminosilicate $\text{Na}_2\text{O} \cdot \text{Al}_2\text{O}_3 \cdot 2\text{SiO}_2$, principally nepheline with a melting point above 1250°C. The reaction rate was faster in steam than in carbon dioxide or nitrogen. Sodium chloride reacted with kaolin, but at a slower rate, also to form sodium aluminosilicate $\text{Na}_2\text{O} \cdot \text{Al}_2\text{O}_3 \cdot 2\text{SiO}_2$, with steam reaction rate much higher than in carbon dioxide. Increasing the process temperature increased the reaction rate.

It is inferred that under FBG temperature conditions, as kaolin is transformed with the preservation of its hexagonal crystal structure into meta-kaolinite $\text{Al}_2\text{O}_3 \cdot 2\text{SiO}_2$ it reacts with sodium into nepheline, with the further preservation of the hexagonal structure. Reactions of sodium with kaolin will prevent reactions of sodium with silica to form liquid silicates. No formation of sodium aluminosilicate albite $\text{Na}_2\text{O} \cdot \text{Al}_2\text{O}_3 \cdot 6\text{SiO}_2$ was established experimentally, contrary to thermodynamic predictions for both forms of sodium.

The results from experiments showed that carbon conversion in steam was considerably higher than in carbon dioxide for coals containing either form of sodium. It was established that coal activation energy is associated with catalytic activity of sodium. For coal containing sodium chloride, activation energies are substantially higher than for coals containing organically-bound sodium. The presence of such minerals as silica and kaolin significantly increases the activation energies for coal gasification reactions with steam and carbon dioxide. However, the impact was lower for coal containing sodium in the form of sodium chloride.

Recommendations made for future work include establishing efficient ways to introduce kaolin to low-rank coal during gasification to reduce the formation of liquid silicates and hence inhibit agglomeration and defluidisation.

TABLE OF CONTENTS

	Page
DECLARATION	iii
ACKNOWLEDGEMENTS	iv
SUMMARY	v
TABLE OF CONTENTS	viii
LIST OF TABLES	xiv
LIST OF FIGURES	xvii
1 INTRODUCTION	1
1.1 BACKGROUND	1
1.2 COAL GASIFICATION	2
1.3 SCOPE AND STRUCTURE OF THESIS	3
2 LITERATURE REVIEW	6
2.1 INTRODUCTION	6
2.2 INORGANIC MATTER IN COAL	6
2.2.1 Definition and Classification	7
2.2.2 Occurrence and Nature of Inorganic Matter	9
2.2.2.1 Minerals in coal	11
2.2.2.2 Sulphur	11
2.2.2.3 Chlorine	12
2.2.2.4 Sodium	14
2.2.2.5 Potassium	15
2.2.2.6 Calcium and magnesium	16
2.2.2.7 Silicon and aluminium	17
2.2.2.8 Iron	18
2.3 TRANSFORMATIONS OF INORGANIC MATTER DURING GASIFICATION	18
2.3.1 Chemical Transformations	19
2.3.1.1 Decomposition of the Inorganics during Pyrolysis	19
2.3.1.1.1 Sulphur transformations	23
2.3.1.1.2 Chlorine transformations	24
2.3.1.1.3 Transformations of the minerals	24
2.3.1.2 Transformations during Combustion	25
2.3.1.2.1 Sodium reaction with sulphur oxides	26
2.3.1.2.2 Sodium reaction with silica and aluminosilicates	26
2.3.1.2.3 Chlorine	30
2.3.1.2.4 Calcium, magnesium and iron	31

2.3.1.3	Transformations during Gasification	32
2.3.1.3.1	Sodium and potassium reactions	33
2.3.1.3.2	Alkali catalysed gasification	34
2.3.1.3.3	Potassium	35
2.3.1.3.4	Chlorine	36
2.3.1.3.5	Sulphur	37
2.3.1.3.6	Calcium and magnesium	38
2.3.1.3.7	Iron	39
2.3.1.3.8	Minerals	40
2.3.1.4	HTW Gasification Process Experience	42
2.3.1.5	Laboratory Gasification Experiments	44
2.3.1.6	Thermodynamic calculations	45
2.3.2	Physical Transformations	46
2.3.2.1	Mineral salt crystallisation	47
2.3.2.2	Melting and sintering	47
2.3.2.3	Vapourisation of inorganic and minerals	50
2.3.2.4	Ash coalescence	51
2.3.2.5	Char porosity	51
2.3.2.6	Particle temperature	52
2.4	AGGLOMERATION and DEFLUIDISATION	52
2.4.1	Agglomeration mechanisms	53
2.4.2	Agglomeration in spouted fluidised beds	55
2.4.3	Sintering and agglomeration	57
2.4.4	Slag viscosity	62
2.4.5	Defluidisation	62
2.4.6	Deposition	62
2.5	SUMMARY	63
2.6	OBJECTIVES OF THE PRESENT STUDY	70
3	THERMODYNAMIC CONSIDERATIONS	72
3.1	INTRODUCTION	72
3.2	OBJECTIVES	73
3.3	PREDICTION OF EQUILIBRIUM COMPOSITIONS	73
3.3.1	Computational method	74
3.3.2	Reaction system	75
3.3.3	System assumptions and limitations	76
3.4	DISTRIBUTION OF SODIUM SPECIES AT EQUILIBRIUM CONDITIONS	77
3.4.1	Coal containing organically-bound sodium	77
3.4.1.1	Effect of nitrogen and hydrogen atmosphere	77
3.4.1.2	Effect of carbon monoxide atmosphere	78
3.4.1.3	Effect of steam atmosphere	79
3.4.1.4	Effect of carbon dioxide atmosphere	79
3.4.2	Coal containing sodium as sodium chloride	79
3.4.3	Coal containing organically-bound sodium and kaolin	80
3.4.4	Coal containing sodium chloride and kaolin	81
3.4.4.1	Effect of nitrogen atmosphere	81
3.4.4.2	Effect of carbon monoxide atmosphere	82
3.4.4.3	Effect of steam atmosphere	83

3.4.4.4	Effect of carbon dioxide atmosphere	83
3.4.4.5	Effect of hydrogen atmosphere	84
3.4.5	Coal containing organically-bound sodium and silica	84
3.4.6	Coal containing sodium chloride and silica	85
3.4.6.1	Effect of nitrogen atmosphere	86
3.4.6.2	Effect of steam atmosphere	87
3.4.6.3	Effect of carbon dioxide atmosphere	87
3.4.6.4	Effect of hydrogen atmosphere	87
3.4.6.5	Effect of carbon monoxide atmosphere	88
3.4.7	Silicon distribution	88
3.4.7.1	Coal containing organically-bound sodium and silica	88
3.4.7.2	Coal containing sodium chloride and silica	88
3.4.7.3	Coal containing organically-bound sodium and kaolin	88
3.4.7.4	Coal containing sodium chloride and kaolin	89
3.5	SUMMARY	90
4	EXPERIMENTAL WORK	93
4.1	INTRODUCTION AND OBJECTIVES	93
4.2	COAL PREPARATION	94
4.2.1	Coal leaching technique	96
4.2.2	Choice of specific compositions for preparation of synthetic coals	96
4.2.3	Preparation of coal samples	97
4.2.3.1	Preparation of dried coal granules	99
4.2.4	Preparation of mineral mixtures	100
4.3	EXPERIMENTAL APPARATUS	101
4.4	EXPERIMENTAL PROCEDURE	104
4.5	ANALYTICAL METHODS FOR COAL AND REACTION PRODUCTS	106
4.5.1	Solubility of sodium and silicates	106
4.5.1.1	Staged water leaching analysis	108
4.5.1.2	Confirmation of sodium forms in prepared synthetic coals	108
4.5.2	FT-IR analysis	109
4.5.3	Electron Microscopy	110
4.5.4	Mineralogical X-Ray diffraction analysis	111
4.6	SUMMARY	111
5	TRANSFORMATIONS OF SODIUM IN HIGH-SULPHUR LIGNITE DURING PYROLYSIS AND GASIFICATION – EXPERIMENTAL RESULTS	114
5.1	INTRODUCTION	114
5.1.1	Transformations of organically-bound sodium.	115
5.2	OBJECTIVES	118
5.3	PYROLYSIS AND GASIFICATION OF COAL CONTAINING ORGANICALLY-BOUND SODIUM	119
5.3.1	Sodium volatilisation during pyrolysis and gasification	120
5.3.1.1	Sodium volatilisation during pyrolysis	120

5.3.1.2	Sodium volatilisation during gasification with carbon dioxide	122
5.3.1.3	Sodium volatilisation during gasification with steam	123
5.3.2	Solubility of sodium present in pyrolysis and gasification char	126
5.3.2.1	Effect of pyrolysis	126
5.3.2.2	Effect of gasification	129
5.3.3	Mechanism of formation of volatile sodium	130
5.3.4	Determination of sodium forms in pyrolysis and gasification char	132
5.3.4.1	Determination of sodium carbonate using FT-IR spectroscopy	132
5.3.4.1.1	Effect of pyrolysis	134
5.3.4.1.2	Effect of gasification	134
5.3.4.2	Determination of sodium carbonate by XRD technique	135
5.3.4.3	Determination of compounds between sodium and sulphur	135
5.4	PYROLYSIS AND GASIFICATION OF COAL CONTAINING SODIUM CHLORIDE	137
5.4.1	Sodium and chlorine volatilisation during pyrolysis and gasification	138
5.4.1.1	Effect of pyrolysis	138
5.4.1.2	Effect of gasification	140
5.4.2	Determination of sodium carbonate in char	143
5.5	SUMMARY	145
6	REACTIONS OF SODIUM WITH SILICA DURING PYROLYSIS AND GASIFICATION OF COAL – EXPERIMENTAL RESULTS	148
6.1	INTRODUCTION	148
6.1.1	Silicate formation and associated agglomeration and defluidisation	148
6.1.2	Formation and properties of silicate glass	150
6.2	OBJECTIVES OF THIS WORK	153
6.3	SILICA AND ORGANIC SODIUM MIXTURE	153
6.3.1	Chemical Analyses	153
6.3.1.1	Results for nitrogen atmosphere experiments	154
6.3.1.2	Results for carbon dioxide atmosphere experiments	156
6.3.1.3	Results for steam atmosphere experiments	158
6.3.2	Evaluation of formation of silicates	161
6.3.2.1	Effect of carbon dioxide and nitrogen atmosphere	161
6.3.2.2	Effect of steam atmosphere	164
6.3.3	Microscopic examination for formation of silicates	166
6.3.3.1	Effect of nitrogen atmosphere	167
6.3.3.2	Effect of carbon dioxide atmosphere	167
6.3.3.3	Effect of steam atmosphere	170
6.4	PYROLYSIS AND GASIFICATION OF COAL CONTAINING SILICA AND ORGANIC SODIUM	177
6.4.1	Chemical Analyses of Char	177
6.4.1.1	Results for pyrolysis char	178

6.4.1.2	Results for gasification with carbon dioxide	180
6.4.1.3	Results for gasification with steam	181
6.4.1.4	Sodium volatilisation during gasification	184
6.4.2	Microscopic examination of char	186
6.4.2.1	Silicate formation during coal pyrolysis	186
6.4.2.2	Silicate formation during gasification with carbon dioxide	187
6.4.2.3	Silicate formation during gasification with steam	190
6.5	SILICA AND SODIUM CHLORIDE MIXTURE	194
6.5.1	Formation of Silicates in Steam Atmosphere	194
6.5.2	Microscopic examination	197
6.6	PYROLYSIS AND GASIFICATION OF COAL CONTAINING SILICA AND SODIUM CHLORIDE	200
6.6.1	Pyrolysis in nitrogen	201
6.6.2	Gasification with carbon dioxide	202
6.6.3	Gasification with steam	202
6.7	SUMMARY	204
6.7.1	Reactions between silica and organic sodium in mineral mixture	204
6.7.2	Pyrolysis and gasification of coal containing organically-bound sodium and silica	205
6.7.3	Reactions between sodium chloride and silica	207
7	REACTIONS OF SODIUM WITH KAOLIN DURING GASIFICATION AND PYROLYSIS OF COAL - EXPERIMENTAL RESULTS	208
7.1	INTRODUCTION AND OBJECTIVES	208
7.2	KAOLIN AND ITS THERMAL TRANSFORMATION	209
7.3	KAOLIN AND ORGANIC SODIUM MIXTURE	211
7.3.1	Mineralogical analysis	211
7.3.1.1	Products of thermal decomposition of kaolin	211
7.3.1.2	Results for carbon dioxide atmosphere experiments	211
7.3.1.3	Results for steam atmosphere experiments	212
7.3.2	Chemical analyses of reaction products	214
7.3.2.1	Solubility of kaolinite and its transformation products	214
7.3.2.2	Solubility of reaction products	216
7.3.2.2.1	Solubility in cold water	216
7.3.2.2.2	Solubility in hot water	218
7.3.2.3	Formation of sodium silicates	220
7.3.3	Microscopic examination	221
7.4	PYROLYSIS AND GASIFICATION OF COAL CONTAINING KAOLIN AND ORGANIC SODIUM	225
7.4.1	Chemical Analyses of Char	225
7.4.2	Microscopic examination of char	228
7.4.3	Mineralogical examination	231
7.5	KAOLIN AND SODIUM CHLORIDE MIXTURE	231
7.5.1	Chemical Analyses	232
7.5.2	Microscopic examination	235
7.5.3	Mineralogical examination	236

7.6	PYROLYSIS AND GASIFICATION OF COAL CONTAINING KAOLIN AND SODIUM CHLORIDE	236
	7.6.1 Chemical Analyses of Char	237
	7.6.2 Mineralogical examination	238
	7.6.3 Microscopic examination	238
7.7	SUMMARY	243
8	KINETICS OF COAL GASIFICATION	246
8.1	INTRODUCTION	246
8.2	MECHANISM OF CATALYTIC GASIFICATION	246
	8.2.1 Catalytic effect of sodium on coal gasification	247
8.3	GASIFICATION KINETICS OF COAL	250
8.4	SUMMARY	256
9	GENERAL DISCUSSION	258
9.1	INTRODUCTION	258
9.2	SODIUM TRANSFORMATIONS	258
	9.2.1 Vaporisation of Sodium	259
9.3	REACTIONS OF SODIUM WITH SILICA	261
9.4	REACTIONS OF SODIUM WITH KAOLIN	264
9.5	IMPLICATIONS FOR AGGLOMERATION	266
10	CONCLUSIONS AND RECOMMENDATIONS	268
10.1	CONCLUSIONS	268
	10.1.1 Thermodynamic Studies	268
	10.1.2 Transformations of Sodium	269
	10.1.3 Reactions of Sodium with Silica during Gasification of Coal	270
	10.1.3.1 Reactions of silica and organically-bound sodium	270
	10.1.3.2 Reactions between sodium chloride and silica	271
	10.1.4 Reactions of Sodium with Kaolin during Gasification of Coal	272
	10.1.4.1 Reactions of kaolin and organically-bound sodium	272
	10.1.4.2 Reactions of kaolin and sodium chloride	273
	10.1.5 Kinetics of Coal Gasification	273
10.2	RECOMMENDATIONS FOR FUTURE WORK	274
	BIBLIOGRAPHY	276

LIST OF TABLES

Figure No	Caption	Page
Table 2.1	Silicate mineral species in coal.	17
Table 2.2	Melting points of selected inorganic compounds and eutectics that may be found in a fluidised bed gasifier conditions (after Dean, 1985; Levin et al., 1979).	48
Table 3.1	Chemical species considered as possible product phases and system component species for the thermodynamic equilibrium predictions.	76
Table 4.1	Analysis of Lochiel coal.	95
Table 4.2	Analyses of additives Silica (quartz) and Kaolin used in preparation of synthetic coals.	95
Table 4.3	Typical levels of sodium and silicon oxides in South Australian Bowmans and Lochiel coals and Victorian Loy Yang coal.	97
Table 4.4	Description of coal samples with desired content of sodium and silica or kaolin.	99
Table 4.5	Actual synthetic coals compositions.	100
Table 4.6	Description of mineral mixture samples.	100
Table 4.7	Experimental conditions for experiments conducted with synthetic coals and mineral mixtures in the Horizontal Tube Furnace.	105
Table 4.8	Sodium and chlorine content in NA1 coal loaded with organically-bound sodium and in NC1 coal impregnated with sodium chloride.	109
Table 5.1	Results of sodium release from NA1 coal containing 0.92% d.b. of organically-bound sodium during pyrolysis in nitrogen and during gasification with carbon dioxide and with steam. The results are shown as per cent loss of the sodium present originally in coal.	120
Table 5.2	Sodium release from coal during pyrolysis or gasification as reported in literature in comparison with the current work.	122
Table 5.3	Surface area and micropore volume data for high-sulphur Lochiel lignite for pyrolysis and gasification char samples obtained in TGA experiments by Poeze (2000).	128

Table 5.4	Results of determination of presence of sodium as sodium carbonate in the residue pyrolysis and gasification chars of NA4 coal obtained by measuring carbon dioxide absorption using FT-IR technique.	133
Table 5.5	Results of analysis of NA1 coal char samples for the presence of sulphides and soluble sulphur compounds formed within char during pyrolysis and gasification of coal.	136
Table 5.6	Results of determination of presence of sodium as sodium carbonate in the NC4 coal pyrolysis and gasification chars by measuring carbon dioxide absorption using FT-IR technique. Char samples from experiments conducted at 750°C were treated with acid to evolve carbon dioxide.	145
Table 6.1	Typical levels of sodium and silicon oxides in South Australian Bowmans and Lochiel coals and Victorian Loy Yang coal.	150
Table 6.2	X-ray diffraction analysis of samples of sodium carbonate and mixture of sodium carbonate and silica exposed to steam atmosphere for various times at temperature between 650°C and 850°C.	161
Table 6.3	Results of solubility in water of silica present in residue char after pyrolysis in nitrogen and gasification in steam and carbon dioxide of NA1S coal containing on dry basis 0.7% of organically-bound sodium and 9.2% of silica.	179
Table 6.4	Results of solubility of silica present in residue chars after gasification at various conditions in steam and in carbon dioxide of NA1S coal containing on dry basis 0.7% weight of organically-bound sodium and 9.2% of silica.	183
Table 6.5	Silica soluble in hot water after exposure of SNC silica and sodium chloride mixture and SAC silica and sodium acetate mixture to steam atmosphere at temperature range of 650°C to 850°C.	196
Table 6.6	Results of solubility in hot water of silica present in residue char after pyrolysis in nitrogen and gasification in steam and carbon dioxide of NC1S coal containing on dry basis 0.85% of organically-bound sodium and 9.6% of silica.	201
Table 7.1	X-ray diffraction analysis of samples of kaolin and KAC kaolin and sodium acetate mixture exposed to carbon dioxide or steam atmosphere at temperature of 650°C to 850°C.	212
Table 7.2	Solubility in acids of kaolin and its breakdown and reaction with sodium products (Dean, 1985).	214

Table 7.3	Solubility of aluminium in sulphuric acid in samples of pure kaolin and kaolin mixed with sodium acetate into KAC mixture exposed respectively to carbon dioxide and to steam for 15 minutes at elevated temperatures.	215
Table 7.4	Solubility in superheated water of silica present in samples of KAC mixtures exposed to steam at elevated temperatures.	220
Table 7.5	Sodium content in char samples of NA1K and NA1S coals gasified with carbon dioxide and pyrolysed in nitrogen, established after leaching the chars in cold water, hot water and in sequences of leaching in water superheated to 120°C.	227
Table 7.6	Results of leaching in cold water, hot water and for 64 hours in water superheated to 120°C of char samples of NA1K coal gasified with carbon dioxide and pyrolysed in nitrogen at 650°C and 750°C showing sodium leached from char as part of the initial sodium present in coal.	228
Table 7.7	Results of SEM-EDAX analysis of sodium chloride and kaolin KNC mixture exposed to carbon dioxide, nitrogen and steam atmosphere at 850°C.	236
Table 8.1	Reactivity values for gasification in steam and in carbon dioxide of NA1 coal.	253
Table 8.2	Activation energy for gasification reactions with steam or with carbon dioxide of coal containing a controlled form and amount of sodium with silica or kaolin and prepared from acid-washed low-mineral Lochiel coal.	254
Table 8.3	Activation energies for gasification reactions with steam or with carbon dioxide for South Australian coals as reported in literature in comparison with current work.	256

LIST OF FIGURES

Figure No	Caption	Page
Figure 2.1	Schematic composition of the brown coal structure (after Lindner, 1988).	10
Figure 2.2	Schematic diagram illustrating high-temperature reactions for minerals in an USA Eastern-type coal under reducing conditions (after Huffman and Huggins, 1986).	41
Figure 2.3	Phase diagram for $\text{Na}_2\text{O}.\text{SiO}_2$ mixtures.	49
Figure 3.1	Equilibrium distribution of the sodium species from sulphur-rich coal containing 1% d.b. organically-bound sodium, in atmospheres of (a) nitrogen or hydrogen, (b) carbon monoxide, (c) carbon dioxide and (d) steam at 1 atmosphere pressure.	78
Figure 3.2	Equilibrium distribution of the sodium species from sulphur-rich coal containing 1% d.b. sodium as sodium chloride in atmospheres of steam and at 1 atmosphere pressure.	80
Figure 3.3	Equilibrium distribution of the sodium species from sulphur-rich coal containing 1% d.b. organically-bound sodium and 10% d.b. kaolin in atmospheres of carbon dioxide, carbon monoxide, steam or hydrogen at 1 atmosphere pressure.	81
Figure 3.4	Equilibrium distribution of the sodium species from sulphur-rich coal containing 1% d.b. sodium as sodium chloride and 10% d.b. kaolin in atmospheres of (a) nitrogen or hydrogen (b) carbon monoxide, (c) steam and (d) carbon dioxide at 1 atmosphere pressure.	82
Figure 3.5	Equilibrium distribution of the sodium species from sulphur-rich coal containing 1% d.b. organically-bound sodium and 10% d.b. SiO_2 in atmospheres of (a) nitrogen, (b) carbon dioxide, carbon monoxide, steam and hydrogen at 1 atmosphere pressure.	85
Figure 3.6	Equilibrium distribution of the sodium species from sulphur-rich coal containing 1% d.b. sodium as NaCl and 10% d.b. SiO_2 in atmospheres of (a) nitrogen, (b) steam, (c) carbon dioxide, (d) hydrogen and (e) carbon monoxide at 1 atmosphere pressure	86
Figure 3.7	Equilibrium distribution of the silicon species from sulphur-rich coal containing (a) 1% d.b. organically-bound sodium and 10% SiO_2 , (b) 1% d.b. sodium as NaCl and 10% SiO_2 , (c) 1% d.b. organically-bound sodium and 10% kaolin and (d) 1% d.b. sodium as NaCl and 10% d.b. kaolin during gasification in carbon dioxide at 1 atmosphere pressure.	89

Figure 4.1	Schematic diagram of the Horizontal Tube Furnace.	102
Figure 4.2	Measured temperature responses at the centre of 4 mm Lochiel coal particles during heating in the Horizontal Tube Furnace heated to specified set point.	103
Figure 4.3	Measured temperature responses at the centre of 4 mm Lochiel coal particles during cooling from specified temperature level in the quencher of the Horizontal Tube Furnace.	104
Figure 4.4	Portion of silica, α , which could be leached out after one hour exposure of sodium silicate glass with water as a function of composition and of temperature - adapted from Eitel (1966) and Lindner (1984).	107
Figure 4.5	Schematic diagram of the apparatus arrangement for analyses of carbon dioxide.	110
Figure 5.1	Sodium losses at various temperatures as a function of time during pyrolysis in nitrogen of NA1 coal only containing 0.9% d.b. of organically-bound sodium.	121
Figure 5.2	Sodium volatilisation at various temperatures as a function of time during gasification of NA1 coal containing 0.9% d.b. of organically-bound sodium (a) with carbon dioxide and (b) with steam.	123
Figure 5.3	Sodium volatilisation as a function of carbon conversion during carbon dioxide and steam gasification (a) at 650°C, (b) at 750°C and (c) at 850°C of NA1 coal containing 0.9% of organically-bound sodium.	125
Figure 5.4	Distribution of sodium between acid-soluble (A.S.) sodium and sodium analysed in post acid leaching char residue (Res.) present in char as a function of reaction time for char generated during pyrolysis of NA1 coal at various temperatures.	127
Figure 5.5	Distribution of sodium present in char between acid-soluble sodium (A.S.) and sodium analysed in char residue post acid leaching (Res.) as a function of reaction time for char generated at various temperatures during gasification (a) with carbon dioxide and (b) with steam of NA1 coal.	129
Figure 5.6	Carbon dioxide absorption measurements using FT-IR spectroscopy to determine presence of sodium carbonate in samples of NA4 coal char. Char samples were generated during pyrolysis in nitrogen and during gasification with carbon dioxide and with steam at 750°C.	133
Figure 5.7	Losses (a) of sodium and (b) of chlorine from NC1 coal during pyrolysis in nitrogen presented for various temperatures as a function of time.	139

Figure 5.8	Losses (a) of sodium and (b) of chlorine during gasification with carbon dioxide of NC1 coal for various temperatures presented as a function of time.	141
Figure 5.9	Losses (a) of sodium and (b) of chlorine during gasification with steam of NC1 coal for various temperatures presented as a function of time.	142
Figure 5.10	Release of sodium and chlorine from NC1 coal presented as a function of carbon conversion during gasification with carbon dioxide and with steam at 850°C.	143
Figure 5.11	Carbon dioxide absorption measurements using FT-IR spectroscopy to determine presence of sodium carbonate in NC4 coal char samples. Char samples were generated during pyrolysis in nitrogen and during gasification with carbon dioxide and with steam at 750°C.	144
Figure 6.1	Sodium carbonate melting temperature trendline presented as a function of steam content: (1) standard melting point, (2) Huttinger and Minges, 1985, (3) Song and Kim, 1993.	152
Figure 6.2	Silica soluble in (a) cold and (b) hot water as part of a sample of SAC mixture containing silica and 6.2% sodium as sodium acetate exposed to atmosphere of nitrogen at 650°C, 750°C and 850°C and presented as a function of reaction time.	154
Figure 6.3	Sodium soluble in (a) cold and (b) hot water as part of a sample of SAC mixture containing 6.2% sodium as sodium acetate and silica exposed to atmosphere of nitrogen at 650°C, 750°C and 850°C and presented as a function of reaction time.	155
Figure 6.4	Solubility of (a) sodium and (b) silica in water superheated to 120°C of SAC samples, the mixtures of silica and sodium acetate, exposed to nitrogen atmosphere at 650°C, 750°C and 850°C temperature, presented as function of reaction time.	156
Figure 6.5	Silica soluble in (a) cold and (b) hot water as part of a sample of SAC mixture containing 6.2% sodium as sodium acetate and silica exposed to atmosphere of carbon dioxide at 650°C, 750°C and 850°C and presented as a function of reaction time.	157
Figure 6.6	Sodium soluble in (a) cold and (b) hot water as part of a sample of SAC mixture containing 6.2% sodium as sodium acetate and silica exposed to atmosphere of carbon dioxide at 650°C, 750°C and 850°C and presented as a function of reaction time.	157
Figure 6.7	Solubility of (a) sodium and (b) silica in water superheated to 120°C of SAC samples, the mixtures of silica and sodium acetate, exposed to carbon dioxide atmosphere at 650°C, 750°C and 850°C temperature, presented as function of reaction time.	158

Figure 6.8	Silica soluble in (a) cold and (b) hot water as part of a sample of SAC mixture containing 6.2% sodium as sodium acetate and silica exposed to atmosphere of steam at 650°C, 750°C and 850°C and presented as a function of reaction time.	159
Figure 6.9	Sodium soluble in (a) cold and (b) hot water as part of a sample of SAC mixture containing 6.2% sodium as sodium acetate and silica exposed to atmosphere of steam at 650°C, 750°C and 850°C and presented as a function of reaction time.	159
Figure 6.10	Solubility of (a) sodium and (b) silica in water superheated to 120°C of SAC samples, the mixtures of silica and sodium acetate, exposed to nitrogen atmosphere at 650°C, 750°C and 850°C temperature, presented as function of reaction time.	160
Figure 6.11	Micrograph of SEM secondary electron images of SAC mixture exposed to nitrogen atmosphere at 650°C for (a) 45 seconds, (b) 5 minutes and (c) 35 minutes.	168
Figure 6.12	Micrographs of SEM secondary electron images of SAC mixture exposed to nitrogen atmosphere at 750°C for (a) 45 seconds, (b) 5 minutes and (c) 35 minutes.	169
Figure 6.13	Figure 6.13 Micrograph of a SEM backscattered image of SAC sample exposed to nitrogen atmosphere at 850°C for 35 minutes.	170
Figure 6.14	Micrograph of SEM secondary electron images of SAC sample exposed to carbon dioxide atmosphere at 650°C for (a) 45 seconds, (b) 5 minutes and (c) 35 minutes.	171
Figure 6.15	Micrograph of SEM secondary electron images of SAC sample exposed to carbon dioxide atmosphere at 750°C for (a) 45 seconds, (b) 5 minutes and (c) 35 minutes.	172
Figure 6.16	Micrograph of SEM (a) secondary electron image of SAC sample exposed to carbon dioxide atmosphere at 850°C for 35 minutes and (b) of backscattered electron image of a cross section of a 15 minutes sample.	173
Figure 6.17	Micrographs of SEM backscattered images of SAC mixture exposed to steam atmosphere at 650°C for (a) 90 seconds and (b) 15 minutes.	174
Figure 6.18	Micrographs of SEM backscattered images of SAC sample exposed to steam atmosphere at 750°C for (a) 90 seconds and (b) 15 minutes.	175
Figure 6.19	Micrographs of SEM backscattered images of SAC sample exposed to steam atmosphere at 850°C for (a) 90 seconds and (b) 15 minutes.	176

Figure 6.20	Content of silica soluble in hot water present in the residue char of NA1S coal pyrolysed in nitrogen atmosphere or gasified with steam or with carbon dioxide at 850°C presented as function of reaction time.	182
Figure 6.21	Fraction of sodium lost during gasification in steam at 650°C, 750°C and 850°C of NA1S coal containing 0.7% wt. of organically-bound sodium and 9.2% of silica, presented as function of reaction time.	185
Figure 6.22	Sodium volatilisation as a function of carbon conversion during carbon dioxide and steam gasification at 850°C of NA1S coal containing 0.7% wt. of organically-bound sodium and 9.2% of silica.	185
Figure 6.23	Micrograph of SEM backscattered electron images of a 50x magnification of cross section of NA1S coal 35 minutes pyrolysis char from (a) 750 °C and (b) 850°C pyrolysis conditions.	186
Figure 6.24	Micrograph of SEM backscattered electron images of cross-section of NA1S coal pyrolyses char sample exposed for 35 minutes to nitrogen atmosphere (a) at 750°C and (b) at 850°C showing formation of silicate joints between silica particles and formation of silicate layers on the surface of silica particles.	188
Figure 6.25	Micrograph of SEM backscattered electron images of cross-section of NA1S coal gasification char samples gasified for 35 minutes with carbon dioxide (a) at 750°C and (b) at 850°C showing silicate joints between silica grains.	189
Figure 6.26	Micrograph of SEM backscattered electron image of a cross-section of NA1S coal char sample after gasification with steam for 35 minutes at 650°C showing signs of silicate formation on the surface of silica grains.	191
Figure 6.27	Micrograph of SEM backscattered electron image of a cross-section of NA1S coal char sample after gasification in steam for 35 minutes at 750°C showing silicate glass joints between silica grains.	191
Figure 6.28	Micrograph of SEM backscattered electron image of 1000x magnification of a cross-section of NA1S coal char sample from gasification with steam for 5 minutes at 850°C showing silicate rims around silica grains and glass joints between silica grains.	192
Figure 6.29	Micrograph of SEM backscattered electron image of 1000x magnification of a cross-section of NA1S coal char sample after gasification in steam for 35 minutes at 850°C showing silicate glass joining silica grains.	192
Figure 6.30	Solubility in hot water of (a) sodium and (b) silica as part of a sample of SNC mixture exposed to atmosphere of steam at 650°C, 750°C and 850°C and presented as a function of reaction time.	196

Figure 6.31	Micrographs of SEM (a) secondary electron image and (b) of backscattered electron image of a cross section of SNC sample exposed to steam atmosphere at 750°C for 35 minutes.	198
Figure 6.32	Micrographs of SEM backscattered electron images of cross sections of SNC samples exposed to steam atmosphere at 850°C for (a, b) 5 minutes and (c) 35 minutes.	199
Figure 6.33	Micrographs of SEM backscattered electron images of cross section of NC1S coal char samples exposed to steam atmosphere for 35 minutes (a) at 650°C, (b) at 750°C and (c) at 850°C.	203
Figure 7.1	Solubility of sodium in cold water present in KAC mixture exposed to atmosphere of (a) nitrogen, (b) carbon dioxide and (c) steam at 650°C, 750°C and 850°C, shown as part of total initial sodium, and presented as a function of reaction time.	217
Figure 7.2	Combined sodium soluble in hot and in superheated water as part of total initial sodium of KAC mixture exposed to atmosphere of (a) nitrogen, (b) carbon dioxide and (c) steam at 650°C, 750°C and 850°C and presented as a function of reaction time.	219
Figure 7.3	Morphology of KAC mixture exposed to steam atmosphere at (a) 650°C, (b) 750°C and (c) 850°C for 35 minutes.	222
Figure 7.4	Micrographs of SEM back-scattered electron images of KAC mixture exposed to steam atmosphere at (a) 650°C, (b) 750°C and (c) 850°C for 35 minutes.	224
Figure 7.5	Micrographs of SEM back-scattered electron images of char of NA1K coal gasified with carbon dioxide for (a) 45 seconds and (b) for 15 minutes at 850°C.	229
Figure 7.6	Micrographs of SEM back-scattered electron images of char of NA1K coal gasified in steam for 35 minutes at (a) 650°C, (b) 750°C and (c) 850°C.	230
Figure 7.7	Combined sodium soluble in cold, hot and superheated water as part of total initial sodium present in KNC mixture exposed at 650°C, 750°C and 850°C to (a) carbon dioxide, (b) nitrogen and (c) steam atmosphere presented as a function of reaction time.	233
Figure 7.8	Insoluble sodium as part of total initial sodium present in KNC mixture exposed to steam at 650°C, 750°C and 850°C and presented as a function of reaction time.	234
Figure 7.9	Morphology of KNC mixture exposed to steam atmosphere at 850°C for 35 minutes.	235

Figure 7.10	Combined sodium soluble in cold, hot and superheated water as part of total initial sodium present in NC1K coal gasified with steam at 650°C, 750°C and 850°C presented as a function of reaction time.	238
Figure 7.11	Micrographs of SEM back-scattered electron images of char of NC1K coal (a) pyrolysed in nitrogen and (b) and (c) gasified with carbon dioxide at 850°C for 35 minutes. Images in (a) and (b) show the edges of char particles, while (c) shows inside of char grain.	240
Figure 7.12	Micrographs of SEM back-scattered electron images of char of NC1K coal gasified with steam at (a) 750°C and (b) 850°C for 35 minutes.	241
Figure 8.1	Catalytic effect of sodium on char carbon conversion during gasification with steam and with carbon dioxide at 750°C and at 850°C for coal containing 1% organically-bound sodium (NA1 coal). LAW designates sodium-free acid-washed low-mineral Lochiel coal used in preparation of NA1 coal.	248
Figure 8.2	Char carbon conversion during gasification with steam at 850°C of NA1 coal containing 1% of organically-bound sodium, NA1S coal containing 1% organically-bound sodium and 10% silica and NA1K coal containing 1% organically-bound sodium and 10% kaolin.	249
Figure 8.3	Fixed carbon conversion as a function of time during gasification with steam at 850°C of NC1 coal containing sodium chloride, NC1S coal containing sodium chloride and silica and NC1K coal containing sodium chloride and kaolin.	250
Figure 8.4	Char carbon conversion data plotted for different temperatures according to Homogenous model for gasification with (a) steam and (b) carbon dioxide of coal containing 1% of organically-bound sodium (NA1 coal).	252
Figure 8.5	Arrhenius plot of reaction rate constants on gasification with steam and carbon dioxide of NA1 coal containing 1% of organically-bound sodium.	254
Figure 8.6	Activation energy for gasification reactions with steam or with carbon dioxide of coal containing controlled form and amount of sodium with silica or kaolin, as prepared from acid-washed low-mineral Lochiel coal.	255



Chapter 1

INTRODUCTION

1.1 BACKGROUND

The current global concern on climate change due to greenhouse gas emissions has cast a shadow on the future development of coal-fired power generation with respect to environmental acceptability.

The gasification of coal, as opposed to the direct combustion of coal, represents an attractive alternative for using coal in a more efficient, clean, low-cost technology for electricity generation. Gasification's primary attribute is that it offers a coal-based substitute for natural gas and fuel oil.

Coal gasification is a process that essentially converts a solid fuel (coal) into gaseous fuels by reacting the coal with oxygen and steam. The product gas can then be burnt in a gas turbine and waste heat recovered through use of a combined cycle system. The coal gasification-combined cycle (CGCC) process offers higher efficiency than other competing coal-based energy-conversion technologies.

1.2 COAL GASIFICATION

The vast reserves of low-rank coals in Australia offer a long term supply of possible feedstock for power generation. Coal deposits in Victoria have a low content of sulphur and ash, with a number of traditional pulverised fired power stations in operation in the Victorian Latrobe Valley based on those deposits. A number of low-rank coal deposits exist in South Australia, such as the Bowmans or Lochiel deposits, from which the use of coal would be difficult with currently used combustion technologies due to high content of sulphur, alkali and chlorine in those coals. Gasification of such coals offers a real hope for their utilisation as it offers better control over sulphur emission and meeting ever more stringent environmental requirements. The gasification process offers many advantages over conventional combustion processes: contaminants such as mineral matter, sulphur and nitrogen compounds can be removed easily and the fuel gas can be processed further into liquid fuels or chemicals.

There are three generic types of coal gasification reactors: fixed-bed, fluidised-bed, and entrained-bed. This classification is based on the method by which the coal and reactant gas are brought in contact. The method of contact also results in different gasification conditions and gasification products. The real life operation of these reactors poses some technical challenges because of the complex nature of coal as a feedstock and its undesirable contaminants.

The more important processes being either at a commercial or at a demonstration stage appear to be entrained-bed slagging ash gasifiers in the Shell or Texaco technology, the fixed-bed Lurgi process, ash-agglomerating fluid bed gasifiers in U-GAS or KRW technology and non-agglomerating fluidised bed gasifiers (FBG) such as HTW technology. The latter technology appears to be more suitable for low-rank coals, which often contain significant quantities of halide and alkali elements. These elements are volatile and are likely to cause deposition in CGCC plants.

During combustion or gasification, the transformation of inorganic matter present in coal is a complex process. The influence of inorganic matter on the performance of a combustor or gasifier may have a profound effect. The agglomeration of bed material or bed defluidisation can be a very common phenomenon. Therefore design of a plant such as a

FBG gasifier requires substantial knowledge on what happens to minerals (such as quartz and clays), salts, organically-bound elements and to sulphur present in the coal. Many of the answers are still unknown, with the current knowledge on the behaviour of coals with the high levels of sodium, chlorine and sulphur during fluidised bed gasification being limited.

Work to establish the suitability of the HTW technology to South Australian lignites showed that inorganic matter present in coal resulted in the agglomeration of bed material and the deposition of ash in the gasifier and its associated equipment (Bellin et al., 1989; Kosminski and Manzoori, 1990). Agglomerates rich in fused silicates and aluminosilicates of sodium were found in the gasifier ash. Condensation of sodium chloride led to deposition in the cyclone, ammonium chloride deposits were found blocking the product gas cooler. These results showed that the chemical and physical transformations undergone by the inorganic matter were different to those under combustion conditions where sodium sulphate is responsible for deposition and agglomeration (Manzoori, 1990).

As FBG technology offers real hopes for the effective utilisation of low-rank coals such as South Australian lignites, there is a need for more fundamental work to be carried out. The principal area of understanding will include inorganic matter transformations, mainly of sodium, its role in agglomeration of fluidised gasifier beds and finding ways to avoid agglomeration, fouling and defluidisation.

1.3 SCOPE AND STRUCTURE OF THESIS

The broad objective of this project is to gain an improved understanding of low-rank coal ash behaviour in fluidised bed gasification systems, particularly related to sodium and silicon reaction. Factors influencing the behaviour of coal ash during gasification include composition of mineral matter and operating parameters. The inorganic matter components in coal are transformed and initially partitioned into intermediate species in the form of inorganic gases, liquids and solids. The state of these species at any given stage or position in the gasifier directly influences their behaviour at that stage.

The literature review presented in Chapter 2 will critically analyse previous published literature related to agglomeration and defluidisation in fluidised bed gasification systems.

The emphasis is on existence of inorganic matter present in coal and its transformation during the process of gasification leading to the phenomena of agglomeration and defluidisation. Particular attention is given to the role of sodium and silicon minerals in coal ash behaviour in the process of gasification of low-rank coals.

The Literature Review presented in Chapter 2 draws attention to the possibility of theoretical prediction of reaction products during coal gasification between various inorganic elements present in coal. Chapter 3 presents results of thermodynamic calculations to predict the equilibrium compositions of sodium and silicon species under conditions relevant to fluidised bed gasification. Chapter 4 presents a description of the experimental equipment, experimental technique and materials used in the present study.

Chapter 5 deals with the transformations of sodium present in a lignitic high-sulphur Lochiel coal during pyrolysis and gasification with carbon dioxide or steam under conditions as prevailing in an atmospheric fluidised bed gasifier. It is important to define products of such transformations as they will play an important part in the possible reactions with silica and kaolin during the coal gasification process. The first part of this chapter deals with the transformation of organically-bound sodium, sodium bound to the coal structure via its carboxylic groups. The second section deals with the transformation of sodium present in coal as sodium chloride.

Chapter 6 concentrates on the reactions between sodium compounds and silica present in coal pyrolysed in an atmosphere of nitrogen or gasified in carbon dioxide or steam atmosphere at conditions similar to those existing in a typical atmospheric fluidised bed gasifier. Sodium and silica, when reacted in such conditions, may form silicates, which in turn may cause the gasifier bed to agglomerate and/or to defluidise. Also presented are the results of reactions in mixtures of sodium salts and silica exposed to the same temperature and atmospheric conditions as the samples of gasified coal. Results of these experiments form the basis for an assessment of products of reaction between sodium and silica in coal gasification.

Chapter 7 reports the results of reactions between sodium compounds and kaolin during the pyrolysis and gasification of coal. When sodium and kaolin react under such environmental conditions, they form aluminosilicates. The formation of these products is

very beneficial for the stable operation of a gasifier, as aluminosilicates remain in the solid state under typical temperatures of operation for a gasifier and may help prevent the creation of silicates. The objective of this Chapter is to provide experimental validation to predictions presented in Chapter 3 on the formation of solid sodium aluminosilicates such as nepheline $\text{Na}_2\text{O} \cdot \text{Al}_2\text{O}_3 \cdot 2\text{SiO}_2$ or liquid albite $\text{Na}_2\text{O} \cdot \text{Al}_2\text{O}_3 \cdot 6\text{SiO}_2$ under coal gasification conditions.

Chapter 8 summarises theoretical aspects of coal gasification: kinetics of gasification, catalytic activity of sodium and the influence of silica and kaolin on the gasification of coal with steam or carbon dioxide. The activation energy for gasification with steam or carbon dioxide of coal containing various forms of sodium and containing silica or kaolin will be presented. A summary of the work presented will be given in Chapter 9 and the implications of the present work for future investigations in the areas of coal agglomeration and defluidisation during gasification will be discussed.

Chapter 2

LITERATURE REVIEW

2.1 INTRODUCTION

This chapter reviews the published literature related to agglomeration and defluidisation in fluidised bed gasification systems. The emphasis is on existence of inorganic matter present in coal and its transformation during the process of gasification leading to phenomena of agglomeration and defluidisation. Particular attention is given to coal ash behaviour in the process of gasification of low-rank coals and the role and the presence in such coals of sodium and silicon minerals. Reactions of sodium with silicon bearing minerals are important as in the process of agglomerating coal ash during fluidised bed gasification. Coal gasification is a complex process involving coal pyrolysis, coal combustion and coal gasification. Understanding coal ash behaviour in the process of gasification requires understanding of coal ash behaviour in all those processes. The literature relevant to these areas is reviewed.

2.2 INORGANIC MATTER IN COAL

Coal is a complex solid organic polymer that originates from the accumulation and decomposition of organic matter millions of years ago. The organic matter may initially be

degraded by aerobic and anaerobic bacteria, but it is the deposition of sediments (sands, clays, etc) to bury this material, that the process of low grade metamorphosis involving the application of heat and pressure, termed *coalification*, results in the transformation into coal.

Coal mainly consists of organic substance (enriched in elemental carbon), mineral substance and moisture. The organic structure of low-rank coals (brown coals or lignites), which are of interest to the CRC Clean Power from Lignite, are at an intermediate stage of development between peat, (which contains significant proportions of cellulose and lignin) and sub-bituminous coal (which have lost the majority of their carboxyl and methoxyl groups). Coal consists of lamellae containing nuclei of aromatic or hydroaromatic ring clusters (low-rank coals typically having between one to three rings), with various substituted heteroatoms (N, O, S) and functional groups (carbonyl, carboxyl, ethers and phenols). These lamellae are cross-linked by covalent polymethylene, etheric-oxygen and sulphur bridges, non-covalent bonds, hydrogen bonds and Van der Waal forces. The inorganic matter is distributed in a heterogenous manner both at the macroscopic and microscopic levels.

Low-rank coals contain significant amount of humic acids formed by the oxidation of plant lignins and cellulose during the coalification process. Humic acids are compounds having a character of polymerised phenols networked by oxygen bridges and having ion-exchangeable carboxylic (-COOH) and hydroxyl (-OH) groups. The number of these functional groups in the coal decreases as coalification proceeds.

2.2.1 Definitions and Classification

The mineral matter present in coal can be in the form of mineral inclusions, as dissolved salts or colloids in coal moisture and as part of the coal chemical structure. The occurrence of mineral matter depends on coal origin and conditions of coal deposit formation and transformation during coalification.

The mineral matter, also known as inorganic matter, can be grouped as follows (Wall et al., 1979; Matl and Tomkow, 1981; Manzoori, 1990):

-
- a) Elements absorbed by plant tissue during growth; predominantly alkali and alkali earth elements, phosphorus and sulphur, and also trace elements including iron, silicon, aluminium, manganese.
 - b) Elements intimately bonded with coal organic substance, particularly to coal humic acids, originating from water, with which plant matter came in contact during coalification.
 - c) Sedimentary minerals, fine discrete particles of mainly clays, other hydrated aluminosilicates and quartz, uniformly distributed within the organic matter.
 - d) Bands of sedimentary minerals, detritus and their weathering product minerals, shale minerals, clays and quartz, periodically depositing and forming partings of final coal deposit.
 - e) Epigenetic minerals, carbonates, sulphates, sulphides, chlorides depositing in fractures from waters infiltrating the deposits.
 - f) Fragments of coal deposit roof and floor rocks included in the coal while mining.
 - g) Colloids dispersed in coal inherent moisture.
 - h) Salts dissolved in coal inherent moisture, often dissociated in the form of free ions.

Various researchers have offered a number of classifications to differentiate between the forms of the inorganic matter in coal. For this study, the adopted classification by Manzoori (1990) was used, where the inorganic matter is divided into the following two categories:

- “Inorganics” - which include the atomically dispersed organically-bound inorganic elements in groups (a) and (b) above; basically sodium Na, potassium K, calcium Ca, magnesium Mg, iron Fe, aluminium Al, chlorine Cl, sulphur S, manganese Mn,

- “Minerals” - substances from groups (c), (d), (e), (f), (g) and (h) above, which occur as discrete minerals: group (c), (d), (e), (f) and those which are in the inherent moisture: as colloids (g) and salts (h) crystallising into fine particles upon drying of coal.

The terms “inorganic matter”, “inorganics” and “minerals” will be used according to the above definitions in this text.

2.2.2 Occurrence and Nature of Inorganic Matter

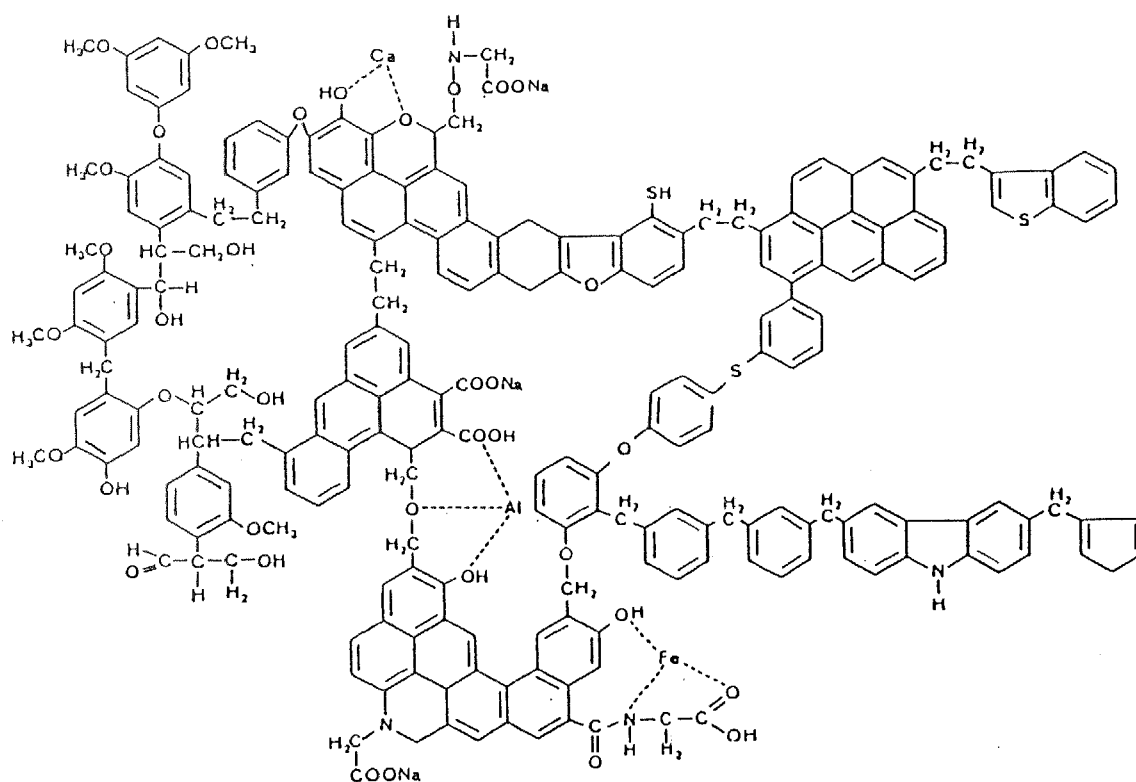
The presence of inorganic matter in coal and its distribution is dependent on the vegetation, from which the coal was formed, depositional and post depositional environment and the coalification degree and conditions (Brayers and Walchuk, 1984).

The low-rank coals contain significant amount of inorganics, due to the high loads of humic acids (10 - 40%) present in these coals. Sub-bituminous coals, on the other hand, contain less than 10% humic acids (Mraw et al., 1983). In some of the Australian low-rank coals elements such as calcium and magnesium are often mostly present only in form of humic acid salts; these elements are ion-exchangeable with hydrogen ion and other ions (Durie, 1961).

The schematic of the structure of a brown coal, given by Lindner (1988) and shown in Figure 2.1, illustrates the presence of oxygen groups in coal and shows how ions, mostly alkali and alkali earth elements may be exchanged into these groups.

The carboxylic groups in coal may exchange their proton with ions present in ground water. Ions bound to the coal structure can be water or acid leached and can be exchanged with other ions. The determination of the presence of organically bound inorganic ions in the coal structure is important for assessing their behaviour and fate in a coal utilisation process. Studying the results of various methods for determination of coal carboxylic and phenolic group contents Singh (1992) found a linear relationship between O/C ratio and coal carboxyl group acidity. Singh proposed the expression for carboxyl group acidity prediction:

$$Y = 11.3873 \text{ O/C} - 0.21$$



lignins

humic acids

structural aromatic elements

Figure 2.1 Schematic composition of the brown coal structure (after Lindner, 1988).

Schafer (1970) reports that pH affects ion-exchange properties of low-rank coal carboxylic groups in the presence of phenolic groups. Increasing the pH above 8.3 will result in phenolic group exchange.

Detailed ion-exchange process description is given by Takarada et al. (1987). The cation addition to a low-rank coal consists of a cation-exchange step and a water-washing step. Takarada et al. (1991) soaked coal in a KCl solution and adjusted the pH with addition of ammonia solution. The washed and dried coal was back-exchanged with HCl to determine loading with potassium.

Analysis of the inorganic matter in some of the US lignites was conducted by Zygarlicke et al. (1990) through staged water leaching. Water extracts were prepared to determine the

content of salts dissolved in the coal inherent moisture. A leachate of ammonium acetate solution of inorganic elements was prepared. This was supposed to represent ion-exchangeable cations present in the coal primarily as the salts of carboxylic acids. Coal residue remaining from such extractions was leached with hydrochloric acid to remove elements held in coordination complexes within the organic structure, as well as acid soluble minerals such as carbonates and oxides. It was found that the sodium and calcium in the coals tested were predominantly present in the ion-exchangeable form.

2.2.2.1 Minerals in coal

Minerals in coals originate from rocks, and their weathering products. These minerals are predominantly sandstones, clays, shale minerals, plagioclase, quartz, dolomite, calcite, siderite, gypsum, pyrite and marcasite. In case of some of the South Australian low-rank coals the minerals, such as halite originate from sea water as seas covered some of those deposits during the deposit formation times.

Minerals generally will be a source of coal's silicon, aluminium, iron, also calcium and magnesium. Determination of mineral species in coal allows prediction of coal ash behaviour in utilisation process. Such determination can be conducted on raw coal, however the results are often not comprehensive, due to small grain size and the distribution of them. The method of low temperature ashing of coal to concentrate the mineral matter in coal also is not fully satisfactory as additional minerals such as carbonates, nitrates and sulphates may form in the process (Morgan et al., 1981; Martinez-Tarazona et al., 1990a).

Martinez-Tarazona et al. (1990a, 1990b) report on using FT-IR spectroscopy for obtaining information on the nature of bonding of inorganic elements to coal carboxyl groups.

2.2.2.2 Sulphur

Sulphur in coal exists in inorganic and organic forms. The inorganic forms are usually sulphides and sulphates. The organic sulphur compounds in coals are mainly components of the macromolecular structures of the coal and are not readily separated from these structures (Calkins, 1994).

The sulphur content of coals varies in wide range and is independent of coal rank. In low-rank Australian coals this range varies from eg. 0.2% d.b. for Yallourn brown coal in Victoria to 6.7% for Sedan coal in South Australia.

Only divalent organic sulphur is present in coals (Attar, 1978). Organic sulphur exists in a number of structures: in form of thiophenic aromatic structures as thiophene, benzothiophene, dibenzothiophene and a number of their methyl-substituted and hydroxylated compounds; in form of heterocyclic sulphur compounds; in form of aliphatic and aromatic sulphides, aryl and aliphatic thiols. Low-rank coals contain more of the organic sulphur in aliphatic form, whereas higher-rank coals contain predominantly heterocyclic sulphur.

Dominant inorganic form of sulphur in coal is its sulphide mineral pyrite (FeS_2), (Gluskoter, 1977, Calkins, 1994). Marcasite (FeS_2), sphalerite (ZnS_2), galena (PbS), chalcopyrite (CuFeS_2) are also often present in coals. Pyrite occurs in micrometre-sized crystals, as framboids of 10 to 40 mm in the diameter and aggregates of up to boulder size.

The sulphate minerals include barite (BaSO_4), gypsum ($\text{CaSO}_4 \cdot \text{H}_2\text{O}$), anhydrite (CaSO_4), a number of iron sulphates and others. As well as being incorporated in solid minerals, sulphate ions can exist in inherent coal moisture, (Readett, 1983 and 1984).

2.2.2.3 Chlorine

The level of chlorine content in coal is usually below 0.3% d.b., but can be even less than 0.01%. Low-rank coals in Australia contain, comparing with these numbers, a significant concentrations of chlorine, eg. Lochiel coal 1.3% d.b., or Esperance coal 2.5 % d.b.

Gluskoter and Rees (1964) studying USA Illinios and Indiana coals established, that the chlorine content of coal is mainly determined by the salinity of the ground waters associated with coal. Chou (1991) concluded studying Illinios coal that chlorine may occur in coal also as chloride ion (Cl^-) adsorbed on the inner surfaces of the micropores in coal macerals. In their most recent work on chlorine in coal, Shao et al. (1994) conclude that the forms of chlorine in Illinios coal are closely associated with the forms of nitrogen. The chlorine may be bonded to the basic nitrogen sites on the inner wall of coal micropores.

Forms of chlorine in UK coals were studied for many years. Edgecombe (1956) and Daybell (1967) postulated that the portion of chloride ions equivalent on a molar basis to the quantity of alkali extracted by water exists in the coal as alkali chloride, while remaining portion is bonded to the coal matter, which acts as an ion-exchange medium. Pearce and Hill (1986) concluded from their research that chlorine is present in one form, with no particular relationship with nitrogen, sodium or other alkali/alkaline earth metals, uniformly distributed in coal and linked ionically to the coal substance and very labile to heat treatment evolving as hydrogen chloride.

Hodges et al. (1983) concluded in their review of the works on the forms of chlorine in UK coals that the major source of chlorine in coals is brine, rich in soluble chlorides. That chlorine can be removed by prolonged washing with water. A large part of chlorine will be removed as hydrogen chloride by heat-treatment at approximately 200°C in either oxidising or inert atmospheres. Their final conclusion was however such, that the nature of the chlorine-coal bond is uncertain.

In a review Oakey et al. (1991), similar to Hodges et al. (1983), postulate that the mode of occurrence of chlorine, and as well of sodium, is not fully defined. Leaching experimental works quoted showed differences in the rates of release of sodium and chlorine suggesting that the two elements were largely independent of each other. The results indicated that both sodium and chlorine are present in UK coals as ions adsorbed on the coal surface. Some NMR works have shown the sodium (as ion) to be surface-bound and hydrated in the raw state. Chlorine (as ion) is believed to be either associated with basic surface groups or in solution in the inherent moisture in a coal's pore structure.

The leaching tests of a South Australian Bowmans coal conducted by Readett (1983, 1984) showed, that the most of the chlorine was extractable, and that it was in stoichiometric equivalent to the removed quantity of sodium. Conducting mechanical dewatering of the same coal Readett and Quast (1987) found the same quantity of chlorine in coal moisture as in leaching tests but less of sodium. They concluded that the chlorine was present in the coal in the form of free chloride ions in the coal inherent moisture.

The chlorine content of the coal, and also that of sodium, can be related to the salinity of the aquifers associated with the coal (Edger and Kaiser, 1984; Brockway and Borsaru, 1985; Gluskoter and Rees, 1964).

The above information on forms of chlorine in coals suggests that the nature of chlorine is dependent on the coal and its rank. In many cases final conclusion by Hodges et al. (1983) may still be valid.

The recently published work on forms of chlorine in lignite coals is that by Heng et al. (1995) who studied forms of chlorine in Victorian coals. They report that their results show that significant proportion of chlorine in those coals can be present in organic form.

Further work on determination of forms of chlorine in South Australian low-rank coal seems to be necessary.

2.2.2.4 Sodium

Sodium is present in some low-rank coals in significant quantities. In high-sodium content coals such as low-rank South Australian coals its content can reach 1.5% d.b. wt. The Victorian Flynn brown coal has its sodium-in-ash content of 20%. Generally a coal is considered as high-sodium coal if the sodium content in coal is greater than 0.5% d.b. or if sodium oxide in coal ash is in excess of 3% value (Lindner, 1988).

The sodium in coal can be in a number of forms. In mineral form it exists as a part of clay minerals. Plagioclases - sodium calcium aluminosilicates, have been identified in many coals by a number of researches: Kemezys and Taylor (1964), Karner et al. (1984), Raask (1985). Some clays, such as zeolites, have ion exchange properties and it is considered possible for sodium in coal to exist in this form (Hale et al., 1980). Sodium also exists in coal in minerals containing sodium: in clays such as montmorillonite or zeolites. Proportion of such mineral sodium is low for low-rank coals and can be considerable for higher rank coals.

Sodium chloride, sodium sulphate and also sodium carbonates are the major salts of sodium present in coal inherent moisture in coals ranging from low-rank coals to

bituminous coals (Edgecombe, 1956; Allan, 1981a and 1981b; Hodges et al., 1983; Readett, 1983 and 1984; Raask, 1985). Sodium then, because of salts solubility and dissociation exists in coal as a free ion. Readett and Quast (1987) concluded from their results of leaching and dewatering of Bowmans coal, that some sodium can be present as a water-soluble sodium weakly bonded to the coal surface.

Due to the nature of the low-rank coal and high content of ion-exchangeable humic acids functional groups, mainly carboxylic and phenolic groups, the sodium ion may exchange the proton in this groups forming humic acid carboxylic and phenolic salts. A significant proportion of the sodium, and of inorganic matter generally, can therefore be present in coal matrix as organically bound.

From his experiments of leaching Victorian Yallourn coal Durie (1961) concluded, that sodium ions and also other cations: calcium, magnesium, ferrous, were bonded to the coal substance via carboxylic acid groups. Murray (1968) established that there is no exchange of sodium on phenolic groups. Murray (1973) reports that the inorganic constituents of low-rank Victorian brown coal are mainly present as inherent inorganic combinations attached to the coal molecule. Durie and Swain (1971) gave further evidence suggesting that in Victorian Latrobe Valley brown coals sodium may be present partly as carboxylate. They also suggest that some carboxyl groups occur in coal in the free acid (-COOH) form.

The distribution of sodium in coal is then very even for that sodium, which is present as salts dissolved in coal inherent moisture or as sodium bound to coal organic substance. Such distribution has been demonstrated by electron microprobe coal analysis of US North Dakota lignites conducted by Sondreal et al. (1977).

The proportion of sodium present in this organic salts form reduces however with increase of coal rank as the high rank coals have a lesser quantity of functional groups than low-rank coals. The sodium content of the coal, as said before, can be related to the salinity of the aquifers associated with the coal (Edger and Kaiser, 1984; Brockway and Borsaru, 1985).

2.2.2.5 Potassium

Potassium exists in coals mainly in illite, a predominantly potassium aluminosilicate clay mineral - ideal formula $KAl_2(AlSi_3O_{10})(OH)_2$. Illite can be present in coal in large quantities. Particularly in bituminous coals illite can be present in as much as 25 wt% of coal total mineral content and it can be in a variety of sizes and association with other minerals (Srinivasachar et al., 1990). Other potassium minerals commonly existing in coals are feldspars or other than illite K-aluminosilicates such as montmorillonite.

Potassium concentration in coal is however not related to coal rank, as it is not that much attached to the coal matrix, like it is the case with sodium. Illite is present also in South Australian and Victorian low-rank coals (Readett and Quast, 1986, Brockway et al., 1991).

Illite appears to be the first molten phase amongst other minerals existing in coal ash of ashed US Eastern coals (Huffman and Huggins, 1986).

2.2.2.6 Calcium and magnesium

Calcium is often one of the major coal inorganic elements. In low-rank coals significant proportion of calcium is uniformly dispersed in the coal macerals as ion-exchangeable cations (Huffman et al. 1990, Mraw et al., 1983). Higher rank coals contain more mineral calcium, mainly in form of calcite $CaCO_3$, as the proportion of organically bound calcium reduces with increase of coal rank.

Other major calcium mineral forms are dolomite $CaCO_3.MgCO_3$, gypsum $CaSO_4.2H_2O$, anhydrite $CaSO_4$ or Ca-aluminosilicate clay minerals such as montmorillonite. Calcium, similarly to sodium, can also exist in zeolites, which exhibit ion-exchange properties. All these mineral inclusions occur of various sizes and concentrations.

Studies by Durie (1961) and Durie and Swain (1971) gave evidence suggesting that calcium and magnesium in Victorian brown coal are invariably present as carboxylates. In high-sulphur low-rank South Australian lignites both elements were found as bound to coal organic structure and calcium in form of gypsum (Readett and Quast, 1987).

Magnesium also exists in low-rank coals as ion-exchangeable cation attached to coal matrix. Brockway et al. (1991) report that in Victorian coals magnesium is concentrated in

the same top seams in coal deposit as are sodium and chloride ions and that it is associated with original coal aquifers.

Major magnesium minerals in coals are dolomite CaCO_3 , MgCO_3 , magnesite MgCO_3 , and various clays and other aluminosilicate minerals.

2.2.2.7 Silicon and aluminium

Silicon exists in coal mainly in form of its oxide, silica. Quartz (SiO_2) is the most common form of silica in both low and high-rank coals. The other such mineral is a basic clay mineral kaolinite $\text{Al}_2\text{O}_3 \cdot 2\text{SiO}_2 \cdot 2\text{H}_2\text{O}$. Other major classes of silicon and aluminium minerals found in coals are feldspars, feldspathoids, mica, chlorites, zeolites and also other basic clays minerals: illites, montmorillonite. A list of minerals most common in both low and high-rank coals compiled from Wall et al. (1979), Raask (1985) and Lindner (1988) is presented in Table 2.1. The chemical formulas for some of these minerals are quoted after Deer et al. (1992).

Table 2.1 Silicate mineral species in coal.

Species	Chemical formula
Silica, clays and silicates - common occurrence	
Quartz	SiO_2
Chalcedony	SiO_2
Kaolinite	$\text{Al}_2\text{O}_3 \cdot 2\text{SiO}_2 \cdot 2\text{H}_2\text{O}$
Illite	$\text{K}_{1.5-1.0}\text{Al}_4(\text{Si}_{6.5-7.0}\text{Al}_{1.5-1.0}\text{O}_{20})(\text{OH})_4$
Montmorillonite	$(1-x)\text{Al}_2\text{O}_3 \cdot x(\text{MgO}, \text{Na}_2\text{O}) \cdot 4\text{SiO}_2 \cdot n\text{H}_2\text{O}$
Muscovite	$\text{K}_2\text{O} \cdot 3\text{Al}_2\text{O}_3 \cdot 6\text{SiO}_2 \cdot 2\text{H}_2\text{O}$
Alkali Feldspars	$(\text{K}, \text{Na})_2\text{O} \cdot \text{Al}_2\text{O}_3 \cdot 6\text{SiO}_2$
Plagioclase	$\text{Na}_2\text{O} \cdot \text{Al}_2\text{O}_3 \cdot 6\text{SiO}_2$ - albite
	$\text{CaO} \cdot \text{Al}_2\text{O}_3 \cdot 2\text{SiO}_2$ - anorthite
Chlorite	$\text{Al}_2\text{O}_3 \cdot 5(\text{FeO}, \text{MgO}) \cdot 3.5\text{SiO}_2 \cdot 7.5\text{H}_2\text{O}$
Silicates - less common occurrence	
Augite	$\text{Ca}(\text{Mg}, \text{Fe}, \text{Al})(\text{Al}, \text{Si})_2\text{O}_6$
Biotite	$\text{Al}_2\text{O}_3 \cdot 6(\text{MgO}, \text{FeO}) \cdot 6\text{SiO}_2 \cdot 4\text{H}_2\text{O}$
Sanidine	$\text{K}_2\text{O} \cdot \text{Al}_2\text{O}_3 \cdot 6\text{SiO}_2$
Kyanite	$\text{Al}_2\text{O}_3 \cdot \text{SiO}_2$
Tourmaline	$\text{Na}(\text{Fe}, \text{Mn})_3\text{Al}_6(\text{BO}_3)_3 \cdot \text{Si}_6\text{O}_{18} \cdot (\text{OH})_4$
Halloysite	$\text{Al}_2\text{O}_3 \cdot 2\text{SiO}_2 \cdot 4\text{H}_2\text{O}$
Epidote	$4\text{CaO} \cdot 3(\text{Al}, \text{Fe})\text{O}_3 \cdot 6\text{SiO}_2 \cdot \text{H}_2\text{O}$
Natrolite	$\text{Na}_{16}(\text{Al}_{16}\text{Si}_{24}\text{O}_{80}) \cdot 16\text{H}_2\text{O}$

Silicon and aluminium constitute most of high-rank coals ash, mainly 60 to 90%. Ash from low-rank coals contains less of silicon and aluminium, often only 50%, as there is higher alkali and alkali earth content in such coals.

Aluminium in low-rank coals is also reported to exist in organically bound forms (Brockway et al., 1991). Murray and Bonafede (1972) report that aluminium in various low-rank coals has been found to be extractable by hydrochloric acid solution. The form of this acid extractable aluminium, which has been found to be evenly distributed in the coal matrix on a micro scale, has not been determined with certainty. Murray (1971) and Murray and Bonafede (1972) proposed, that in the Latrobe Valley brown coal the acid extractable aluminium was present as a hydrated aluminium oxide. The existence of an aluminium based (Al complex)⁺ ion-exchanged onto a carboxylic group has not been discounted by those workers.

2.2.2.8 Iron

Dominant iron minerals present in low and high-rank coals are pyrite FeS_2 and its weathering products such as sulphates. Often there is also present in coal polymorphic form of pyrite: marcasite. High rank coals frequently contain substantial amounts of iron as siderite FeCO_3 and in some clay minerals (Huffman et al., 1990). Siderite is a very common coal mineral present in considerable quantities in South Australian Leigh Creek coal. Fe-aluminosilicates, probably a type of montmorillonite clay can also be a source of iron (Zygarlicke et al., 1990). Iron can also be present as iron associated with coal matrix. Zygarlicke et al. (1990) report that some 50 % of a US Texas Monticello lignite total iron content may be as organically bound ions. Brockway et al. (1991) report on iron organically-bound as present in some of Australian low-rank coals.

2.3 TRANSFORMATIONS OF INORGANIC MATTER DURING GASIFICATION

The behaviour of the coal inorganic matter in fluidised bed gasifiers may be different, and will be substantially different from the behaviour of such matter in combustion systems, both pulverized system and fluid bed combustors.

Coal is introduced to a fluidised bed gasifier with a top grain size of a few millimetres. Temperature conditions in a gasifier are rather uniform. Initially a particle will undergo drying and devolatilisation. Reactions of the volatiles and the formed char with oxygen, steam and hydrogen and carbon dioxide will follow. Combustion will then be a part of these reactions. Therefore an attempt was made to find in the published literature information about behaviour of inorganic matter in both oxidising and reducing environments and in temperatures up to 1000°C or even above, if it is well related to a fluidised bed gasification process. However the temperature range of the most interest was between 700°C and 1000°C.

It is important to understand individual mineral transformations in predicting the formation and behaviour of ash. During all these processes the inorganic matter present in coal will also undergo both physical and chemical transformations. These may be:

- physical transformations: drying, dehydration, crystallisation, fusion, coalescence, vaporisation
- chemical transformations: thermal decomposition, oxidation, reduction, reaction between the species forming inorganic matter, reactions with volatiles and gaseous species, reactions with char.

Following is a review of information available in the literature covering these transformations. This gives an indication of the behaviour of the inorganic matter during gasification of coal in fluidised bed gasifier.

From now on the definition “inorganic matter” will include inorganic species formed as a product of transformations undergone by the coal inorganic matter.

2.3.1 Chemical Transformations

2.3.1.1 Decomposition of the Inorganics during Pyrolysis

Heating of coal will cause its devolatilisation and consequently depending on the temperature conditions lead to decomposition of the coal functional groups containing the inorganic elements. Devolatilisation starts below 400°C and is usually over at about 900°C.

Murray (1973), Schafer (1979a) report that in low-rank Victorian brown coals carboxylic groups containing the inorganic constituents begin to decompose on carbonisation below 400°C and their decomposition is completed by 600°C and the rate of carbon dioxide evolution is directly proportional to the decomposition of these carboxyl groups. Murray reports that sodium carbonate, calcium oxide, magnesium oxide and iron oxides are usually the chief compounds that may be formed. Murray also reports that there is no evidence of the presence of inorganics as phenates in studied coals.

Schafer (1979a) has also found that for coals in which those carboxylic groups were in a salt form, such for example as with calcium, that calcium was acid extractable for chars prepared at temperatures up to 400°C. Amounts of calcium extracted from higher temperature prepared chars was markedly less for 500°C and 600°C, increasing again at 700°C and 800°C. Schafer then reports that fine grinding of higher temperature char samples markedly improved the extractability of calcium from 500°C, 600°C and 700°C prepared char but was only slightly increased for the 800°C. He suggests that changes in char pore structure affects accessibility of the char to reagents.

Schafer (1979b) has also reported that chemical forms of decomposition products during pyrolysis of brown coal of cations associated with the coal carboxylic groups depend on temperature and type of cation. For example magnesium forms initially carbonate which decomposes to oxide above 600°C. Calcium and barium form cyanide and cyanamide at 900°C with carbonates formed at lower temperatures. With complete oxygen elimination from coal at 900°C, sodium and potassium are volatilised or form cyanides.

Schafer (1979b) also reports that carboxyl groups in the salt forms undergo less decomposition than those in the acid form, however more CO₂ is generated from cation loaded coals. Work by Ogunsola (1993) shows that less carboxyl groups decompose when lignite coal is exposed to heat treatment in steam atmosphere than in nitrogen atmosphere in temperature range between 200-500°C.

Manzoori (1990) concluded from pyrolysis experiments of single particles of a high-sulphur, high-sodium South Australian lignite (Lochiel) that under reducing conditions prevailing within the coal particles the organically bound sodium transforms mostly into a

water soluble form, whereas, calcium and magnesium transform into acid insoluble compounds. Manzoori also found that chlorine and sodium present in studied Lochiel coal were partially disproportionately evaporated during pyrolysis, suggesting that mechanisms other than vaporisation of sodium chloride were involved.

Otake and Walker (1993) report from their pyrolysis work with demineralised and cation loaded Texas lignite that the presence of exchangeable cations associated with carboxyl groups affects composition of the gas released upon pyrolysis to 1000°C. They identified using XRD technique that resultant products of coal loaded with calcium and magnesium for chars produced at 1000°C were respectively CaO and Ca(OH)₂ and MgO. However, they made no identification of these compounds for the same coal chars at 375 and 630°C. For sodium and potassium loaded coals they report several unknown peaks and found that inorganic phases, which existed at 1000°C were already formed at 630°C. The weight loss results reported from their experiments do not indicate any sodium loss at higher temperatures during pyrolysis.

Takarada et al. (1986) found that alkali exchanged into low-rank Yallourn coal structure forms alkali carbonate during pyrolysis in nitrogen atmosphere and during steam gasification at 650°C temperature. Alkali remained as carbonate when remaining low carbon content char was ashed. Alkali chloride was used to exchange alkali into the coal structure.

Matsukata et al. (1992) heat-treated in argon atmosphere at 850°C carbon impregnated with alkali carbonate solutions. They concluded that sodium and also other alkali species migrated into the bulk of carbon in the course of heat treatment and stabilised there. Those species were becoming not extractable with HCl solution.

Yamashita et al. (1991) claim, that they have presented, for the first time, clear evidence that Na₂CO₃ is the principal sodium species in the char after pyrolysis of coal exchanged with sodium into the structure in a form of carboxylates. Coals and their chars were examined by X-ray absorption near edge structure (XANES) using soft X-rays. Yamashita et al. used in their experiments Victorian Loy Yang coal impregnated with Na₂CO₃ and sodium ion-exchanged into coal structure using NaCl solution. They observed aggregation

of sodium species: NaCl and Na₂CO₃ in their coals heat-treated to temperatures 550°C and 650°C, but not at 350°C. These findings are in an agreement with work by Murray (1973), showing that decomposition of carboxylic groups starts at below 400°C and is completed at 600°C.

Radovic et al. (1983) report finding CaO in the severely pyrolysed chars by using X-ray diffraction technique. But they also suggest that short pyrolysis time may result in reduced aggregation and accessibility of dispersed ions due to very small pyrolysed chars micropores size.

Huggins et al. (1988a, 1988b) established that in rapidly pyrolysed chars, for few seconds only, the calcium state remained highly dispersed and only little different from its state in un-pyrolysed lignite. They did not find evidence of any spectra characteristic for CaO or other discrete calcium compounds in these chars. It appeared that the calcium in the rapidly pyrolysed chars remained bound to oxygen originally present in carboxyl groups in the lignite or polymer. Slowly pyrolysed chars showed that significant fractions of the calcium had been transformed to bulk CaO. They conducted their experiments at 800°C and 1000°C and used rich in organically bound calcium North Dakota lignite, and a Ca-loaded phenol-formaldehyde polymer.

They used EXAFS and XANES, X-ray absorption spectroscopies for sample examination. EXAFS spectroscopy determines the atomic structure of an element by analysis of the fine structure associated with an X-ray absorption edge of that element. EXAFS, and X-ray absorption near edge spectroscopy is an excellent method for investigating the atomic structure of a specific element in a complex sample, with concentration of element of interest at levels 100ppm to 1% (Huffman et al., 1989).

Huhn et al. (1983) concluded from their pyrolysis experiments conducted with K₂CO₃ impregnated coke that in the inert atmosphere there is a reduction of potassium carbonate by carbon resulting in formation of metal potassium at temperature already of about 700°C, with maximum rate of reduction at 720°C. Such reduction they report also for Na₂CO₃ and Rb₂CO₃. They also report condensation of potassium metal in the cooler part of their reactor after prolonged heating of the samples at temperatures approximating 1000°C.

Formation of metallic potassium has been also reported by Kapteijn et al. (1983), who exposed K_2CO_3 -activated carbon and K_2CO_3 -coal in a nitrogen flow at 830°C.

McKee (1983) in his review on mechanisms of the alkali metal catalysed gasification of carbon also reports a presence of potassium vapour in the gas phase for K_2CO_3 and carbon mixtures heated in a vacuum environment at temperatures in the range of 500-700°C. The presence of such potassium vapour was not contributed to the dissociation of the K_2CO_3 salt.

2.3.1.1.1 Sulphur transformations

During pyrolysis organic and inorganic coal sulphur compounds will transform mostly into the gaseous products: SO_2 , H_2S , COS , CS_2 , mercaptans. Transformation rate of sulphur into the gas phase will depend mainly on the temperature conditions and forms of sulphur in the coal (Ma et al., 1989). Calcium sulphide is often the most common sulphur solid product of pyrolysis. Hydrogen sulphide H_2S is mostly found in the volatiles (Attar, 1978).

Decomposition of pyrite liberates sulphur, which becomes trapped in the coal matrix (Cleyle et al. 1984). Gryglewicz and Jasienko (1992) report sequential changes in the sulphur distribution in the char formed during pyrolysis of a low-rank coal pyrolysed in the atmosphere of the evolved gas. They report an enrichment of the organic sulphur observed between 330-600°C when conversion of pyrite into ferrous sulphide occurred. Only thiophenic sulphur was present in the higher temperature char. A higher content of the thiophenic sulphur in the char than in the original coal, suggest reactions between sulphur or hydrogen sulphide and the char.

Manzoori (1990) quotes several sources also reporting on significant retention of organic sulphur in low-rank coal chars after pyrolysis at temperature as high as 900°C. From the results of his own work with low-rank Lochiel coal and the reported works carried by other workers, Manzoori suggests formation during pyrolysis of complex compounds involving sulphur and certain organically-bound inorganic elements. Sodium and calcium sulphide have been identified as the main products.

Sugawara's et al. (1994) work using fixed bed pyrolyser showed that the release rate of sulphur during coal pyrolysis was higher with increased heating rate. They tested a bituminous coal with near even content of organic and inorganic sulphur content. The optimum desulphurisation temperature range they found was 500°C to 700°C.

2.3.1.1.2 Chlorine transformations

Gibb and Angus (1983) concluded that British coals give off 97% of its chlorine as HCl in oxygen-free nitrogen (pyrolysis) environment at 258°C. Shao et al. (1994) found that more than 95% of chlorine in USA bituminous Illinois coal is evolved as HCl between 300°C and 600°C during pyrolysis.

Mulholland et al. (1993) found studying the effects of organic chlorine on the composition and distribution of pyrolysis tar products that chlorine preferentially incorporates into HCl due to relative instability of carbon-chlorine and chlorine-chlorine bonds at high temperatures.

Kosminski and Manzoori (1990) report from their experiments with high-salt content South Australian Bowmans lignite that under carbonisation conditions sodium and chlorine are released from coal disproportionately. The loss of chlorine started at below 400°C and that of sodium started above 750°C and increased with temperature probably due to direct vaporisation of sodium chloride. The disproportionate release of sodium and chlorine was considered to be due to sodium chloride dissociation in coal and/or reactions of sodium chloride with other species.

2.3.1.1.3 Transformations of the minerals

Minerals on heating will be dried, dehydrated, decomposed or transformed into new minerals. The degree of change will depend on type of a mineral, exposure time but mainly on temperature conditions. Investigations on effect of heating on minerals structures and behaviour have been for many years investigated by numerous workers (Mitchell and Gluskoter, 1976; Warne, 1983). Comprehensive summaries are given by Wall et al (1979) and Warne (1983).

Clays will start losing their water of hydration at temperatures above 300°C. This process ends below 600°C. At higher temperatures clays may decompose or various new species will form. The dehydration products will be a new form of arrangement of aluminosilicate structures. Kaolinite will transform to meta-kaolinite, to be transformed to mullite at high temperatures. Illite, montmorillonite transform to amorphous aluminosilicates.

Sulphides, such as pyrite, will decompose with loss of sulphur, new sulphides formed may transform further into oxides. Decomposition of pyrite takes place between 500 and 550°C and pyrrhotite is formed (Cleye et al., 1984). Carbonates will lose carbon dioxide and become oxides at temperatures approaching 500°C. Sulphates will decompose to oxides and sulphur dioxide at temperatures higher than 1200°C. Quartz remains unchanged in the temperature regions concerned.

2.3.1.2 Transformations during Combustion

During combustion most of inorganics will undergo further transformations to those happening to them during pyrolysis. These will be reactions with gaseous phases such as SO₂, with minerals present in coal, and reactions with products of transformations of other inorganics.

Fine distribution of inorganics in coal leads them to being more reactive than minerals, which usually occur in larger grain forms (Falcone and Schobert, 1986). The reactions by transformed coal inorganics with minerals or products of their decomposition will result in formation of variety of aluminosilicates, silicates. The extent of these reactions will mostly depend on temperature conditions. More complex will be products of such reaction in pulverized coal boilers, where temperatures are usually in excess of 1200°C.

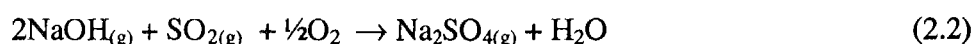
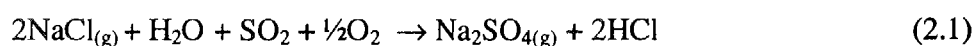
Less complex products may result from fluid bed combustors, in which burning particles reach temperatures below 1100°C. Many minerals may not react with inorganics due to too low temperatures. Quartz or aluminosilicates present originally in coal often are unchanged chemically in fluid bed combustor ashes.

2.3.1.2.1 Sodium reaction with sulphur oxides

Sodium and calcium sulphates form during combustion of coal containing sulphur and organically bound sodium, calcium, magnesium, aluminium. The last two elements may form their individual or combined (spinel, $MgAl_2O_4$) oxides, as established by Domazetis (1985).

These findings have been confirmed by work of Manzoori (1990). Manzoori (1990) reports that molten sodium-calcium sulphates matrix had formed on the surface of high-sulphur and high-sodium low-rank coal particles burnt in a fluidised bed environment. The matrix embedded solid oxides and aluminates of calcium and magnesium.

Behaviour and reactions of sodium species is the major concern in utilisation of many low-rank coals in pf-fired boilers. Sodium sulphate is found as a cause of fouling of heat transfer surfaces and sodium silicates as cause for ash agglomeration. Particularly vaporised sodium species such as chlorides, sulphates, hydroxides may react with silica to form silicates or sulphates. Many researchers showed substantial evidence for formation of sodium sulphate from vaporised sodium species (Durie and Swain, 1971, Raask, 1985, Lindner, 1988). Lindner (1988) reviews mechanisms of such reactions, mainly for higher temperature conditions prevailing in pf boilers. Halstead and Raask (1969) propose the following reactions:



Lindner (1988) shows that during combustion of coal with high sulphur content, in high temperatures prevailing in pf-fired boilers sodium silicates will be dominant species. Sodium sulphate will form at lower temperatures prevailing in fluidised beds (Manzoori, 1990).

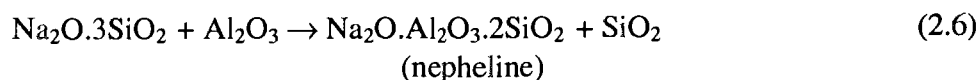
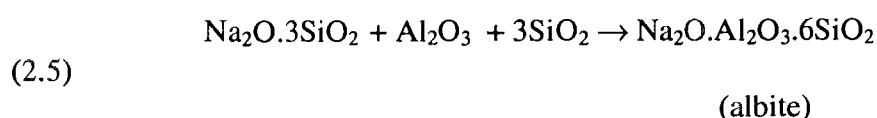
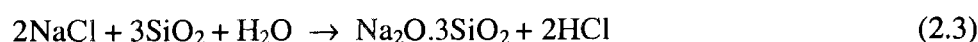
2.3.1.2.2 Sodium reaction with silica and aluminosilicates

The most research over the years has been devoted to the research of coal combustion and ash formation during combustion process. What has been learnt about ash formation during combustion may be helpful in determining what is happening during coal gasification.

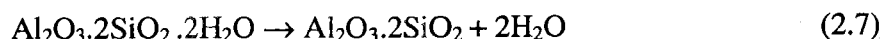
Many researchers devoted their work particularly to establishing reactions between sodium species and silica and aluminosilicates to find ways for the removal of sodium or other alkali from gas streams from various types of combustors and gasifiers.

Studying corrosion inhibitors Nelson and Lisle (1965) established that kaolin reacted with alkali sulphates at 600°C when mixed together in a fixed bed. Reaction between kaolin and sodium sulphate has also been described earlier by Niles and Siegmund (1963).

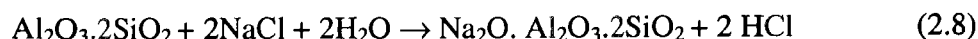
Wall et al. (1975) suggest using clays to absorb sodium into sodium aluminosilicates and silicates during fluidised bed combustion of salty sludges to avoid formation of melting at low temperatures sodium salts or their eutectics: NaCl-Na₂CO₃, NaCl-Na₂SO₄, Na₂CO₃-Na₂SO₄. Chemical reactions involved in the fixation of alkali chlorides by aluminium silicate clays have been well established according to Wall et al. (1975). Offering fluidised bed combustion technology to burn salty sludges Wall et al. propose reactions, which will take place between NaCl or Na₂SO₄ and silica, aluminosilicates and metal oxides leading to formation of higher melting silicates and aluminosilicates than NaCl-Na₂CO₃ eutectic, which melts at 633°C.



For reaction with kaolin clay, the clay first dehydrates:



and then reacts with NaCl and H₂O:



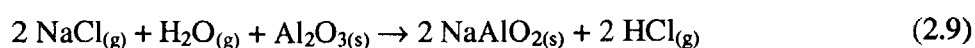
Lee and Johnson (1980) testing sorption by six different sorbents of NaCl, KCl and K₂SO₄ vapours from air stream or simulated dry flue gas at temperatures of 800°C and 880°C showed that:

- diatomaceous earth absorbed alkali vapours by forming silicates that were water-insoluble; the rate of reaction of NaCl with diatomaceous earth in their experiments increased with temperature. Diatomaceous earth is a sedimentary rock of marine or lacustrine deposition; chemically it consists primarily of silicon dioxide and various amounts of impurities such as clays, carbonaceous matter, iron oxides, etc.
- kaolinite based clays retained NaCl vapours through chemical reactions to form water-insoluble products such as sodium aluminium silicates.

Lee and Johnson (1980) also concluded that for both, activated bauxite and diatomaceous earth sorbents the rate of NaCl capture is not mass transfer controlled, but it is controlled by either the diffusion of NaCl vapour through internal pores, the adsorption of NaCl vapour on the active sites of the sorbent, or by the chemical reaction.

Lee and Carls (1990) studied removal of sodium vapours from flue gas. Analysis of that flue gas from a pressurised fluidised bed combustor burning Beulah lignite from North Dakota showed that 0.24% of sodium leaving the bed operating at 800-875°C and 9.2 bar abs. with 1 m/s fluidising velocity was in the vapour state. They conducted sorption tests using activated bauxite and diatomaceous earth as in the former test involving Lee (Lee and Johnson, 1980). Lee and Carls found that the bauxite they used was twice as effective sorbent as the diatomaceous earth. Alkali captured by bauxite was completely water soluble. Diatomaceous earth captured and reacted with sodium vapours present in the flue gas to form primarily water-insoluble silicates.

In earlier works Lee et al. (1985) reported that in the absence of water vapour activated bauxite captures NaCl vapour through both physical adsorption and by chemical fixation by clay minerals present in bauxite. Adsorbed alkali was removable by water leaching, reacted formed water-insoluble products. However in the presence of water the NaCl vapour sorption capacity of bauxite was found to be significantly increased as compared with that observed for dry gas environment. In addition to the chemical fixation of NaCl vapour by clay minerals, NaCl vapour was found to form water soluble sodium aluminate compounds, with the proposed overall reaction:

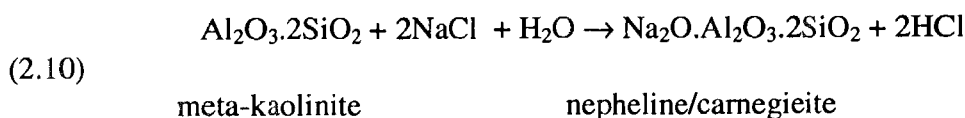


Luthra and LeBlanc (1984), who found that sorption on Al_2O_3 conducted in argon atmosphere of NaCl and KCl at 800-900°C was a physical adsorption process and that no reaction of sodium with alumina was observed.

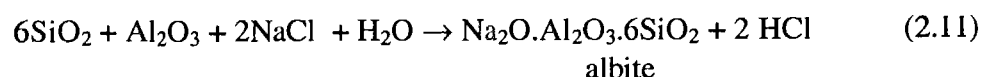
Effective reduction of sodium vapour in pressurised fluidised bed combustor by addition of clay to the combustion zone is also reported in literature quoted by Lee and Johnson (1980).

Punjak and Shadman (1988) studying the kinetics and mechanism of sorption on kaolinite of NaCl vapour under both nitrogen and simulated flue gas atmospheres at 800°C found that kaolinite captured approximately five times more alkali in the simulated flue gas environment. Under N_2 atmosphere, both chlorine and sodium were retained, while only sodium was retained under simulated flue gas conditions. They concluded that overall process was influenced by chemical reaction and diffusion of alkali in the sorbent.

Similar results were reported by Punjak et al. (1989) reporting works on alkali sorption at 800°C using bauxite, kaolinite and emathlite, material consisting of alpha quartz, cristobalite and kaolinite. They established that kaolinite forms with removed alkalis the nepheline and carnegieite, which are sodium aluminosilicate polymorphs with the chemical formula $\text{Na}_2\text{O}.\text{Al}_2\text{O}_3.2\text{SiO}_2$ and with a melting point of about 1600°C. The following reaction scheme between meta-kaolinite, the dehydration product of kaolinite and sodium chloride has been proposed:



The product of alkali sorption with emathlite had a melting point of approximately 1100°C and was found to be albite $\text{Na}_2\text{O}.\text{Al}_2\text{O}_3.6\text{SiO}_2$, which overall formation reaction has been proposed by Punjak et al. as follow:



Punjak et al. (1989) concluded than, that bauxite and kaolinite are suitable for *in situ* removal of alkali and proposed a sorption model, which agreed with their experimental

data, to describe the simultaneous physical and chemical processes that occur during alkali removal by sorbent particles.

Uberoi et al. (1990) report their work on sorption of NaCl at the temperature of 750, 800 and 845°C using the same sorbents as reported by Punjak et al. (1989). Uberoi et al. observed that carnegieite formed at 750°C, with nepheline dominating the kaolinite sorption reaction products at higher tested temperatures. Albite formed from NaCl sorption on emathlite at 800°C temperature was found to exist as a glassy phase. Uberoi et al. (1990) suggest that under the simulated flue gas atmospheres sodium is captured by these sorbents through adsorption followed by chemical reaction.

Sodium solubility decreased considerably when heated in air as NaCl/kaolinite and Na₂SO₄/kaolinite mixtures as reported by Botting et al. (1989). At all temperatures tested the extent of reaction of NaCl was greater than Na₂SO₄ and reactions occurred at temperatures below the sodium salts melting points and resulted in formation of insoluble sodium aluminosilicates.

The NaCl present in coal can also react with H₂ and with silica as proposed by Halstead and Raask (1969):



Falcon and Schobert (1986) observed the formation of nepheline Na₂O.Al₂O₃.2SiO₂ for a 1:1 molar mixture of sodium acetate (chosen to simulate the carboxylate-bound sodium cations in low-rank coals) with kaolinite ashed in oxidising atmosphere at 800°C. They generally found, that organically-bound sodium and calcium were more reactive in producing new mineral species with pre-existing minerals than cations bound in mineral forms.

2.3.1.2.3 Chlorine

Chlorine present in coal during combustion is transformed basically into hydrogen chloride (Boll and Patel, 1961; Hodges and Richards, 1989). Works by Ershov et al. (1992) on formation of hydrogen chloride in a flame showed that transition of chlorine into gaseous

phase exceeded the rate of burnout of coal particles. Ershov et al. also found that CaO added to the coal reacts with HCl present in the gas phase and that this reaction is favoured at temperatures below 1000°C. They further established that HCl formation in the gases is qualitatively independent of the nature, reducing or oxidising, of the medium in which the pf coal is burnt. Ershov et al. concluded that at such stoichiometric conditions, the HCl concentration rises due to increase in the quantity of fuel burnt in unit volume of oxidant.

Chlorine may leave coal also in form of sodium chloride. Lee et al. (1993) studying alkali vapour content in flue gas from PFBC involving Illinois high-sulphur coals, concluded that sodium-vapour emission could be a result of a direct vaporisation of NaCl present in coal.

Disproportionate, to that of sodium, release of chlorine during combustion in a fluidised bed environment is reported by Manzoori (1990). Suggestion of sodium chloride reaction with other compounds is given as a reason for this disproportionate release. Earlier Brinsmead and Kear (1956) concluded, from burning sodium chloride and carbon mixtures, that other phenomena than a straight vaporisation of sodium chloride had to be involved, particularly at low to medium temperatures, that is below 1000°C.

2.3.1.2.4 Calcium, magnesium and iron

Calcium being organically-bound in coal and forming during pyrolysis carbonate or oxide during combustion will predominantly form calcium sulphate by reacting with sulphur dioxide released during the combustion process. Calcium originating from lime or calcite, may remain as oxide or it also may react with aluminosilicates or silica, and also with product of sodium reactions with the same (Wall et al., 1975).

Magnesium in combustion mostly will finish as magnesium oxide, identified in combustion ashes as periclase, and as magnesium aluminate - spinel (Manzoori, 1990; Readett and Quast, 1987).

Iron during combustion forms mostly oxides: magnetite and hematite, with magnesium or aluminium oxide it often forms oxides of spinel structure. Iron also forms silicates and aluminosilicate, usually in direct reactions of iron oxides silica and clay minerals or with already formed other alkali or alkali earth silicates and aluminosilicates.

2.3.1.3 Transformations during Gasification

The behaviour of the coal inorganic matter in fluidised bed gasifiers may be substantially different from the behaviour of such matter in fluidised bed combustion systems. Coal introduced into a gasifier undergoes a sequence of physico-chemical transformations: drying, devolatilisation and combustion/gasification of the residual char. The extent of each of these processes will influence transformations, reactions and behaviour of coal inorganic matter.

In gasification process oxygen supply is insufficient for full carbon combustion to form CO_2 . Instead carbon monoxide CO is wanted as the main product of coal conversion. Reactions of a char with steam also lead to formation of carbon monoxide and hydrogen. This creates reducing atmosphere in the reactor, consequently not fully oxidised forms of inorganic elements may form. Elements able to exist in various valency levels may tend to form the least oxidised states. The reduction of some inorganic compounds formed in the process or introduced into the reactor may take place.

As during combustion, the devolatilisation process will also be the first step during gasification. This will lead to coal decomposition. That is the decomposition of carboxylic groups containing inorganics, and reactions involving inorganic matter. Devolatilisation may last longer than during combustion. This may be influenced particularly by particle temperature expected not to be much higher than bed temperature.

Fluidised bed gasification is characterised by lower particle temperatures, longer residence times than during combustion, and what is more significant, low partial pressures of oxygen. These parameters amongst other effects may cause formation of more reduced chemical forms of ash components and may influence physical forms of coal ash differently than seen in combustion systems. They may cause the effect of devolatilisation on the inorganic matter behaviour in coal gasification process be more pronounced than in combustion process.

During fluidised bed combustion volatiles are released very quickly. The devolatilisation time depends on the bed temperature, type of coal and the particle size. The

devolatilisation times are 20 to 400 seconds for lignite particle of size 5 to 35 mm (Jia et al., 1993). Combustion times also depend on coal type and particle size, and will be much longer than devolatilisation time; a 1 mm particle will burn for about 200 seconds (Davidson, 1992). Gasification of such a particle may take yet much longer as gasification reactions, those of char with steam or carbon dioxide will be slower than reactions with oxygen. Particularly, char - carbon dioxide reaction is much slower than char - steam reaction (Shakaryan et al., 1989; Davidson, 1992). The rates of those reactions depend on a number of parameters such as bed temperature, particle size, type of coal.

Consequently the longer char reaction times may influence the behaviour of inorganic matter originating from carboxylic groups in coal by causing different degree of aggregation of resultant products such as oxides or carbonates (Huggins et al., 1988a).

Gururajan et al. (1991) concluded from studying coal gasification work results by others, that the results in pilot-scale gasifiers of the carbon conversion and product gas yields are mainly determined by the fast rate of devolatilisation of coal, volatiles combustion/decomposition and char combustion, rather than by the slow rate of char gasification reactions. They state that char combustion is very rapid compared to the steam or carbon dioxide gasification reaction.

The following paragraphs highlight reactions and the products formed with participation of the most common coal inorganic matter and coal minerals during gasification of coal.

2.3.1.3.1 Sodium and potassium reactions

Behaviour of both sodium species and potassium species during gasification will depend on their original form in coal, temperature conditions and distribution. Depending on those conditions the species may be in a solid, liquid or a gaseous state. And this will influence very considerably their behaviour and tendency to react with other species.

Mojtahedi et al. (1989) report on gasification tests at pressurised fluidised bed gasifier test facility operating at 830°C and up to 10 bar pressure gasifying high-alkali, high-chlorine content peat. Sodium and potassium were found in high concentration in vapour species in the gas leaving the gasifier. The total concentrations of the alkali metals in the product gas

were found to be at least an order of magnitude higher than allowable in a gas turbine, but not quite as high as the thermodynamic equilibrium calculations would suggest (Mojtahedi and Backman, 1989a, 1989b).

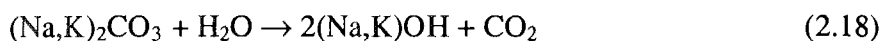
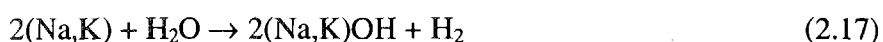
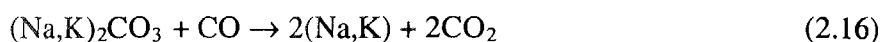
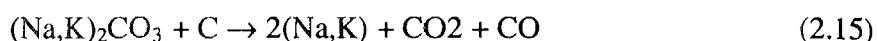
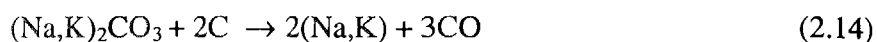
Studying sorbents for sodium compounds vapours Bachovin et al. (1986) found emathlite to be a good sorbent for the capture of NaCl in pressurised gasification systems. Bachovin et al. concluded that that capture was due to a chemical reaction, controlled by diffusion of alkali through a sodium rich glass layer around the emathlite particles. Bachovin et al. also, the base of thermodynamic considerations, predicted the formation of sodium aluminosilicate albite.

2.3.1.3.2 Alkali catalysed gasification

It has been well established that alkali and alkali earth metals catalyse coal gasification reactions as numerous studies have been conducted on the subject for various types of coal (McKee et al., 1983, 1985; Matsukata et al., 1992; Meijer et al., 1994; Sams et al., 1985; Spiro et al., 1983; Suzuki et al.; 1989, Takarada et al., 1986, 1987, 1991; Yamashita et al., 1991). These catalytic effects may contribute to an improvement in the rate of coal gasification and could be used to lower the reaction temperatures by 100-200°C according to Douchanov and Angelova (1983).

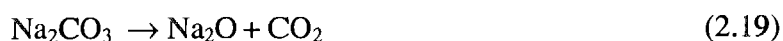
The research on the catalytic effect of alkali and alkali-earth elements led to a better understanding of their molecular distribution within coal matrix. The major sodium compound formed in a gasified coal is believed to be sodium carbonate. This is regardless whether it was sodium chloride, acetate or carbonate used by researches for ion-exchanging onto coal structure. If coal was impregnated only with a sodium salt, chloride or carbonate, these salts remain in their chemical form and aggregate as the surface of the gasified char recedes.

It is suggested that alkali catalytic reactions of char gasification with carbon dioxide or steam may involve principally reduction of sodium carbonate to metallic form, as a part of a possible catalytic mechanism, in reactions as presented below (Mims and Pabst, 1983; Kikuchi et al., 1983; McKee, 1983; Suzuki et al., 1989):



Some of these reactions are happening even at temperatures below 600°C (Suzuki et al., 1989). It may be that as a consequence of these reactions and in the presence of the minerals in coal, liberated alkali elements may react with the coal minerals. McKee et al. (1983) report that the catalytic activity of alkali suffered a progressive loss during a steam gasification of coal due to reaction of the alkali with mineral matter present in the coal.

Wigmans et al. (1983) report that decomposition of Na_2CO_3 in the presence of carbon starts at temperature far below the decomposition temperature of 851°C of the bulk carbonate. They further suggest that during gasification, Na-O-C bonds in sodium carbonate will be broken in the initial stage of gasification, after which sodium becomes active in a redox cycle. This will involve reduction of sodium carbonate to sodium oxide and further to metallic sodium with the release of carbon monoxide.



Oxidation with carbon dioxide may then follow:



The results of above presented studies on catalytic effects of sodium on gasification process allow to follow the transformations of various forms of sodium during gasification. In consequence, of all these above reactions, leading to formation of elemental alkali metals or their respective oxides or hydroxides, may lead to the volatilisation of elemental metal vapour or reactions with the mineral matter such as quartz, clay and shale minerals present in coal.

2.3.1.3.3 Potassium

Huggins et al. (1988b) report on formation of K_2CO_3 from organically-bound potassium during coal char gasification conducted at 420°C.

Sams et al. (1985) concluded from their studies on a catalytic effect of potassium on gasification of coal that the vaporisation of potassium from K_2CO_3 catalyst under reducing atmosphere was faster than that under oxidising conditions. Vaporisation of potassium occurred above $700^\circ C$, which is below the melting point of K_2CO_3 catalyst of $891^\circ C$. It is concluded that a reduced form of a potassium-carbon complex is formed, which then vaporises readily. This vaporisation was faster in an inert atmosphere of nitrogen than in gasification with carbon dioxide.

Kikuchi et al. (1983) report formation of K_2S and K_2O from K_2SO_4 in H_2 or CO stream, respectively, in temperature about $840^\circ C$. They report reduction of this sulphate to K_2S by graphite in a stream of helium.

2.3.1.3.4 Chlorine

Hydrogen chloride is believed to be the basic chloride product during devolatilisation of coal (Shao et al., 1994; Lang, 1986; Bjorkman and Stromberg, 1997).

Also, as chlorine is most often believed to be associated in low-rank coals with sodium, sodium chloride has been identified as another basic chlorine compound to be present in a gasifier. Sodium chloride may evaporate in a fluidised bed gasifier and then condense on heat transfer surfaces or on the surface of particles downstream of the process. Sodium chloride deposits were found during a pilot plant testing of a high-sodium, high-chlorine South Australian Bowmans coal in Rheinbraun's HTW process (Bellin et al., 1987)

Manzoori and Agarwal (1992) report disproportionate release of sodium and chlorine from coal containing sodium chloride during pyrolysis process. Disproportionate release of sodium and chlorine during gasification of South Australian lignites containing sodium chloride is reported by Kosminski and Manzoori (1990).

Chlorine was also found in form of ammonium chloride, as reported by Kosminski and Manzoori (1990), in the deposits from the HTW plant collected from those parts of the plant, where gas temperature was below $300^\circ C$. Reaction between ammonia, formed from the fuel nitrogen and the HCl supposed to lead to the formation of ammonium chloride.

2.3.1.3.5 Sulphur

Gaseous species are the major products of transformations of both organic and inorganic sulphur compounds. They are H₂S, CS₂, COS, with the highest concentrations of H₂S (Attar, 1978; Ma et al, 1989). Their relative concentrations depend on oxygen to coal ratio, and steam to oxygen ratio. Higher oxygen to coal ratio promotes formation of SO₂, steam reduces the formation of sulphur dioxide (Price et al., 1983; Highsmith et al., 1985; Nichols et al., 1989). Increased process pressure yields more H₂S and less CS₂ and SO₂ and tends to increase the trapping back of H₂S by char (Nichols et al., 1989).

Hydrogen sulphide H₂S is produced during pyrolysis and in char hydrodesulphurisation and from reaction of sulphur and hydrogen (Attar, 1978). Thiophenes are also major products of coal pyrolysis. They may also form during pyrolysis and gasification due to reaction of sulphur and H₂S with organic molecules (Attar, 1978). This may be a reason for increasing sulphur content in coal char reported by Gryglewicz and Jasienko (1992). Formation of thiophenes may be catalysed by some mineral matter: alumina, silica.

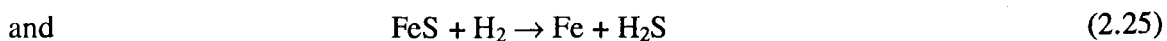
During gasification, inorganic sulphur, mostly present in coal as pyrite, will break down into iron sulphide and elemental sulphur (Attar, 1978):



The rate of this reaction becomes very high between 550 and 600°C (Attar, 1978). Sulphur is released from smaller particles faster than from larger particles (Atogi et al., 1986). Depending on operating conditions, iron sulphide may be in a solid or in a liquid state (Huffman et al., 1981). At lower temperatures reaction with carbon monoxide, mainly during pyrolysis, may also lead to iron sulphide formation (Cleyle et al., 1984):



Attar (1978) also reports that in the presence of many organic compounds, pyrite is reduced to the sulphide at temperatures as low as 250-300°C, which is substantially lower than the temperatures at which it would be reduced in the presence of hydrogen:



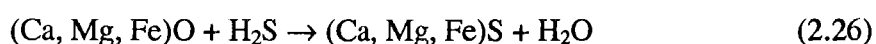
Attar (1978) reports that material balance of the sulphur suggests that reactions between pyrite and organic hydrocarbons lead to the formation of elemental iron at temperatures below 700°C. These reactions will lead than to the formation of iron forms melting at temperature conditions prevailing in the fluidised bed gasifiers.

Telfer (1999) reports formation of calcium sulphide in gasification ash of high-sulphur Bowmans and Lochiel coals. McCarthy (1986) reported the identification of sodium sulphate in gasifier ash, collected at the bottom of the gasifier, in which North Dakota lignite coal was gasified.

2.3.1.3.6 Calcium and magnesium

During gasification initial product of organically-bound calcium and magnesium will be their very dispersed respective oxides (Huffman et al., 1989). It is probable that aggregation of these oxides will take place (Huffman et al., 1989) before some of them are involved in further reactions involving other gaseous, liquid or solid state compounds.

According to Attar (1978), hydrogen sulphide reacts very rapidly with calcium, magnesium and iron oxides and carbonates to form corresponding sulphides. Under reducing conditions prevailing in fluidised bed gasifiers the reaction of calcium and sulphur compounds is expected to result in the formation of calcium sulphide CaS. Thermodynamically the most favoured is reaction of H₂S with CaO, CaCO₃, FeO and FeCO₃ in the temperature range prevailing in fluidised bed gasification (Attar, 1978):



Reaction of calcium carbonate with H₂S stops after a while at temperatures below 600°C because the CaS formed is not permeable to CO₂. The reaction of H₂S with MgCO₃ is not favoured below 570°C. Kinetically the reactions of calcium and magnesium oxides with H₂S at 570°C are about five times faster than those involving carbonates.

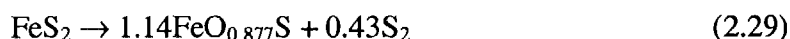
Calcium and magnesium chlorides were found in a fluidised bed gasifier deposits on the down-stream plant walls of HTW gasification plant during a test with a Bowmans coal (Kosminski and Manzoori, 1990).

Huffman et al. (1981) report that in a reducing atmosphere calcium reacts with sulphurous gases to form CaS. Jensen et al. (1982) report that a significant sulphur capture may occur during a gasification even at high temperatures through the conversion of CaO to CaS within the char due to the pore diffusion effects, even though CaS formation is not feasible at bulk gas conditions.

Considering thermodynamic aspects of regenerating CaO from calcium sulphate using CO Hayhurst and Tucker (1991) calculated, that at high CO concentrations formation of CaS will be favoured. Such situation is applicable to gasifier atmosphere.

2.3.1.3.7 Iron

Decomposition of pyrite and formation of iron sulphide and pyrrhotite will happen in a fluidised bed gasifier already during coal devolatilisation (Cleyle et al., 1984).



The second reaction, as suggested by Srinivasachar and Boni (1989), is endothermic and happens at rapid rate once pyrite reaches its average 600°C dissociation temperature. Products of the above two reactions were identified by Huffman and Huggins (1978) studying the products of high-temperature (950-1100°C) carbonisation of coal. These sulphides may oxidise to ferrous oxide FeO.

Studies by Hinckley et al. (1980), using iron Mössbauer spectroscopy on a selection of ash samples coming from a Lurgi gasification process, showed that 40% or more of iron was present in the divalent form in molten silicates form, with the remainder present in form of oxides.

Iron transformations during gasification can lead to the formation in char and in ash of five or six different iron-bearing compounds in three different oxidation states, according to Huffman and Huggins (1986). Example gasified char contained iron metal, iron sulphide (principally FeS), fayalite (Fe_2SiO_4), magnetite (Fe_3O_4), hematite (Fe_2O_3), glass, wüstite (FeO) and other minor phases.

Mason and Patel (1980) report that in ash-agglomerating U-GAS® fluidised bed gasifiers agglomerates are produced from relatively low-melting products of reaction of iron with the siliceous components produced from clays and quartz. Iron comes from pyrite (FeS_2), which is decomposed to iron sulphide FeS and other iron-sulphur species, and is further oxidised to FeO , which reacts with silicates. This oxidation of iron-sulphur species is required for formation of oxides, the presence of which is a prerequisite for formation of the low-melting silicate mixture and for agglomerate formation. The matrix of formed agglomerates consisted predominantly of ferrous aluminosilicates of variable composition together with smaller amounts of other oxides. Formation of agglomerates was reported to occur only in the vicinity of the oxygen reaction region, where the temperatures were higher than in other regions of the bed.

From other studies Mason et al. (1982) concluded that a temperature substantially higher than 1035°C is required for these ferrous aluminosilicate agglomerates to form. Later Mason (1992) reported that in the U-GAS® ash-agglomerating fluidised bed gasifiers liquid iron-sulphur species derived from pyrite were responsible for the unwanted formation of ash agglomerates, the formation which happened at the too low temperature. Mason further reports that formation of liquid iron-sulphur species in the gasifier or in the inert atmosphere cannot be explained on the basis of equilibrium considerations. Instead he suggests a kinetic explanation, based on increased concentration of iron in the exterior regions of the decomposing pyrite particle, as sulphur is removed from their surface.

2.3.1.3.8 Minerals

Behaviour of minerals in reducing environments in temperatures up to 1000°C , or even above it, relates well to fluidised bed gasification process. There is evidence that during gasification minerals exhibit different physical behaviour: melting, volatilisation or crystallisation, than during combustion (Huffman and Huggins, 1986). Minerals present in coal may in gasification environment be in form of liquid, and reactions in liquid-liquid state or liquid-solid state may take place at the temperature conditions, expected in combustion environment for solid-solid state reactions.

High temperature reactions of minerals present in US Eastern coals are schematically illustrated after Huffman and Huggins (1986) in a schematic diagram shown in Figure 2.

That diagram shows results of both chemical and physical transformations of coal minerals. There are indications that iron oxide - wüstite may react with aluminosilicates to form glass phases already at temperatures below 900°C.

Detailed mineralogical studies of ashes of the same lignite gasified in three different gasifiers using grain picking, size separation, magnetic enrichment, dissolution in water and other strategies were used by McCarthy (1986). This allowed McCarthy to identify at least twenty crystalline phases in each specimen. The ashes were from gasifiers with maximum temperature in the 1100-1250°C. Despite this and other operating condition differences, like gasification with air or oxygen, at atmospheric or increased pressure, all of the ashes had the same basic crystalline phase assemblage: silicates and aluminosilicate (calcium silicates, melilite, nepheline and solidate structure phase, oxides (ferrite spinel, hematite and periclase), calcite and residual lignite minerals (quartz, plagioclase).

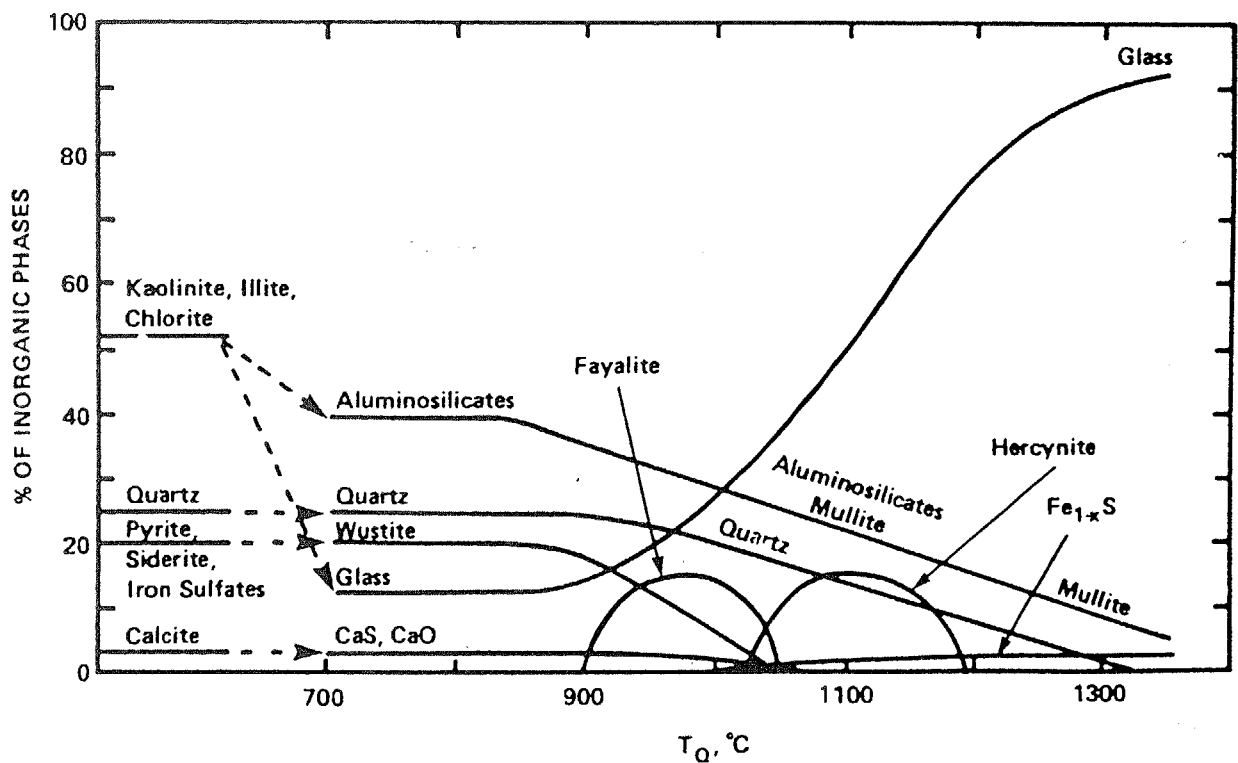


Figure 2.2 Schematic diagram illustrating high-temperature reactions for minerals in an USA Eastern-type coal under reducing conditions (after Huffman and Huggins, 1986).

Douchanov et al. (1992) impregnated coal char separately with K_2CO_3 and Na_2CO_3 and found that at temperature reduced to 850°C no agglomeration was happening. Conducting detailed mineralogical ash examinations they found that these additives formed feldspars,

sanidine ($K_2O \cdot Al_2O_3 \cdot 2SiO_2$) and albite ($Na_2O \cdot Al_2O_3 \cdot 6SiO_2$) respectively, likely due to reaction with kaolinite present in coal. Addition of these carbonate additives also caused more than 50% increase of retention of sulphur in the gasifier ash. When no additives were used kaolinite transformed to mullite. Fe_2O_3 was reduced to Fe_3O_4 during gasification of char with or without additives.

The role of kaolinite in reduction and formation of deposits has been studied for many processes. Spiro et al. (1990) report that addition of kaolinite to a molten slag shifted the composition of the melt from the anorthite phase field into the mullite phase field being characteristic for higher melting temperature.

2.3.1.4 HTW gasification process experience

First significant experience with gasification of high-sodium coal was that from gasifying a South Australian Bowmans coal in a non-agglomerating gasification process. Bowmans coal is characteristic of high content of sodium, chlorine and sulphur and also of high quartz content (Lindner et al., 1988; Readett, 1984).

A preliminary technology evaluation indicated, that non-slagging and non-agglomerating fluidised bed gasification may offer potential solution to the known problems associated with alkali in lignites. The reason being, amongst others, that in the fluidised bed gasification low and relatively uniform bed temperature maintained below the ash agglomeration temperature may prevent clinker formation and subsequent defluidisation of the bed. Consequently, the High Temperature Winkler (HTW) process was selected for detailed investigation. Tests were carried out in the 1.2 tonnes/hour HTW pilot plant owned and operated by Rheinbraun AG, and located at Frechen, Germany. Detailed analyses of the results of those HTW gasification tests are given by Bellin et al. (1987) and by Kosminski and Manzoori (1990).

The pilot plant comprised coal handling equipment, a gasifier, two cyclones and a product gas cooler. Oxidant and steam were injected to the gasifier at various levels. For gasification of lignites, the fluid bed normally operated in the range 700 to 800°C and the entrained zone in the range 900°C to 1000°C. The gasifier was equipped with a quench system prior to the primary cyclone to reduce the product gas temperature to about 850°C

and that supposed to prevent fused ash leaving the gasifier and entering the cyclone. After the cyclones, the product gas was cooled in heat exchangers to about 250°C.

During Bowmans coal gasification tests, the coal ash formed large fused agglomerates in the gasifier and deposits on the gasifier walls. Deposits also formed on cyclone walls and in the gas cooler. The agglomerates were falling with the most of the ash to the bottom of the gasifier.

Chemical composition of ash collected in the gasifier showed accumulation in this ash of coal original minerals, mostly quartz, and formation of quartz based glassy silicates. Sodium silicates were prevailing in the matrix of the agglomerates, with sodium oxide content being about 20% of the matrix content. Fine, 10 micron or more in size, and colloidal silica uniformly distributed in coal was suggested by Kosminski and Manzoori (1990) as participating in the formation of the silicates. Sodium aluminosilicates were also reported as part of agglomerates and their matrix.

Silicates of iron, magnesium and calcium were also present in agglomerate molten matrix and also in crystalline forms in the ash. Organically bound calcium, magnesium, sodium and iron are suggested to participate in their formation of those silicates.

Sodium chloride was found to be the basic component of deposits formed in the downstream plant. Chlorides of iron, magnesium and calcium were also suggested as part of these deposits as chlorine content in deposits was exceeding that of stoichiometrically corresponding content of the sodium. Fused alkali earth silicates were also reported by Kosminski and Manzoori (1990) as a part of the deposits. Ammonium chloride was a significant contributor to deposits in the coolest part of the plant gas heat exchangers.

Various mineral forms were identified in gasifier ash and in some deposits but mostly in the fine ash collected in the gasifier cyclone. They included iron and calcium sulphides, magnesium oxide, magnesium aluminate - spinel, iron aluminate - hercynite, iron magnesium silicate - ringwoodite, sodium aluminosilicates, both nepheline and carnegieite.

2.3.1.5 Laboratory gasification experiments

The results of HTW gasification tests with Bowmans coal led to the conclusion that better basic knowledge is needed to understand coal ash behaviour. Coal gasification laboratory studies based on fixed bed gasification were set up. Results of this study were reported by Kosminski and Manzoori (1990). Those studies confirmed chemistry of the ash formed during gasification formation Bowmans coal in the HTW pilot plant. Under gasification conditions sodium present in coal as inorganic salts and inorganics would form sodium silicates, aluminosilicates, carbonates, chlorides and sulphates, which could enhance formation of ash agglomerates and deposits.

During the experiments sodium loss from the char was observed. More sodium was lost during gasification than during coal pyrolysis, particularly at higher temperature. Kosminski and Manzoori (1990) report that sodium vaporisation may be reduced by gasification of coal with steam and by gasification of coal with high silica content.

Kosminski and Manzoori (1990) observed that ash formed not only on the surface of char grains but also evidently inside the char particles. Microscopic analysis, using electron microprobe analyser, of residual chars from carbon dioxide or steam gasification experiments allowed for identification of areas of very high concentration of sodium, which could correspond to sodium oxide, hydroxide, carbonate or even metallic sodium present within those chars. Crystallisation of sodium chloride was also taking place inside char particles. Char samples from gasification tests carried at the temperature as high as 950°C showed content of crystalline sodium chloride.

Rims of fused sodium silicates were formed around silica grains inside the char. It was established that formation of sodium silicates was particularly enhanced under steam gasification. Such rims also formed when coal was exposed to carbon monoxide atmosphere. Composition of those silicates corresponded to sodium disilicate $\text{Na}_2\text{Si}_2\text{O}_5$ and sodium metasilicate Na_2SiO_3 .

Alkali metals also formed silicates. Organically-bound calcium was engaged in formation of calcium silicates, calcium magnesium silicates and sodium calcium silicates.

2.3.1.6 Thermodynamic calculations

Various researchers have used thermodynamic calculations to predict formation from inorganic matter present in coal of particular phases during a process of combustion and gasification of coal. Such predictions could help to understand ash behaviour and also help to reduce experimental work to define coal ash behaviour.

Wibberley and Wall (1982) report results of thermodynamic calculations for equilibrium conditions of burning coal. Part of the results relate to ash formation in reducing atmosphere. For high-sodium and high-chlorine coal for a lower temperature range (750-850°C) Wibberley and Wall showed high sodium sulphate content and high sodium chloride and sodium silicate presence in ash and an absence of sodium sulphate at higher temperatures (850-1000°C). Wibberley and Wall concluded that alkali silicate layer formation on the silica or ash grains would depend on the rate of diffusion of the sodium into the particles, so the real sodium distribution in practice will likely see more sodium chloride than the calculated amount.

Results of thermodynamic calculations quoted by Lee and Johnson (1980) indicate that gaseous NaCl is the major sodium carrier in the flue gas of a fluidised bed combustor burning coal with NaCl being principal form of sodium.

Scandrett and Clift (1984) examined some of the thermodynamic considerations involved in removing alkali salts from hot gases. Scandrett and Clift state that in a reducing environment of a gasifier the volatile species should exist as vapour, mainly chlorides. In combustion systems with sulphur present, alkali will condense as sulphates in temperatures prevailing in fluidised bed combustor. Thermodynamic calculations by these researchers confirmed work by Lee and Johnson (1980), that aluminosilicates are potentially attractive 'getters' for alkali vapours, but suggested that equilibrium constraints require the reaction to be carried out below about 930°C.

A thermodynamic study by John (1986) on slag/deposit/gas equilibrium in a coal gasifier for a variety of conditions showed, that in a temperature range characteristic for fluidised bed gasifier, volatilisation of some metal sulphides: PbS and ZnS may cause ash deposition. John also showed that low temperature deposition of NH₄Cl would be possible

if NH_3 concentration were well above temperature equilibrium values. Formation of NH_4Cl would also be favoured with high HCl concentrations.

Mojtahedi and Backman (1989a, 1989b) conducted extensive thermodynamic equilibrium calculations for combustion and gasification conditions involving high-alkali and high-chlorine content peat. Mojtahedi and Backman showed that the concentration of the vapour-phase alkali metal compounds in the flue gas was strongly dependent on the operating temperature and pressure conditions. This concentration increases sharply with temperature but decreases markedly only with an increase in the total pressure of the system in the temperature range of 600-1100°C. According to Mojtahedi and Backman's results a greater percentage of alkali metals would be released in the vapour phase during gasification than during combustion. The dominant species in gaseous state during gasification for both, sodium and potassium will be chlorides and hydroxides. Whereas in combustion conditions the condensed phase will consist almost entirely of sulphates, under gasification conditions condensed chlorides and carbonates will prevail. Mojtahedi and Backman's results show, that sulphur concentrations exert no influence on alkali forms under gasification conditions.

Kurkela et al. (1990) in their assessment of results of a pressurised fluidised bed gasifier gasifying peat state, that release of alkali metals was comparable with theoretically predicted values. The plant bed was operated at 700 to 800°C with the freeboard temperature of up to 1000°C.

There are some limitations of such thermodynamic calculations and they relate to data used for calculating the predictions according to Harb et al. (1993). Harb et al. recommend, that results of thermodynamic calculations from models based on the stoichiometric approach be compared to both, experimental results and predictions from other thermodynamic models.

2.3.2 Physical Transformations

It has been indicated earlier in this report that during gasification process inorganics will undergo physical transformations such as drying, dehydration, crystallisation, fusion, coalescence and vaporisation.

2.3.2.1 Mineral salt crystallisation

During drying of a coal, salts dissolved in the coal inherent moisture will go from solution to a solid form. A particle of coal, depending on the size, loses all the moisture before it is heated to 200°C. It is reasonable to expect that salts like sodium chloride will crystallise out. As the solution of sodium chloride in the coal moisture becomes more concentrated during the drying process a consequent growth of detectable crystals may take place. There is however little evidence showing such aggregation or any migration of such sodium chloride within coal structure. The crystals are therefore believed to be very evenly and intimately distributed in dry coal.

2.3.2.2 Melting and sintering

Inorganic species originally present in coal, and those formed from inorganics present in coal, may include various salts characteristic of having relatively low melting point. Many of these salts or minerals may form eutectic mixtures, which may melt at much lower temperature than their individual components. Table 2.2 contains a list of individual inorganic compounds and their eutectics, which are likely to exist in coal ash at some stage of a gasification process.

The data shown in Table 2.2 may however be different, if the measurements were done in other than in air exposure conditions. Song and Kim (1993) report much lower melting temperature for alkali salts and their mixtures when measured in steam atmosphere. For Na_2CO_3 Song and Kim measured melting temperature as 725°C in steam-nitrogen 80-20% molar mixture, against reported in literature standard melting temperature of 851°C measured in pure nitrogen. Huttinger and Minges (1985) report Na_2CO_3 melting temperature as 801°C in 50-50 % steam-argon molar ratio gas.

The melting points of many inorganic species fall in the temperature range characteristic for the operation of fluid bed gasifier. Additionally to obvious salts of common inorganic acids, a large variety of silicates and aluminosilicates may form from silica and clays present in coal and from various forms of sodium, potassium and other elements. Sodium compounds may with silica, such as quartz, form solid solutions with melting points even below 800°C in oxidising conditions. Many of these compounds will form glass. Figure 2.3 shows a phase diagram for compounds of sodium and silicon oxides.

Table 2.2 Melting points of selected inorganic compounds and eutectics that may be found in a fluidised bed gasifier conditions (after Dean, 1985; Levin et al., 1979)

Pure compounds	Melting point, °C	Eutectics	Melting point, °C
CaO	2927	Na ₂ SO ₄ -CaSO ₄	900
Ca ₂ SiO ₄	2130	NaCl-Na ₂ SO ₃	633
CaSO ₄	1400	NaCl-Na ₂ SO ₄	623
CaO.Al ₂ O ₃ .2SiO ₂	1551	Na ₂ SO ₄ -MgSO ₄	670
Na ₂ CO ₃	851	NaCl-CaSO ₄	721
Na ₂ O	1132	NaCl-Na ₂ CO ₃	633
NaOH	322	Na ₂ O-SiO ₂	789
Na ₂ SiO ₃	1089	NaCl-Na ₂ CO ₃ -Na ₂ SO ₄	612
Na ₂ Si ₂ O ₅	874	Na ₂ O-Al ₂ O ₃ -SiO ₂	732, 740, 780
Na ₂ S	950	Na ₂ O.SiO ₂ -Na ₂ SO ₄	635
Na ₂ SO ₄	884		
Na ₂ O.Al ₂ O ₃ .6SiO ₂	1100		
Na ₂ O.Al ₂ O ₃ .2SiO ₂	1270		
NaCl	801		
NaAlO ₂	>1650		
MgFeO ₄	1750		
FeS ₂	1171		
FeS	1195		
Fe _{1-x} S	-		
FeSiO ₃	1140		
FeO	1377		
FeCl ₃	304		
NH ₄ Cl	520		
CaS	2400		
CaCl ₂	772		
MgCl ₂	714		

Formation during combustion and gasification of many compounds, and particularly glasses, from inorganics and minerals are related by researches (Mitchell and Gluskoter, 1976) to the reactions between

- acid oxides: SiO₂, Al₂O₃ and TiO₂ and
- basic oxides: Na₂O, K₂O, CaO, MgO, FeO.

Results of a coal ash fusion temperatures measured in accordance to standard methods are often related to a ratio of these oxides: acid/basic oxide ratio.

Huffman and Huggins (1986) found that formation in the ash of significant amount of molten silicate phases occurred at 200°C to 400°C temperatures below the Initial Deformation Temperature (IDT) and a partial melting was markedly accelerated in

reducing as compared with oxidising conditions. Huffman and Huggins also observed that IDT is not the temperature, at which ash melting begins. The samples they quenched from the IDT consisted primarily of glass.

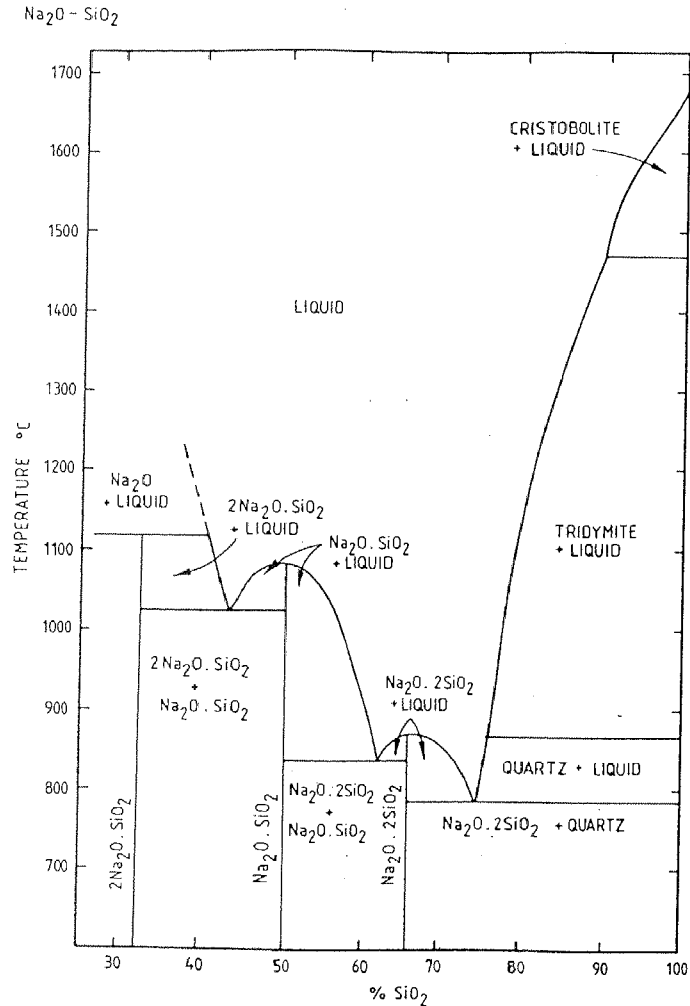


Figure 2.3 Phase diagram for Na₂O.SiO₂ mixtures.

Huggins et al (1981) report that all of the ash fusion temperatures were dependent on ash composition in a manner, which mirrored liquidus curves and not the solidus curves of ternary oxide phase diagrams. They also observed that transformation from the IDT to the Flow Temperature (FT) primarily reflects deformation of a viscous slag and decreasing slag viscosity rather than increasing amounts of molten ash.

Huffman and Huggins (1986) also showed that for those coals samples from reducing atmosphere they have tested, there was a correlation between the variation of the

percentage of the total sample iron content in glass with the parameter $\text{Base} \times \text{SiO}_2$ ($\text{Base} = \% \text{Fe}_2\text{O}_3 + \% \text{CaO} + \% \text{K}_2\text{O} + \% \text{Na}_2\text{O}$). Ashes from coals with value of this factor being below 600 exhibit relatively low deposition in full-scale combustion operation.

Huggins et al. (1981) established that iron rich coal ash was dominated by wüstite and iron-rich ferrites for ashes formed at temperature 700°C to 850°C in reducing environment as the iron minerals, pyrite, siderite, sulphate were converted to wüstite or ferrites. Some molten phases were already observed, but mainly coming from illites. But above 900°C molten silicates were formed by reactions of iron compounds with dehydrated kaolinite and with quartz, and their formation was accelerated by the presence of additional base elements.

Huffman et al. (1981) studied ash-fusion temperatures, and reactions between mineral-derived phases, in reducing and oxidising atmospheres of coal ash for a large number of US bituminous and sub-bituminous coals of widely different mineralogy for ashes prepared in air at 750°C temperature and quenched at various temperatures. There were no significant solid-state reactions between different mineral components during ash preparation. Ash melting in reducing atmospheres was found to be controlled primarily by reactions involving iron-bearing compounds forming glass phases. Significant amounts of melting were associated with the eutectic in the FeS-FeO liquidus curve.

Studying estimation of ash fusion temperatures in reducing atmosphere for seventy coals Lloyd et al. (1993) concluded that a simple chemical analysis, ignoring mineralogical species, might not be expected to be sufficient for the prediction of an ash fusion temperature.

2.3.2.3 Vaporisation of inorganic and minerals

Parts of inorganic species may vaporise at fluidised bed gasification conditions. In gasification conditions, the melting of some compounds may happen at temperatures lower than in combustion (Song and Kim, 1993), and the vaporisation may then take place and a partial pressure of a compound may then be higher for that given temperature than it would be in combustion conditions.

Volatilisation of chlorides of sodium, ammonium chloride and other chlorides in fluidised bed gasification conditions was confirmed by theoretical calculations (Kosminski and Manzoori, 1990). Their gasification experimental results also suggest direct vaporisation of sodium chloride. Sodium chloride may then cause formation of deposits in gasifier, through vapour condensation mechanism.

2.3.2.4 Ash coalescence

Depending on the gasification conditions, a part of the coal ash may vaporise with the remaining inorganic matter to be distributed within char particle.

This remaining inorganic matter will form most of the ash. During combustion, particularly pf combustion, char recedes and inorganic matter is exposed to the char surface (Quann and Sarofim, 1986). With the progress of combustion of char particle this inorganic matter is drawn together. Formed molten ash may coalesce or may sinter. Solid phases may agglomerate with the molten phase. The exact mechanisms of retention of both molten phases and solid particles are still investigated.

Ash formation mechanisms during gasification gained so far little attention. From work by Kosminski and Manzoori (1990) it appears that ash forms inside the char particle while it forms also on the char surface. Diffusion of reacting gases, such as steam and carbon dioxide, into the porous char might be causing these char reactions not only on the surface but also inside. This may have a positive effect on a formation of larger ash particles as more ash coalescence may take place within a char particle.

2.3.2.5 Char porosity

Reduction in coal char porosity and pore surface area of the char were found by Koyama et al. (1992) to be strongly effected by the gasification temperature. From their experiments Koyama et al. concluded that char particles exposed to temperatures higher than the ash melting point are less reactive, less porous and have smaller surface area than particles exposed to lower temperatures. They suggest that for example before introducing coal to an entrained bed gasification process the coal should be gasified at lower oxygen/carbon ratio at temperatures lower than ash melting point.

So, the inorganic matter present in coal can not only cause physical problems such as agglomeration or deposition but also can reduce process efficiency.

2.3.2.6 Particle temperature

During gasification a part of coal reacts with oxygen in exothermic reactions. Temperature of particles may increase to above that of the gasifier environment temperature. But it also may not exceed the bed temperature. Frederick et al. (1994) report that the temperature of the surface of black liquor droplets pyrolysed in N_2/CO_2 gas environment was reaching a temperature somewhat below the furnace temperature during devolatilisation and remained such as long as gasification continued. For droplets gasified in an $800^\circ C$ furnace in 20% CO_2 , the surface temperature during gasification was about $760^\circ C$.

Kojima et al. (1993) studied temperature of the inside of the burning char for bituminous coals, using 13-18 mm particles with a thermocouple installed inside a particle. The temperature inside burning particles was 20 to $400^\circ C$ higher than the surrounding temperature in tested range of $600^\circ C$ to $1400^\circ C$. That difference corresponded with the quality of coal. For the coals with low ash melting point, the maximum temperature almost linearly decreased with the increased surrounding temperature. Inside the particles Kojima et al. measured the temperature of $1000^\circ C$ for the surrounding temperature of $800^\circ C$. Doing X-ray diffraction analyses Kojima et al. found that for most minerals present in tested coals, their peak intensities decreased with particle temperature. These results suggested the progress of the ash vitrification with temperature increments.

Linjewile et al. (1994) found that the temperature of a burning particle in the bubble phase of a fluid bed combustor could be up to $170^\circ C$ higher than in the emulsion phase. Linjewile et al. also established that there was always an excess of particle temperature against that of the bed. This difference increased with particle diameter and with the bed temperature.

2.4 AGGLOMERATION and DEFLUIDISATION

Agglomerating fluidised bed gasifiers (FBG) rely on agglomerating of ash during gasification, and agglomerates are removed by falling off from the bed during the process. Ash agglomeration is therefore a very important part of the process.

In a non-agglomerating gasifier, such as HTW gasifier, the process of agglomeration is not a welcomed phenomenon. It is important then for this type of gasifier to operate at conditions to avoid agglomeration and associated problems. Experience with Bowmans coal (Bellin et al., 1987; Kosminski and Manzoori, 1990) showed that these problems might exist. Non-agglomerating gasifiers operate usually with bed inventory formed mostly by coal char with little ash content to avoid ash agglomeration. To sustain a high carbon conversion the gasification processes require higher temperature. But the high temperatures then may lead to unwanted ash agglomeration, clinkering, deposition and defluidisation.

2.4.1 Agglomeration mechanisms

A comprehensive summary of research into agglomeration phenomena is given by Manzoori (1990). Quoted are works and findings by Godel (1966), Yerushalmi et al. (1976), Gluckman et al. (1976), which relate to operation of fluidised bed gasifiers. Godel (1966) found from work with FBG at high fluidisation velocity, that the bed might be operated at temperatures higher than ash melting point.

Smaller agglomerates may form at higher fluidisation velocity and their growth may also be restricted. But they may be sufficient in size to be separated and removed from the gasifier without causing the bed to defluidise. Ignifluid process was designed on this discovery. This process is described by Yerushalmi et al. (1976) and Gluckman et al. (1976).

Yerushalmi et al. (1976) suggested for fluidised bed gasifier agglomeration process the following steps of agglomeration phenomena:

1. Occurrence of small molten beads on the surface of the char particles.
2. Growing of these beads on the char surface by further char gasification or by capturing of molten ash from other particles during particle collision.
3. Separation of beads from char during the growth due to the high interfacial tension between the molten phase and the char.
4. Remaining sticky at the gasifier temperature the beads continue to grow either by coalescence with other agglomerates or with other beads.

The agglomerates formed in fluidised bed gasifiers usually contain little of organic matter. This is due to the fact of a high interfacial tension between the molten inorganic matter and the char. Merry et al. (1975) give examples of a number of ash agglomerating processes developed and based on this phenomena.

Manzoori (1990) concentrated his work on the mechanism of bed agglomeration in a circulating fluid bed when burning high-sodium, high-sulphur, high-chlorine coal. Manzoori concluded that agglomeration could proceed only when the temperatures in the bed were above the initial sintering temperature of the ash and that the bed particles have to reach a minimum "critical" thickness. If these conditions existed in a combustor, then the rate of agglomeration and possibility of defluidisation will increase with the furnace temperature, with the amount of melt in the particle coating, lowering content of mineral inclusions in the coating and with increasing of the thickness of coating.

Langston and Stephens (1960) postulated that in the fluidised bed the tendency of particles to stick together and agglomerate, when they collide, is directly proportional to their adhesive force and area of contact and inversely proportional to their momentum. Langston and Stephens found in their experimental work on reducing iron ore in fluidised bed in hydrogen atmosphere that with coarse particles bed temperature could be maintained at 870°C but the bed was defluidised already at 760°C when only fine ore particles were in the bed. Langston and Stephens concluded that as larger particles have higher mass, and thus higher momentum, they could tolerate greater adhesive force and be fluidised at higher temperature than finer particles.

Mason and Patel (1980) report that in a single-stage ash-agglomerating fluidised bed U-GAS gasifier for a given coal the rate of agglomeration, the size of agglomerates and the ash content of the agglomerates are dependent on: fluidised-bed temperature and ash concentration, average feed-particle size, superficial gas velocity, and fluidised-bed height. Carty et al. (1986) report on the same U-Gas process on using coals rich in iron. They report that agglomeration of ash in that process was caused by molten iron.

Vora et al. (1980) report the chemistry of ash agglomerate matrix from coke breeze as being based on ferrous aluminosilicate. Agglomerates from bituminous coals contained mainly ferrous silicates, calcium ferrous silicates and calcium aluminosilicates.

Interesting conclusions were drawn by Hsieh and Roberts (1985) working on an assessment of agglomeration of various sub-bituminous and lignite coal ashes. They prepared ashes by heating coal in air to 538-649°C and screened all samples to pass between 100-mesh and 200-mesh US standard screen. Then they exposed prepared ashes in a fixed beds to reducing and oxidising atmospheres for various times and temperature range 1038-1150°C. No agglomeration was observed in a nitrogen atmosphere and a more rapid agglomeration was observed in a reducing than in an oxidising atmosphere. Hsieh and Roberts suggest that an agglomeration temperature is a several hundred degrees lower than the ASTM temperature and that the ASTM initial deformation temperature cannot be correlated to the agglomeration temperature.

Stallmann and Neavel (1980) also found that agglomeration in fluidised beds begins at temperatures few hundred degrees lower than the initial deformation temperature of the coal ash determined in accordance with the ASTM standard methods.

Hsieh and Roberts (1985) further found that agglomeration depends on coal type and on process operating conditions. With up to 80% conversion of coal the agglomeration was negligible. At higher carbon conversions the agglomeration can be controlled, by diluting the reacting material with inert materials. Hsieh and Roberts also report that agglomeration occurs on a shorter time scale than the nominal residence time in all but the most kinetically rapid gasification systems. Hsieh and Roberts found that agglomeration temperature for coal ashes they tested decreased linearly with increasing content of sodium in the coal ash.

2.4.2 Agglomeration in spouted fluidised beds

Laughlin and Reed (1991) have shown that the tendency for a certain coal to form agglomerates during gasification in spouted beds is dependent on:

- composition
- concentration

- size and distribution of the inorganic components (coal ash and sorbent) in the gasifier;
- maximum particle temperature attained in the gasifier spout;
- particle mobility in the spout and cone regions of the bed.

Laughlin and Reed recent studies (1993) have shown that the temperature at which the bed material agglomerates defines an ultimate boundary of operability of pressurised fluidised bed gasifier. While operating a spouted fluidised bed gasifier at atmospheric pressure they found that the maximum temperature attained in the gasifier spout was typically 50°C higher than that recorded for the bed. Their studies into ash agglomeration mechanisms have shown that interactions of pyrite iron species and calcium species with aluminosilicate minerals in the coal ash can occur to form relatively low-melting phases in the gasifier bed. In addition, an iron/iron sulphide eutectic melt can form. Both these liquid phases can act as binding media for the agglomeration of ash. Laughlin and Reed (1993) found that agglomeration temperature decreased as the coal ash and iron content increased and the C:O ratio decreased. They also found, that ash fusibility measured with accordance to the standards would not correlate with temperatures, at which ash agglomerates form in the gasifier.

Arastoopour et al. (1989) worked on determining the rate and extent of agglomeration in fluidised beds with central jets. Their results showed that the extent of agglomeration increased with increasing temperatures and/or decreasing velocities of the jet and fluidising air. The rate of agglomerate formation was particularly sensitive to the jet temperature.

Watkinson et al. (1983) studied gasification of coal in fluidised and spouted bed gasifiers. The comparison of results for Canadian bituminous and sub-bituminous coals used in that study showed generally a little difference in the influence of either of the systems on the gas yield or the gas heating value. Spouted bed system showed, as expected, a slightly higher maximum bed temperature, with fluidised bed showing more uniform bed temperature distribution. Sand inert bed was used in each system.

Watkinson et al. also report that neither of those systems could support gasification of a low-rank coal, with sodium content in coal ash at 8% Na₂O, due to a significant bed agglomeration followed by the bed defluidisation. Agglomerates recovered after cooling

the bed were very loose and easily broken, contained little carbon and showed measurable Na_2O levels. The bed temperature in the gasifiers was not reaching softening temperature of the ash of coal used in the experiments. No combination of air, steam and coal rates attempted led them to obtaining any satisfactory operation of either the spouted or fluidised bed.

Interesting results come from spout bed experiments conducted by Kojima and Tanaka (1989). Kojima and Tanaka gasified coal in spout beds with different diameter nozzle and angled or flat additional gasifier distributor. They recorded the highest temperature in excess of 1300°C in the zone formed by the central nozzle jet and did not record ash agglomeration or clinker formation. Clinker and agglomerates however formed when wide nozzle was used and when temperature reached only 1080°C . Kojima and Tanaka's results show that gas velocity and shear forces do prevent formation of agglomerates even at favourable temperature conditions.

Also, according to Rehmat et al. (1992), the rate of agglomeration depends upon the size and the intensity of the jet stream zone. Rehmat's et al. work, with spout beds, showed that agglomeration increased with time and jet temperature. Rehmat et al. found that at higher bed temperatures, the particles attained higher temperatures before they were entrained into the jet and therefore had a better chance to melt and become sticky. Rehmat's et al. work also showed that a fluidised bed with a multi-jet gas distributor could tolerate higher jet temperature without the formation of sinters.

Silica sand was found to cause agglomeration in a spout bed gasification process developed by British Coal Corporation. Gale et al. (1991) report that by substituting bauxite for sand as the gasifier bed material allowed to overcome the problem. A coal ash coating formed on sand particles: due to its high content of iron oxide, which reacted with sand to form low melting-point eutectic mixtures causing particle agglomeration at 1020°C process temperature.

2.4.3 Sintering and agglomeration

Sintering mechanisms of fluidised bed combustion ashes were studied by Skrifvars et al (1994). These mechanisms are identified as partial melting, viscous flow and gas-solid

reaction. Ash sintering laboratory tests were conducted on laboratory prepared ashes under oxidising and reducing conditions. Partial melting was found to be a dominant sintering mechanism for high-sodium, high-chlorine brown coal ashes; in reducing atmosphere these ashes were sintering already at 500°C. Viscous flow sintering was found mostly for silicate systems.

Mann et al. (1990) suggest the sintering mechanism for ash agglomeration and deposition in fluidised bed combustors burning lignites to be caused by coal based organically-bound alkali and alkali earth metals and sulphur. Sodium calcium sulphates are giving matrix to agglomerates and deposits. Mann et al. suggest the same mechanism for agglomerates and deposits to be initiated and formed: volatilisation of alkali species during combustion and gas-to-solid condensation on bed material forming partially fused or solid crystals. Mann et al. definitely state, and quote other researches evidence, that the alkali must be in a form that will allow it to be volatilised during combustion, i.e. organically bound. Mann et al. also find that aluminosilicate phases present in FBC systems can compete for the released alkalis and form higher melting point clays, rendering the alkalis inert in terms of agglomerate and deposit formation.

Hupa et al. (1989) report on a method for measuring sintering tendency of peat-gasification ashes. The method is based on compression-strength measurements of sintered pellets made from pre-melted, crushed and screened synthetic ash samples. Hupa et al. results showed that silicate ashes with high sodium content tend to sinter more rapidly than ashes with low sodium content.

Moilanen et al. (1989) report on High-Temperature-Winkler gasification process using peat relatively rich in iron with some sodium and potassium, observed no ash agglomeration in the fluidised bed gasifier. They were testing this peat ash sintering properties and report that sintering in reducing environments was more rapid than in oxidising atmosphere and that sintering strength showed good correlation with basic-acid ash oxide ratio. The reported sintering of ash was referred to the content of iron and in general to the ratio between alkaline and acid oxides present in the ash. No specific alkali silicates were identified as being a major phase of the binding matrix in the identified deposits.

Results of Moilanen's (1990) studies suggest that sintering seems to correlate best with the base-to-acid oxide ratio (B/A) rather than with a component only, such as iron. Under reducing conditions the iron content of molten slag can change, so that part of iron is reduced to metal and is precipitated out of the melt. This indicates that high iron contents can cause inconvenience in fluidised bed gasifiers also due to reduction of iron to metal, which can be manifested, for example, in fluidising difficulties. Sintering by viscous flow is dependent on the viscosity, which rapidly decreases while the temperature rises. Moilanen's viscosity measurements indicated, that an increase in the B/A-ratio of ash also results in a reduction of the ash viscosity, which in consequence intensifies ash sintering.

Moilanen et al. (1991) reports that viscous flow is a characteristic mechanism of sintering of peat ash during gasification of peat. Sintering of ash was identified under reducing conditions at temperatures significantly lower than those measured with standard methods for ash fusion. The strength of the ash sample sintered in laboratory tests at 700°C could correspond to that measured for real deposit samples coming from HTW process.

They found that at 1000°C the measured viscosities well correlated with B/A ratio of the peat ashes and the rates of sintering calculated from Frenkel formula were in general agreement with Moilanen's (1990) fly-ash sintering studies.

Marinov et al. (1992) studying agglomeration of ash during fluidised bed gasification of Bulgarian Elhovo high-sulphur lignite found that two kinds of ash agglomeration centres can be distinguished: the centres of melting and the centres of sintering. Marinov et al. considered that FeS.FeO eutectic has been responsible for being a melting centre of agglomerates and the heavy ash agglomeration happening at 930°C temperature. Sintered centres consisted of a magnetite and mixtures of various separate calcium or iron or magnesium aluminosilicates.

Viscous sintering of coal ashes proceeds by the formation of closed pores and their shrinkage, and /or by the diffusion and reactive diffusion of a liquid phase along surface or grain boundaries according to Nowok et al. (1989). Nowok et al. found that pellets of ash sintered in a reducing atmosphere had higher strength than those sintered in air at the same test temperature.

Studying granular bed filters Thambimuthu and Clift (1989) found adhesion of the sodium sulphate additive at temperatures below the ash self softening range of 750 to 800°C. Liquid phase formed by sodium sulphate and sodium chloride eutectic was aiding the adhesion.

Measuring electrical resistance of a lignite coal ash, Khan and Williford (1989) report that sintering temperature is higher in an oxidising atmosphere than in an inert atmosphere and that increase of pressure increases ash sintering temperature in both atmospheres.

Jung and Schobert (1991) conducted a fixed bed ash sintering tests of lignite ashes prepared in accordance with ASTM coal ashing procedures at 750°C. Jung and Schobert found that the sinter point decreased with decreasing particle size, and that, at a given sintering temperature, the strength of the sintered ash was inversely proportional to the particle size. The onset of sintering point was due to the formation of a liquid phase from the lowest melting point components, which might have formed from the interactions of alkali and alkaline earth metal sulphates with aluminosilicates and silica. Ash of Beulah lignite was sintering at temperature as low as 448°C for particle size smaller than 38 microns and at 550°C for particles larger than 75 microns. Jung and Schobert suggest that the coal ashes have electrical conductivity behaviour similar to that of glasses.

In later work Jung and Schobert (1992a) report that the onset of sintering correlates with the sodium content of the ash, and presumably reflects the formation of the sodium-containing aluminosilicate phases having the lowest melting point. The sintering behaviour of the ashes is also governed by calcium content. Jung and Schobert found that minimum sintering temperatures determined by the drop tube furnace method, which they adopted in their study, were lower than those reported by them previously (Jung and Schobert, 1991) using electrical resistance measurement technique. The Beulah lignite ash was sintering already in the temperature range of 430-455°C.

Jung and Schobert (1992b) demonstrate prediction of the liquid-phase composition at a temperature, and based on that prediction they calculated that phase viscosity. Jung and Schobert based their classification criteria on ash composition, base-to-acid (B/A) ratio, silica ratio, and lignite factor. Their predicted value average deviation was within 30%

from experimental measurements for most of the coal ashes, ranging from bituminous to brown coals, they tested. They found that the predicted liquid-phase composition changed slightly as a function of temperature in the range of 1000-1500°C, for which they compared predicted and experimental viscosity data.

Interesting results on ash sintering and agglomeration are given by Falcone (1989). Studied ash samples showed that bulk of non-agglomerating ash contained more silicon dioxide than agglomerating ash. Agglomerating ash had great amounts of calcium oxide and contained less silicon dioxide. Falcone's work results show that under reducing atmosphere ash viscosity decreases, while surface tension increases, given a constant ash composition and that formation of a slag is greater under reducing conditions than under oxidising conditions. Falcone further suggests that increased silicon dioxide content increases both the viscosity and surface tension of a slag while increased sodium oxide or total alkali content decreased them both.

Falcone further established that ashes which tend not to sinter or agglomerate from molten phases have higher viscosities relative to their surface tension and agglomerating ashes have lower viscosities relative to their surface tension at a given temperature.

Falcone suggests that the viscosity factor is considerably more sensitive to compositional parameters than the surface tension. Ashes with higher silicon dioxide to sodium oxide ratios at a given temperature tend to have higher viscosities relative to their surface tension. And therefore tend to exhibit reduced sintering and agglomeration. While sodium oxide tends to decrease surface tension, it tends to decrease viscosity at a greater rate resulting in increased viscous flow sintering.

Nowok et al. (1991) studying ash sintering under gasification conditions have shown that interfacial surface tension/viscosity ratio increases with base/acid ratio. This is indicated by the systematic increase of the depolymerisation of silicate network structure. Steadman and Nowok (1991) report that in amorphous coal ashes, crystals of silicate/aluminosilicates may precipitate at grain boundaries and may generate tensile or compressive strength. In a sample of Beulah coal ash, which has a high sodium/silica content ratio, mineral gehlenite crystallised at 800-880°C. Steadman and Nowok also report that other parameter

responsible for the coal ash strength development is the sintering factor - viscosity/surface tension ratio.

2.4.4 Slag viscosity

There is several gasification technologies based on slagging the ash during gasification process. Some of the aspects of formation of slags, their properties and behaviour may relate to the fluidised bed gasifiers, where some components may be in a viscous state similar to that of slag. The following is collected information related to fluidised bed gasification.

Working on slag flow behaviour Watt and Federay (1969) proposed a formula for slags formed from British coals expressed as a function of temperature and chemical composition in terms of five oxides present in coal ash.

Benson and Nowok (1990) found in their studies, that there was a prominent increase of interfacial surface tension and viscosity ratio with the basic/acid oxide ratio of coal ash exposed to reducing environment.

Gasification slag leachability of was studied by Federer and Lauf (1985). They concluded that the leachability of the slags increased substantially with increasing sodium content. Federer and Lauf also found that slag containing 37% of Na_2O contained no crystalline phases and consisted only of glass.

2.4.5 Defluidisation

Davies et al. (1989) investigated thermal agglomeration and defluidisation in fluidised beds using wood chips and iron sand. They report on work by others in defining minimum fluidisation velocity U_{mf} and defluidisation parameters. Davies et al. found that there could be large changes in U_{mf} even when only very small quantities of wetting ash existed in the system. Davies et al. also found that iron sand became sticky at 750°C in its own right, even when no ash was used in their experiments.

From his research Basu (1982) concluded that defluidisation of a fluidised bed is governed by the sintering characteristic of the bed material.

Manzoori (1990) suggests that defluidisation is caused by the interactions of the bed particles coated with coal ash what results in high minimum fluidisation velocity required to maintain the bed particles in suspension. Defluidisation can occur with bed particles having very little coating but being at extreme temperatures and with the coal ash having high content of melt-forming inorganic matter (Manzoori and Agarwal, 1994).

2.4.6 Deposition

Deposition of ash in the gasifier, its cyclone or other parts of installation can be of concern as it may cause operational problems. Experience with gasification of high-chlorine high-alkali Bowmans coal in HTW process (Bellin et al., 1987) shows that salts may deposit in the gasifier or in the following plant. Alkali and alkali earth chlorides and silicates were found as major material deposited in the gas path (Kosminski and Manzoori, 1990).

Mason et al. (1982) report on ferrous sulphide and iron-rich ferrous aluminosilicates as being responsible for deposition of ash in the U-GAS gasifier cyclone. Mason et al. report that deposits grow in a direction counter to gas flow and that the impact of particles on the growing surface also plays a role. Tsao et al. (1982) suggest reducing wall temperature and reducing gas velocity, as a part of operating criteria to avoid such situation in the high temperature cyclones.

2.5 SUMMARY

The information presented in this chapter relates substantially to the inorganic matter present in coal, the mechanisms of formation of ash and its behaviour in conditions prevailing in fluidised bed gasifiers. The formation of ash involves a range of chemical reactions and physico-chemical processes undergone by the coal inorganic matter. Not only physical parameters, but also the modes of occurrence of the inorganic matter influences this ash formation, as, due to their heterogeneous nature, the low-rank coals can be rich in the inorganic matter.

Occurrence of inorganic matter

- The inorganic matter can exist in coal as:

- a) Inorganics: metal ions organically bound to coal structure, mostly in form of carboxylic salts, and as inorganic salts dissolved in coal moisture.
- b) Minerals: in bands, inclusions or finely distributed in coal matter. Mineral distribution in coal is generally uneven.
- In low-rank coals, considerable quantities of metal ions are often in the form of salts of carboxylic groups associated mostly with humic acids present in the coal structure. Calcium, magnesium and sodium ions often exist in these forms but may contain other minor metallic elements such as iron and aluminium.
 - Sodium also exists in coal inherent moisture in dissolved form as chloride, or sulphate.
 - Chlorine mainly exists in ionic form in the coal inherent moisture, with the forms of chlorine in low-rank coals and its association with metal ions other than sodium has not been established with certainty.
 - Sulphur mainly exists in the forms associated with the coal organic structure and as sulphides of iron, mainly pyrite. Sulphates, such as gypsum are other forms of occurrence for sulphur.
 - Silicon is the principal inorganic material present, mainly in the forms of quartz, clays and shale minerals. Aluminium is typically associated with silicon as it is another fundamental component of clays and shale minerals present in coals.
 - Clays, quartz and other minerals may often be uniformly distributed. The particle size can be smaller than 1 micron. This is attributed to the distribution of deposited minerals during the coalification period. Quartz is sometimes present in colloidal form in the moisture.
 - Other minerals often found in low-rank coals are carbonates, mostly of calcium and magnesium.

Ash formation during gasification

The gasification of coal will lead to the reactions of its organic matter and transformations of its inorganic matter to form ash. The coal structure will change upon drying, heating, devolatilisation and chemical reaction with gaseous reactants during which, the coal inorganic matter will also change in its physical and chemical forms.

New forms of inorganic compounds will materialise by the process of crystallisation, melting, vaporisation, aggregation and coalescence. Chemical transformations will be by

thermal decomposition, reactions in all phases between inorganic species, reactions with char, coal gaseous products. These transformations can be outlined in following way:

a) Devolatilisation

- Coal particles lose moisture during the beginning of a heating up period. Upon drying the crystallisation of salts dissolved in the inherent moisture takes place within particles. The salts and colloidal matter will be finely distributed in the coal matrix.
- At high temperatures, coal devolatilises and releases some of its organic and inorganic matter. Many organic sulphur compounds will be released into the gas phase. Some inorganic species, such as chlorides, may vaporise. Aggregation of remaining salts may occur in the coal char.
- During devolatilisation the coal functional groups, including the carboxylic groups, decompose. This results in the formation of molecularly dispersed reactive inorganic species. The species formed are carbonates, oxides, sulphides. Sodium carbonate Na_2CO_3 is reported always to form from organically-bound sodium.

b) Combustion

- Particle temperature in a fluidised bed combustor may be 100-200°C higher than the bed temperature.
- Chlorine will be released mainly as hydrogen chloride and will be released disproportionately to the amount of sodium present as sodium chloride. Sulphur will be oxidized to sulphur dioxide.
- Sodium, both organically-bound and sodium chloride reacts with sulphur to form sodium sulphate. This sulphate together with calcium sulphate, will form a molten phase.
- The organically-bound calcium will form calcium sulphate, silicates and aluminosilicates. Magnesium mainly will form magnesium oxide and magnesium aluminate - spinel. Iron will form oxides. Sodium silicates may be an intermittent reaction product, with which calcium, magnesium or iron will react to form various combined silicates.
- Silica and clays, particularly kaolinite, will react with sodium salts, sodium sulphate and sodium chloride to form silicates and aluminosilicates. Water promotes these reactions. Sodium chloride was found to be more reactive than sodium sulphate.

Reactions with silica and clays may reduce the content in ash of sodium salts melting at low temperature and increase the content of sodium species having a higher melting point. These reactions are intensified by an increase in temperature, but may already proceed at temperatures below the melting point of sodium salts, as low as 600°C. Reactions with aluminosilicates lead mainly to a formation of nepheline and albite, sodium aluminosilicates melting above 1000°C.

- Bauxite is reported to only adsorb sodium chloride vapours with little proof of chemical reactions.

a) Gasification

- Alkali and alkali earth chlorides may melt at fluid bed gasification temperatures. Gasification conditions promote the vaporisation of sodium chloride. Results of thermodynamic calculations suggest that vaporisation of sodium chloride will be more intense in gasification conditions than in combustion conditions. Vaporisation of sodium, whether as sodium chloride or via other species is reported to be reduced by the presence of steam. The condensation of sodium chloride vapours is the major form of deposition in a gasifier plant.
- Increasing the silica content in the coal reduces sodium loss into the gaseous phase.
- The organically-bound sodium is reported to form sodium carbonate during coal pyrolysis. For high-sulphur containing coal, thermodynamic calculations predict the formation of sodium sulphide.
- Sodium present in low-rank coals is reported to form silicates, aluminosilicates, sulphates and chlorides during coal gasification. Organically-bound sodium is reported to react with silica as reported from laboratory and pilot plant gasification tests.
- Sodium chloride (molten and vapour) reacts with minerals to form silicates and aluminosilicate, with glass phases dominating the products of such reactions and form the base for formation of agglomerates. The details on the extent of reactions during gasification of a low-rank coal of particular original forms of sodium with silica and aluminosilicates are however scarce.
- Hydrogen chloride and ammonia may form ammonium chloride, which condenses to a solid phase at a temperature below 350°C and may cause operational difficulties in gas cooling equipment of a gasifier.

- Reactions of inorganic matter during gasification depend on the composition of gas and the partial pressure of the steam. Steam promotes sodium reactions with quartz and the formation of glass phases.
- Sulphur will be released in gaseous form, principally as hydrogen sulphide. Carbonyl sulphide, sulphur dioxide, mercaptans will also form. Hydrogen sulphide will react with coal inorganics and minerals' transformation products. Calcium sulphide and other sulphides will be the main inorganic sulphur compounds in the ash from a fluidised bed gasification process.
- Calcium, both mineral and organically-bound will form mostly calcium sulphide in sulphur rich coals and will also form oxides, silicates and aluminosilicates. Magnesium will mainly form magnesium oxide. The presence of calcium and magnesium chlorides in gasifier ash deposits has been suggested. However, there is little information regarding the mechanism of their formation. Sodium silicates may be an intermittent reaction product, with which calcium, magnesium or iron will react to form various combined silicates
- It has been reported that alkali carbonates are reduced during gasification to their respective metal forms by reactions with carbon or carbon monoxide. Reactions with steam are suggested to lead to the formation of their respective hydroxides. These reactions are suggested to be a part of the reactions involving alkali metals in catalysis of coal gasification reactions. The reduction reactions are suggested to take place already at temperatures below 600°C. Vapour of metallic potassium was identified in a reactor environment in pyrolysis conditions at 700°C.
- Clays and other hydrated minerals will dehydrated up to a temperature of 600°C. Above this temperature they may further decompose into various new species of which, oxides, silicates and aluminosilicate will dominate. They will participate in reactions with alkali and alkali earth salts and oxides to form often low-temperature melting compounds and eutectics. These compounds may melt at temperatures hundreds of degrees below the gas temperature found in fluidised bed gasifiers. The extent of formation, kinetics and conditions for reactions of alkali and alkali earth salts and oxides with silicates and aluminosilicate to form silicates and aluminosilicates are not well represented in the literature.
- Iron compounds are the most common compounds initiating formation of agglomerates in agglomerating fluidised beds. Pyrite will decompose to iron sulphide and part of the

sulphur will be liberated. The formed sulphide may decompose further to pyrrhotite, oxidized to FeO and also reduce to metallic iron. FeO, by forming silicates, is a prerequisite for agglomeration in agglomerating fluidised beds; FeS-FeO eutectics and metallic iron also initiate agglomeration. Iron based agglomerates melt below 900°C and their formation is accelerated by the presence of an alkali.

- During a gasification process, the reactions involving inorganic matter happen not only on the char surface, but also extensively inside the char. This may lead to the coalescence or sintering of that matter into larger and better-consolidated ash particles.

Ash Agglomeration

In a fluidised bed gasifier, char particles with molten ash exposed on their surface may collide with each other or with ash particles. This may result in the formation of larger particles, or agglomerates. This agglomeration may include fused material as well as unfused particles. Agglomerates are collected at the bottom of a reactor and fine particles may leave the reactor with the gas stream.

With fluidised bed systems, such as in combustion systems, inert particles form the bed. In gasification systems an initial bed is created mostly by char particles.

- Agglomerates formed in fluidised bed gasifiers usually contain little of the organic matter. The collision between particles other than char results in the majority of the particle adhesion. This is due to high interfacial tension between the molten inorganic matter and the char.
- Many researches have studied the mechanisms of agglomerate formation and no definitive answer has yet been given to explain this phenomenon. It has been established that agglomeration depends on the stickiness of the ash and other particles in the bed.
- Sintering temperature is the lowest temperature below which ash will not start to agglomerate. For agglomeration to happen, the fusion temperature of particles in the bed must be higher than the sintering temperature. In reducing conditions the sintering temperature of coal ash is lower than in oxidising conditions, and is much lower than ash fusion temperature measured using standard methods.

- Agglomerate formation may be dependent on coal type, the form and composition of inorganic matter in coal, on its characteristic, and on gasifier operating conditions: process temperature, particle size, gas velocity.
- With carbon conversion below 80% no agglomeration should take place during gasification. Agglomeration occurs on a shorter time scale than a nominal residence time.
- It is reported that an increase of sodium in ash will result in a linear decrease of ash agglomeration temperature.
- Partial melting is suggested as sintering mechanism for high-sodium, high-chlorine coal. Viscous flow is suggested for silicate systems.
- Agglomeration of ash is reported at temperature hundred of degrees lower than ash initial deformation temperature. Molten phases appear in gasification environment at temperatures 200 to 400°C lower than in combustion process. Their coalescence or sintering with solid particles is leading to agglomeration of ash particles in the gasifier chamber.
- Formation of bonds between agglomerated particles is by surface diffusion or viscous flow. Agglomeration at lower temperature leads to formation of sintered agglomerates. At higher temperature agglomerated particles experience significant coalescence. The bonds between the particles are strengthening with time and temperature.

Sintering

Sintering of ash may initiate ash agglomeration in a fluidised bed gasifier.

- Sintering onsets due to formation of a liquid phase from the lowest melting point component.
- Ash sinter point decreases with particle size. The temperature of 448°C is reported as temperature, at which smaller than 38 μm particles in size of ash of lignite had sintered. At a given temperature strength also increases with decrease of particle size.
- Ash surface tension to viscosity ratio is called "sintering factor". This ratio is suggested as being responsible for initial particle joint strength development and consequently the agglomeration, and a final strength of agglomerates. The sintering factor will increase with increase in base/acid (B/A) oxide ratio.

- An increase in base/acid oxide ratio causes a reduction of ash viscosity and consequently intensifies sintering. Most researches suggest such a relation to B/A ratio and not to a single ash component, as some of components, such as iron, may precipitate out. Viscosities are reported to correlate well with B/A ratio for an ash from peat rich in sodium and potassium.
- High $\text{SiO}_2/\text{Na}_2\text{O}$ ratio in ash is reported to give higher viscosity relative to surface tension and exhibit reduced sintering and agglomeration. Viscosity and surface tension increase with increase of SiO_2 while increases in Na_2O decreases viscosity and surface tension. Viscosity is reported to be more sensitive to composition than for surface tension.
- Non-agglomerating ash contains more silicon dioxide than agglomerating ash.
- Under reducing conditions viscosities decrease, surface tension increases for a given ash composition.
- More slag forms under reducing conditions than under oxidizing conditions.

Defluidisation

Defluidisation is affected by the same variables of the fluidising process, as is agglomeration. Defluidisation is caused by particle interactions, which result in an increase in the minimum fluidisation velocity required to maintain bed fluidisation. Defluidisation is dependent on bed temperature and the thickness of coating on bed particles.

Agglomeration of ash and bed material is therefore suggested by most researches to be the reason for defluidisation. Operation of a fluidised bed system containing sticky particles is possible by maintaining high gas velocity. At the same time agglomerates may form at controlled rate.

2.6 OBJECTIVES OF THE PRESENT STUDY

The main objective of this study is to elucidate the role of sodium and silicon minerals in the formation of liquid phases potentially responsible for fluidised bed agglomeration during gasification of high-sulphur low-rank coals in order to identify methods to prevent the formation of such phases. A study will be undertaken to investigate the transformations of sodium present in high-sulphur low-rank coal and reactions and reaction mechanisms of

sodium with silicon bearing minerals, silica and kaolin, during fluidised bed gasification of coal. The knowledge gained is expected to assist in the development of tools required for the successful design and operation of a coal gasification plant.

Experimental work and published literature (Bellin et al., 1987; Kosminski and Manzoori, 1990; Watkinson et al., 1983; Skrifvars et al., 1994; Falcone, 1989) have shown, that sodium is the most important inorganic element in low-rank coals in relation to coal ash tendencies to deposition and formation of agglomerates during a process of coal gasification. Laboratory scale experiments, under controlled conditions, will ultimately provide a greater understanding of the reactions and mechanisms leading to agglomeration and should be directed specifically at the effect of sodium forms and content on agglomeration.

To determine the critical fundamental parameters and mechanisms of coal ash formation and agglomerating behaviour during low-rank coal gasification in a non-agglomerating fluidised bed gasification process it is important therefore to obtain fundamental information on the kinetics and the mechanism of reactions between sodium and silicon compounds.

The key milestones of this project are:

1. To determine the effect of gasification atmosphere, gasification temperature, forms of sodium in coal, sodium transformation products on reactions between sodium and silicon in forms of quartz and kaolinite.
2. To determine mechanisms and assess kinetics of interactions between forms of sodium and forms of silicon.
3. To determine effect of individual gaseous atmospheres, temperature and time on sodium chloride evaporation.
4. To assess the formation of ash on the surface and inside the char particles during gasification.
5. To establish influence of gasification agents such as carbon dioxide or steam on formation of fused phases.
6. To relate agglomeration and defluidisation to the chemical composition and the forms of inorganic matter.

Chapter 3

THERMODYNAMIC CONSIDERATIONS

3.1 INTRODUCTION

The literature review presented in Chapter 2 brought to attention the fact of the possibility of theoretical prediction of reaction products between various inorganic elements present in coal during coal gasification. A number of such theoretical predictions reported in the literature were found to be comparable with experimental observations.

The theoretical calculations reported in literature were specifically directed to the gasification conditions resembling the particular experimental or plant operating condition used. No examination was conducted on the influence of individual gases such as carbon dioxide, steam or hydrogen on the equilibrium products. Importantly, the results were mostly concerned with vaporised alkali species rather than condensed phase species.

It has been considered that for the current study and future work, it would be of significant value to refer and compare experimental results with theoretical predictions on the behaviour of individual gases such as carbon dioxide, steam or nitrogen on the equilibrium products of coal components during gasification. This chapter therefore presents results of thermodynamic calculations, which were conducted to predict the equilibrium compositions of sodium and silicon species for the conditions representative for the fluidised bed gasification of low-rank coal.

3.2 OBJECTIVES

There is little evidence, and no clear understanding of the influence of individual gases of a gasifier atmosphere on sodium transformations and its reactions with silicon compounds and with sulphur in a FBG. Such reactions can be investigated experimentally and also theoretically by thermodynamic predictions of equilibrium of chemical reactions. Predictions were therefore sought for the behaviour of sodium present in coal as organically-bound or chloride form and its reactions with silica or kaolin during exposure to individual gaseous atmospheres of carbon dioxide, steam, carbon monoxide, hydrogen and nitrogen.

3.3 PREDICTION OF EQUILIBRIUM COMPOSITIONS

Thermodynamic equilibrium represents a composition towards which chemical reactions proceed. Thermodynamic calculations can be used to evaluate products of reactions, which can proceed under given conditions of pressure and temperature and composition. Such calculations for the equilibrium conditions for chemical reactions however do not consider the kinetics of such reactions and specific parameters of the process, which may result in equilibrium conditions not being reached. Therefore results of predictions may not find their full confirmation in practice, but they still form a valuable guide to experimental investigation (Harb et al., 1993).

The prediction of the quantity and composition of products in the coal ash, particularly the liquid phase is important in the determination of ash agglomeration and defluidisation in a fluidised bed environment. Further to this, the nature of the gaseous phase present effects the ash condensation and deposition behaviour in downstream gasifier plant equipment.

During combustion in a fluidised bed combustor (FBC) of coal containing sodium and sulphur species, sodium is mainly transformed into sodium sulphate. For the typical operating temperature range in a FBC, this sulphate forms a eutectic that is considered to be responsible for causing agglomeration and defluidisation of ash and bed material (Manzoori, 1990). There is substantial evidence from the published literature that reactions also occur between sodium and silica/kaolin species in combustion systems (Halstead and

Raask, 1969, Wall et al., 1975, Lee and Johnson, 1980, Lee et al., 1985, Punjak et al., 1989, Uberoi et al., 1990) and during coal gasification (Bachovin et al., 1986, Kosminski and Manzoori, 1990).

The formation of sulphate under reducing environment is thermodynamically not favoured (Mojtahedi and Backman, 1989a). Hence, during the fluidised bed gasification of coal, silica present in coal may react with sodium and form liquid silicates, which, similar to sulphates in combustors, may cause ash agglomeration and bed defluidisation. However, the reactions of sodium and kaolin may form solid aluminosilicates and by that, reduce the amount of ash agglomeration.

Thermodynamic calculations have been conducted for gasification at atmospheric pressure in the temperature range of between 450°C and 950°C, to predict the equilibrium composition of reactions between sodium and silicon species present in a high-sulphur South Australian Lochiel coal. It is important to note that sulphur has a major influence on the products of sodium transformations. Theoretical predictions were also evaluated for an assumed sulphur-free coal and the results are reported elsewhere (Kosminski, 2000). However, this is outside the scope of objectives of the current thesis, which is directed solely at high-sulphur content coals typical in origin for South Australia.

3.3.1 Computational method

The calculations were performed using a CSIRO/MONASH THERMOCHEMISTRY SYSTEM VSN: 1.00 IBM-PC DOS system (Turnbull and Wadsley, 1994). This system has been developed for Gibbs free energy minimisation. A CHEMIX program, being part of this system, was used for calculations.

The CHEMIX program allows for reaction systems to be defined by specifying possible phases and their component species, the phase and quantities of each input component, the temperature and the pressure conditions. The program calculates possible equilibrium phases and their composition by minimising the total Gibbs free energy of the system. The thermodynamic data required for calculations are the standard Gibbs free energy of formation for all species. These data are included in the program data files and also can be introduced to the data files.

3.3.2 Reaction system

Calculations were conducted for reaction systems based on experiments conducted in this study. Calculations were performed for coal Lochiel coal containing on dry basis (d.b.) 3.2% sulphur and exposed to atmospheres of carbon dioxide, carbon monoxide, steam, hydrogen or nitrogen. A series of calculations were carried for the coal containing either organically-bound sodium or as sodium chloride and in the presence of silica or kaolin.

The quantities of sodium and silicon compounds present in coal and used in calculations on a coal dry basis were as follow:

- 1.0% sodium (organically-bound sodium)
- 1.0% sodium, 1.54% chlorine (sodium as NaCl)
- 1.0% sodium (organically-bound sodium), 10% kaolin
- 1.0% sodium (organically-bound sodium), 10% silica
- 1.0% sodium, 1.54% chlorine (sodium as NaCl), 10% kaolin
- 1.0% sodium, 1.54% chlorine (sodium as NaCl), 10% silica

The total mass input used in calculations was the sum of the quantities of individual elements of carbon, sulphur, hydrogen, oxygen, nitrogen, silicon, sodium and chlorine present in coal and in reacting gas. Levels of sodium and silicon were corresponding to the levels of concentration of sodium and silicon in coal used in experiments. Quantities of carbon dioxide or steam reacting with coal used in the calculations corresponded to a flow of 4 litres per minute passing for 15 minutes over 1 gram of coal containing controlled amounts of sodium and silicon compounds. The amounts of carbon dioxide and steam were several times higher than required by stoichiometry for full gasification of coal.

The temperature range used in calculations was from 450°C to 950°C in incremental steps of 50°C. The calculations were carried out for atmospheric pressure conditions. Table 3.1 lists the chemical species that were considered as possible product phases and system component species for the thermodynamic equilibrium predictions.

Table 3.1 Chemical species considered as possible product phases and system component species for the thermodynamic equilibrium predictions.

Gas phase:	CO, CO ₂ , CH ₄ , H ₂ O, H ₂ , N ₂ , O ₂ , Cl, HCl, NH ₃ , NaOH, NaCl, Na ₂ Cl ₂ , Na, H ₂ S, CS, CS ₂ , COS, SO ₂ ,
Liquid phase:	
Melt 1:	NaCl, NaOH, Na ₂ CO ₃ , Na ₂ S, Na ₂ SO ₄
Melt 2:	SiO ₂ , Na ₂ O, Na ₂ SiO ₃ , Na ₂ Si ₂ O ₅ , NaAlSiO ₄ , NaAlSi ₂ O ₆ , NaAlSi ₃ O ₈
Solid phase:	C, S, Na, Na ₂ SO ₄ , Na ₂ S, NaOH, Na ₂ O, NaCl, Na ₂ CO ₃ , SiO ₂ , Na ₂ SiO ₃ , Na ₂ Si ₂ O ₅ , Na ₄ SiO ₄ , Na ₆ Si ₂ O ₇ , Al ₂ O ₃ , NaAlO ₂ , NaAlSiO ₄ , NaAlSi ₂ O ₆ , NaAlSi ₃ O ₈ , Al ₂ SiO ₅ , Al ₂ Si ₂ O ₅ .2H ₂ O, Al ₂ Si ₂ O ₇

3.3.3 System assumptions and limitations

Equilibrium compositions were calculated assuming that the gas mixtures were ideal. For solid phases it was assumed that all of the solid condensed species were immiscible and each was forming a separate phase. For atmospheric pressure conditions used in the calculations such an assumption is not a significant limitation on calculation results.

Two liquid phases were assumed for the systems: Melt 1, containing sodium salts and the Melt 2, containing oxides and silicates. Despite partial miscibility between some of the components of the two assumed phases, such as limited solubility of sodium sulphate in sodium silicates (Pearce and Beisler, 1965), generally the components of the two phases are mostly immiscible. Each phase was then assumed to be separate and in an ideal solution. The above assumptions do not reduce the risk of inaccuracies in calculations, which are subject to limitations of thermodynamic data accuracy. It is particularly important for the data on species at high temperatures. The computer program uses several data bases for the relevant species and it is believed that they are the most accurate data sets available.

Also, by assuming an ideal phase it was assumed for each of the phases that activity of a phase was equal to unity. This assumption may bear consequences of obtaining false results if activity of a phase is different from the assumed value. Harb et al. (1993) reported that

this may be the case for the liquid phase of silica, $\text{SiO}_2(\text{l})$. Harb et al. reported poor predictions for systems containing $\text{SiO}_2(\text{l})$.

3.4 DISTRIBUTION OF SODIUM SPECIES AT EQUILIBRIUM CONDITIONS

The mass, number of moles and the mole fractions for each component present at equilibrium for a given system were calculated for each phase possibly present as the reaction product. The distribution of each elemental species in the equilibrium products as a percentage of the total content of each element was also calculated. The results of sodium distribution for a high-sulphur Lochiel coal were calculated separately for each atmosphere; carbon dioxide, carbon monoxide, steam, hydrogen or nitrogen, and are presented graphically in Figures 3.1 to 3.6 and for silicon distribution in Figure 3.7.

The results for the combustion of all coal mixtures predict the formation at 800°C of liquid sodium sulphate, representing all sodium present in coal regardless of sodium form or the presence of silica or kaolin. Several exceptions from the norm were predicted for coal containing kaolin and either form of sodium, with approximately 20 to 30% of total sodium expected to form liquid aluminosilicate, albite above 750°C . While some 20% of sodium present in coal as sodium chloride is predicted to exist at equilibrium as sodium chloride vapour above 900°C .

3.4.1 Coal containing organically-bound sodium.

This section presents the results of equilibrium calculations for a coal containing 1% d.b. organically-bound sodium. The results are presented in Figure 3.1.

3.4.1.1 Effect of nitrogen and hydrogen atmosphere

The results of the equilibrium distribution of sodium species after exposure of coal to nitrogen atmosphere are presented in Figure 3.1a. Sodium sulphide is predicted to be the dominant sodium species in the temperature range of 450°C to 900°C and it will be the only sodium species thermodynamically favoured up to 800°C . Sodium vapour will start to form at 800°C and will reach nearly 35% of the total sodium at 950°C temperature. A hydrogen atmosphere has the same effect as pyrolysis in nitrogen.

3.4.1.2 Effect of carbon monoxide atmosphere

In a carbon monoxide environment (Figure 3.1b) sodium is predicted to be present as solid carbonate below 800°C. At 800°C, solid sodium sulphide is predicted to be the stable species at equilibrium and metallic sodium vapour will also appear. At 950°C, half of the sodium will be in this vapour phase.

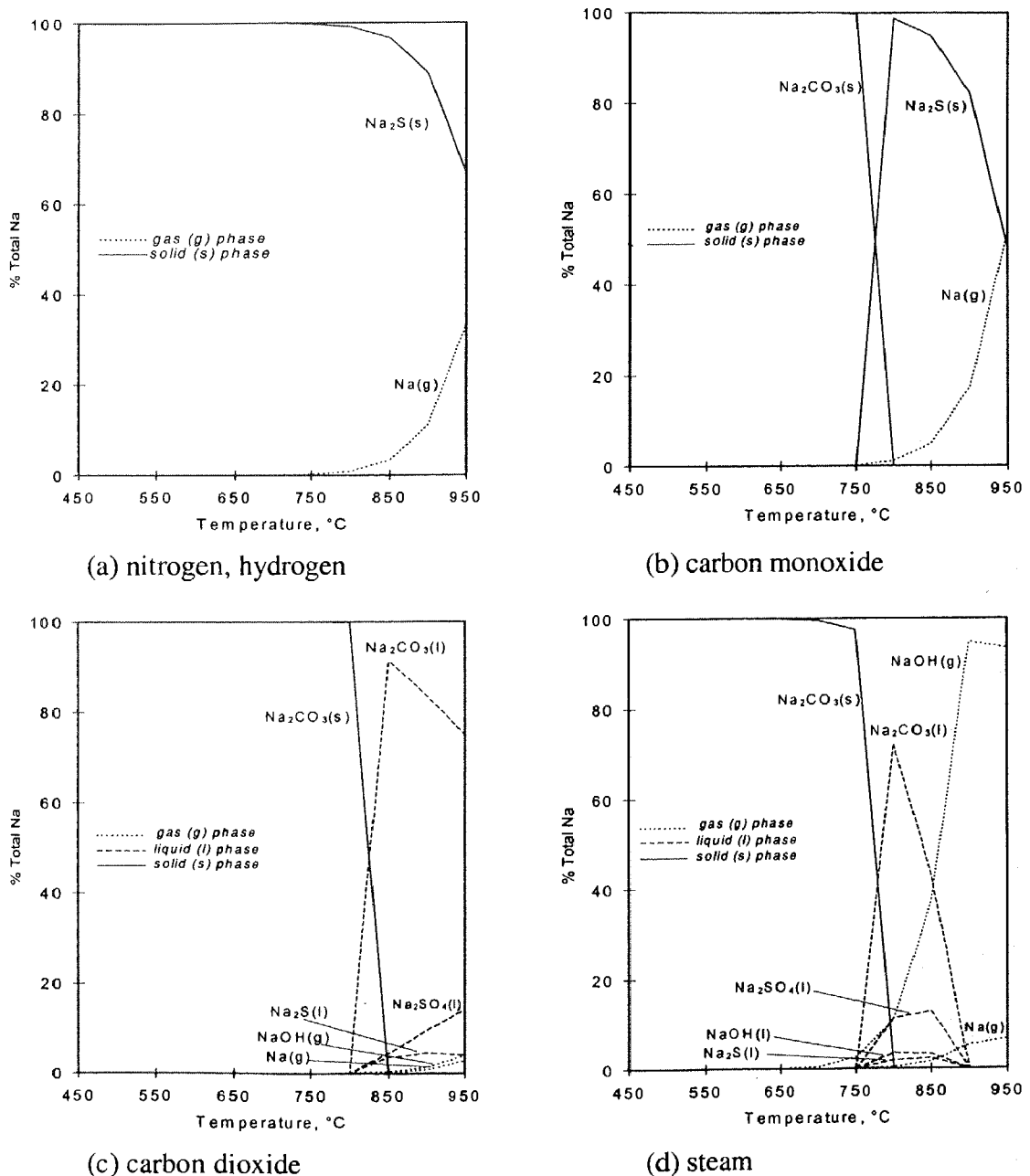


Figure 3.1 Equilibrium distribution of the sodium species from sulphur-rich coal containing 1% d.b. organically-bound sodium, in atmospheres of (a) nitrogen or hydrogen, (b) carbon monoxide, (c) carbon dioxide and (d) steam at 1 atmosphere pressure.

3.4.1.3 Effect of steam atmosphere

The gasification of coal in steam atmosphere shows a more complex situation, as presented in Figure 3.1d, compared with carbon dioxide gasification. Solid sodium carbonate will melt into liquid at 800°C, which is 50°C lower than in predictions for carbon dioxide gasification. Additionally, above 750°C some sodium is predicted to be present as gaseous sodium hydroxide. The carbonate liquid phase is predicted to be the dominant sodium specie between 800°C and 850°C, with up to 75% of total sodium predicted to exist in this form at 800°C. At equilibrium at 850°C 50% of the sodium is predicted to be in the vapour phase as sodium hydroxide. Condensed phases should disappear above 900°C and sodium hydroxide in vapour is predicted as the dominant volatilised sodium form.

3.4.1.4 Effect of carbon dioxide atmosphere

During the gasification of coal with carbon dioxide, solid phase sodium carbonate is predicted as only sodium specie below 850°C. At 850°C solid sodium carbonate will melt into a liquid phase (Figure 3.1c). The formation of some liquid sodium sulphate and sodium sulphide are also predicted for temperatures above 800°C, with sodium carbonate retaining 80% of the total sodium at 950°C.

Sodium carbonate melts in air at 851°C. The prediction of it melting at 800°C in the steam atmosphere is in a fair agreement with the experimental data reported by Song and Kim (1993) and Huttinger and Minges (1985) who have reported, as presented in Section 2.3.2.2, that sodium carbonate melts at lower temperature in an environment in which steam is present.

The fact that the carbonate melts in a steam atmosphere at lower temperature than in the other atmospheres may increase the possibility of carbonate reactions with minerals, such as silica and kaolin present in coal.

3.4.2 Coal containing sodium as sodium chloride

The equilibrium distribution of sodium product species from coal containing 1% d.b. sodium chloride are presented in Figure 3.2. The results of equilibrium calculations for all the tested gas atmospheres are basically very similar.

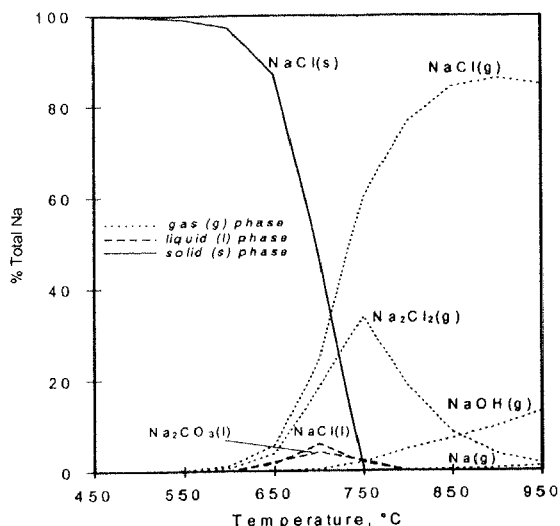


Figure 3.2 Equilibrium distribution of the sodium species from sulphur-rich coal containing 1% d.b. sodium as sodium chloride in atmospheres of steam and at 1 atmosphere pressure.

A solid phase of sodium chloride is predicted to be dominant specie below 750°C in all atmospheres. At and above 750°C, sodium is predicted to exist almost entirely in the vapour phase as sodium chloride, as both monochlorides and dichlorides, in all but hydrogen atmosphere. In hydrogen, full sodium chloride evaporation will take place at 800°C. Negligible metallic sodium vapour is predicted above 850°C for other than steam atmospheres. Some sodium hydroxide vapour is predicted to form above 750°C in steam, but not exceeding 10% of the total sodium at 950°C. A negligible part of less than 5% of the total sodium is predicted in the temperature range of between 650 to 750°C to form liquid phase sodium chloride and sodium carbonate for gasification with steam and carbon dioxide.

3.4.3 Coal containing organically-bound sodium and kaolin

Calculations have been performed for coal containing 1% d.b. of organically-bound sodium and 10% d.b. of kaolin $\text{Al}_2\text{O}_3 \cdot 2\text{SiO}_2 \cdot 2\text{H}_2\text{O}$. The results of the calculations presented in Figure 3.3 are very similar for all tested atmospheres showing no influence of individual gaseous conditions on the distribution of sodium species.

A solid phase sodium aluminosilicate nepheline, $\text{NaAlSi}_3\text{O}_8$ is predicted to be the dominant sodium specie in the temperature range between 450°C and 950°C as shown in Figure 3.3. Another solid aluminosilicate phase, albite $\text{NaAlSi}_3\text{O}_8$, is predicted to combine 20% of the

total sodium below 650°C. This solid phase of albite is predicted to melt completely at 700°C and the liquid albite together with some liquid nepheline will dominate the liquid phase from 700°C to 950°C. The total content of the sodium in the liquid aluminosilicate phase is predicted to be 20% at 700°C and 30% at 950°C.

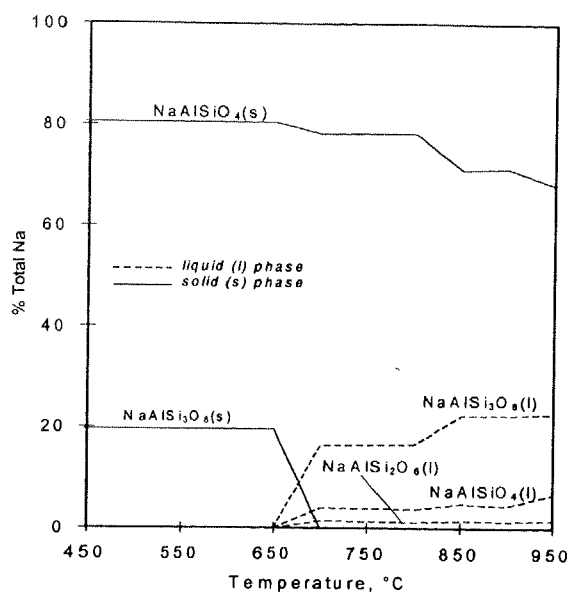


Figure 3.3 Equilibrium distribution of the sodium species from sulphur-rich coal containing 1% d.b. organically-bound sodium and 10% d.b. kaolin in atmospheres of carbon dioxide, carbon monoxide, steam or hydrogen at 1 atmosphere pressure.

Elemental sodium vapour is predicted to form only in pyrolysis conditions in nitrogen. The vaporisation of sodium will start above 800°C with up to 20% of the total sodium predicted to be in the metallic sodium vapour phase at 950°C.

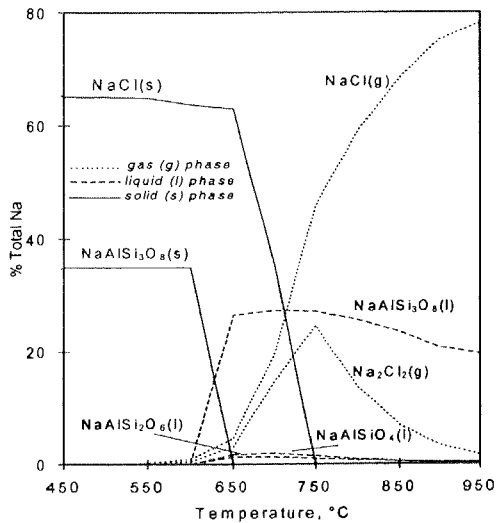
3.4.4 Coal containing sodium chloride and kaolin

Results of calculations carried out for the coal containing 1% d.b. sodium as NaCl and 10% d.b. of kaolin presented in Figure 3.4 are showing significant influence of a gas atmosphere on distribution of sodium species at equilibrium conditions.

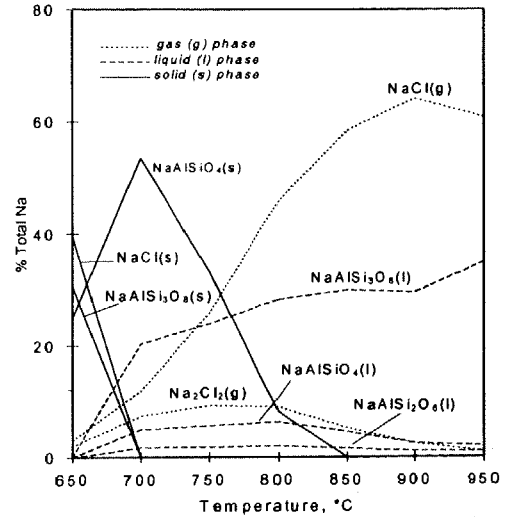
3.4.4.1 Effect of nitrogen atmosphere

During pyrolysis in nitrogen, sodium is predicted to exist in the solid phase up to 700°C, with two thirds of total sodium present as sodium chloride and one-third as sodium aluminosilicate albite (Figure 3.4a). At 650°C, albite is predicted to melt. This prediction is 50°C lower than the prediction for the organically-bound sodium for gasification of coal

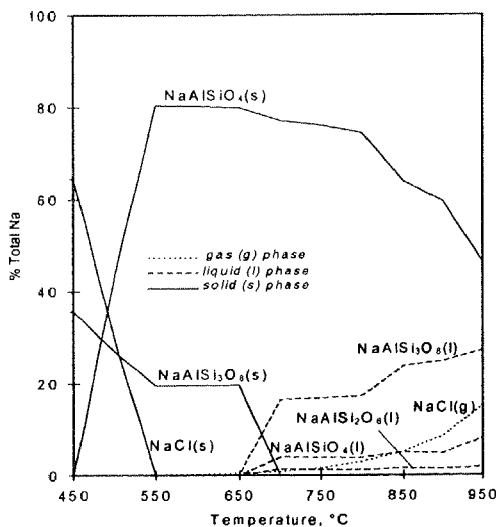
with carbon dioxide or with steam. Vaporisation of sodium chloride is predicted to start at 650°C, and sodium chloride vapour will become dominant sodium specie at 750°C. No solid sodium chloride phase is predicted to be present at this and above temperatures.



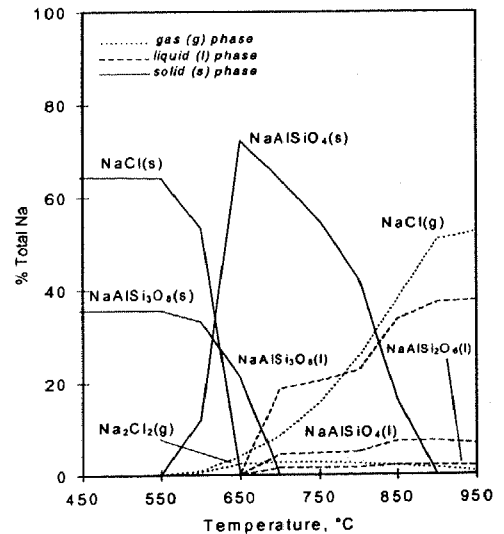
(a) nitrogen



(b) carbon monoxide



(c) steam



(d) carbon dioxide

Figure 3.4 Equilibrium distribution of the sodium species from sulphur-rich coal containing 1% d.b. sodium as sodium chloride and 10% d.b. kaolin in atmospheres of (a) nitrogen or hydrogen (b) carbon monoxide, (c) steam and (d) carbon dioxide at 1 atmosphere pressure.

3.4.4.2 Effect of carbon monoxide atmosphere

Exposure to a carbon monoxide atmosphere (Figure 3.4b) is predicted to result in a somewhat similar product distribution to that predicted for the pyrolysis in nitrogen but for

temperatures above 800°C. Sodium chloride vapour is predicted to be the major species above 800°C. Liquid albite is predicted to exist above 700°C with 30% of the total sodium to be in this form. A solid nepheline is predicted as major sodium specie up to 750°C but disappears above 800°C.

3.4.4.3 Effect of steam atmosphere

During gasification with steam for coal containing sodium chloride and kaolin, sodium is predicted to exist as a solid phase, mainly as nepheline between 550°C and 950°C, as shown in a Figure 3.4c. Albite in the solid phase is predicted as another, more thermodynamically stable solid phase below 650°C.

A liquid phase containing mostly albite is predicted to form above 650°C with 20% of the total sodium at 700°C and 30% of the total sodium at 950°C. Only up to 10% of total sodium is predicted to be in the vapour phase as sodium chloride for temperatures above 850°C.

The results for the effect of steam on the distribution of sodium species clearly show that the solid nepheline is predicted as the dominant phase for a wide temperature range and that at equilibrium, there should be much less vapour and liquid phase formation than in the nitrogen or the carbon dioxide atmospheres.

3.4.4.4 Effect of carbon dioxide atmosphere

The predictions for carbon dioxide atmosphere, as presented in Figure 3.4d, show that nepheline molecular structure should be the dominant sodium species between 650°C and 800°C, while solid sodium chloride and solid albite are more thermodynamically stable species below 650°C. The formation of the albite liquid phase is predicted to commence at 700°C, which is 50°C higher than for pyrolysis conditions in nitrogen.

A steady increase of sodium chloride vapour is predicted from 650°C. Some 60% of the total sodium should be in the sodium chloride vapour form at and above 800°C, with the liquid aluminosilicates predominantly albite taking the rest of the sodium.

3.4.4.5 Effect of hydrogen atmosphere

Exposure to a hydrogen atmosphere is predicted to result in similar product distribution to that observed in pyrolysis conditions. The main difference being that in a hydrogen atmosphere the solid phases of both albite and sodium chloride, are predicted to exist up to 800°C, which is a temperature 50°C higher than that predicted for the nitrogen atmosphere. The same influence of hydrogen atmosphere on sodium chloride evaporation was observed for coal containing only sodium chloride.

All the calculation results for coal containing sodium chloride and kaolin show that in the temperature range of between 450°C to 950°C, the final sodium products can be expected to exist in all phases, with almost all of the sodium in the form of solid nepheline during gasification with steam, or mainly sodium chloride vapour for coal pyrolysed in nitrogen.

This shows how widely sodium forms can change and that these forms do depend on the gas composition of the gasifier.

3.4.5 Coal containing organically-bound sodium and silica

Calculations were performed for coal containing 1% d.b. organically-bound sodium and 10% d.b. silica SiO₂. The results are presented in Figure 3.5 and show similarity to the results for coal containing organically-bound sodium and kaolin for all tested gasification and pyrolysis atmospheres. No influence of individual gaseous conditions on sodium species distribution is predicted for temperatures below 850°C. Only in nitrogen atmosphere some 10% of the total sodium is predicted to form elemental sodium vapour above 850°C.

No solid phases at equilibrium conditions above 600°C are predicted to exist. A liquid phase is predicted above 600°C and is to contain sodium disilicate Na₂Si₂O₅(l), accounting for 90% of the total sodium, and sodium metasilicate Na₂SiO₃(l) accounting for the rest of the sodium.

These predictions indicate the formation of the liquid phase at temperatures approximately 200°C lower than that observed experimentally for Na₂O-SiO₂ systems (Levin et al., 1979). This may be caused by the fact that the system is not able to predict the immiscibility gap

often found in silica-rich systems (Harb et al., 1993). Such is the case with the coal tested in these calculations, where silica forms 90% of the total inorganic element input. Silica is known to polymerise in the liquid phase. Consequently, the liquid phase may contain silica species not introduced in calculated reaction system.

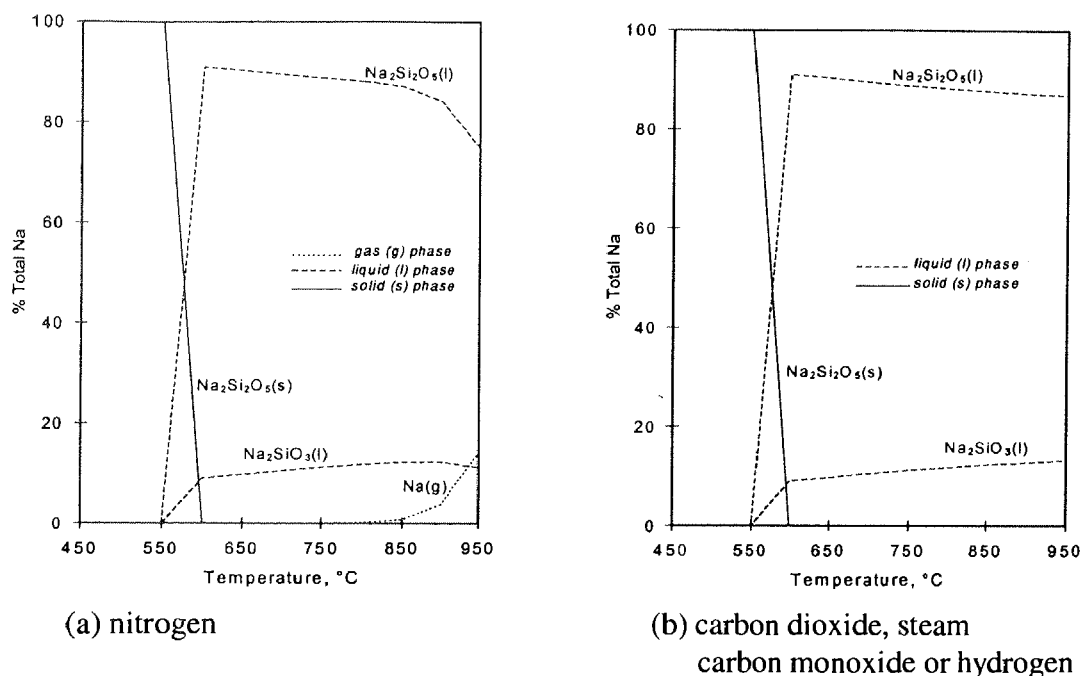


Figure 3.5 Equilibrium distribution of the sodium species from sulphur-rich coal containing 1% d.b. organically-bound sodium and 10% d.b. SiO_2 in atmospheres of (a) nitrogen and (b) carbon dioxide, carbon monoxide, steam or hydrogen at 1 atmosphere pressure.

Substituting silica by a single more complicated silica species such as Si_2O_4 or Si_4O_8 instead of SiO_2 in the liquid phase may give an improved agreement between experimental and calculated results. But the extent of the silica polymerisation varies with silica concentration and with the temperature. This represents a problem in choosing a single silica specie to reflect experimental results over the range of conditions for a given system.

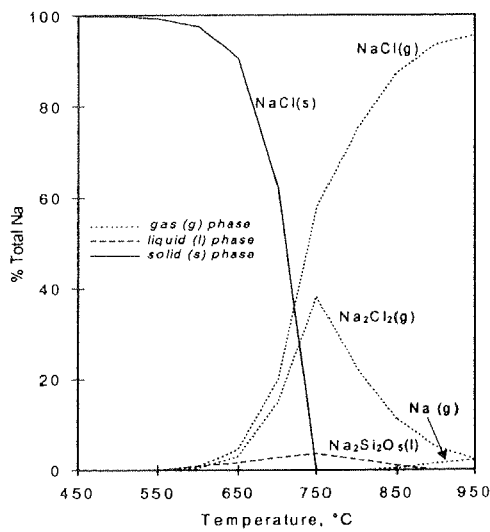
The differences between predictions and published experimental data reinforce the need for experimental investigations of the behaviour of the sodium and the silica present in coal gasified under various conditions.

3.4.6 Coal containing sodium chloride and silica

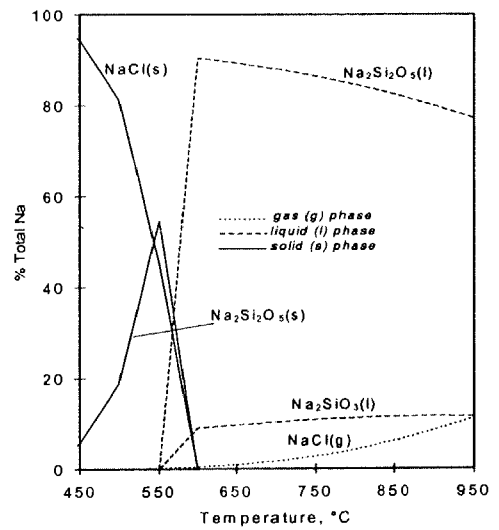
Calculations were carried out for the coal containing 1% d.b. sodium in the form of sodium chloride and also containing 10% d.b. silica. The results are presented in Figure 3.6.

3.4.6.1 Effect of nitrogen atmosphere

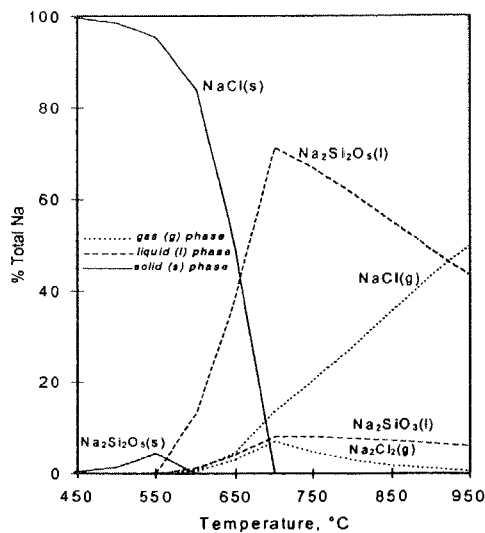
For pyrolysis in nitrogen conditions, sodium present as the solid sodium chloride is predicted to be the dominant sodium species below 700°C (Figure 3.6a). Sodium chloride vaporisation is predicted to commence at 650°C and its vapour will contain more than 98% of total sodium at 750°C. The remainder of the total sodium is attributed to a liquid silicate phase of sodium disilicate.



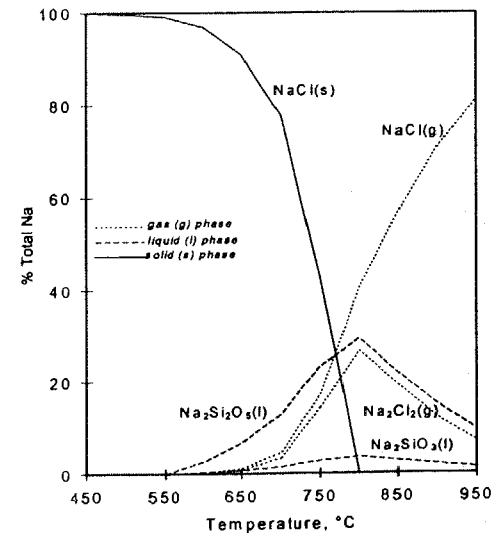
(a) nitrogen



(b) steam



(c) carbon dioxide

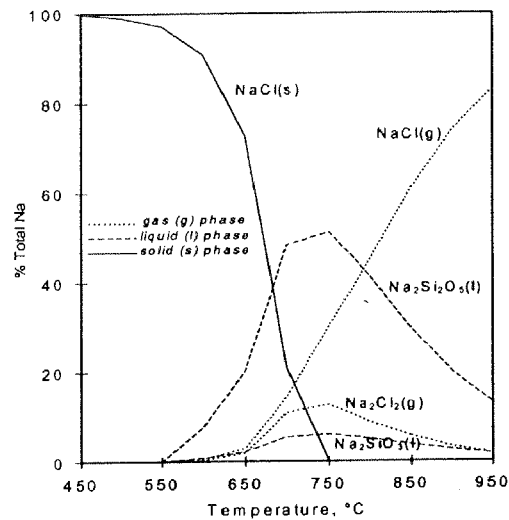


(d) hydrogen

Figure 3.6 Equilibrium distribution of the sodium species from sulphur-rich coal containing 1% d.b. sodium as NaCl and 10% d.b. SiO₂ in atmospheres of (a) nitrogen, (b) steam, (c) carbon dioxide, (d) hydrogen and (e) carbon monoxide at 1 atmosphere pressure.

3.4.6.2 Effect of steam atmosphere

For gasification with steam as shown in Figure 3.6b, the predicted equilibrium distribution shows that at and above 600°C, 90% of the sodium exists in the liquid phase as silicates, principally as sodium disilicate. Some less than 10% of the sodium is predicted to be at 950°C as gaseous sodium chloride.



(e) carbon monoxide

Figure 3.6 Continuation.

3.4.6.3 Effect of carbon dioxide atmosphere

During gasification with carbon dioxide, the solid phase of sodium chloride is predicted to be the dominant sodium specie up to 600°C, with the liquid phase of sodium disilicate $\text{Na}_2\text{Si}_2\text{O}_5(\text{l})$ predicted to contain 50% of total sodium at 650°C. No solid phase containing sodium is predicted at and above 700°C. A steady increase of the NaCl vapour phase is predicted from 650°C and this vapour phase will contain 50% of the total sodium at 950°C.

3.4.6.4 Effect of hydrogen atmosphere

For coal exposed only to a hydrogen atmosphere, solid sodium chloride is the most stable sodium specie below 800°C as shown in Figure 3.6d. Sodium chloride vapour is predicted to be the dominant sodium species at and above 800°C. A liquid phase of sodium disilicate $\text{Na}_2\text{Si}_2\text{O}_5(\text{l})$, is predicted to be present in the temperature range of Between 600°C to 950°C and would contain up to 30% of the total sodium.

3.4.6.5 Effect of carbon monoxide atmosphere

Exposure to carbon monoxide atmosphere is predicted to result in similar equilibrium distribution of the sodium species to that predicted for the carbon dioxide gasification. However, more sodium chloride vapour will form under carbon monoxide conditions. Almost 50% of the sodium is predicted to be in the sodium chloride vapour at 750°C and 80% at 900°C, as shown in Figure 3.6e. Solid sodium chloride should exist below 700°C. Liquid silicates are predicted to start forming at 600°C and their liquid phase would contain some 50% of sodium at 750°C.

3.4.7 Silicon distribution

Equilibrium calculations to predict the distribution of silicon species in the products are also considered important for reference. For example, gaining knowledge on whether liquid silica additionally to liquid silicates or aluminosilicates will form during coal gasification.

3.4.7.1 Coal containing organically-bound sodium and silica

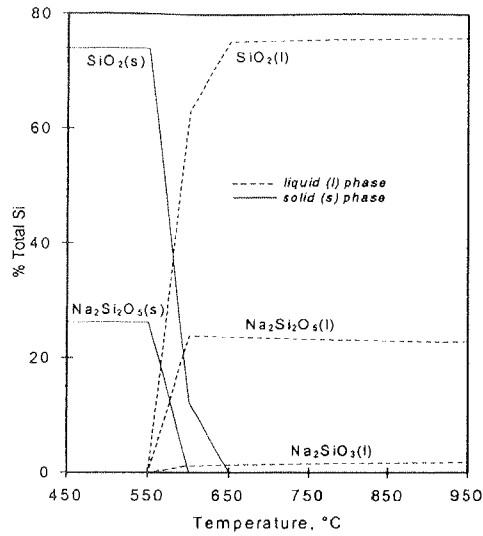
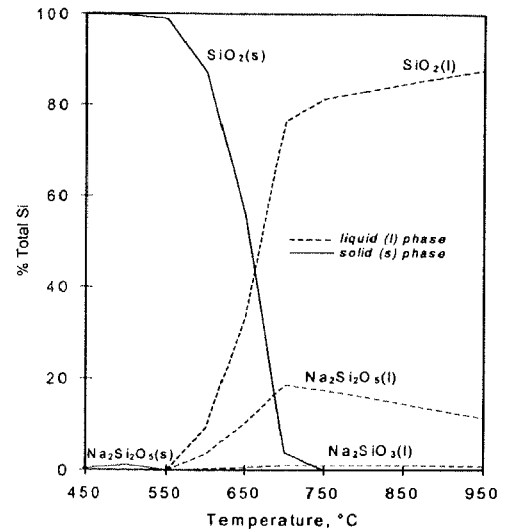
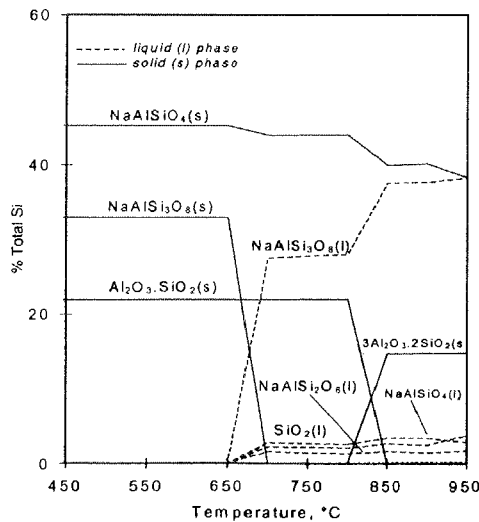
Gasification with carbon dioxide of coal containing organically-bound sodium and silica is predicted to result in 90% of the silicon in the liquid phase above 600°C. Above 600°C, all the silicon is predicted to exist in the liquid phase; three quarters as liquid silica SiO_2 (l), and the rest as silicates, mainly $\text{Na}_2\text{Si}_2\text{O}_5$ (l), as shown in Figure 3.7a.

3.4.7.2 Coal containing sodium chloride and silica

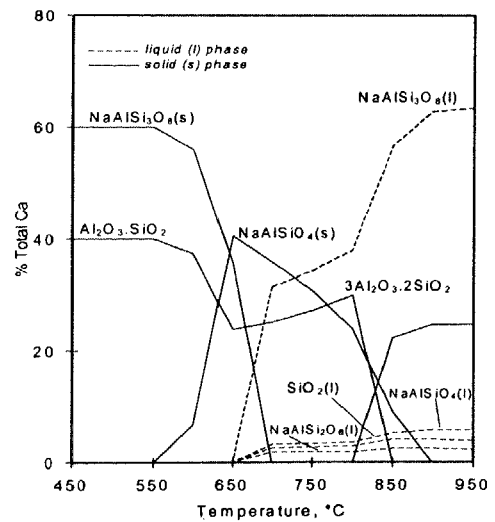
Gasification in carbon dioxide of the coal containing sodium chloride and silica is predicted to result in a similar distribution of silica species as predicted for coal containing organically-bound sodium. However, as shown in Figure 3.7b, full melting of silica into liquid SiO_2 (l) is predicted at 700°C, while for the other coal it is predicted to be at 600°C. The liquid phase silica should form 80% of the silicon liquid phase and sodium disilicate $\text{Na}_2\text{Si}_2\text{O}_5$ (l) almost 20% of the that phase.

3.4.7.3 Coal containing organically-bound sodium and kaolin

Results presented in Figure 3.7c show that above 700°C and up to 950°C some 30% to 40% of the total silicon is predicted to be present in the liquid phase, mostly as albite. Liquid silica SiO_2 (l) may consist of some 20% of the liquid phase. The solid phases above 850°C are predicted to be mullite $3\text{Al}_2\text{O}_3 \cdot 2\text{SiO}_2$ forming from the disappearing $\text{Al}_2\text{O}_3 \cdot \text{SiO}_2$.

(a) 1% organically-bound sodium and 10% SiO₂(b) 1% sodium as NaCl and 10% SiO₂

(c) 1% organically-bound sodium and 10% kaolin



(d) 1% sodium as NaCl and 10% kaolin

Figure 3.7 Equilibrium distribution of the silicon species from sulphur-rich coal containing (a) 1% d.b. organically-bound sodium and 10% SiO₂, (b) 1% d.b. sodium as NaCl and 10% SiO₂, (c) 1% d.b. organically-bound sodium and 10% kaolin and (d) 1% d.b. sodium as NaCl and 10% kaolin during gasification in carbon dioxide at 1 atmosphere pressure.

3.4.7.4 Coal containing sodium chloride and kaolin

Carbon dioxide gasification of coal containing sodium chloride and kaolin is predicted to result in the distribution of silicon as presented in Figure 3.7d. A liquid phase, mostly

albite, is predicted to exist above 650°C and contain 30% of the total silicon at 700°C and 80% above 850°C. In the temperature range of 650°C to 850°C, the solid phases are predicted to be nepheline and aluminosilicate $\text{Al}_2\text{O}_3 \cdot \text{SiO}_2$, and above the 850°C mullite $3\text{Al}_2\text{O}_3 \cdot 2\text{SiO}_2$ is predicted as only solid silicon phase.

These results show that at and above 850°C, the gasification of coal containing kaolin and organically-bound sodium will result in 55% of total silicon existing in a solid form, while if sodium is in the form of sodium chloride, only 20% of the silicon will exist in a solid form at equilibrium conditions.

3.5 SUMMARY

The results reported here for the thermodynamic equilibrium calculations show that during gasification of high-sulphur low-rank coal at temperature conditions characteristic for a fluidised bed gasification process, the distribution of sodium among the produced species will be a complex problem.

Sodium species formed in such a process will depend on the form of sodium in the coal, the gas atmosphere and the forms of silicon present in the coal. The dependence of the gas atmosphere is observable for behaviour of the organically-bound sodium and for behaviour of sodium chloride in the presence of silicon minerals.

The major findings of the work reported here are listed below.

- Organically-bound sodium is predicted to be transformed below 800°C into a solid phase of sodium sulphide in nitrogen and hydrogen atmospheres. In the same temperature range in atmospheres of carbon monoxide, carbon dioxide or steam, the sodium is predicted to form a solid phase of sodium carbonate.
- In nitrogen, hydrogen or in carbon monoxide, some elemental sodium vapour may form above 800°C. Liquid sodium carbonate is predicted as the dominant sodium species in either carbon dioxide or steam atmosphere above 850°C or 800°C, respectively.
- In a steam atmosphere, sodium hydroxide vapour is predicted as the major sodium form at and above 900°C.

- For the same coal burnt in air, molten sodium sulphate will form at 800°C and will be the only sodium species.
- Consequently, the gas composition in a gasifier can be expected to influence the nature of the sodium species formed. Gasifying coal in fluidised bed with air only, may result in liquid carbonate forming at 850°C, while gasification with air and steam may result in formation of this liquid phase at a lower temperature and also result in significant sodium volatilisation above 850°C.
- During gasification or pyrolysis of coal containing organically-bound sodium and kaolin, most of the sodium is predicted to react into a solid phase aluminosilicate nepheline with some 20 to 30% of the sodium forming liquid aluminosilicate phase at temperatures above 700°C.
- No influence of gas environment was predicted on transformations of sodium in coal containing organically-bound sodium and silica. Sodium silicates in liquid phase are predicted as the only sodium species at temperatures above 600°C.
- Sodium chloride vapour is predicted as the dominant sodium species above 750°C in carbon dioxide, carbon monoxide, steam or nitrogen, and in hydrogen above 800°C, when sodium was present in coal as sodium chloride. The gasification atmosphere was predicted to have little influence on sodium chloride transformations.
- For coal containing sodium chloride and kaolin, the chloride vapour will be the most dominant sodium species above 750°C for pyrolysis in nitrogen and above 800°C for reducing atmospheres of carbon monoxide or hydrogen. The solid phase of nepheline will be the dominant sodium species during gasification in steam and carbon dioxide in the temperature range of between 450°C and 950°C and 650°C and 800°C respectively.
- Also, for coal containing sodium chloride and kaolin, liquid aluminosilicate albite is predicted to contain 20 to 35% of total sodium in all atmospheres above 700°C. More liquid albite was predicted to form in a reducing atmosphere of hydrogen or carbon monoxide than during gasification with steam or carbon dioxide.
- If coal contains only sodium chloride and silica, sodium chloride vapour is predicted to be the dominant species at and above 750°C in nitrogen and 800°C in hydrogen atmosphere.

- In steam, all of the sodium chloride is predicted to form liquid silicates at 600°C. Less liquid silicates are to form under carbon dioxide gasification conditions, while very little liquid silicates are predicted to form in nitrogen or hydrogen atmospheres.
- The proportion of sodium in sodium chloride vapour is predicted to be the same for each atmosphere if either silica or kaolin were present in the coal.
- The results of the thermodynamic calculations also show that during gasification and pyrolysis, silica may transform into the liquid phase. When sodium is predicted to be present as liquid silicates, part of the silica not participating in the formation of silicates is predicted to be in the liquid phase as liquid silica. The existence of silica in the liquid phase may considerably contribute to increasing the mass of total liquid phase existing in a fluidised bed gasifier.
- Combustion of high-sulphur coal containing sodium and silica or kaolin is predicted to result in the formation of sodium sulphate. Silica is predicted to remain in the solid form. Given that a quantity of sodium will form sulphates during combustion of coal, the same amount of sodium may cause the formation of more liquid phase during gasification. If silica present in coal enters into the liquid phase additionally to the silicates formed, there will be substantial increase of the total liquid phase in the gasifier. However, the formation of liquid phase silicate will depend on the reaction rates between sodium and silica. Consequently, there is substantial likelihood for agglomeration of ash from sulphur-rich coal during coal gasification, similarly to what happens during combustion of such coal.
- The results from the thermodynamic prediction also show that during pyrolysis or gasification, other than in steam, there is greater reactivity of organically bound-sodium with silica in comparison with sodium chloride reactivity with silica. This will lead to more liquid phase formation from organically-bound sodium and greater likelihood of agglomeration if this form of sodium is present in coal. The formation of sodium chloride vapour will cause problems in cooler parts of gasifier due to condensation of its vapour.

Chapter 4

EXPERIMENTAL WORK

4.1 INTRODUCTION AND OBJECTIVES

This chapter presents description of the experimental equipment, experimental technique and materials used in the present study.

The experimental program has been designed to achieve a better understanding of how sodium and silicon influence the process of fluidised bed gasification of low-rank coal, with the following objectives:

- To determine the transformations of sodium during pyrolysis and gasification of coal.
- To establish the extent of vaporisation of sodium from coal during pyrolysis and gasification.
- To establish conditions and mechanisms of reactions between sodium and silicon minerals during coal pyrolysis and gasification.
- To establish the influence of gasification environment, steam and carbon dioxide on the transformations of sodium and its reactions with silicon minerals.
- To determine the catalytic activity of various forms of sodium present in the coal.
- To determine the rate of conversion of char during gasification with steam and carbon dioxide and obtain a relation of the conversion and reaction time for gasification of coal under various conditions.

To achieve these aims, the strategy was to use a simple reaction system to pyrolyse and gasify the coal. Synthetic coals, in which the concentrations, physical sizes, forms and distribution of inorganic constituents were controlled and known, were used.

To verify and support this investigation on the interactions between sodium and silicon minerals present in the coal, a separate investigation was carried out on a series of specially prepared mixtures of just sodium salts and silica and kaolin. These mixtures were exposed to the same experimental conditions as synthetic coal samples.

4.2 COAL PREPARATION

The low-rank coals of interest to be investigated occur in large deposits in the states of South Australia and Victoria and are in sufficient abundance to be considered for utilisation in a commercial-scale gasification process and the reason, for which this study was initiated. Although these coals differ in their inorganic components, they all contain silica and silica-based minerals, sodium, chlorine and sulphur. Therefore, preparation of the synthetic coals for this study was based on one of the South Australian lignites, Lochiel coal, which generally contains high levels of sulphur, sodium and chlorine.

Eight synthetic coals were prepared to contain various desired concentrations and forms of sodium and silicon minerals for the pyrolysis and gasification program. The aim was to prepare the coal particles of a size characteristic for use in a fluidised bed with properties similar to the general low-rank coals, but with known and controlled physical forms, size and distribution of inorganic components.

A low-mineral Lochiel coal was used for the preparation of synthetic coals. Several pockets of coal with unusually low minerals content were found within Lochiel trial pit and a large sample of coal was collected for this research work. This coal has all the characteristics of "normal" run-of-mine Lochiel coal, but it has a very low content of mineral inclusions with an inorganic matter content of 8-10% on dry basis. The inorganic matter is based on cations in ion-exchangeable forms. Run-of-mine Lochiel coal typically contains 14-16% on dry basis of inorganic matter, based on the additional contribution of both silica and other mineral bearing inclusions. The analyses of low-mineral Lochiel coal and of run-of-mine coal are presented in Table 4.1.

Table 4.1 Analysis of Lochiel coal.

Coal analysis:	Low-mineral coal	Acid-washed low-mineral coal	Run-of-mine coal
Proximate analysis, % wt			
Moisture	61.1	-	60.3
Ash, d.b.	10.3	3.9	15.7
Volatile matter, d.b.	49.2	54.3	46.2
Fixed carbon, d.b.	40.5	41.8	38.1
Additional assays, % wt. d.b.			
Sulphur	3.4	3.5	3.5
Sodium	0.9	0.00	1.0
Chlorine	0.9	0.01	0.5
Ash composition, %wt.			
Fe ₂ O ₃	4.26	2.95	4.05
Al ₂ O ₃	7.93	14.5	8.30
SiO ₂	4.04	79.0	31.40
CaO	13.80	0.85	9.97
MgO	16.95	0.54	8.58
K ₂ O	0.25	0.00	0.30
Na ₂ O	11.53	0.90	8.68
SO ₃	38.55	1.22	27.54
TiO ₂	0.10	-	0.48

The soluble minerals and ion-exchangeable cations were removed from this low-rank coal by prolonged leaching with cold acid. Sodium and silicon minerals were then added to the coal. Sodium was added in the form of sodium acetate or sodium chloride.

Table 4.2 Analyses of additives Silica (quartz) and Kaolin used in preparation of synthetic coals.

Additive:	Composition, %wt.	
	Silica (quartz)	Kaolin
SiO ₂	97.3	46.8
Al ₂ O ₃	1.27	38.3
Fe ₂ O ₃	0.10	0.70
CaO	0.02	0.03
MgO	0.04	0.22
Na ₂ O	0.02	0.10
K ₂ O	0.10	0.95
L.O.I.*	0.58	13.5

*L.O.I. - Loss on ignition determined at 950°C.

Commercial grade, high purity silica was added to coals to simulate the coal quartz content. The silica size was chosen between 25 and 36 µm, as to best represent the range of

sizes of quartz present in Lochiel and other coals (Lindner, 1988). Analytical grade washed kaolin with a particle size 80% less than 10 μm , was added to selected samples. Analysis of the silica (quartz) and kaolin used in preparation of synthetic coals are presented in Table 4.2.

The following outlines all steps taken to prepare the synthetic coals.

4.2.1 Coal leaching technique

A batch of low-mineral Lochiel coal was crushed to less than 10 mm particle size and air dried to approximately 15% moisture content. The coal was then pulverised in a laboratory scale Richmond mill to a particle size less than 125 micron, with 70 per cent being in the size range between 38 and 125 microns. Approximately 4 kg of air dried pulverised coal was leached in a large plastic drum with 2N hydrochloric acid with the ratio of coal to acid equal 1:10. Leaching was carried out for approximately 60 hours with frequent stirring of the drum content. After leaching, the leachate was decanted and coal rinsed with deionised water and allowed to settle. This process was repeated until the pH of filtrate water was exceeding 4.5 units. The water was then decanted and coal was filtered out using a vacuum Böhem filter. The filtered coal was rinsed with deionised water until Cl^- ions were not detectable in the filtrate using silver nitrate as the indicating solution.

This prepared sample is denoted in the text as low-mineral Lochiel acid-washed (LAW) coal. The coal was analysed for sodium content and was determined to be below 0.02% of the coal on a dry basis. The moisture content was approximately 60%.

4.2.2 Choice of specific compositions for preparation of synthetic coals

Synthetic coals were prepared to contain on dry basis a combination of 1% sodium and 10% of silica or kaolin as coal mineral matter. The levels of both sodium and silicon minerals were chosen as they the best represent concentrations of sodium and the characteristic of ash content for high-sulphur South Australian coals, particularly Lochiel coal. They also represent a ratio of sodium to silicon oxide in coal similar to that in the coals listed in Table 4.3. By considering the levels of chlorine present, approximately half of the sodium in the Lochiel coal could be associated with chlorine (NaCl) and the other half present as organically-bound sodium.

Table 4.3 Typical levels of sodium and silicon oxides in South Australian Bowmans and Lochiel coals and Victorian Loy Yang coal.

Coal	Lochiel	Bowmans	Loy Yang
Ash value, % wt. d.b.	15.7	11.6	1.6
Na in coal, % wt. d.b.	1.0	1.4	0.07
SiO ₂ in ash, %	31.4	29.1	21.2
Na ₂ O in ash, %	8.7	15.0	9.5
Ratio Na/SiO ₂ in coal	0.202	0.415	0.206

It was decided for best representation of the sodium and silicon oxide content in an Australian lignite coal, to prepare batches of coal on dry basis (d.b.) containing a combination of 1% sodium as either organically-bound or as sodium chloride and with or without 10 % silica or kaolin. Table 4.4 shows designations for prepared synthetic coals.

4.2.3 Preparation of coal samples

Preparation of each coal listed in Table 4.4 was in two stages:

- preparation of the chemically altered coal with minerals added where required, and
- preparation of coal slurry, drying the slurry and obtaining the required coal particle size.

A commercially available kitchen blender was used for blending the coal and additives into a slurry. A 3N sodium acetate solution based on Analytical Reagent grade sodium acetate was used to prepare coal with organically-bound sodium. A 15% concentration of sodium chloride solution adjusted with nitric acid HNO₃ to a pH value of approximately 1.0 was used to prepare the coal with sodium in the form of sodium chloride. The pH adjustment was needed to prevent sodium from exchanging with a proton on the coal ion-exchangeable groups.

NA1 coal

300 grams (d.b.) of wet LAW acid-washed coal and approximately 400 ml of 3N sodium acetate solution were mixed in a plastic container and left for 24 hours. The mixture was frequently stirred. The coal was then filtered out in a vacuum Böhem filter and rinsed with 250 ml of de-ionised water. The prepared coal was used directly for preparation of coal slurry.

NA1S and NA1K coals

300 grams (d.b.) of wet LAW acid-washed coal and approximately 400 ml of 3N sodium acetate solution were mixed in a plastic container and left for 24 hours. The mixture was frequently stirred. The coal was then filtered out in a vacuum Böhem filter and rinsed with 250 ml of de-ionised water. The prepared coal was blended with 33 grams of silica or kaolin and used directly for preparation of coal slurry.

NC1 coal

300 grams (d.b.) of wet LAW acid-washed coal and 52 grams of 15% concentration sodium chloride solution were blended into slurry together with an additional small amount of de-ionised water.

NC1S and NC1K coals

300 grams (d.b.) of wet LAW acid-washed coal and 52 grams of 15% concentration sodium chloride solution were blended into slurry together with 15 grams of silica or kaolin and an additional small amount of de-ionised water.

NA4 coal

200 grams (d.b.) of air dry LAW acid-washed coal and approximately 400 ml of 5N sodium acetate solution were mixed in a plastic container and left for 24 hours. The mixture was frequently stirred. The coal was then filtered out in a vacuum Böhem filter and rinsed with 250 ml of de-ionised water. The prepared coal was used directly for preparation of coal slurry.

NC4 coal

100 grams (d.b.) of air dry LAW acid-washed coal and 70 grams of 15% concentration sodium chloride solution were blended into slurry together with an additional small amount of de-ionised water.

LiAC4 coal

This coal, used in two experiments only, was prepared to experiment with coal, in which ion-exchangeable groups would be exhausted by lithium ions and in which sodium would exist as sodium chloride impregnated into coal. 100 grams (d.b.) of air dry LAW acid-washed coal and approximately 400 ml of 10N lithium bromide solution were mixed in a

plastic container and left for 24 hours. The mixture was frequently stirred. The coal was then filtered out in a vacuum Böhem filter and rinsed with 250 ml of de-ionised water, and then dried in air. Then 100 grams of 15% concentration sodium chloride solution was added to the coal and coal was blended into slurry.

The three coals, NA4, NC4 and LiAC4 were specially prepared to contain a greater quantity of sodium, whether organically bound or in the form of NaCl, so as to provide a better resolution in the identification of the possible formation of Na_2CO_3 in the respective chars.

Table 4.4 Description of coal samples with desired content of sodium and silica or kaolin.

Coal designation	Sodium organically-bound, % wt.	Sodium as Sodium chloride, % wt.	Silica, % wt.	Kaolin, % wt.
NA1	1	-	-	-
NA1S	1	-	10	-
NA1K	1	-	-	10
NC1	-	1	-	-
NC1S	-	1	10	-
NC1K	-	1	-	10
NA4	4	-	-	-
NC4	-	4	-	-
LiAC4	-	4	-	-

4.2.3.1 Preparation of dried coal granules

The prepared coals were made into slurry with the addition of small quantities of water till a toothpaste consistency of so created thixotropic slurry was achieved. The water content in the slurry was approximately 73%. The slurry was then firmly packed into sample container lids, each 8 cm in diameter and 75 ml in volume. The lids were then placed in a pre-warmed 80°C laboratory oven and dried. The dry coal lumps were gently crushed in a mortar and pestle and then sieved to recover 1.18 to 2.0 mm sized particles. The size chosen was considered to be representative of coal particle feed size applicable to fluidised bed technology. It was also important that the generated char particles be large enough in diameter to be examined for distribution of sodium and silica and kaolin using microscopic techniques. This selected coal size batches were dried in a laboratory oven at 100°C and then stored in a desiccator before being used in experiments. Table 4.5 shows actual content of sodium and chlorine and ash values for these prepared coals.

4.2.4 Preparation of mineral mixtures

Mixtures of sodium and silicon minerals used in the preparation of the synthetic coals were prepared for tests of exposure to the same conditions as coal samples in pyrolysis and gasification tests. It was desired to keep the ratio of sodium to silicon mineral at 1:10, the same as in prepared synthetic coals. Table 4.6 lists the sets prepared.

Table 4.5 Actual synthetic coals compositions.

Coal designation	Sodium, % wt. d.b.	Chlorine, % wt. d.b.	Ash, % wt. d.b.
LAW	-	-	1.9
NA1	0.92	-	2.9
NA1S	0.70	-	12.6
NA1K	0.76	-	11.8
NC1	0.91	1.36	3.5
NC1S	0.85	1.35	11.9
NC1K	1.11	1.52	12.5
NA4	3.28	-	4.1
NC4	3.32	5.35	6.7
LiAC4	3.44	5.51	8.4

Preparation of SAC mixture

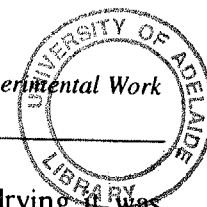
10.7 grams of AR grade of sodium acetate was dissolved in 25 ml of deionised water in a 50 ml beaker and 30 grams of silica sized in the range of 25-32 μm was added. The mixture was then dried in a laboratory oven and mixed during the process. After drying it was crushed and kept in storage in a desiccator.

Table 4.6 Description of mineral mixture samples.

Sample designation	Sodium present as	Mineral	Desired Na/mineral mass ratio	Actual sodium, % wt	Ash, % wt. at 750°C
SAC	acetate	silica	1 : 10	6.16	87.2
SNC	sodium chloride	silica	1 : 10	23.5	98.2
KAC	acetate	kaolin	1 : 10	5.67	77.0
KNC	sodium chloride	kaolin	1 : 10	8.18	80.4

Preparation of SNC mixture

10 grams of AR grade of sodium acetate was dissolved in 30 ml of deionised water in a 50 ml beaker and 30 grams of silica sized in the range of 25-32 μm was added. The mixture



was then dried in a laboratory oven and mixed during the process. After drying it was crushed and kept in storage in a desiccator.

Preparation of KAC mixture

10.7 grams of AR grade of sodium acetate was dissolved in 25 ml of deionised water in a 50 ml beaker and 30 grams of kaolin was added. The mixture was then dried in a laboratory oven and mixed during the process. After drying it was crushed and kept in storage in a desiccator.

Preparation of KNC mixture

10 grams of AR grade of sodium acetate was dissolved in 30 ml of deionised water in a 50 ml beaker and 30 grams of kaolin was added. The mixture was then dried in a laboratory oven and mixed during the process. After drying it was crushed and kept in storage in a desiccator.

4.3 EXPERIMENTAL APPARATUS

Reports in the literature (Riley and Judd, 1987; Kwon et al., 1988; Ye, 1994) show that the gasification rate of low-rank coals at temperatures up to 900°C for gasification with carbon dioxide or steam is reaction-rate controlled and is independent of diffusion rates for mass transfer between reacting coal and gases. On this basis, the choice of a simple reaction environment in which coal particles could be gasified reflecting the conditions present in a fluidised bed gasifier was made. It was considered that exposure of the coal to a reactive atmosphere of carbon dioxide or steam would be the same for given temperature conditions regardless whether the particles were suspended (fluidised) in a gas stream or stagnant with gas flow passing-by.

The prepared samples were pyrolysed and gasified in a Horizontal Tube Furnace (HTF). The use of a HTF offers a well-defined and relatively constant heating environment for studying transformations of sodium present in the coal, the mechanisms of its reactions with silicon minerals present and its catalytic effect on the coal gasification process and subsequent kinetics of such a process. This furnace arrangement offers a great advantage for handling the fragile synthetic coal particles, which would otherwise be prone to

fragmentation in a robust agitated environment like a fluidised bed, in which handling of the coal, its char and over all material balance would be difficult to obtain.

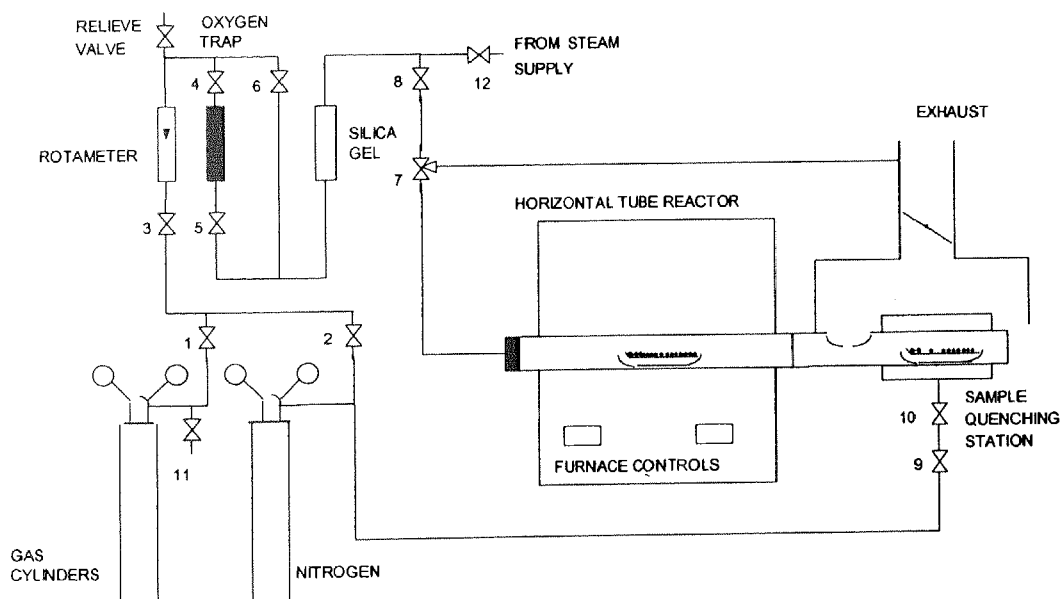


Figure 4.1 Schematic diagram of the Horizontal Tube Furnace.

The HTF used was a Carbolite Model CFM 14/2 furnace. The furnace was controlled by Eurotherm 91e temperature controller/programmer. A schematic diagram of the HTF is presented in Figure 4.1. A 25 mm I.D. x 500 mm long non-porous "Pythagoras" type ceramic tube housed inside the refractory lined furnace was heated by four Kanthal silicon carbide heating elements capable of delivering a maximum of 2.25 kW. The HTF could be heated to 1400°C and the heating rate was 10³°C/min. An 80 mm hot zone in the centre of the furnace was maintained along the ceramic tube at uniform temperature. Carbon dioxide and nitrogen gases were supplied directly from G size high purity gas bottles. The gas flow rate was controlled by a rotameter and prior to entering the furnace the gas passes through a moisture trap packed with silica gel to ensure that it was free of moisture. Steam was supplied from a flask electrically heated with a steady supply of distilled water to it. The steam leaving the flask was partly released to atmosphere and approximately 8 grams per minute of steam was entering the reactor.

Gases entered from one end of the tube through a 10 mm metal plug. At the other end of the ceramic tube, a 25 cm long stainless steel tube was mounted onto the ceramic tube so

the inner wall of the steel tube formed an extension of the ceramic tube. This tube was fitted with two unique features. An opening in the top of the tube close to the tube connection allowed the gases to leave the ceramic tube immediately via the exhaust hood.

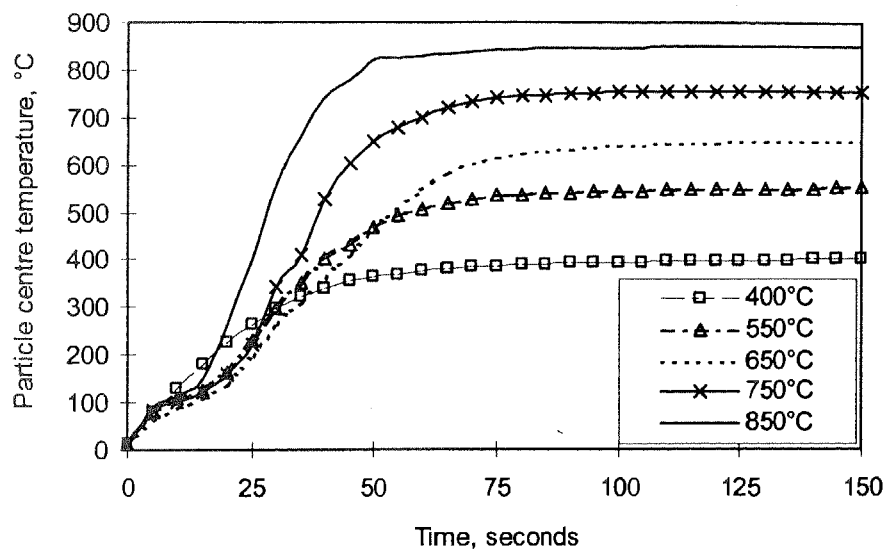


Figure 4.2 Measured temperature responses at the centre of 4 mm Lochiel coal particles during heating in the Horizontal Tube Furnace heated to specified set point.

Further down from that exhaust opening the tube was doubled wall for the length of 15 cm with numerous small holes drilled in the bottom part of the inner tube. A supply of nitrogen was connected to the outer section of this tube. This section acted as a quenching and purging zone for sample crucibles to be withdrawn from the furnace.

To assess the coal heating rate in the HTF, a measurement of the temperature profile in the centre of a dry 4 mm particle of Lochiel coal using a 1.0 mm standard K type thermocouple was carried out for various temperature set points. The thermocouple was attached to the crucible and the tip with a particle placed on it was in the centre of crucible. Figure 4.2 shows the typical temperature response at the centre of particle during heating and Figure 4.3 temperature response during cooling.

The rate of heating of the particles was found to be approximating 10^3 °C/minute, a typical heating rate obtained for coal particles in a fluidised bed combustor or gasifier (Davidson et al., 1985).

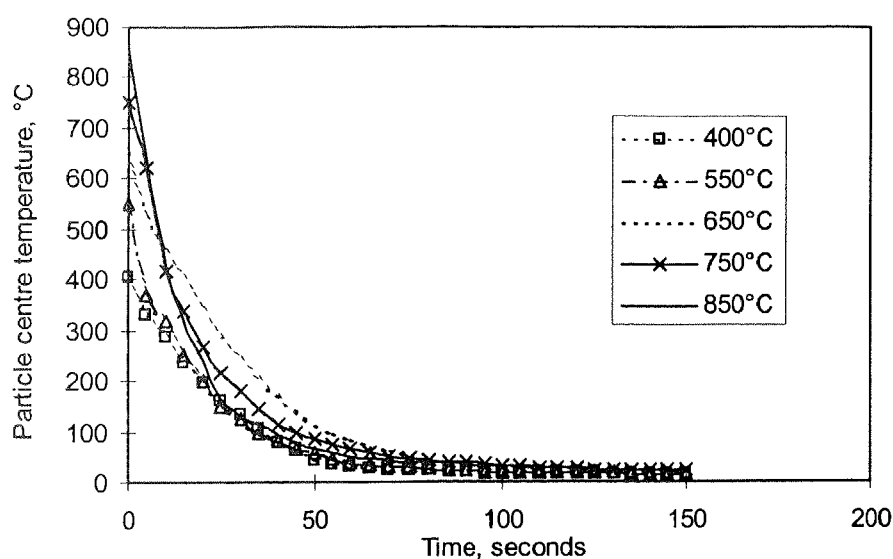


Figure 4.3 Measured temperature responses at the centre of 4 mm Lochiel coal particles during cooling from specified temperature level in the quencher of the Horizontal Tube Furnace.

4.4 EXPERIMENTAL PROCEDURE

Pyrolysis experiments involved heating the coal to a pre-set temperature in an inert atmosphere of nitrogen. The pyrolysis process allowed for the determination of the amount of volatiles released from coal at any given temperature and exposure times required. Gasification with carbon dioxide or steam results in volatile matter release due to devolatilisation and reaction of remaining char with these gases. The rate of gasification of char could then be calculated for gasification with carbon dioxide or steam by subtracting the amount of volatile matter released in a nitrogen atmosphere from the residual amount of solid generated during gasification.

Coal samples were placed in a 45 mm long, 7mm high and 10 mm wide platinum (Pt) crucible with a Pt/Au gauze placed in at the half height of the crucible. Coal particles were spread over the gauze. The gauze was used to facilitate better gas penetration amongst coal particles. The crucible was inserted and withdrawn from the HTF using a steel rod, approximately 1.2 metres in length. Upon withdrawing the crucibles from reaction zone, the crucibles were left for up to 3 minutes in the quencher to avoid oxidation of remaining material.

A known sample mass, approximately 0.5 grams of coal or 0.2 grams of a mineral mixture was placed in the crucible. The mass of crucible was measured after it was withdrawn from the furnace to obtain mass values of solid residue remaining in the crucible. This allowed mass data collection used in the calculation of the char carbon conversion and determination of chemical kinetic values for the gasification reactions, as well as for use in the mass balance of the inorganic components. Each sample was emptied from a crucible into a marked container and retained for chemical and instrumental analyses. Each experiment was carried out in duplicate.

Reactant gases were passed over a bed of coal maintained at reaction temperature. Carbon dioxide and nitrogen supply to the furnace were kept at approximately 3.5 NI/minute. A steam flow rate of 8 grams/minute was supplied to the furnace. These flows allowed for significant over supply of gas reagent against stoichiometric requirements to gasify given mass of coal. The samples of mineral mixtures were exposed to the same gaseous, temperature and time conditions as the coal samples. No sampling of the exhaust gas was undertaken as the investigation was aimed at reactant influence on char conversion and inorganic reactions occurring within char.

A reaction time of 45 seconds was chosen as a reference time, in which it was expected that coal particles introduced to the furnace reaction zone would attain the desired temperature. This reaction time was judged on balance between the three temperature levels to be investigated, these being 650°C, 750°C and 850°C. The overall experimental conditions for synthetic coals and mineral mixtures are set out in Table 4.7. The samples of each coal or mineral mixture were exposed to each given reaction time, temperature and atmosphere conditions.

Table 4.7 Experimental conditions for experiments conducted with synthetic coals and mineral mixtures in the Horizontal Tube Furnace.

Coal and mineral mixture samples used	Temperature, °C	Atmosphere	Reaction time, minutes
NA1, NA1S, NA1K, NC1, NC1S, NC1K SAC, SNC, KAC, KNC	650°C 750°C 850°C	Nitrogen, Carbon dioxide, Steam	0.75 1.5 5.75 15 35
LAW, NA4, NC4, LiAC4	750°C	Nitrogen, Steam, Carbon dioxide,	15

4.5 ANALYTICAL METHODS FOR COAL AND REACTION PRODUCTS

Lochiel coal, all synthetic coals, mixtures of minerals and salts of sodium and all post-reaction char and mineral residues were analysed for: moisture, ash, chlorine and sulphur content, ash constituents in coal ash and in mineral mixtures, in accordance with appropriate Australian Standard method as follows:

Moisture	AS 2434.1 – 1991
Ash	AS 2434.8 - 1993
Volatile matter	AS 2434.2 - 1983
Fixed Carbon	AS 2434.6 - 1986
Chlorine	AS 1038.8 – 1980
Sulphur	AS 1038.6 – 1996
Sodium	AS 2434.9 - 1995
Ash constituents	AS 1038.14.1 – 1995

Sulphide ions were analysed in solutions by ion selective electrode and by Ion Chromatography. Chlorine in water leachates after digestion of product samples was analysed by colorimetric method with mercuric thiocyanate. Silicon in water leachates was analysed also by calorimetric method using molybdenum blue method. Both chlorine and silicon methods were developed into Torrens Island Power Station (TIPS) Chemical Laboratory standard methods. Residue from acid extraction (acid-washing) were analysed by, first ashing, and then analysed for ash constituents in accordance with AS 1038.14.1 – 1995 method.

4.5.1 Solubility of sodium and silicates

The assessment of the sodium and silica reactions was based on the solubility of sodium silicates. Sodium metasilicate Na_2SiO_3 is soluble in cold (15–25°C) water, while sodium disilicate $\text{Na}_2\text{Si}_2\text{O}_5$ is soluble in hot (90–100°C) water. Extrapolation of the data on solubility of silicates in water as reported by Eitel (1966), for the silicates with silicon oxide content higher than 80% would, according to Lindner (1988), allow complete solubility of such silicates in water superheated at 120°C or higher. The process of digestion in superheated water at 120°C would be however a slow process. Solubility of a glass of the composition $\text{Na}_2\text{O}, m\text{SiO}_2$ depends on the coefficient $\alpha = n_{\text{SiO}_2}/m.n_{\text{Na}_2\text{O}}$ which

reflects on the amounts of sodium oxide $n_{\text{Na}_2\text{O}}$ and silicon oxides n_{SiO_2} going into solution. For $\alpha = 1$ whole silicate glass dissolves (Eitel, 1966). Figure 4.4 shows, that sodium silicates with increasing silica content can be completely dissolved in water as the temperature is increased.

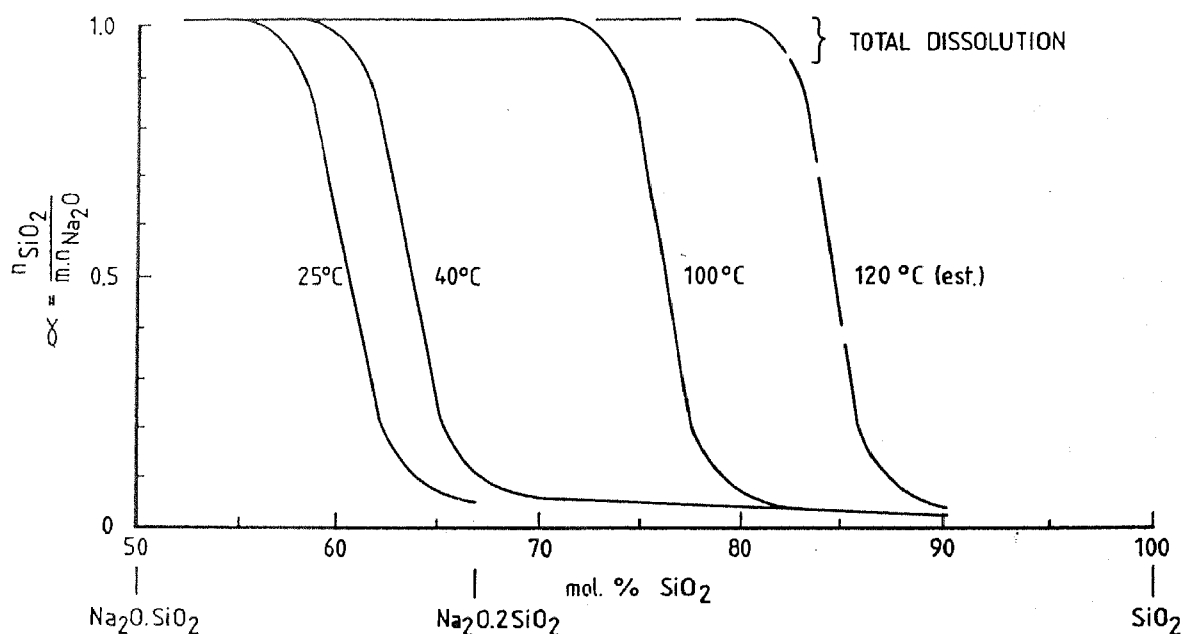


Figure 4.4 Portion of silica, α , which could be leached out after one hour exposure of sodium silicate glass with water as a function of composition and of temperature - adapted from Eitel (1966) and Lindner (1984).

Water digestion of char and post-reaction mineral mixtures was then intended as a principal part of the analytical process aimed at assessment of transformations of sodium and of formation of reaction products of sodium with silica and kaolin, i.e. silicates and aluminosilicates.

Figure 4.4 shows, that hot water can dissolve silicate glass with composition of sodium disilicate. Hot water will also dissolve glass with composition of the lowest melting eutectic in the system between sodium oxide and silica. That eutectic, as shown in Figure 2.3, melts at 789°C and has the composition on molar basis of 27% Na_2O and 73% SiO_2 ,

or on mass basis 27.7% Na₂O and 72.3% SiO₂. Silicates with higher content of silica should be dissolved after prolonged digestion in water superheated at 120°C.

4.5.1.1 Staged water leaching analysis

Samples of coal, char or mineral mixture products were digested in deionised water in stages; first for 30 minutes in cold water, than for 30 minutes in hot - near boiling point, followed by digestion in superheated water at 120°C for periods of 4, 16, and 44 hours. The cold and hot water leaching was carried in 100 ml beakers in 50 ml of water with some addition of ethyl alcohol for wetting char sample with magnetic stirrers immersed in solutions. The leachates from cold and hot water leaching were gently transferred out from the beaker with pipette to a flask for analysis.

The leaching at 120°C was carried out in 150 ml culture test tubes immersed in water bath of an autoclave heated to 120°C in an oven preheated to 120°C. A commercially available kitchen pressure cooker was used as the autoclave. The leachates from each stage of leaching in the superheated water were, after being centrifuged, carefully decanted with pipettes from the tubes to flasks for analysis.

Leachates were analysed as required for sodium, sulphides, chlorine, silicon and aluminium in accordance with methods listed earlier in this Section.

4.5.1.2 Confirmation of sodium forms in prepared synthetic coals

An examination of prepared synthetic coals was carried out to assess the quality of the preparation process of the coals desired to contain sodium in a particular organically-bound form or in the form of sodium chloride. Table 4.8 presents the results of stage water-leaching carried out on NA1 coal loaded with organically-bound sodium and NC1 coal impregnated with sodium chloride.

Sodium attached to the organic structure of the NA1 coal was nearly completely leached out from coal structure in almost equal proportions in the five stages of water-leaching process. From NC1 coal, impregnated with NaCl, both sodium and chlorine were almost completely leached in first cold water digesting stage.

Table 4.8 Sodium and chlorine content in NA1 coal loaded with organically-bound sodium and in NC1 coal impregnated with sodium chloride.

Sample designation	Sodium form	Cold water leaching	Hot water leaching	4 hours leaching @ 120°C	16 hours leaching @ 120°C	44 hours leaching @ 120°C	96 hours leaching @ 120°C	Residue
		% total Na	% total Na	% total Na	% total Na	% total Na	% total Na	% total Na
NA1	organically-bound	15.22	14.37	14.53	25.42	20.97	7.44	2.11
NC1	chloride	88.34	5.57	3.61	1.96	0.1	0.1	0.1
		% total Cl	% total Cl	% total Cl	% total Cl	% total Cl	% total Cl	% total Cl
NC1	chloride	97.98	1.65	0.37	0.0	0.0	0.0	0.0

These results show that both forms of sodium were present as those desired. They show then the difference between dispersion of sodium into the organic structure of coal and impregnation of sodium into the mass of coal. These results thus provide evidence that the techniques of preparation of the synthetic coals allowed for preparation of coal samples to contain two distinctly different forms of sodium.

4.5.2 FT-IR analyses

To assess whether sodium transformation within the coal char results in the formation of sodium carbonate, a simple experimental test was devised whereby acid treating the char and sampling the evolved gases for the presence of carbon dioxide were undertaken. Figure 4.5 shows a schematic diagram for the apparatus arrangement. Sodium carbonate in reaction with acid would decompose and carbon dioxide would be liberated.

Char samples were simmered in a 20% HCl solution in an apparatus under continuous flow of sweeping nitrogen taking any evolving gases into a Perkin-Elmer System 2000 FT-IR spectrometer for carbon dioxide detection. The method proved to be very successful for determination of carbon dioxide released from char. However, due to a relatively short scanning time of 100 seconds used for FT-IR readings, the results cannot be used for a precise quantitative assessment of sodium carbonate in char, although still a very good appreciation of its presence in analysed chars was gained.

A pure analytical reagent grade sodium carbonate was used as a standard reference material. Char of a low-mineral Lochiel acid-washed coal (LAW) free of sodium pyrolysed at 750°C was used as the char reference sample. The NA4, NC4 and LiAC4 synthetic coals samples were specially prepared for this carbon dioxide determination and for mineralogical analysis of chars.

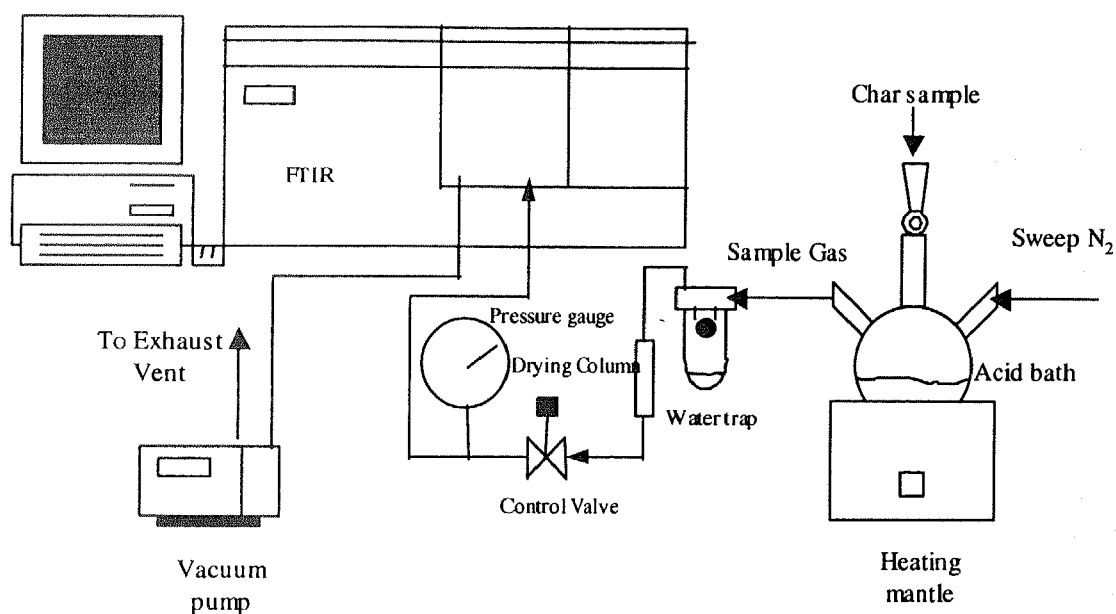


Figure 4.5 Schematic diagram of the apparatus arrangement for analyses of carbon dioxide.

4.5.3 Electron Microscopy

Samples of prepared synthetic coals, char samples and samples of mineral mixtures exposed to experimental conditions were subject to extensive microscopic examinations using Scanning Electron Microscope (SEM). A Phillips SEM XI-20 equipped with lanthanum hexaboride emitter and with an energy dispersive X-ray detection system (EDAX).

The SEM was operated in the secondary electron imaging process to examine morphology of examined samples, particularly formation of fused phases and for elemental analysis. Images of polished cross-sections of samples mounted in epoxy resin blocks were examined under backscattered electron image for carrying elemental analyses and clear identification of various phases, particularly within coal char and for identification of boundaries between formed phases.

The samples for SEM backscattered electron image for elemental analysis were prepared by embedding the coal, char or mineral mixture sample in an epoxy resin block. The surface of the block was then ground, polished and coated with carbon. The samples for SEM secondary electron imaging to examine morphology were mounted directly with double-sided adhesive tape onto special aluminium stubs and then coated with carbon.

4.5.4 Mineralogical X-Ray diffraction analysis

Samples of coal, chars, minerals, mineral mixtures exposed to experimental conditions were analysed using X-Ray powder diffraction (XRD) analysis to identify the mineral forms of species present in the examined samples in order to establish transformations of the inorganic matter present in the coal. The XRD method was considered as qualitative, although fair quantitative results can be assumed from this analysis. The method was complimentary to electron microscopic examinations and chemical analyses.

The analyses were performed by the Commonwealth Scientific and Industrial Research Organisation (CSIRO), Division of Soils. XRD patterns were recorded with Philips PW 1800 microprocessor-controlled diffractometer using Co K α radiation, variable divergence slit and graphite monochromator. The phases identified in samples were reported as dominant (>60%), co-dominant (sum of phases >60%), sub-dominant (20-60%), minor (5-20%) or as at trace (<5%) quantity level.

3.6 SUMMARY

This chapter has dealt with the apparatus and techniques used in the experimental investigations carried out in this study for the results to be reported in Chapters 5, 6, 7 and 8. The experimental program has been designed to achieve a better understanding of how sodium and silicon influence the process of fluidised bed gasification of low-rank coal.

To achieve these aims, a simple reaction system was used to pyrolyse and to gasify the coal. Batches of specially prepared synthetic coals were used. Concentrations, physical sizes, forms and distribution of inorganic constituents in these coals were controlled and known. Further to this, a series of specially prepared mixtures of just sodium salts and silica and kaolin were prepared for reference to investigate the interactions between

sodium and silicon minerals present in the coal. All coals and mixtures were exposed to the same experimental conditions.

Low-mineral Lochiel coal was used for preparation of the synthetic coals. Eight synthetic coals samples were prepared to contain various desired concentrations and forms of sodium and silicon minerals for the pyrolysis and gasification program. The soluble minerals and ion-exchangeable cations were removed from the coal by prolonged leaching with cold acid. Sodium and silicon minerals were then added to the coal. Sodium was added in the form of sodium acetate, which resulted in organically-bound form of sodium or it was impregnated as sodium chloride. Commercial grade, high purity silica was added to coals to simulate the coal quartz content.

The prepared samples were pyrolysed and gasified in a Horizontal Tube Furnace (HTF). The use of a HTF offers a well-defined and relatively constant heating environment for studying transformations of inorganic mineral matter present in the coal.

Pyrolysis experiments involved heating the samples to a pre-set temperature in an inert atmosphere of nitrogen, while gasification was conducted in either a pure environment of carbon dioxide or steam. The samples were exposed for reaction times of between 45 seconds to 35 minutes at three operating temperatures of 650°C, 750°C and 850°C. A known sample mass of approximately 0.5 grams of synthetic coal or 0.2 grams of a mineral mixture was placed in a crucible. The mass of loss of the sample was taken for each time period after exposure to the reaction environment and that allowed mass data collection to be used in the calculation of the char carbon conversion, the determination of chemical kinetic values for the gasification reactions and for use in the mass balance of the inorganic components.

Water digestion of char and post-reaction mineral mixtures was then principle part of analytical process aimed to assess transformations of sodium and to assess formation of sodium reaction products with silica and kaolin, silicates and aluminosilicates. The assessment of the sodium and silica reactions was based on solubility of sodium silicates. Sodium meta-silicate Na_2SiO_3 is soluble in cold water, while sodium disilicate $\text{Na}_2\text{Si}_2\text{O}_5$ is soluble in hot water. Silicates with higher silicon content will dissolve slowly in superheated water at 120°C.

To assess whether sodium transformation within the coal char results in the formation of sodium carbonate, a simple experimental test was devised whereby acid treating the char and sampling the evolved gases for the presence of carbon dioxide were undertaken using a FTIR spectrometer. Sodium carbonate in reaction with acid would decompose to produce carbon dioxide.

The samples of prepared synthetic coals, char samples and samples of mineral mixtures were subject to extensive microscopic examinations using Scanning Electron Microscope (SEM). The SEM was operated in the secondary electron imaging process to examine morphology of examined samples, particularly formation of fused phases and elemental analysis. The SEM was also operated under backscattered electron image mode for elemental analysis. Further to this, X-Ray powder diffraction (XRD) analysis to identify mineral forms of species present in the examined samples complimented the SEM analysis.

Chapter 5**TRANSFORMATIONS OF SODIUM IN HIGH-SULPHUR LIGNITE
DURING PYROLYSIS AND GASIFICATION – EXPERIMENTAL
RESULTS****5.1 INTRODUCTION**

This chapter deals with the transformations during pyrolysis and gasification, with carbon dioxide or with steam, of sodium present in high-sulphur lignite (Lochiel coal) at typical atmospheric fluidised bed gasifier conditions. Sodium is generally present in such coal as organically-bound sodium and as sodium chloride.

It is important to define products of such transformations, as they will play an important part in possible reactions with silica and kaolin during the pyrolysis and gasification processes. The products of such reactions may cause bed agglomeration and defluidisation.

The first part of this chapter deals with the transformation of sodium present in coal as organically-bound sodium, bound to coal mainly in its carboxylic groups. The second part deals with the transformation of sodium present in coal as sodium chloride.

5.1.1 Transformations of organically-bound sodium.

Generally accepted and proven knowledge on sodium, and other inorganic cations, organically-bound to coal structure is that it is bonded to the coal matrix containing oxygen functional groups, principally carboxylic groups (Schafer, 1970). This is as a result of an ion exchange process during coalification by substituting the hydrogen ion in carboxylic groups by the sodium ion.

Coal when heated will devolatilise. Usually organic, even more complex, compounds will start breaking above 400°C. Coal devolatilisation usually is concluded by 900°C. An exact coal structure is still being worked on by scientists, but it is fair to say that low-rank coal is mostly composed of aromatic structure based on the basic structure of benzene and some cyclic compounds, with a variety of functional groups attached to it together with very short or long aliphatic groups also containing various functional groups attached to them, such as carboxylic groups. Carboxylic groups contain metal ions, such as sodium or other very common ions such as calcium, potassium or magnesium. On heating as the bonds break and volatilisation of the components broken away takes place, the carboxylic groups break away chemically from char structure and form carbonates (Hendrickson et al., 1972). Carbonates of the above mentioned elements are much more stable than organic compounds and do not dissociate below 800°C, with the exception of magnesium carbonate (Dean, 1985).

Sodium carbonate broken away from the coal structure will remain within the char and it may react with char carbon. Carbon is a well-known reducing agent used in high temperature metallurgical processes to obtain metals from their respective oxides. But the main effect of reduction of sodium carbonate by carbon to metallic sodium will be the reason for sodium evaporation. With its very low melting point, just below 100°C, sodium vapour pressure will be high at elevated temperatures with its boiling point at 881°C. Therefore it is expected that quantities of sodium present in coal originally organically-bound can upon pyrolysis become metal and evaporate from char. At higher temperature of pyrolysis or char gasification more sodium carbonate may react with char carbon and more sodium may evaporate.

Release of volatiles from char will depend on the structure of pores in the formed char. The sizes of pores are considered as low as one Ångstrom (Simons, 1984). It is, therefore, reasonable to expect that some coal devolatilisation products will be trapped inside the char for some time before leaving during extensive heating or char consumption process such as gasification. Size of char pores can also be the defining parameter for sodium staying in the char rather than leaving the char if sodium metal was formed from reduced sodium carbonate. Slow diffusion to external surface of the char particle may limit sodium release from char.

Recent literature reports on coal pyrolysis (Pang et al., 1999; Sathe, 1998) speculate decomposition of carboxylates into carbon dioxide and organometallic compounds in which sodium, or calcium, would be directly attached to the char matrix. This assumption of direct bonding by sodium to char appears unfounded. As char during pyrolysis is dehydrogenated, it is difficult to assume that such char will react at high temperatures with metal ions. Also, contradictory to those above speculations, information given in the same reports has shown that the same metals engage carbon dioxide to form carbonates and consequently reduce the yield of volatile matter from coal. Therefore suggestions by Pang et al. (1999) and Sathe (1998) are not considered as indicating a valid path of transformations of organically-bound sodium.

During pyrolysis, organically-bound sodium is transformed from carboxylic form to sodium carbonate. This is established for a coal containing minor proportions of sulphur. Sodium carbonate has been reported as a product of decomposition of coal carboxylic groups containing sodium. Murray (1973) reported formation of sodium carbonate at 400-800°C when pyrolysing Morwell coal containing sodium carboxylates. More recently Yamashita et al. (1991) established the presence of sodium carbonate in pyrolysed lignite char samples using XANES spectroscopy. The lignite used in that work was also a Victorian (Loy Yang) coal.

However the thermodynamic calculations presented in Chapter 3 suggest formation of sodium sulphide during pyrolysis of high-sulphur Lochiel coal. Manzoori (1990), who investigated combustion of similar coal in a fluidised bed reactor, suggests that sodium will be transformed into sodium sulphide during pyrolysis at typical fluidised bed conditions.

Those sodium transformation products, both, sodium carbonate and sodium sulphide, are suggested to be in condensed forms.

There are however reports in the literature about volatilisation of metallic sodium during a prolonged pyrolysis process. Dunderdale et al. (1963) report formation of a mirror of metallic sodium on a cold metal surface at the end of a tube in which a coal containing sodium was heated to 800°C in a nitrogen atmosphere. Huhn et al. (1983) report of reduction of sodium carbonate to metallic sodium when heating a coke impregnated with sodium carbonate to temperature below 1000°C in an inert atmosphere. Takarada et al. (1995) report sodium volatilisation from Yallourn lignite coal containing 0.3% wt d.b sulphur impregnated with 5% of sodium carbonate and charred or gasified at 840°C. The coals studied by above quoted researchers contained no or little sulphur. Results of thermodynamic calculations for coal containing no sulphur predicted that all sodium will be in sodium metallic vapour in nitrogen atmosphere at temperature above 650°C (Kosminski, 2000).

Huhn et al. (1983) report on conducting pyrolysis in an inert atmosphere of coke impregnated with alkali carbonates, including sodium carbonate. Report on results of that work say that some of the sodium present in the carbonate form was reduced to metallic sodium. Huhn et al. work concentrated on fate of potassium and no details on sodium experiments have been given.

More information on sodium release comes from work reported by Dunderdale et al. (1963). They conducted a series of experiments using heated tube experimental arrangement principally the same as the one used in this study. In that study sodium salts of brown coal and sodium salts, mainly carbonate and sodium chloride in one of the reported experiment, mixed with carbonaceous matter were heated in argon atmosphere for 2 hours at temperature of 850°C, 900°C or 920°C. Sodium salt of a brown coal (this is how it is reported - what is probably to mean that sodium was present in that brown coal in a form of a carboxylic salt, i.e. as organically-bound sodium) was used in one of the reported experiments. In the other experiments were used mixtures of sodium carbonate with graphite or char, including brown coal char and char from fluidised-bed (probably either

Morwell coal or Yallourn coal char was used). Sodium carbonate consisted of one third, by mass, of those mixtures.

Results of all of those experiments indicated the formation of a sodium mirror in the cool part of the tube wall, formed by condensation of sodium vapour. It was reported that graphite mixture gave deposit only ca. 10% of that produced in experiment with brown coal mixed with sodium carbonate. It is also reported that in experiments with sodium carbonate approximately 40% of the sodium was lost from the samples heated for two hours at 920°C. It is reported further that appreciable quantities of sodium cyanide were formed during carbonisation in nitrogen atmosphere, and that is why argon was used in the reported experiments.

Another study on volatilisation of sodium has recently been conducted by Takarada et al. (1995). In that study sodium-loaded coal was pyrolysed in nitrogen and gasified in carbon dioxide atmosphere. Victorian Yallourn coal leached with hydrochloric acid and then impregnated with sodium carbonate or mixed with sodium chloride or sodium silicate was used in reported experiments. Effects of sodium chemical form and process temperature on volatilisation of sodium were examined. Takarada et al. (1995) conclusions and findings were similar to those reported by Dunderdale et al. (1963). Dunderdale et al. (1963) concluded that a fair quantity of sodium might be released as sodium vapour during high temperature heating of coal containing sodium salts. This may happen also during gasification as reported by Takarada et al. (1995).

These conclusions led to this study to establish extent of sodium release during carbonisation in nitrogen atmosphere and during coal gasification from coal containing high levels of sulphur. The study was then carried out on release of sodium organically-bound in coal and also on release of sodium from coal containing sodium strictly in form of sodium chloride.

5.2 OBJECTIVES

Assessment of sodium mass balance from pyrolysis and gasification experiments was considered very important in the present work. Literature reports bring to attention a fact

that sodium present in coal can enter the gas phase during coal pyrolysis in an inert atmosphere at fluidised-bed gasifier temperatures. It was therefore necessary to validate the reported information and make a detailed assessment of extent of the sodium release during pyrolysis or gasification.

All the above reports do not give a clear picture on the fate of organically-bound sodium present in high-sulphur lignites, such as Lochiel coal, during pyrolysis. Thermodynamic predictions show that only sodium sulphide will be formed at equilibrium conditions during pyrolysis in nitrogen at temperature conditions of interest. In addition, limited information exists in the literature on transformations of sodium during gasification of coal either in carbon dioxide or steam atmosphere.

Therefore the objectives of this study were:

- to investigate the behaviour of organically-bound sodium present in high-sulphur Lochiel coal during pyrolysis in nitrogen,
- to investigate the behaviour of organically-bound sodium present in high-sulphur Lochiel coal during gasification with either carbon dioxide or steam at typical fluidised bed gasifier conditions,
- to investigate volatilisation of sodium present in high-sulphur Lochiel coal in form of sodium chloride during both pyrolysis and gasification with possible implications for equipments down stream of fluidised bed gasifier.

5.3 PYROLYSIS AND GASIFICATION OF COAL CONTAINING ORGANICALLY-BOUND SODIUM

A series of experiments was carried out with NA1 and NC1 prepared coal samples containing organically-bound sodium or sodium chloride, respectively. This was to provide data and information for the determination of transformations of sodium compounds during pyrolysis and during gasification of organically-bound sodium and sodium chloride present in a high-sulphur Lochiel coal. Samples of NA1 and NC1 coal were pyrolysed in nitrogen or gasified with carbon dioxide or with steam. Detailed parameters of experiments are given in Table 3.7.

The following sections present the results of experiments and interpretation of these results, to establish relevant sodium chemical forms for reactions with silica and kaolin. Products of such reactions might lead to a formation of products enhancing agglomeration in fluidised bed gasifiers.

5.3.1 Sodium volatilisation during pyrolysis and gasification

5.3.1.1 Sodium volatilisation during pyrolysis

Results of pyrolysis and gasification experiments using NA1 coal containing 0.92% on dry basis of organically-bound sodium are presented in Table 5.1 and in Figures 5.1 and 5.2. Comparison of some of these results with results by Takarada et al. (1995) and by Dunderdale et al. (1963) is presented in Table 5.2.

Table 5.1 Results of sodium release from NA1 coal containing 0.92% d.b. of organically-bound sodium during pyrolysis in nitrogen and during gasification with carbon dioxide and with steam. The results are shown as per cent loss of the sodium present originally in coal.

Process	Pyrolysis			Gasification			Gasification		
Reagent	Nitrogen			Carbon dioxide			Steam		
Temperature, °C	650	750	850	650	750	850	650	750	850
Reaction time, min.									
0.75	0.1	0.8	2.3	1.0	1.2	4.0	2.1	2.6	2.1
1.5	0.8	1.4	3.9	2.6	3.5	6.6	4.6	6.6	6.6
5	1.1	1.2	6.3	5.1	6.1	33.6	5.7	9.7	14.6
15	2.5	3.8	12.7	6.4	12.3	53.4	7.1	11.8	33.2
35	3.5	8.1	18.7	8.2	15.2	57.2	8.9	14.8	42.7 ^{**}

^{*}, ^{**} - 10 and 15 minutes reaction time respectively

During pyrolysis sodium volatilisation was found to depend on temperature as well as on the duration of coal pyrolysis. As shown in the Table 5.1 almost 19% of original sodium in coal was released after 35 minutes of pyrolysis at 850°C. Release of sodium was the highest at 850°C, while at 650°C there was hardly any loss of sodium measured. Sodium loss from char increased slowly with time, as is shown in Figure 5.1.

Thermodynamic calculations presented in Chapter 3 predicted formation of some sodium metal vapour above 850°C. Sodium metal would form as transformation product of the organically-bound sodium. It was expected that sodium carbonate rather than sodium sulphide would form under the experimental conditions. In reports by Takarada et al.

(1995) and by Dunderdale et al. (1963), sodium carbonate was mixed with coal or coal char. The results for the sodium release at 850°C during pyrolysis and gasification reported by those researchers, although for different experiment times, are in a good agreement with those found in this work as shown in Table 5.2. It can therefore be concluded that sodium metal forms from sodium carbonate during pyrolysis experiments reported by others and in the current experiments. This may lead to a speculation that organically-bound sodium during pyrolysis of sulphur-rich coal is transformed into sodium carbonate and not into sodium sulphide. In a subsequent section it will be shown that that is the case.

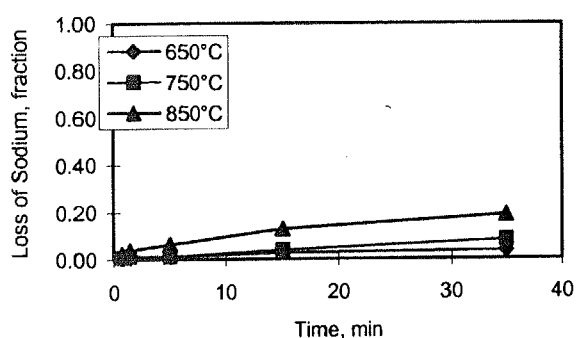
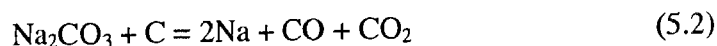


Figure 5.1 Sodium losses at various temperatures as a function of time during pyrolysis in nitrogen of NA1 coal only containing 0.9% d.b. of organically-bound sodium.

As indicated earlier in this chapter, for coal containing no sulphur, sodium vapours are predicted to form above 650°C during pyrolysis in nitrogen atmosphere. This could happen as a result of reduction of sodium carbonate by coal char in a form of one of the following reactions:



Sodium melting point is 98°C and the boiling point 881°C. Much higher sodium loss results at 850°C than at 650°C, suggesting that the reaction of sodium carbonate with carbon is a limiting factor in sodium release, rather than the rate of sodium evaporation at tested temperatures of 650°C to 850°C. Considerable vapour pressure of sodium would exist at 650°C as well as at near boiling point at 850°C. However much lower sodium vaporisation at 650°C than at 850°C suggests that formation of sodium metal (i.e. reaction of sodium carbonate with carbon) would be that limiting factor.

Table 5.2 Sodium release from coal during pyrolysis or gasification as reported in literature in comparison with the current work.

Work by	Coal/Sodium form/ sodium concentration	Atmosphere	Duration, hours	Temperature °C	Sodium loss
Dunderdale et al., 1963	Brown coal char + Na ₂ CO ₃ - 33%	Argon	2	920	40%, sodium mirror reported
Takarada et al., 1995	Yallourn coal impregnated with Na ₂ CO ₃ - 5%	Nitrogen	1	840	35%
Takarada et al., 1995	Yallourn coal impregnated with Na ₂ CO ₃ - 5%	Carbon dioxide	1	840	80%
Current study	Lochiel - organically-bound sodium, 0.9%	Nitrogen	0.5	850	19%
Current study	Lochiel - organically-bound sodium, 0.9%	Carbon dioxide	0.6	850	57%
Current study	Lochiel - organically-bound sodium, 0.9%	Steam	0.25	850	43%

5.3.1.2 Sodium volatilisation during gasification with carbon dioxide

The fastest release of sodium during gasification with carbon dioxide was measured at 850°C, when more than a half of originally present sodium vaporised from coal after 35 minutes of gasification. Gasification with carbon dioxide at both 650°C and 750°C showed sodium losses much higher in comparison with pyrolysis results by approximately a factor of two, as shown in Figure 5.2a and also in Table 5.1. Comparing with results for 850°C experiments, these sodium vaporisation results were, however, considerably lower. Again this was in a good agreement with results reported by Takarada et al. (1995), who have found very low sodium release at 650°C during carbon dioxide gasification. For experiments at 750°C those researchers report hardly any increase of sodium release, up to a fixed-carbon conversion level of 70%, beyond which the release rose strongly.

During gasification of coal with carbon dioxide, carbon dioxide presence could slow sodium carbonate reduction through reaction (5.2). However, then this reduction would be happening as per reaction (5.1), as carbon monoxide partial pressure would still be very low under the experimental conditions. Therefore the formation of sodium metal during gasification in carbon dioxide is as possible as during pyrolysis in nitrogen.

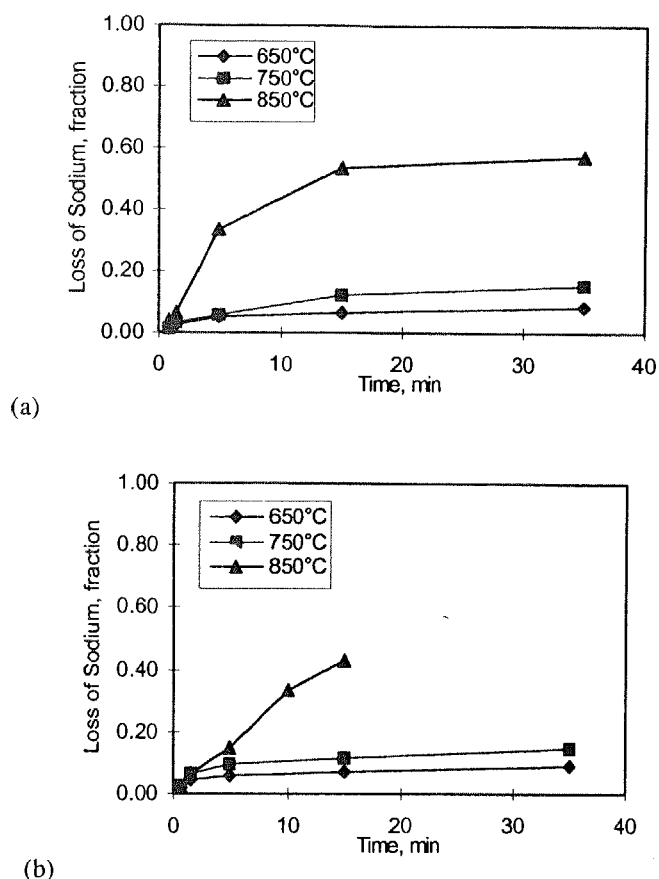


Figure 5.2 Sodium volatilisation at various temperatures as a function of time during gasification of NA1 coal containing 0.9% d.b. of organically-bound sodium (a) with carbon dioxide and (b) with steam.

5.3.1.3 Sodium volatilisation during gasification in steam

Gasification of NA1 coal with steam resulted less sodium volatilisation (Figure 5.2b), than that measured for carbon dioxide gasification; but still significantly higher than measured during pyrolysis in nitrogen. Again there was high sodium release at 850°C with nearly a half of original sodium lost from char to the gaseous state.

Thermodynamic calculations predict no formation sodium vapour in a carbon dioxide gasification atmosphere at 850°C, as only formation of liquid sodium carbonate is predicted. In steam atmosphere, however, half of sodium has been predicted to be in the form of sodium hydroxide vapour, the other half as liquid sodium carbonate at equilibrium conditions at 850°C. This suggests that different forms of sodium in the gaseous state may result from gasification reactions under carbon dioxide and under steam conditions.

It is still possible for steam gasification conditions that sodium evaporates as metal, when it forms as a product of reduction of sodium carbonate by char carbon (Reactions 5.1 and 5.2). As stated earlier sodium boiling point is 881°C , while sodium hydroxide boiling point is 1557°C and the melting point 322°C . So at 850°C the metallic sodium vapour pressure would be considerably higher than that of the sodium hydroxide. According to Jackson (1963) sodium hydroxide vapour pressure at 850°C would be only 5 torr. On the other hand the fact that sodium vaporisation in steam was measured slightly lower than that in carbon dioxide gasification atmosphere, may suggest that sodium reduced to the metallic state reacted with steam to form sodium hydroxide. The formation of sodium hydroxide would reduce sodium volatilisation.

However as shown in later sections (Section 5.3.3) sodium hydroxide was not identified in any steam gasification char, as only sodium carbonate presence was established. And once again equilibrium thermodynamic calculations do not predict sodium hydroxide formation in condensed form for the experimental conditions considered in this work.

Therefore it can be inferred that sodium metal evaporates from coal char gasified with steam or with carbon dioxide.

When comparing results for sodium volatilisation from coal char in relation to the coal fixed carbon conversion during gasification with carbon dioxide and with steam, sodium volatilisation in carbon dioxide was higher for comparable carbon conversion, as shown in Figure 5.3. This can be particularly concluded for gasification at 850°C .

The maximum measured sodium losses after 35 minutes for both gasification atmospheres at 750°C were around 12% of original sodium content in coal and were nearly double those at 650°C . But at 850°C gasification with steam the loss of sodium was 43% for almost full carbon conversion, while during gasification with carbon dioxide it was 57% for slightly lower carbon conversion, and was four times higher than sodium loss measured for gasification at 750°C . These results indicate that reduction of sodium to a volatile form of metallic sodium was much faster at 850°C as nearly a half of original sodium present in coal evaporated from gasified NA1 char. Takarada et al. (1995) report 80% sodium loss for 70% carbon conversion during gasification with carbon dioxide of Yallourn coal impregnated with 5% sodium carbonate.

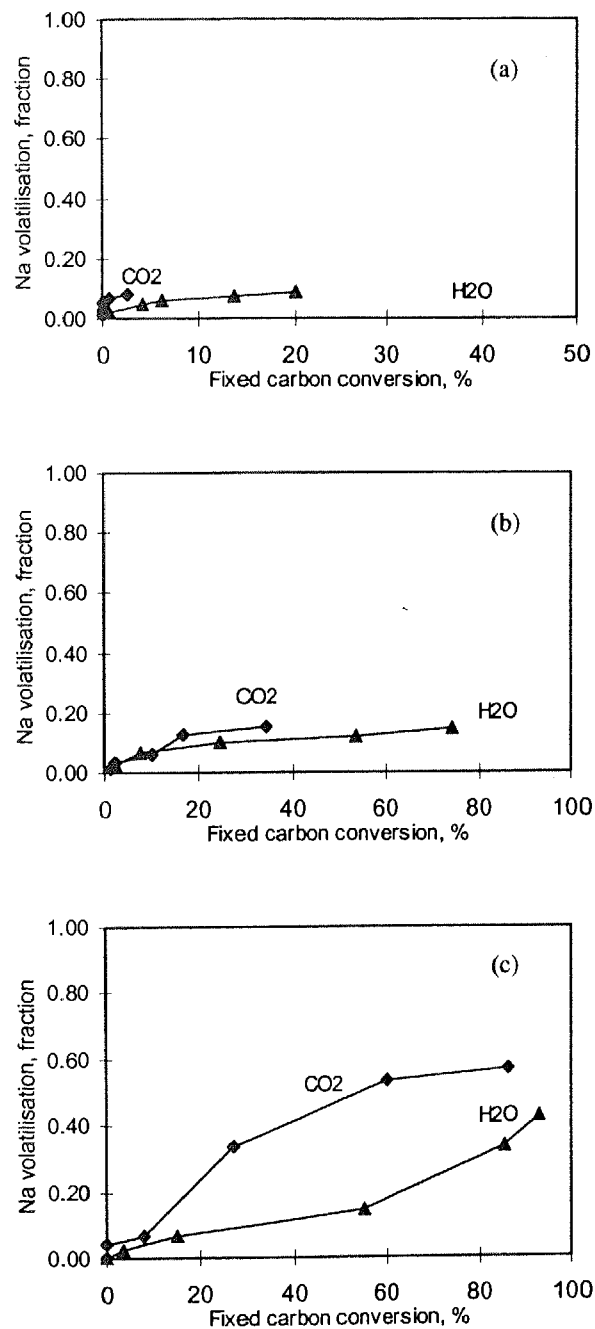


Figure 5.3 Sodium volatilisation as a function of carbon conversion during carbon dioxide and steam gasification (a) at 650°C, (b) at 750°C and (c) at 850°C of NA1 coal containing 0.92% of organically-bound sodium.

Figure 5.3 shows that higher losses of sodium during gasification with steam or with carbon dioxide at the tested temperatures were observed for higher carbon conversion under steam conditions. Reactions (5.1) or (5.2), as shown in Section 5.2.1, between sodium carbonate and char carbon are solid state reactions and gas atmosphere would have little influence on them, particularly on reaction (5.1). It appears that faster over all char

gasification reaction in steam involving catalytic action of sodium (Section 2.3.1.3.2) results in shorter life of metallic sodium and consequently lesser sodium vaporisation in steam.

5.3.2 Solubility of sodium present in pyrolysis and gasification char

Sodium mass balance and loss assessment analyses were carried out in two stages. First, finely ground char was digested in a hot acid solution and sodium was analysed in that solution. In the second step char residue from the first step was filtered out, ashed and that ash was analysed for any unleached sodium.

The nature of sodium in char whether leachable or not is important from the point of view of its possible reactions with silicon bearing minerals, as different sodium compounds will react in different way. There are reports published in the literature by Telfer (1999), Manzoori and Agarwal (1992), suggesting that during pyrolysis of coal containing organically-bound sodium, that sodium may transform into acid-insoluble form. In those reports sodium not leached out from char during acid leaching is called acid-insoluble sodium. However the sodium not leached out not necessarily must be insoluble in acids, it may be inaccessible. Equilibrium thermodynamic calculations predict formation of only soluble forms of sodium. Therefore the following assessment of solubility has been considered.

The coal used in this work contained organically-bound sodium totally soluble in acid. Analyses of the pyrolysis chars and gasification chars show that some part of original sodium present in coal is not leached from chars by acid. The results are shown graphically in Figure 5.4 for pyrolysis and in Figure 5.5 for gasification.

5.3.2.1 Effect of pyrolysis

Most of the sodium was leached out from char generated at all tested temperatures during pyrolysis. Some sodium however was still found in post-leaching residue. Nearly a third of all the sodium present in 650°C pyrolysis char was not leached by acid after pyrolysis lasting longer than 5 minutes. But for shorter lasting pyrolysis at 650°C some 90% of the total sodium has been found as leachable by acid. This result for short pyrolysis could be

contributed to the fact that the char physical structure has not yet been much altered in comparison with the coal structure and that allowed for almost full acid penetration of char.

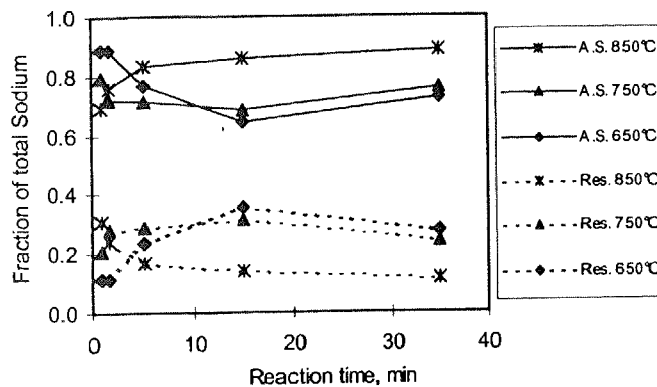


Figure 5.4 Distribution of sodium between acid-soluble (A.S.) sodium and sodium analysed in post acid leaching char residue (Res.) present in char as a function of reaction time for char generated during pyrolysis of NA1 coal at various temperatures.

For pyrolysis chars generated at 750°C and 850°C, more sodium was leached in acid solution. Char produced at 850°C had only a half of unleachable sodium of that found in the 650°C char.

This difference could be due to an increase of pore size upon prolonged char exposure to higher temperature. However also the reduction of sodium carbonate to metallic sodium in reaction with char carbon would release some carbon dioxide, which in turn would gasify the char before leaving it. That would increase char pore size and ease penetration of the finely ground char when mixed into acid for sodium leaching.

Pore development within coal char during pyrolysis leads to formation of a complex pore structure with pore radii ranging from the order of Angstroms to tens of microns (Simons, 1984). If sodium-compound molecules were present in the smallest pores they would not be able to leave such size pores even if the char was ground to few micron sizes. And also such pores will not be entered by acid solution as being too small for H_3O^+ hydronium ion to penetrate into them. Schafer in his early research (1983) suggests that it is really the case of the pore size of the particle used in the leaching to achieve full leaching of alkali ions. Schafer established, that finer grinding of brown coal char allowed for leaching of more cations present in char. These cations were originally present in coal in form of carboxylic

salts. Radovic et al. (1983) also reports reduced accessibility of dispersed ions due to very small micropore size in chars.

The fact that some sodium is still found in char residue post acid leaching can therefore be related to physical status of the char pores, rather than to the actual chemical form(s) of sodium and be called insoluble.

Studies by Poeze (2000) into catalytical effect of calcium and sodium on gasification rates of the Lochiel coal as used in this study well support the above conclusion. They show, in comparison with original coal, an increase of char surface area and micropore volume with both the temperature and experiment time for both pyrolysis and gasification chars. Poeze's experiments were conducted in a TGA apparatus at the same temperature range and for similar duration as experiments in this study. Examples of Poeze's results are presented in Table 5.3.

Table 5.3 Surface area and micropore volume data for high-sulphur Lochiel lignite for pyrolysis and gasification char samples obtained in TGA experiments by Poeze (2000).

Sample	Process	Temperature, °C	Time, minutes	Surface area, m ² /g	Micropore volume, cm ³ /g
Raw coal	-	ambient	0	185	0.150
Char	Pyrolysis in nitrogen	600	20	515	0.138
Char	Pyrolysis in nitrogen	600	30	550	0.146
Char	Pyrolysis in nitrogen	800	20	590	0.158
Char	Gasification in CO ₂	800	10	655	0.175
Char	Gasification in CO ₂	800	15	730	0.195
Char	Gasification in CO ₂	900	15	750	0.201

These surface area and micropore volume results give good support to the already presented evaluation of sodium leaching in relation to the char pore size. These results also support data presented in the next section on sodium leaching from gasification char.

Most sodium salts are soluble in water and it would be expected that in the process of sodium transformations during coal carbonisation sodium remains in a soluble form, as carbonate, sulphide, hydroxide or even metallic sodium. Therefore, if the sodium had not been leached out into acid solution it should not be considered as acid-insoluble, as those

quoted researchers suggest, but be labelled as unleachable by acid solutions, what would be due to physical restrictions within the char.

5.3.2.2 Effect of gasification

Chars generated during gasification with carbon dioxide or with steam contained much more acid-leached sodium than the pyrolysis chars. Carbon dioxide gasification chars still contained some 10% of the total sodium remaining in the post-leaching residue, as shown in Figure 5.5a, while sodium was almost fully leachable by acid from chars generated during steam gasification, as shown in Figure 5.5b.

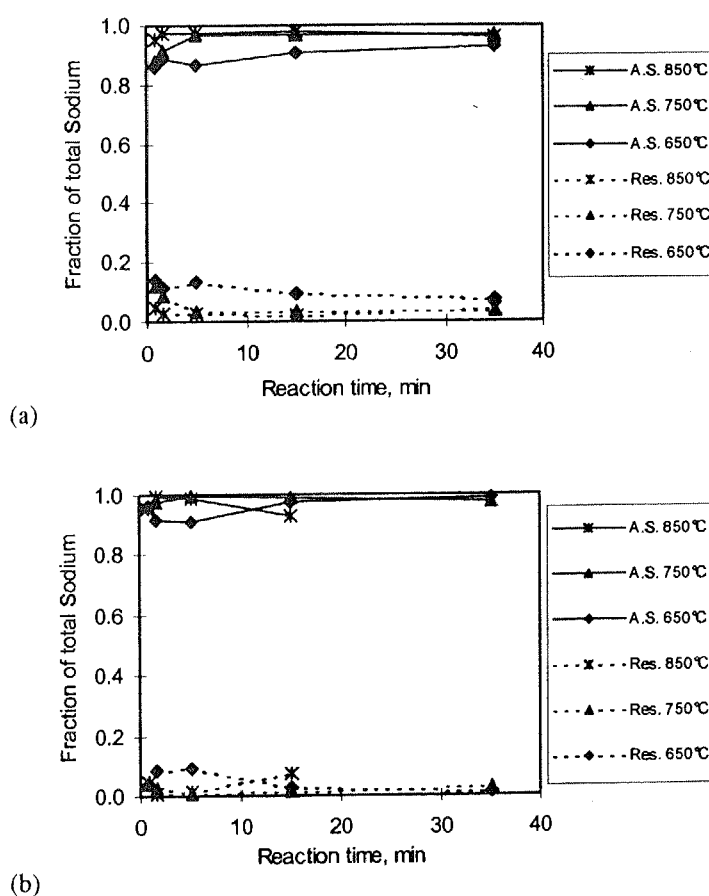


Figure 5.5 Distribution of sodium present in char between acid-soluble sodium (A.S.) and sodium analysed in char residue post acid leaching (Res.) as a function of reaction time for char generated at various temperatures during gasification (a) with carbon dioxide and (b) with steam of NAI coal.

Considering char gasification, there was nearly 10 times less of the original sodium remaining in the post-leaching steam char residue compared to that in pyrolysis char.

Those differences can further support an argument that the size of pores limits the accessibility of sodium. Gasification in steam resulted in much higher carbon conversion than in carbon dioxide at all experimental temperatures. It has been established (Ye, 1994) that for a few millimetre large lignite coal particles char gasification is a phenomenon taking place in the whole volume of the char particle, in difference to combustion process when oxygen is reacting with char on char surface. So, as the steam and carbon dioxide penetrate the char pores, the oxidation of carbon and a subsequent evolution of carbon monoxide and pore enlargement take place.

The results presented in both Figure 5.4 and 5.5 are based on one set of analyses carried out on one appropriate set of samples. Despite that, the trends in the results are clearly observable, and are ensuring of the good representation of the measured values and of the negligible possible error in analyses.

The chemical form(s) of sodium at the onset of gasification will be the same as from pyrolysis, as pyrolysis precedes gasification. Any changes to that form or forms may then be influenced by gasification atmosphere when the reactant gas diffuses into char particles.

5.3.3 Mechanism of formation of volatile sodium

Reduction of sodium carbonate by carbon has been reported widely in literature as presented in Chapter 2. Gow and Phillips (1992) show evidence of metallic sodium present in pyrolysis char of coal containing sodium carbonate. Li and Heiningen (1990) show the same for pyrolysis of black liquor char. Reactions leading to sodium formation would be the same during both gasification and during pyrolysis. The solid state reaction (5.1) between sodium carbonate and char carbon is according to McKee (1993) a rate controlling reaction in the redox cycle of reactions involving sodium and sodium carbonate as a proposed mechanism for sodium participation in catalytical gasification of carbon.

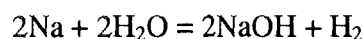


However for gasification with steam it may not necessarily be a solid-state reaction. As reported by Song and Kim (1993) sodium carbonate melts in steam much below its normal melting point of 851°C determined in air. Song and Kim (1993) report that in 80-20%

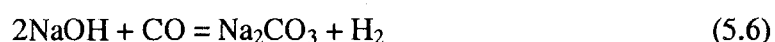
molar mixture of steam and nitrogen, respectively, sodium carbonate melts at 725°C. Consequently in the conditions reported in this study, for steam gasification sodium carbonate would be wetting the char in both 750°C and 850°C experiments. Thermodynamic calculations predict that for gasification with steam sodium carbonate will exist in a liquid form at 800°C, but for gasification with carbon dioxide at 850°C. The reactions involving sodium in a catalytic cycle for carbon dioxide gasification are proposed by McKee (1993) as follows:



and for steam gasification:



(5.5)



During gasification there was no nitrogen added to the reactor atmosphere. Therefore sodium released from char would be in the form of sodium metallic vapour, without possible formation of sodium cyanide. As already indicated earlier, the rate of sodium release was higher during gasification than during pyrolysis. This can be attributed to a steady increase of the char pore size, as gasification progressed and carbonaceous matter was gasified. That could lead to lower sodium vapour pressure within pores and consequently faster evaporation. Another reason for higher sodium release during gasification would be a fact of a constant re-creation of sodium carbonate, resulting in greater frequency of reaction (5.1) between char carbon and sodium carbonate.

The results on sodium release showed that less sodium evaporated in steam conditions than under carbon dioxide gasification. Therefore the reaction of sodium with steam to form sodium hydroxide as proposed reaction (5.5) could be considered as faster than reaction (5.3) between sodium and carbon dioxide. Further, it was shown earlier in Figure 5.3, that for similar level of sodium loss, carbon conversion during gasification with steam was twice of that measured during gasification with carbon dioxide.

As both reactants produce carbon monoxide in reaction with carbon, partial pressure of carbon monoxide would than be higher in the reaction environment of steam than that of

carbon dioxide. Therefore the reaction (5.6) re-creating sodium carbonate with participation of steam would need to be faster than reaction (5.4). This re-creation of sodium carbonate would increase frequency of the metallic sodium re-creation in repeated cycles and likely would also increase sodium evaporation. But as sodium loss was found higher in carbon dioxide atmosphere than in steam, it strengthens above conclusion that the reaction (5.5) in steam, reducing metallic sodium life, could be considered faster than the reaction (5.3) between sodium and carbon dioxide.

5.3.4 Determination of sodium forms in pyrolysis and gasification char

A mass balance for sodium obtained during experiments of pyrolysis and gasification of NA1 coal shows that most of the sodium remained in the char during conducted experiments, particularly at lower temperatures of 650°C and 750°C. It has then been important to identify the forms of sodium, as that question brought some doubts for sulphur-rich lignite coal. Literature reports such as by Schafer (1979b) or Yamashita et al. (1991) report on formation of sodium carbonate for low-sulphur coals or formation of sodium sulphide as suggested by Manzoori (1990). It was therefore necessary to define the forms of transformations during pyrolysis and gasification of coal containing organically-bound sodium and high levels of sulphur.

5.3.4.1 Determination of sodium carbonate using FT-IR spectroscopy

An indirect method was employed to establish the presence of sodium carbonate in pyrolysis and gasification chars by determining an evolution of carbon dioxide from char samples treated with acid. If chars from coal with organically-bound sodium contained sodium carbonate, as it has been inferred in the previous sections, then when treating such chars with acid, the carbon dioxide gas would be released to the atmosphere as sodium carbonate would be decomposed.

Char samples were simmered in acid and evolved gases were analysed for carbon dioxide content in FT-IR spectrometer. Details of the method and equipment arrangement have been presented earlier in Section 4.5.2.

Samples of chars from NA4 coals containing organically-bound sodium from gasification and pyrolysis experiments conducted at 750°C were chosen for carbon dioxide

determination by the FT-IR method. The NA4 coal, with sodium more than three times that in NA1 coal, was specially prepared for this carbon dioxide determination and for mineralogical analysis of chars.

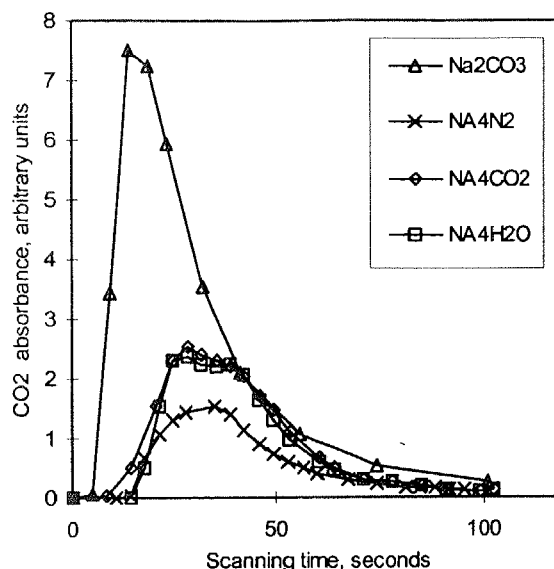


Figure 5.6 Carbon dioxide absorption measurements using FT-IR spectroscopy to determine presence of sodium carbonate in samples of NA4 coal char. Char samples were generated during pyrolysis in nitrogen and during gasification with carbon dioxide and with steam at 750°C.

Results of using infra-red absorption to determine any presence of carbon dioxide evolving from the chars treated with acid proved to be very helpful and informative. The results for carbon dioxide absorption evolved from pyrolysis and gasification chars of NA4 coal are shown in Figure 5.6. Results of carbon dioxide emission from several NA1 pyrolysis and gasification char samples are not included in that Figure, as due to much less sodium in the NA1 coal sample their peaks were considerably lower than those recorded for NA4 chars.

Table 5.4 Results of determination of presence of sodium as sodium carbonate in the pyrolysis and gasification char residues of NA4 coal obtained by measuring carbon dioxide absorption using FT-IR technique.

Sample	Process	Reaction time minutes	Sodium content %	Sample weight, grams	Residue char as part of used coal %	Estimated relative CO ₂ FTIR peak area	Sodium in char as carbonate, as part of sodium present in coal %
Na ₂ CO ₃		0	43.3	0.0387	-	1.00	100
LAWN2	Pyrolysis	15	0	0.1527	49.5	0	0
NA4N2	Pyrolysis	15	3.29	0.3096	51.4	0.27	44.1
NA4CO2	Gasification	30	3.29	0.2065	25.4	0.42	104.6
NA4H2O	Gasification	10	3.29	0.1940	25.0	0.40	105.4

The integrated relative area under absorbance lines allow relating carbon dioxide emission from the tested samples to their sodium content. Sodium content was then recalculated to its original content in coal to assess the sodium retention in char and results of that are shown in Table 5.4.

5.3.4.1.1 Effect of pyrolysis

There was no carbon dioxide release detected from the char of the acid-washed coal pyrolysed at 750°C, as shown in Table 5.4. That coal was free of any organically-bound sodium or any other ion-exchanged cations. Therefore no carbonates had been formed in that char. Also, as there was no carbon dioxide released from LAW coal char, there were no carboxylic groups left in that char, as they had all decomposed, as expected, during the process of pyrolysis. This result is in agreement with studies published by Schafer (1979b), that at 750°C all of carboxylic groups present in the lignitic coals decompose during pyrolysis process.

But there was substantial carbon dioxide evolving from NA4 coal pyrolysis char as it has been shown in Figure 5.6. The area under the NA4N2 pyrolysis char carbon dioxide absorbance line corresponds to 27% of the area under the line for the standard sodium carbonate released carbon dioxide. This result showed that at least some 44% of the total sodium present in NA4 coal was transformed during pyrolysis into sodium carbonate. As discussed in an earlier section, some of the sodium carbonate could still be trapped in the char pores and remain in there during the acid leaching.

5.3.4.1.2 Effect of gasification

Samples of NA4 coal were gasified till approximately 50% of fixed carbon conversion was reached. The actual gasification time in steam was three times shorter than gasification in carbon dioxide.

The amounts of carbon dioxide evolved from the chars obtained during gasification with steam and during gasification with carbon dioxide gasification were very similar, as shown in Figure 5.6. Integrating the area under the corresponding absorbance line showed no loss of sodium during gasification in either atmosphere, and even some gain has been

calculated, as shown in Table 5.4. This result may suggest some error in the integration technique or some analytical discrepancies. The amount of determined sodium carbonate was double that determined for pyrolysis char. This again can be related to the char pore size.

5.3.4.2 Determination of sodium carbonate by XRD technique

Mineralogical examination using XRD technique was carried out on selected NA1 char samples. This was to determine presence of mineral phases present in chars, particularly sodium compounds: sodium carbonate, sodium chloride, sodium sulphide or sodium hydroxide. Sodium carbonate in NA1 char samples has not been identified by XRD. Poor crystallinity and no aggregation to the grain size to give sufficient diffraction pattern could be the reason for sodium carbonate to be not determined in this analytical method.

Therefore the NA4 coal was prepared to experiment with coal containing higher levels of sodium, but still in the same organically-bound form. Pyrolysis and gasification chars of NA4 coal from experiments conducted for 30 minutes at 750°C showed a significant presence of sodium carbonate, natrite, in each examined sample. Diffraction patterns were stronger for gasification samples than for pyrolysis chars. No other sodium compounds were identified in examined samples.

The XRD results in addition to the FTIR results confirmed the formation of sodium carbonate from sodium organically-bound to the structure of a sulphur-rich coal during gasification or pyrolysis of such coal.

5.3.4.3 Determination of compounds between sodium and sulphur

The determination of sodium sulphide formation as stated earlier, was considered very important in this study, as it was necessary to determine the forms of sodium after transformations during thermal processes of organically-bound sodium present in high-sulphur coal. Literature report (Manzoori, 1990) and results of theoretical calculations as presented in Chapter 3 suggest formation of sodium sulphide during pyrolysis of such a coal.

Pyrolysis is the process of coal devolatilisation and diffusional forces are driving gases out from the particle to its outside. During that process there is a release of sulphur from coal, mainly in the form of hydrogen sulphide (Attar,1978). This hydrogen sulphide may react with sodium present in the char.

Analyses of char samples were carried out to determine possible presence of sodium sulphide generated during pyrolysis or during gasification of NA1 coal. The most suitable method for determination was considered to establish any presence in char of sulphide ions or sulphides in form of minerals. Wet chemical methods results are presented in Table 5.5.

Table 5.5 Results of analysis of NA1 coal char samples for the presence of sulphides and soluble sulphur compounds formed within char during pyrolysis and gasification of coal.

	Temperature, °C	Reaction time, min.	Leachate type	Sulphide S ⁼ %	Total soluble Sulphur, %
Pyrolysis in Nitrogen	850	0.75	Hot water	0	0
		15		0	0
		35		0	0
Gasification with carbon dioxide	850	0.75	Hot water	0	0
		15		0	0
		35		0	0
Gasification with steam	850	0.75	Hot water	0	0
		15		0	0
		35		0	0

There were no sulphides or other soluble forms of sulphur identified in the examined char samples. There were also no sulphides determined by mineral determination with XRD technique. These results differ from equilibrium predictions for pyrolysis conditions for temperature conditions below 850°C. According to these predictions sodium sulphide would be the most stable species in such conditions.

The NA1 coal contained 3.5% d.b. sulphur and 0.9% sodium. On a molar basis this gives four times more sulphur than stoichiometrically required to form sodium sulphide. Yet analyses of chars from pyrolysis and gasification experiments showed no presence of either sodium sulphide or sodium sulphate.

Ibarra et al. (1989) studied coal sulphur retention during pyrolysis at 600°C under helium by alkali and alkali earth elements present in Spanish lignites. They used FT-IR technique

to identify any possible changes to coal inorganic matter content. They report formation of calcium sulphide in char but found no traces of sulphides of either sodium or magnesium.

Telfer (1999) in her thesis on the fate of sulphur during pyrolysis of high-sulphur Bowmans coal, observed the same results as in this study. No sodium sulphide was identified in chars generated during pyrolysis in a slow heating process or during fluidised bed pyrolysis at temperature conditions corresponding to those in current study.

All these findings indicate that sodium sulphide does not form during pyrolysis or during gasification of high-sulphur lignite coal in temperature range characteristic for fluidised bed gasification process nor, again according to Telfer (1999), at lower temperatures. Instead, sodium carbonate is formed during pyrolysis or gasification of coal as the principal form of sodium, originally present in coal in organically-bound form.

The same will be the effect of sodium transformation during combustion of such coals in fluidised bed combustors. As shown in this Chapter, sodium carbonate forms in the char during coal pyrolysis. Therefore, it must be that sodium carbonate reacts with sulphur dioxide and oxygen to form sodium sulphate responsible for the formation of a sticky, agglomeration causing, ash component. Manzoori (1990) has suggested that the formation of sodium sulphate takes place after oxidation of initially formed sodium sulphide. This suggestion can be considered invalid.

5.4 PYROLYSIS AND GASIFICATION OF COAL CONTAINING SODIUM CHLORIDE

Sodium chloride is a major form in which sodium exists in some low-rank lignites. Sodium chloride has been identified in high-sulphur South Australian coals, as well as in the low-sulphur Victorian coals (Readett and Quast, 1986).

It was therefore necessary to investigate during both pyrolysis and gasification, the behaviour of sodium and chlorine present in coal as sodium chloride. Coal specially impregnated with sodium chloride (NC1 coal) was used in gasification and pyrolysis experiments. An additional sample, NC4 coal, was also prepared for mineralogical

assessments. For both these coals, sodium leached into cold water exceeded 95% of the total sodium impregnated into coal, proving that sodium was not organically-bound to the coal structure, but in the form of sodium chloride.

5.4.1 Sodium and chlorine volatilisation during pyrolysis and gasification

Reports in the literature (Shao et al., 1994; Lang, 1986; Bjorkman and Stromberg, 1997) say that chlorine leaves coal during pyrolysis as hydrogen chloride. Release of chlorine from coal or biomass can start at 300°C. Muchmore et al. (1995) report that during gasification of lignite coal most of the chlorine present in coal is released at temperatures below temperatures of fluidised bed gasification process. Disproportionate release of sodium and chlorine during gasification of South Australian lignites containing sodium chloride has been reported by Kosminski and Manzoori (1990).

Chemical analyses of NC1 coal gasification and pyrolysis chars were carried out by digesting the chars in stage leaching them in cold water, hot water and for 4 hours in water superheated to 120°C. and than analysing obtained leaching solutions for the presence of sodium and chlorine.

5.4.1.1 Effect of pyrolysis

Results of sodium and chlorine release from NC1 coal char during pyrolysis in nitrogen are presented in Figures 5.7. Pyrolysis of NC1 coal resulted upon heating in an almost immediate release of chlorine from coal. At 650°C 30% and at 750°C approximately 50% of original chlorine was released after 1.5 minute of pyrolysis. For 850°C this value was nearly 70%. At the same time sodium loss was insignificant at 650°C, approximately 8% at 750°C and just less than 20% at 850°C.

Similar results were reported by Manzoori and Agarwal (1992) who studied sodium and chlorine release during pyrolysis from single coal particles of similar coal. Results reported by Takarada et al. (1995) also correspond well with the results observed in this work. Takarada et al. (1995) concluded, that sodium release from coal on heating in an inert atmosphere is dependent on the chemical form of sodium. The organically-bound sodium volatilised less than sodium from coal loaded with sodium chloride. For coal containing

sodium chloride and pyrolysed for 1 hour at 840°C those workers report 90% of sodium as released from coal.

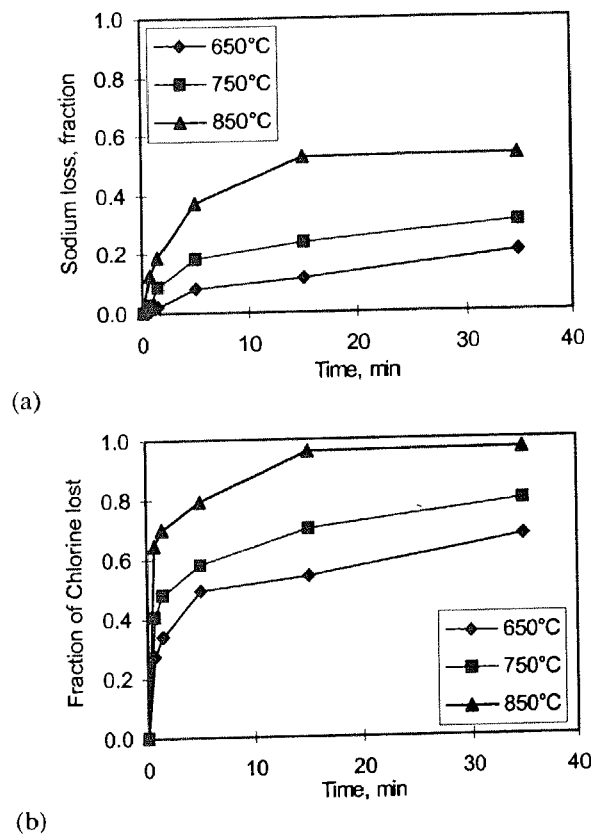


Figure 5.7 Losses (a) of sodium and (b) of chlorine from NCl coal during pyrolysis in nitrogen presented for various temperatures as a function of time.

These results clearly confirm earlier quoted sources that the release of both, sodium and chlorine from coal containing sodium chloride is disproportionate. But this disproportionate release would not be due to sodium chloride dissociation, as the experimental temperature conditions would be too low for that to happen. Therefore it had to be caused first, by a reaction or reactions of sodium chloride with coal, or with char, and then the formed products of those reactions would, depending on their nature, be released from char to the atmosphere.

With increased pyrolysis time more chlorine was released from char. That increase was observed at all three temperatures. After 35 minutes of pyrolysis at 650°C, 60% of chlorine was released, while at the same time at 850°C conditions almost all chlorine was released. At the same time maximum sodium loss from 650°C char was 20% and for 850°C char it was nearly 53%. As both sodium and chlorine release at 850°C was considerably higher, it

can be concluded that partial sodium chloride vaporisation took place at that temperature in addition to any other process, which caused release of both at lower temperatures.

Literature reports quoted earlier indicate release of chlorine from coal as hydrogen chloride, HCl. So, for HCl to be formed from the very early heating of coal, a reaction between sodium chloride and coal matter had to take place and sodium had to replace hydrogen in the coal/char structure. Hydrogen for formation of hydrogen chloride can originate from carboxylic groups -COOH, from groups such as -SH, or =NH or other groups. Lignites, as indicated earlier, are full of functional groups containing hydrogen. The hydrogen to form HCl could come from those groups or from hydrogen bound directly to carbon forming major coal structure, i.e. benzene rings. Identification of sodium carbonate in pyrolysis char of NC4 coal, as shown in the next section, would suggest reaction of sodium chloride with hydrogen of the carboxylic groups.

Upon prolonged heating the sodium was also released from char. The forms of that sodium can be speculated only and most likely it would be the elementary sodium vapour. If sodium attached itself to the formed char in reaction of sodium chloride with coal/char at early stage of heating up the coal, then that sodium upon further heating would break away from the formed char the same way hydrogen breaks from coal structure during pyrolysis. And that sodium would then vaporise most likely as elementary sodium vapour.

The results of the experiments reported by Dunderdale et al. (1963) of heating at 920°C sodium chloride mixed with fluidised bed char did not result in formation of a metallic sodium mirror; the mirror formed only from organically-bound sodium as has been discussed in previous sections. The explanation suggested by Dunderdale et al. is, that recombination of the sodium atoms with hydrogen chloride occurred in the vapour phase because of relatively low temperature prevailing in the experiments. But it appears that at those conditions a direct NaCl evaporation took place and no reaction between NaCl and char occurred.

5.4.1.2 Effect of gasification

As during pyrolysis, chlorine loss from NC1 coal during gasification of coal with either steam or carbon dioxide was almost immediate, as shown in Figure 5.8. Chlorine release

for short gasification times was slightly higher than that in pyrolysis for 650°C experiments in both gasification atmospheres. Generally that was the trend also at 850°C. For longer gasification times at 850°C however, results for carbon dioxide gasification showed less release of chlorine and as well of sodium than during pyrolysis. While in the steam atmosphere the release of both elements was higher than during pyrolysis. Chlorine release reached almost 100% for longer gasification time in steam, while in carbon dioxide atmosphere it was just above 90% for the equivalent gasification conditions.

Generally gasification results show for all experimental conditions that sodium release was 40% to 50% lower than that of chlorine, as can be seen in Figure 5.8 for gasification with carbon dioxide and Figure 5.9 for gasification with steam. It is inferred that the same mechanism governed reactions between sodium chloride and the coal/char at the beginning of gasification, as it did during coal pyrolysis in nitrogen. This would be because the initial process during gasification was coal devolatilisation.

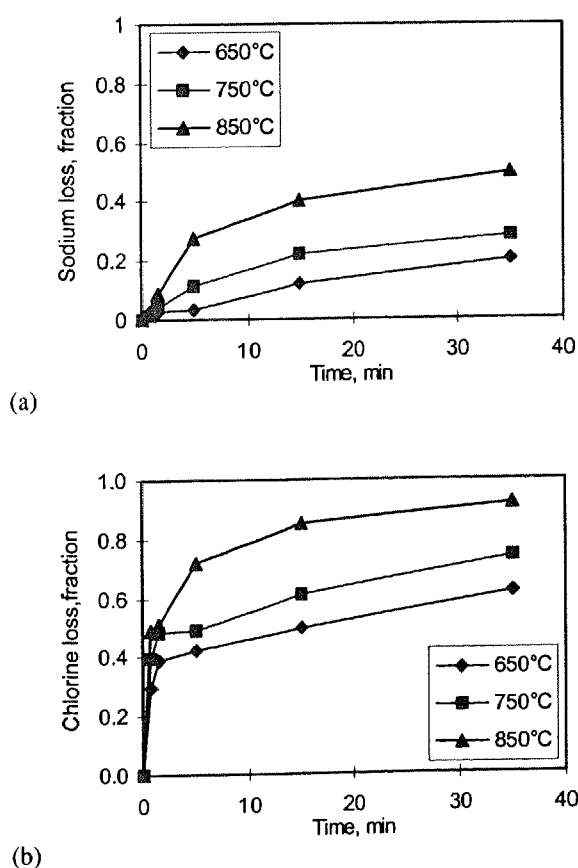


Figure 5.8 Losses (a) of sodium and (b) of chlorine during gasification with carbon dioxide of NCI coal for various temperatures presented as a function of time.

The thermodynamic equilibrium calculations for carbon dioxide atmosphere predicted existence only of sodium chloride vapour above 750°C, while coal gasification with steam would result in some 10% of total sodium to be in sodium hydroxide vapour form above 850°C, while other 90% in form of sodium chloride vapour.

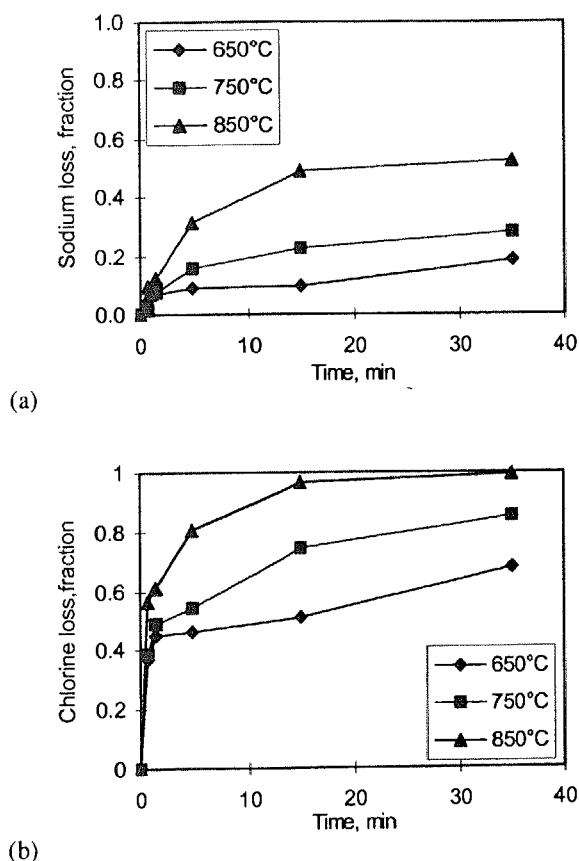


Figure 5.9 Losses (a) of sodium and (b) of chlorine during gasification with steam of NCl coal for various temperatures presented as a function of time.

Direct sodium chloride evaporation, the same way as during pyrolysis, would be expected at the 850°C temperature conditions. As evaporating sodium chloride would diffuse into a given gas environment, a lower sodium chloride evaporation could be expected into carbon dioxide environment due to higher molecular weight of CO₂ compared to steam environment.

A comparison of release from NCl coal char at 850°C of both, sodium and chlorine as a function of fixed carbon conversion is plotted in Figure 5.10 and results appear similar for both gasification environments. If there was no effect of any experimental error, chlorine loss was slightly lower in steam, particularly above 50% carbon conversion. That could be

reflecting direct sodium chloride evaporation being lower into higher molecular weight of CO_2 gas.

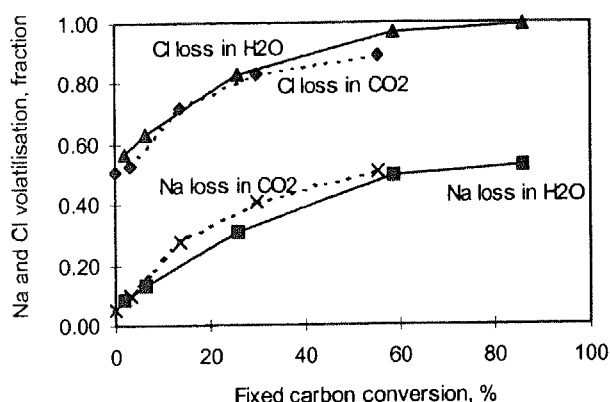


Figure 5.10 Release of sodium and chlorine from NCl coal presented as a function of carbon conversion during gasification with carbon dioxide and with steam at 850°C.

5.4.2 Determination of sodium carbonate in char

Treatment of gasification chars with acid and analysing gases using the FT-IR technique, as described in previous Section 5.3.3.1, showed evolution of carbon dioxide from the NCl chars. More carbon dioxide was evolved from the NC4 coal chars. These chars were produced at 750°C during pyrolysis in nitrogen and through gasification with steam and with carbon dioxide.

Results of carbon dioxide evolution from NC4 chars are shown in Figure 5.11. Results for sodium loss calculated from carbon dioxide absorption are presented in Table 5.6. Those results show that approximately 5% of the total sodium present in NC4 coal was transformed into sodium carbonate form during gasification in steam. Some 3% of the NC4 coal sodium has been identified as sodium carbonate in the carbon dioxide gasification char. This was a half of sodium carbonate identified in pyrolysis char.

For the sodium to be present in the pyrolysis or gasification char as sodium carbonate, the sodium would be expected to be present in coal in the form of carboxylate, which upon heating transforms into sodium carbonate. As discussed in the previous section on pyrolysis results, sodium chloride reacting with coal, or with char in its formation-stage, could react with carboxylic groups. This would result in formation of sodium carboxylates, which in turn, would decompose on subsequent heating and sodium carbonate would form.

If reaction with other hydrogen-containing groups is a mechanism of hydrogen supply for the formation of hydrogen chloride, then sodium in a new form would need to react with carbon dioxide from gasification atmosphere and form sodium carbonate in this way, or with steam possibly via reactions (5.5) and (5.6) presented earlier. As sodium carbonate was identified in chars from NC4 coal after gasification with both carbon dioxide and with steam, it suggests that various mechanisms of sodium carbonate formation could be involved. However as sodium carbonate was identified in NC4 pyrolysis char, where no carbon dioxide or steam was involved, direct reaction of sodium chloride with carboxylic groups and formation of sodium carboxylates still could be the most likely mechanism.

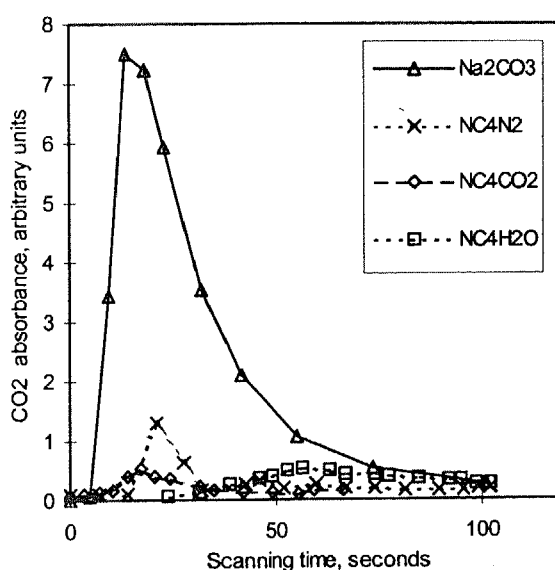


Figure 5.11 Carbon dioxide absorption measurements using FT-IR spectroscopy to determine presence of sodium carbonate in NC4 coal char samples. Char samples were generated during pyrolysis in nitrogen and during gasification with carbon dioxide and with steam at 750°C.

Mineralogical assessment with XRD also established the presence of sodium carbonate in NC4 coal gasification chars. Sodium carbonate, natrite, was identified in trace quantities in the steam gasification char. Natrite was also probably present in the char from carbon dioxide gasification. Natrite was not identified in NC4 pyrolysis char. Neither sodium sulphide nor sodium hydroxide was identified in any of the examined samples.

To further test this hypothesis of reaction of sodium chloride with hydrogen from carboxylic groups, another sample of coal was prepared, LiAC4 coal, in which lithium was organically-bound into coal carboxylic groups and sodium chloride was impregnated into

the coal. This coal was then used in pyrolysis and gasification experiments to generate char for XRD examination. As expected, sodium carbonate was not identified in pyrolysis char and in either char from carbon dioxide gasification or from steam gasification. These results seem to support above hypothesis, that sodium carbonate may form by reaction of sodium chloride with hydrogen from carboxylic groups.

The results of examination of NC4 coal chars lead to the following conclusion. If a coal contained sodium chloride and free carboxylic groups, then reaction of sodium chloride with these groups could increase formation of sodium carbonate in the char. This carbonate could enhance reactions with mineral inclusion present in coal and formation of liquid phases and that could further lead to the formation of ash agglomerates.

Table 5.6 Results of determination of presence of sodium as sodium carbonate in the NC4 coal pyrolysis and gasification chars by measuring carbon dioxide absorption using FT-IR technique. Char samples from experiments conducted at 750°C were treated with acid to evolve carbon dioxide.

Sample	Process	Reaction time minutes	Sodium content %	Sample weight, gram	Residue char as part of used coal %	Sodium in char sample, no loss assumed, gram	Estimated relative CO ₂ FTIR peak area	Sodium in char as carbonate, as part of sodium present in coal %
Na ₂ CO ₃			43.3	0.0387	-	0.0168	1.00	100
LAWN2	Pyrolysis	15	0	0.1527	49.5	0	0	0
NC4N2	Pyrolysis	15	3.32	0.0870	52.0	0.0029	0.13	6.1
NC4CO2	Gasification	45	3.32	0.0537	36.8	0.0018	0.07	5.4
NC4H2O	Gasification	30	3.32	0.1776	36.4	0.0059	0.14	3.1

5.4 SUMMARY

This chapter has dealt with the physico-chemical transformations of sodium present in a high-sulphur lignite coal during pyrolysis, and gasification with carbon dioxide or with steam under temperature conditions relevant to an atmospheric fluidised bed gasifier. Sodium transformation products will play important part in possible reactions with silica and kaolin during the coal gasification process. These transformations are summarised below.

1. Sodium release has been observed during pyrolysis in nitrogen atmosphere and during gasification with both, carbon dioxide and with steam of coal containing sodium organically-bound to coal carboxylic groups. Sodium volatilisation increased with temperature and time. Formation of elemental sodium metal in a process of reduction of sodium carbonate by char carbon followed by sodium vaporisation is believed to take place during gasification and pyrolysis.
2. Significantly higher sodium vaporisation was observed during gasification in carbon dioxide and in steam than during pyrolysis in nitrogen. For similar carbon conversion sodium vaporisation was higher during gasification with carbon dioxide than during gasification with steam, particularly at 850°C.
3. The size of char pores limits the accessibility of sodium. More sodium was acid-leached from chars generated during gasification than during pyrolysis. Physical status of the char pores and accessibility of sodium, not its actual chemical form(s), can then be considered a limiting factor on sodium reactions with coal mineral inclusions such as silica or kaolin.
4. Sodium carbonate forms as the principal form of sodium in char during both pyrolysis and gasification of coal containing originally organically-bound sodium.
5. Sodium sulphide does not form during pyrolysis or during gasification of high-sulphur lignite coal in the temperature range characteristic for fluidised bed gasifier.
6. During combustion in a fluidised bed combustor of coal with high sulphur content, sodium sulphate is predicted to form from reactions of sodium carbonate with sulphur dioxide and oxygen.
7. Release of both sodium and chlorine from coal containing sodium chloride is disproportionate. Almost full chlorine release has been measured during gasification and pyrolysis at 850°C. Release of sodium was nearly a half of that of chlorine and inferred to be in the form of sodium chloride vapour.

8. Sodium chloride reacts with hydrogen present in coal/char and chlorine is released in the form of hydrogen chloride. Identification of sodium carbonate in pyrolysis char confirms the reaction of sodium chloride with hydrogen from the coal carboxylic acid groups. Neither sodium sulphide nor sodium hydroxide was identified in pyrolysis or gasification char of coal containing sodium chloride.
9. Reaction of sodium chloride with free carboxylic acid groups present in ROM coal could enhance formation of ash agglomerates during coal gasification.

The results presented in this chapter will be used to explain reactions between sodium and silicon minerals during both pyrolysis and gasification in subsequent chapters.

Chapter 6

REACTIONS OF SODIUM WITH SILICA DURING PYROLYSIS AND GASIFICATION OF COAL - EXPERIMENTAL RESULTS

6.1 INTRODUCTION

This chapter concentrates on results of reactions between sodium compounds and silica present in coal pyrolysed in an atmosphere of nitrogen or gasified with carbon dioxide or with steam at conditions similar to those existing in a typical atmospheric fluidised bed gasifier. When sodium and silica react in such conditions, molten silicates may form, which in turn may cause the gasifier bed to agglomerate and/or to defluidise. Formation of molten silicates has been predicted by thermodynamic calculations presented in Chapter 3.

Additionally presented in this chapter are the results of reactions of mixtures of sodium salts and silica exposed to the same temperature and atmospheric conditions as the samples of gasified coal. The results of these experiments form a basis for the assessment of products of reaction between sodium and silica in coal gasification.

6.1.1 Silicate formation during gasification of coal

The literature reports reviewed in Chapter 2 referred to iron playing major role in agglomeration of ash in fluidised bed gasifiers for fuels rich in iron and in general to the

ratio between alkaline and acid oxides present in the ash (Carty et al., 1986; Moilanen et al., 1989, 1990). No specific alkali silicates were identified as being a major phase of the binding matrix in the identified agglomerates and deposits. Generally there is limited information on ash agglomeration of sodium-containing lignites gasified in fluidised bed gasifiers.

It is expected for temperature conditions relevant to fluidised bed gasification, that organically-bound sodium present in coal will react with silica to form sodium silicates. Silicates may serve as a cementing agent, embedding other ash particles to form agglomerates, which may electively drop out of the fluidised bed, or may stick to gasifier walls or cause bed defluidisation. A higher reaction rate near and above the carbonate melting point can be expected due to an improvement in carbonate-silica contact with an increase in temperature, due to a reduction of carbonate viscosity and the expected better contact at the silica grain surface.

Thermodynamic equilibrium predictions, as presented in Chapter 3, show that silicates, basically sodium disilicate, would be the principal liquid phase sodium silicate forming under conditions relevant to fluidised bed gasification of atmospheres containing nitrogen, steam, carbon dioxide, hydrogen or carbon monoxide above 600°C. Sodium metasilicate would also form and all silica present in the coal is predicted to be in a liquid form.

Therefore, it can be expected that during gasification of coal in a fluidised bed silica and sodium will react and form silicate products, which are likely to be the source of the bed material agglomeration and possibly defluidisation. Early trials on gasification of South Australian Bowmans coal in a pilot plant resulted in the agglomeration of ash rich in silica (Kosminski and Manzoori, 1990). From the trials it was concluded that the silicates and aluminosilicates of sodium were the major components of fused matrix binding agglomerate samples examined.

Gasification of low-rank coal may be conducted in a fluidised bed at temperature conditions between 700°C to 1000°C. Temperature conditions above 850°C will represent a region in which sodium carbonate formed from organically-bound sodium will be

transformed into a molten state. But both thermodynamic equilibrium predictions and literature data indicate that in steam sodium carbonate may melt at lower temperature.

For South Australian Bowmans or Lochiel coals, or Victorian Loy Yang coal, which have relatively high sodium and silica contents, agglomeration and defluidisation during fluidised bed gasification could be a real and a significant problem. Typical levels of silica and sodium oxide for these coals are presented in Table 6.1.

Table 6.1 Typical levels of sodium and silicon oxides in South Australian Bowmans and Lochiel coals and Victorian Loy Yang coal.

	Lochiel	Bowmans	Loy Yang
Ash value, % wt. d.b.	15.7	11.6	1.6
Na in coal, % wt. d.b.	0.8	1.4	0.07
SiO ₂ in ash, %	23.0	29.1	21.2
Na ₂ O in ash, %	7.2	15.0	9.5
Ratio Na/ SiO ₂ in coal	0.222	0.415	0.206

6.1.2 Formation and properties of silicate glass

If sodium carbonate was mixed with silica and heated to a temperature higher than 850°C, this would then correspond to glass-making conditions. The sodium carbonate standard melting temperature is 851°C and when molten, it will react with silica and form the simplest form of glass. The composition of basic glass may vary from Na₂O.xSiO₂, where 1 < x < 3.75, to 2Na₂O.SiO₂ (Hlavac, 1983). Silica will dissolve in such glass. Sodium disilicate Na₂O.2SiO₂ melts at a temperature of 874°C (Dean, 1985), but the lowest melting temperature for the above glass composition range is 789°C and corresponds to a eutectic composition of 27% mol Na₂O and 73% mol SiO₂.

The viscosity of sodium disilicate glass, according to Hlavac (1983), is about 3 poise at 1000°C and increases to 8.5 poise at 550°C. These values correspond to the requirement for glass forming and an upper range of glass working viscosities in the glass-making process. The glass-making process takes place at various temperatures depending on the

type of glass, but it is still carried out at comparable viscosity values. It may well be expected that the above quoted viscosity range will be characteristic for silicates formed during coal gasification.

Viscosity of the liquid material causing agglomeration is important as it influences ash sintering and agglomeration phenomena. Surface tension is also shown to influence sintering and consequently agglomeration (Falcone, 1989). Silicon dioxide to sodium oxide ratios at a given temperature influence melt viscosities and surface tension and exhibit influence on sintering and agglomeration (see Section 2.4.3). Reducing conditions particularly influence ash sintering. Water vapour may also play a role. Parikh (1958) established, that surface tension of a soda-lime silica glass can be significantly lowered by the presence of water-vapour atmosphere in the temperature range 500°C to 700°C.

A lot of research has been conducted into glass making in the temperature regions at the higher end of the range prevailing in fluidised bed gasifiers. Reactions between molten sodium carbonate and silica and other glass components, as well as reactions, which occur during heating up period between them, may as well occur within coal char containing the same materials.

Harrington et al. (1963) have shown that in the two-component system of silica and sodium carbonate, with $\text{SiO}_2/\text{Na}_2\text{O}$ molar ratio equal to four, reaction between these two components takes place in a temperature range of 630 - 780°C. This reaction proceeds in accordance with the following proposed equation:



Metasilicate Na_2SiO_3 was identified as the reaction product. In that study, powdered mixtures of silica and sodium carbonate were used. Harrington et al. (1963) established that a solid-state reaction with the release of CO_2 occurs at the surface of silica grains and a thin layer of metasilicate Na_2SiO_3 (melting at 1089°C) is produced.

The reaction rate between sodium carbonate and silica increases when the first melt occurs. As shown in Figure 2.3, the first melt should occur at 789°C and the resulting eutectic will

contain 73% mol of SiO_2 . The melt improves the contact area between the reactants and at the same time un-reacted SiO_2 begins to dissolve in the melt.

Steam may influence the reaction between sodium carbonate and silica. Thermodynamic predictions results show that in steam, sodium carbonate will melt at 800°C . Song and Kim (1993) reported Na_2CO_3 melting point temperature as 725°C in 80-20% molar mixture of steam and nitrogen and Huttinger and Minges (1985) reported a temperature of 801°C for Na_2CO_3 in a 50-50 % steam-argon molar gas environment. Standard Na_2CO_3 melting point is 851°C measured in pure nitrogen. Figure 6.1 shows a comparison of these sodium carbonate melting temperatures in relation to steam content in the gas mixture. It can be assumed from Figure 6.1 that as sodium carbonate melting temperature steadily declines in a 100% steam environment sodium carbonate will melt at ca. 700°C .

This short review of relation between sodium and silica at high temperatures and possible influence of gasification atmosphere requires a good understanding of the influence of gasification process parameters on the formation of silicates. This is critically important in avoiding problems associated with bed material agglomeration and defluidisation.

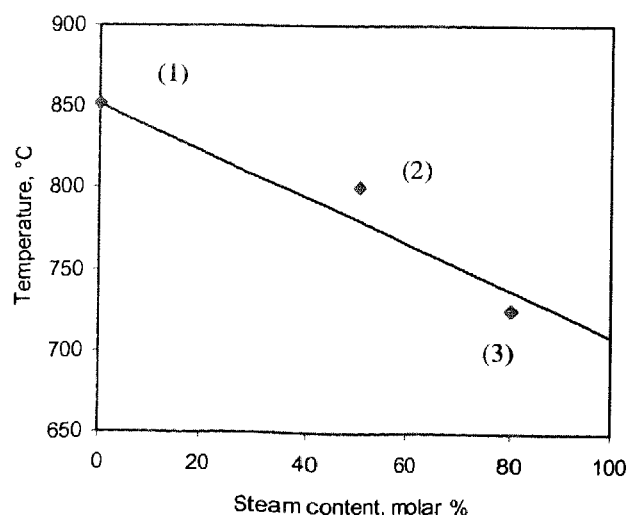


Figure 6.1 Sodium carbonate melting temperature trendline presented as a function of steam content: (1) standard melting point, (2) Huttinger and Minges, 1985, (3) Song and Kim, 1993.

6.2 OBJECTIVES OF THIS WORK

The objective in this Chapter is to provide experimental validation to the thermodynamic predictions presented in Chapter 3. A series of experiments for coal gasification and pyrolysis have been designed and outlined in Chapter 4. Coal samples with silica and controlled forms of sodium, as well as mixtures of silica with sodium salts to reflect sodium and silica forms present in coal are investigated.

6.3 SILICA AND ORGANIC SODIUM MIXTURE

The investigations to establish the reaction products and reaction mechanisms between sodium and silica under conditions prevailing in a fluidised bed gasification process were first carried out with silica and sodium acetate SAC mixture, prepared as shown in Section 4.2. The mixture was exposed to pure atmospheres of nitrogen, carbon dioxide or steam. The description of the experiments is presented in Section 4.4. Details of the analytical method of products and analytical approach are presented in Section 4.5.

These experiments with SAC mixtures were followed by pyrolysis and gasification experiments of NAIS coal containing silica and organically-bound sodium, and further followed by the same type of experiments for silica and sodium chloride SNC mixture and pyrolysis and gasification of NCIS coal containing silica and sodium chloride.

6.3.1 Chemical Analyses

The assessment of sodium and silica reactions in SAC mixtures during the experiments was based on solubility of sodium silicates. The results of silica solubility show a change of solubility of silica from initially insoluble form to solubility in cold, hot and in superheated water as the silicates form. At the same time, the solubility of sodium was changing from that of original sodium present in mixtures being soluble in cold water to sodium becoming soluble in hot and in superheated water, as silicates formed.

6.3.1.1 Results for nitrogen atmosphere experiments

The experimental results for solubility of sodium and silica reaction products formed during the exposure of SAC mixture of silica and sodium acetate exposed to the atmosphere of nitrogen are presented in Figures 6.2 and 6.3 for silica and sodium, respectively. The initial content of sodium, which was completely soluble in cold water, in SAC mixture was 6.2%. Results presented are shown as mass per cent of soluble silica or soluble sodium present in the total analysed sample. Both, solubility in cold and hot water are presented in these two figures. Results for solubility of both, sodium and silica in water superheated to 120°C are shown in Figure 6.4.

Although silica was mixed with sodium acetate, on exposure to experimental conditions the acetate was almost immediately decomposed and sodium carbonate formed. The formation of sodium carbonate from acetate was evident from the mass balance data for the shortest experiment time. Further mass loss was observed due to the carbon dioxide emission as reaction of silica with sodium carbonate continued.

XRD analyses of SAC mixtures exposed to experimental conditions showed no presence of sodium acetate in the samples for either short or long exposure time experiments. The presence of sodium carbonate in the examined samples, as shown in Table 6.2 further in Section 6.3.4, was positively identified.

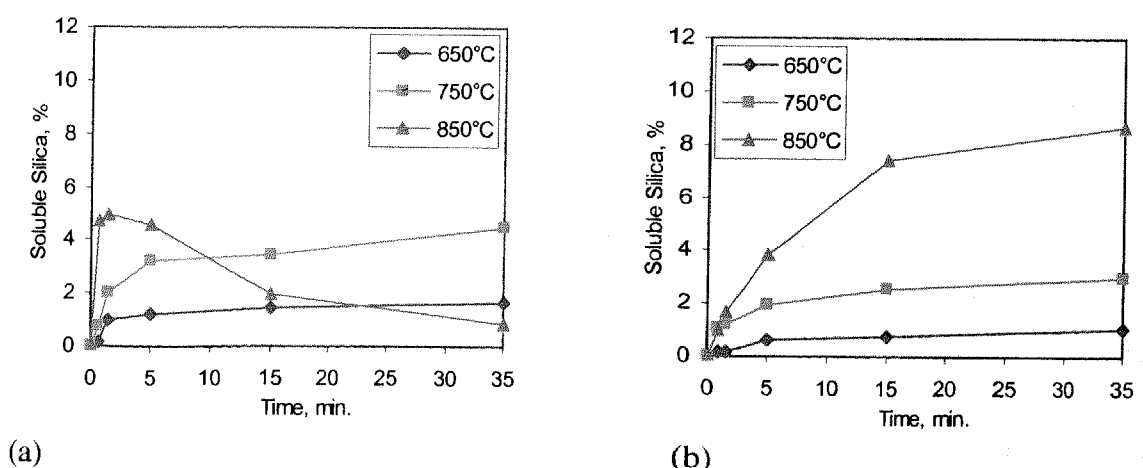


Figure 6.2 Silica soluble in (a) cold and (b) hot water as part of a sample of SAC mixture containing silica and 6.2% sodium as sodium acetate exposed to atmosphere of nitrogen at 650°C, 750°C and 850°C and presented as a function of reaction time.

Consequently all results of this series of experiments for SAC mineral mixture can be viewed as results of reaction between silica and sodium carbonate, and reflecting the chemistry of sodium and silica present in coal char during gasification.

From Figure 6.2, it appears that part of the silica has already reacted with sodium at 650°C as part of silica became soluble in cold water. The amount of silica soluble in cold water equalled nearly 1% of the total sample after 5 minutes, and increased to approximately 2% after 35 minutes. For the same reaction times at 750°C approximately two times more of silica became soluble in cold water and similar amount became soluble in hot water. At the same time sodium solubility in cold water reduced from 6.2% to just below 5%, and part of the sodium became soluble in hot water with more than 1.0% of the sample being sodium soluble in hot water.

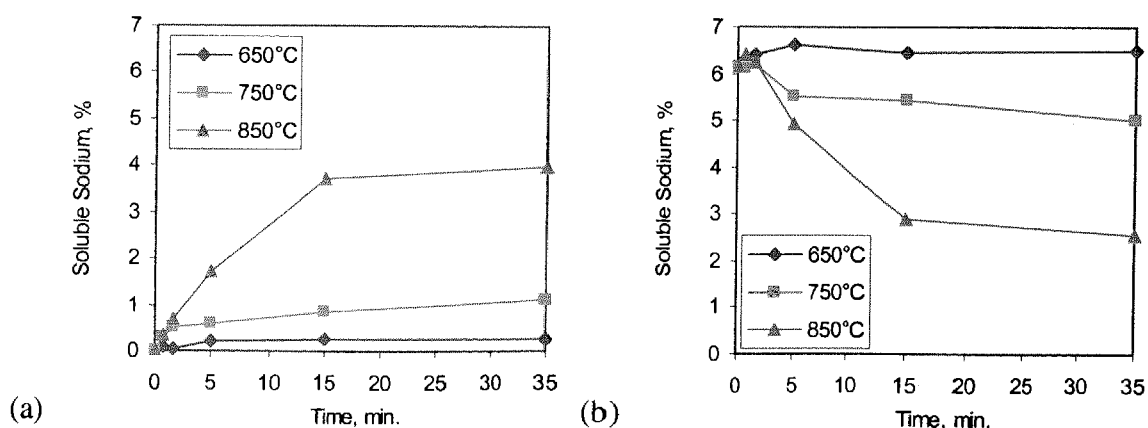


Figure 6.3 Sodium soluble in (a) cold and (b) hot water as part of a sample of SAC mixture containing 6.2% sodium as sodium acetate and silica exposed to atmosphere of nitrogen at 650°C, 750°C and 850°C and presented as a function of reaction time.

Results for silica solubility in SAC samples exposed to nitrogen atmosphere at 850°C are different from those exposed at 650°C and 750°C. Initially, after very short reaction times silica became soluble in cold water reaching almost 5% of total sample mass. For longer reaction times, silica solubility in cold water dropped below 1% of the mass of the total sample. At the same time silica solubility in hot water increased from just under 1% for 45 seconds to nearly 8.5% after 35 minutes. These differences in water solubility of the reaction products suggest the formation of different compounds.

Samples of SAC mixtures exposed to 850°C were found to have different characteristics with respect to sodium solubility. Less than a half of the sodium remained soluble in cold water, while the rest became soluble in hot water. After 35 minutes of reaction sodium soluble in hot water constitutes 4% of the sample.

The change in silica solubility suggests initial formation of soluble, in cold water, metasilicate, and as reaction progressed the formation of sodium disilicate soluble in hot water. The formation of sodium disilicate has been confirmed by changes in solubility of sodium, as less sodium was soluble in cold water, and part of sodium became soluble in hot water.

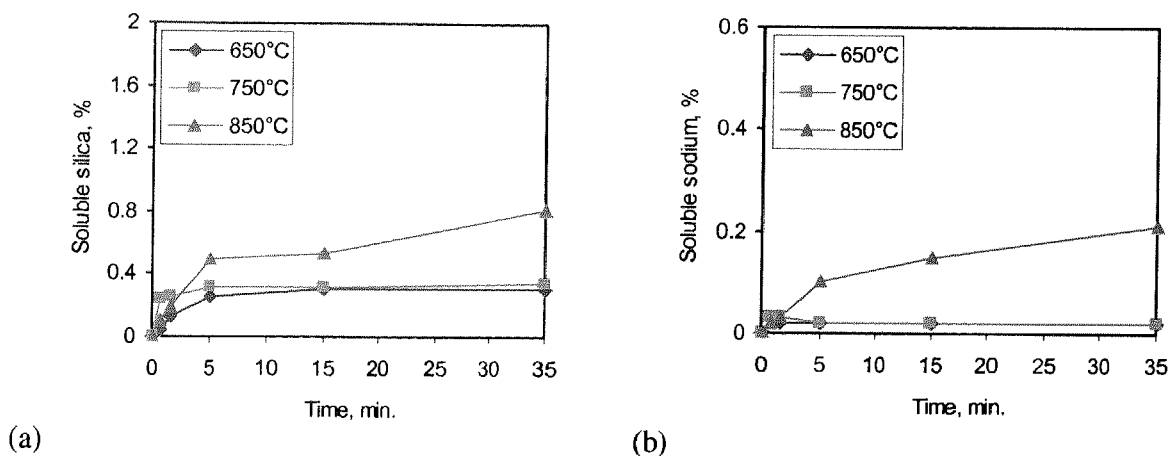


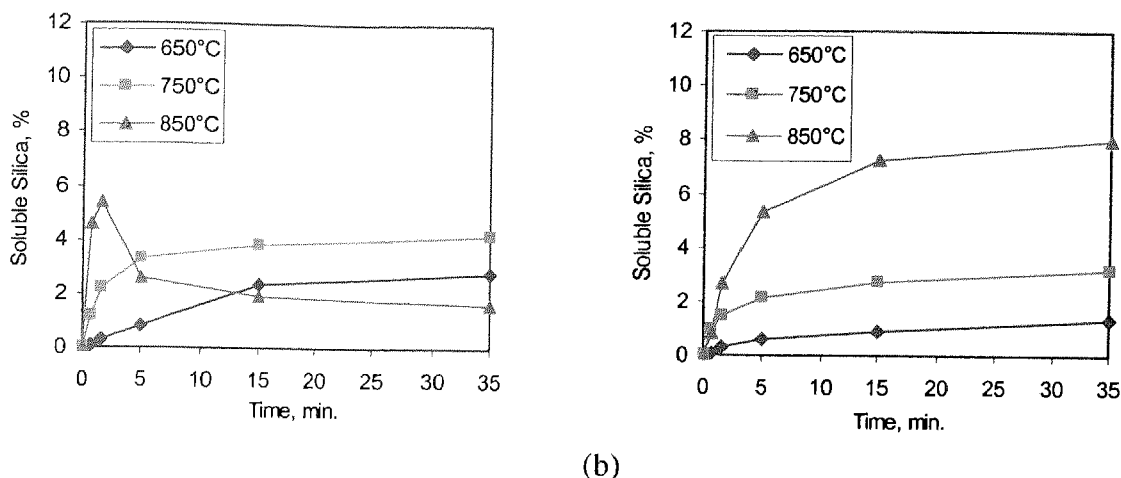
Figure 6.4 Solubility of (a) sodium and (b) silica in water superheated to 120°C of SAC samples, the mixtures of silica and sodium acetate, exposed to nitrogen atmosphere at 650°C, 750°C and 850°C temperature, presented as function of reaction time.

Residues from the hot water leaching were digested in water superheated to 120°C. The results are shown in Figure 6.4. The solubility of both sodium and silica was an order of magnitude less than in hot water at 850°C. For the 650°C and 750°C samples, no sodium was detected and silica levels were very low and could be considered at detection limits in the analysed water leachates. These results indicate no diffusion of sodium into the silica structure at the lower temperatures after the formation of product soluble in hot water.

6.3.1.2 Results for carbon dioxide atmosphere experiments

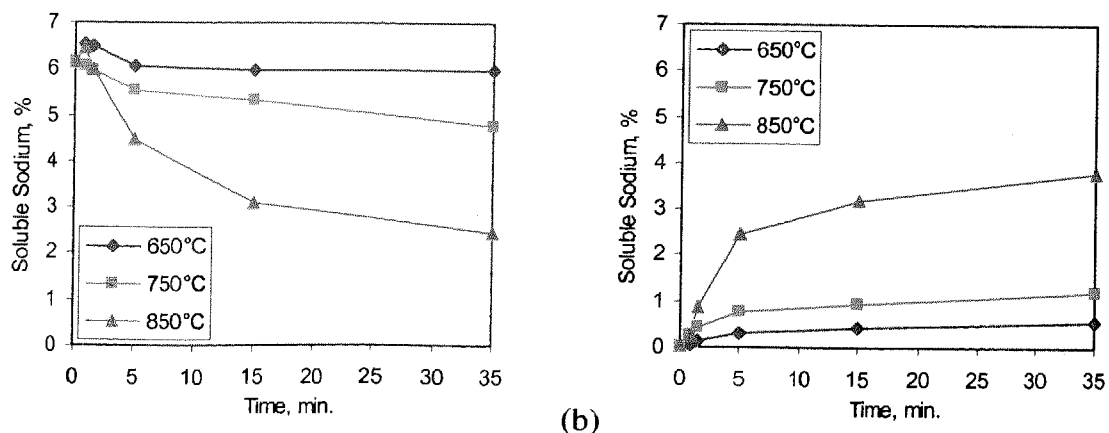
The solubility of silica and sodium reaction products for SAC mixture samples exposed to carbon dioxide atmosphere is shown in Figure 6.5 and Figure 6.6. The results for solubility

in water superheated to 120°C are shown in Figure 6.7. The solubility of products from the carbon dioxide results is similar to that observed for a nitrogen atmosphere.



(a) (b)
Figure 6.5 Silica soluble in (a) cold and (b) hot water as part of a sample of SAC mixture containing 6.2% sodium as sodium acetate and silica exposed to atmosphere of carbon dioxide at 650°C, 750°C and 850°C and presented as a function of reaction time.

Silica solubility in cold water after 35 minutes of reaction reached just over 2% and 4% of the total mass for the 650°C and 750°C samples, respectively. The formation of product soluble in hot water is near zero at 650°C and some 3% of the total silica soluble in hot water after 35 minutes of reaction at 750°C.



(a) (b)
Figure 6.6 Sodium soluble in (a) cold and (b) hot water as part of a sample of SAC mixture containing 6.2% sodium as sodium acetate and silica exposed to atmosphere of carbon dioxide at 650°C, 750°C and 850°C and presented as a function of reaction time.

However, at 850°C there was an initial large formation of silica soluble in cold water, as after only 1.5 minute of reaction more than 5% of the sample was silica in this form. As the reaction progressed, this value dropped to below 2%. At the same time, the concentration

of silica soluble in hot water was quickly rising with increasing reaction time and after 15 minutes levelled off at near 8%.

Results for sodium solubility are also similar to those reported in the nitrogen atmosphere. Only 1% of sodium from SAC mixture exposed to 750°C for 35 minutes in the carbon dioxide atmosphere is soluble in hot water. For the 850°C reaction, sodium soluble in cold water dropped to below 3% while sodium soluble in hot water increased to near 4%.

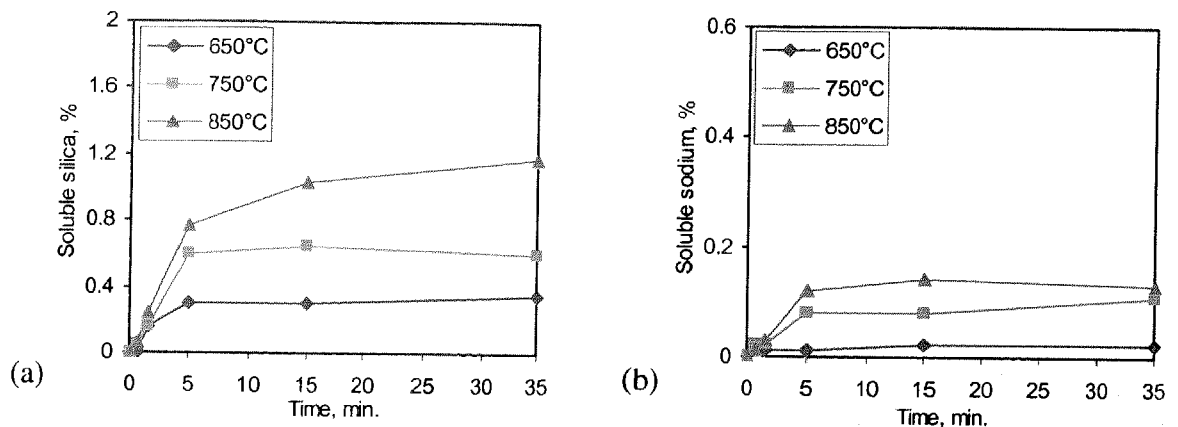
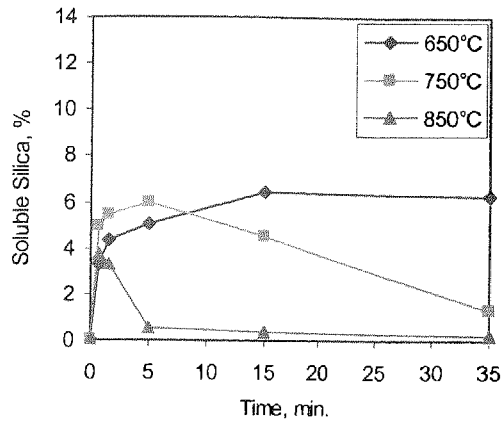


Figure 6.7 Solubility of (a) sodium and (b) silica in water superheated to 120°C of SAC samples, the mixtures of silica and sodium acetate, exposed to carbon dioxide atmosphere at 650°C, 750°C and 850°C temperature, presented as function of reaction time.

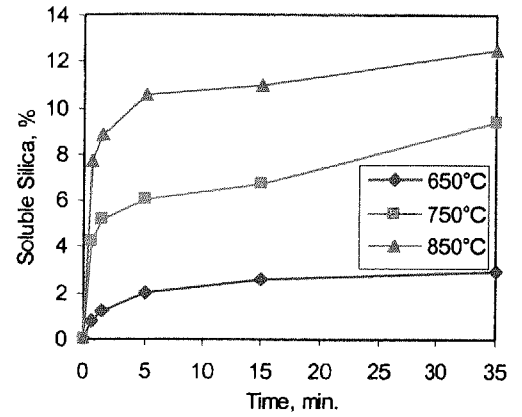
The solubility of silica in water superheated to 120°C was near an order of magnitude less than in hot water for the 650°C and 750°C experiments. The SAC samples exposed to 850°C showed higher silica solubility results than for those exposed to a nitrogen atmosphere. A value of around of 1% of the total sample mass still shows a low level of diffusion of sodium into the silica. Sodium solubility was more than an order of magnitude lower than the concentration of sodium soluble in hot water.

6.3.1.3 Results for steam atmosphere experiments

The results of the solubility analysis in cold and hot water of sodium and silica from experiments conducted in a steam atmosphere are shown in Figures 6.8 and 6.9, respectively. Solubility results in water superheated to 120°C are shown in Figure 6.10. Both Figure 6.8 and 6.9 show much higher solubility of silica in cold water as well as in hot water in comparison to the results observed for carbon dioxide or nitrogen atmosphere.



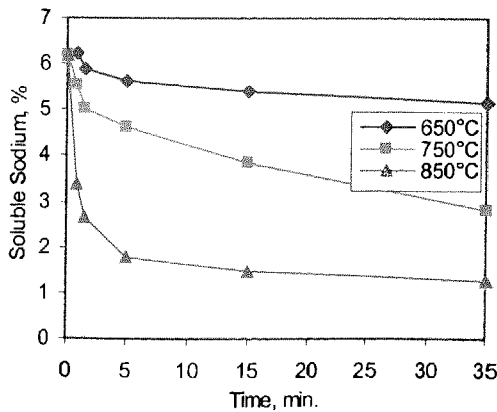
(a)



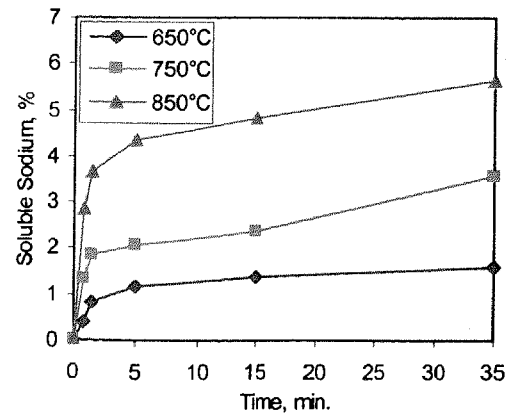
(b)

Figure 6.8 Silica soluble in (a) cold and (b) hot water as part of a sample of SAC mixture containing 6.2% sodium as sodium acetate and silica exposed to atmosphere of steam at 650°C, 750°C and 850°C and presented as a function of reaction time.

The formation of silica reaction product soluble in cold water was almost immediate for all tested temperatures. At 650°C, silica soluble in cold water was more than 6% after 35 minutes of heating. At 750°C, the initially high silica soluble in cold water was reduced to 1% after 35 minutes of reaction. While at 850°C, some 3.5% of the silica was soluble in cold water after only 45 seconds of heating. As the heating progressed, silica became mostly soluble in hot water.



(a)



(b)

Figure 6.9 Sodium soluble in (a) cold and (b) hot water as part of a sample of SAC mixture containing 6.2% sodium as sodium acetate and silica exposed to atmosphere of steam at 650°C, 750°C and 850°C and presented as a function of reaction time.

Corresponding with the increase of silica soluble in cold water for the 650°C products, some silica also became soluble in the hot water. At 750°C there was immediate formation

of products containing silica soluble in hot water, reaching 9.0% after 35 minutes. At 850°C, silica soluble in hot water increased to 12.5% of the reaction product's mass.

Sodium soluble in cold water for samples heated at 650°C dropped from the initial 6.2% to 5%. At 750°C, this reduction was to 3%, while the content of sodium soluble in hot water increases to the same level. At 850°C, after 35 minutes of heating most of the sodium was transformed and was soluble in hot water, reaching a value of 5.5% of the total sample.

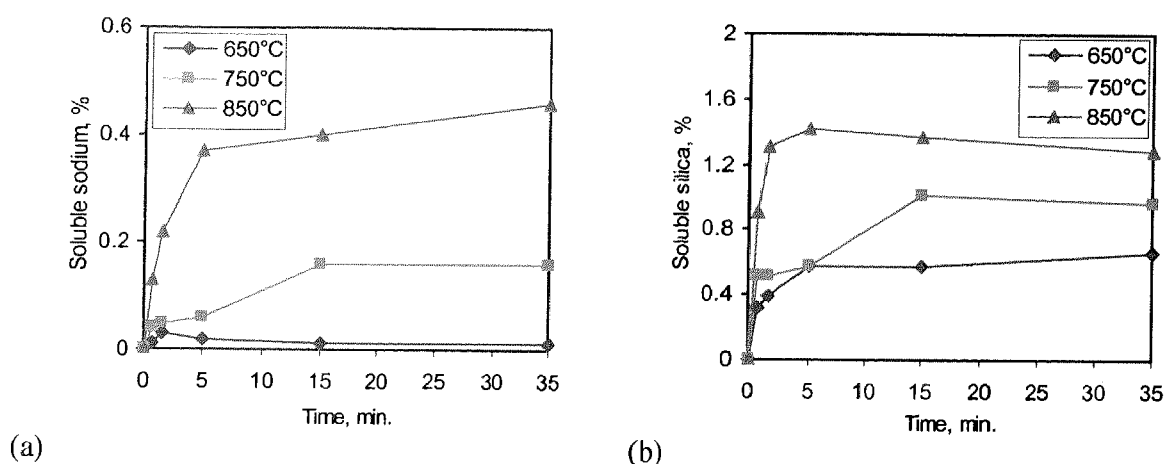


Figure 6.10 Solubility of (a) sodium and (b) silica in water superheated to 120°C of SAC samples, the mixtures of silica and sodium acetate, exposed to nitrogen atmosphere at 650°C, 750°C and 850°C temperature, presented as function of reaction time.

The solubility of reaction products in superheated water was negligible for sodium and somewhat noticeable for silica for 650°C conditions. At 750°C, sodium solubility was similar to that observed at 850°C in carbon dioxide and nitrogen atmospheres, at the 0.2% level, while values for silica reached to 1.0% and was higher than for corresponding carbon dioxide atmosphere value. The values for 850°C samples for sodium were near 0.45%, which was more than two folds higher than from other atmospheric experiments, but still an order of magnitude lower than those for solubility of sodium in hot water. The silica content was at approximately 1.3% of the total sample mass and appeared independent of the reaction time.

6.3.2 Evaluation of formation of silicates

6.3.2.1 Effect of carbon dioxide and nitrogen atmosphere

When a mixture of silica and sodium carbonate is heated towards the sodium carbonate melting point, there is a possible solid-state reaction between sodium carbonate and silica resulting in the formation of sodium metasilicate, as suggested by Eitel (1965) and by Harrington et al (1963). This solid-state reaction precedes the reaction between molten sodium carbonate and silica.

Solubility analyses for silica performed on products of SAC mixture exposed to various temperature and atmosphere conditions allow some differentiation between forms of silicates formed. Silica dissolved in cold water would represent formed metasilicate of sodium. At the same time, sodium present in metasilicate would also be soluble in cold water. The ratio of silica to sodium found in the cold water leachates, whether from samples exposed to carbon dioxide or nitrogen atmosphere, can not be considered as a measure of Na_2SiO_3 formation, as some the sodium would be un-reacted sodium carbonate. Sodium carbonate presence has been shown by XRD examination as presented in Table 6.2

Table 6.2 X-ray diffraction analysis of samples of sodium carbonate and mixture of sodium carbonate and silica exposed to steam atmosphere for various times at temperature between 650°C and 850°C.

Sample	Atmosphere	Time, min.	Temp. °C	Mineralogical Composition*		
				Dominant**	Minor	Trace
NA1 coal	Steam	15	750	sodium carbonate		thermonatrite
NA1 coal	Steam	15	825	sodium carbonate	thermonatrite	
SAC	CO ₂	1.5	850	quartz		
SAC	CO ₂	35	850	quartz		amorphous material
SAC	Steam	15	650	quartz		thermonatrite and natrosilite
SAC	Steam	1.5	850	quartz	amorphous material	thermonatrite and unidentified material
SAC	Steam	5	850	quartz	amorphous material	trona and thermonatrite

* The phases identified were: sodium carbonate (Na_2CO_3), thermonatrite ($\text{Na}_2\text{CO}_3 \cdot \text{H}_2\text{O}$), natrosilite ($\text{Na}_2\text{Si}_2\text{O}_5$), trona ($\text{Na}_3(\text{HCO}_3)(\text{CO}_3) \cdot 2\text{H}_2\text{O}$),

** Dominant (>60%), minor (5-20%), trace (<5%).

The results presented in Figures 6.2 and 6.5 show the formation of metasilicate had taken place at 650°C and more had been formed by 750°C. These results are in agreement with similar results published by Harrington et al. (1963), who reported on the reaction between silica and sodium carbonate at conditions also below the sodium carbonate melting point. In a batch reaction between soda and quartz at molar ratio 1:2, this solid-state reaction starts at 730°C. Eitel (1965) quotes studies in which it was established that in a mixture between sodium carbonate and silica, the solid-state reaction is the first stage of reaction and is followed by “polyeutectic” melt phase formation

No particular influence of either nitrogen or carbon dioxide atmospheres on the formation of metasilicate can be concluded, as the rate of formation of this silicate is similar. However, the formation of metasilicate was 200°C below the sodium carbonate melting point of 851°C. Therefore, it can be concluded that the reaction between silica and sodium carbonate at 650°C leading to the formation of metasilicate was a solid-state reaction.

Silica, which dissolves in both hot water and superheated water, represents a range of sodium silicates containing more silica than in metasilicate. Any sodium insoluble in cold water but becoming soluble in hot water must come from sodium silicates with increased silica content. Consequently, the silica to sodium ratio in hot water leachates can be used as a measure of the formation of sodium silicates, particularly of sodium disilicate $\text{Na}_2\text{Si}_2\text{O}_5$. The formation of this silicate is important and significant, as it may form a molten phase at reaction conditions prevailing in a fluidised bed gasifier.

The hot water mass ratio of silica to sodium for all of the examined nitrogen and carbon dioxide samples, and steam samples as well, is similar to that in sodium disilicate $\text{Na}_2\text{Si}_2\text{O}_5$, suggesting that this is the major form of silicate formed.

The formation of sodium disilicate starts taking place at 750°C, as some of the silica and sodium became soluble in hot water, as occurred for the results for both nitrogen and carbon dioxide atmospheres. The product solubility of SAC mixtures heated at 850°C is much higher than at lower temperatures. The initial formation of sodium metasilicate at 850°C is immediately taken over by the formation of sodium disilicate as reaction between molten sodium carbonate and silica progressed. These results also show that at higher

temperature conditions, not all of the sodium reacts with silica, as nearly half of the sodium remained in cold water soluble exceeding the stoichiometric amount required for formation of metasilicate, amount of which would correspond to silica found soluble in cold water.

The results of silica solubility showed that sodium disilicate should be considered as the major silica form after heating at 850°C and a considerable part of the silica after heating the SAC mixture at 750°C in carbon dioxide or nitrogen atmospheres. However, as shown in Figure 3.4, hot water can dissolve silicate glass with a composition of not only sodium disilicate but also of the lowest melting eutectic in the system between sodium oxide and silica. This has a melting temperature of 789°C and a composition on a molar basis of 27% Na₂O and 73% SiO₂. If a silicate glass of a composition similar to that of this eutectic is cooled down and the eutectic point is reached, solid quartz and sodium disilicate would form. However, if the cooling of the glass is a fast process, as it would be the case in the experiments reported here, then there would be no precipitation from the melt of these two components and the glass will cool down with preservation of its composition.

Therefore, the interpretation of the silica and sodium solubility results must be careful in defining sodium disilicate as the only silicate soluble in hot water, as other glass with a composition of greater silica content will also be soluble in hot water. However, as stated above, the mass ratio between silica and sodium oxide in the analysed hot water leachates closely corresponds to that of sodium disilicate.

The mechanism of the individual batch-melting reactions, as one carried out in experiments discussed in this chapter, is not clearly known, even for the simplest batches of mixture of silica and sodium carbonate. The apparent reaction rate of the solid phase reactions in the system Na₂CO₃-SiO₂ is affected by the particle size distribution and quantities of reactants in the reaction batch (Eitel, 1966). According to Hrma (1985), who quotes many investigations, melting reactions and their products are affected by soda-silica ratio, grain size, and other factors, including the melt size. The matrix of silicate melt formed in such reactions can range from almost pure orthosilicate 2Na₂O.SiO₂ to silica-rich melt. In the case of experiments reported here, if the local sodium carbonate concentration is lower than in the bulk of sample, the reaction with silica may result in much lower sodium content in the formed silicate than that of sodium disilicate. This may correspond to silica

content varying from 66% wt., as in sodium disilicate, to the extreme of almost total silica. Such silicates would still be expected to exist in a liquid form at temperatures higher than 789°C.

With the SAC mixture sodium to silica mass ratio near 1:10, ultimately it may be expected that sodium disilicate should be the major form of silicates formed relevant to conditions prevailing in a fluidised bed gasifier. This would not disqualify the formation of silicate glass with a much higher content of silica.

6.3.2.2 Effect of steam atmosphere

The formation of more silicates in steam atmosphere at very short reaction times and at lower temperatures than in carbon dioxide or nitrogen atmosphere is clearly evident. There is some formation of disilicate after a longer reaction time at 650°C. At 850°C, the formation of this silicate is almost an instantaneous process. The amount of hot water soluble silica from immediate exposure of mineral mixture to the steam atmosphere at 850°C is two times higher than the silica content in the cold water leachate. This suggests a very fast reaction and the straight formation of sodium disilicate and can be related to sodium carbonate melting at much lower temperature when exposed to steam atmosphere against the reported literature standard sodium carbonate melting temperature of 851°C. Figure 7.1 shows values of sodium carbonate melting temperature, as quoted in the literature, when it is heated in atmosphere containing steam. Eitel (1966) reported on the effect of moisture on batch reactions of sodium carbonate-silica mixtures, and observed the formed eutectic of Na_2CO_3 (with 17% soda), Na_2O (formed by dissociation of the carbonate) and H_2O melting at only 255°C to 280°C.

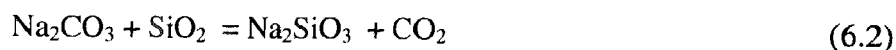
It was conjectured that the melting of sodium carbonate in a steam atmosphere was lower than standard temperature may be associated with partial formation of sodium hydroxide, and lower melting temperature for sodium carbonate and sodium hydroxide mixture. Sodium hydroxide melts at 322°C and it may form with sodium carbonate eutectic melting at lower than sodium carbonate melting temperature. To investigate this idea a few grams of AR grade sodium carbonate were exposed at temperature of 750°C, 800°C, 825°C and 850°C in steam atmosphere for 15 minutes.

Samples exposed at 750°C and at 825°C were dissolved in water and determination of solution pH due to carbonate and hydroxide was carried out in accordance with a standard procedure. The results showed that the solutions pH was neutral and therefore indicated no presence of sodium hydroxide from the sodium carbonate/sodium hydroxide eutectic.

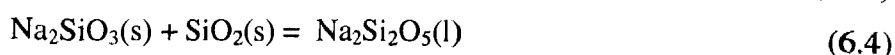
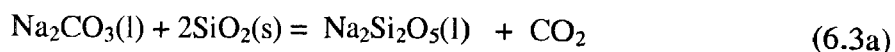
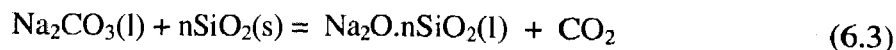
The above two sodium carbonate samples were also subjected to mineralogical analysis using XRD technique. Sodium hydroxide was not detected in these samples, as shown in the results presented in Table 6.2. Examination of all carbonate samples with the naked eye after cooling showed that the amount of molten sample at the surface increases with temperature from 800°C to 850°C.

The diffusion of sodium into the silica structure, and the formation of higher silica content silicates other than sodium disilicate, was low and similar as the levels observed for carbon dioxide and nitrogen atmospheres. The level of silica solubility in water superheated to 120°C was still an order of magnitude lower than solubility of silica in hot water. The mass ratio between silica and sodium soluble in water superheated to 120°C suggests that the silicates leached at 120°C in fact correspond to the composition of sodium disilicate.

The reaction of sodium carbonate with silica, sodium metasilicate Na_2SiO_3 is formed, as it has been proposed in Reaction (6.2):



This reaction would be a solid-state reaction between sodium carbonate and silica according to Eitel (1965) and Harrington et al. (1963). It may also be between a liquid sodium carbonate and solid silica according to Hrma (1985). Formation of liquid disilicate according to Hrma (1985) may take place due to Reaction (6.3) or Reaction (6.4).



Reaction (6.3) results in the formation of sodium silicate melt in a molten sodium carbonate-silica batch and it is a dominating reaction at higher temperatures. The formation of sodium disilicate as in Reaction (6.3a), is a specific case of Reaction (6.3) for $n=2$. For

the solid-state Reaction (6.4) to progress it would require sodium metasilicate to diffuse into solid silica and it can be reasonably expected that this is a slow process.

The observed immediate formation of sodium disilicate $\text{Na}_2\text{Si}_2\text{O}_5$ for the SAC mixtures exposed to steam atmosphere allows the conclusion that sodium disilicate will form in accordance with proposed Reaction (6.3a). Other composition silicate melts may also form as per general Reaction (6.3).

The results of mineralogical analyses shown in Table 6.2 show the formation of sodium disilicate, natrosilite, at trace level in one of the samples exposed to steam atmosphere for short time at 650°C. These mineralogical analyses, although not directly showing the presence of sodium silicates, do indicate that an amorphous phase has formed. It could be expected that this phase was sodium disilicate.

All of the above results and the literature data of Song and Kim (1993), and Huttinger and Mingos, (1985) show that sodium carbonate melts in a steam at lower temperatures than the standard reference temperature. Consequently, sodium carbonate forms a liquid phase and reacts with silica to form silicates principally constituting of sodium disilicate at considerably lower, in the order of 200°C, temperatures.

6.3.3 Microscopic examination for formation of silicates

Microscopic examinations of SAC mixtures were conducted with electron microscopy technique SEM. SAC samples exposed to all tested atmospheres and temperatures were examined for their morphology. The cross sections of a number of samples were also analysed using the SEM to analyse silicate layers formed around silica grains and backscattered electron images were recorded. Conditions, at which analyses and images, such as accelerating voltage, electron beam spot size and magnifications obtained are shown on a bar shown at the bottom of each image. Additionally on each image a bar size is also shown. Analyses of chosen spots of interest, particularly formed melts and joints between silica grains are also shown. These analyses show weight per cent content of component analysed and are expressed on an oxide basis.

The remaining, or rather un-reacted cores of silica grains can be easily recognized in the micrographs, particularly those showing cross-sections of samples. Clear borders between silica grains and silicate rims or silicate glass melts are shown in these images. Therefore in most images there is no marked analysis of the centre of the silica grains, which obviously constitutes only of silica.

6.3.3.1 Effect of nitrogen atmosphere

Morphologies of SAC mixture samples exposed to nitrogen atmosphere at 650°C for various times are presented in Figure 6.11. These images show that there is little change to the sample appearance for short exposure times.

Considerable agglomeration of the silica grains can be observed in Figure 6.12 showing the morphology of samples exposed to nitrogen at 750°C. Analysis of the material appearing to undergo fusion is nearly 30% wt. of sodium oxide and this may correspond to sodium disilicate.

Figure 6.13 shows the backscattered image of a cross-section for 850°C sample. Silica grains are embedded in a melt. Analysis of the glass melt joining silica grains show that sodium oxide content in the melt is only near half of that of sodium in sodium disilicate. This could be the result, particularly after longer reaction time of 35 minutes, that some of the silica is dissolving in the formed sodium disilicate and thus reducing the sodium oxide content.

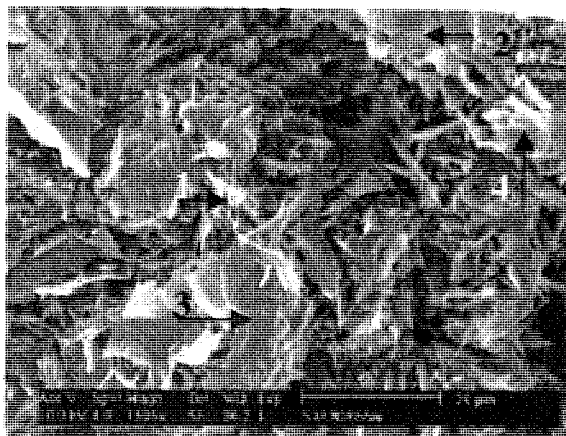
6.3.3.2 Effect of carbon dioxide atmosphere

The morphology of SAC mixture exposed to carbon dioxide at 650°C for various times is presented in Figure 6.14. Similarly to the morphology of samples exposed at the same temperature to nitrogen, there are no signs of reaction between sodium carbonate and silica.



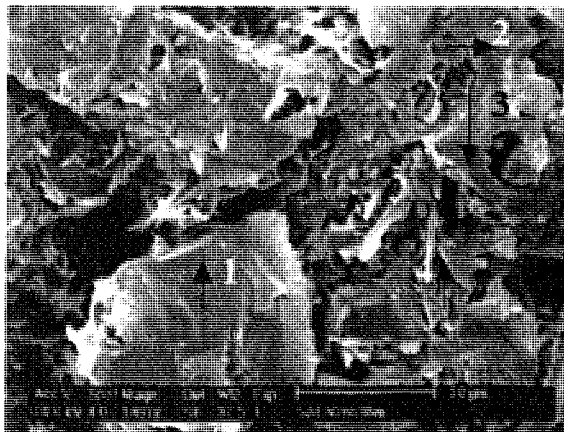
(a)

Analyses, wt %:	Na ₂ O	SiO ₂
1	82.4	17.6
2	20.5	79.5
3	29.0	71.0
4	0.0	100.0



(b)

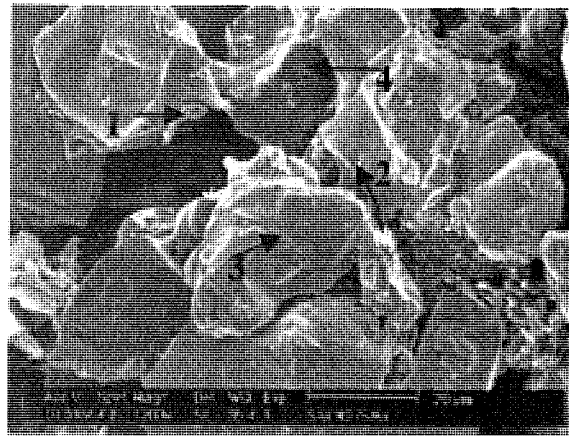
Analyses, wt %:	Na ₂ O	SiO ₂
1	69.2	38.8
2	11.5	88.5
3	13.7	86.3
4	63.4	36.6



(c)

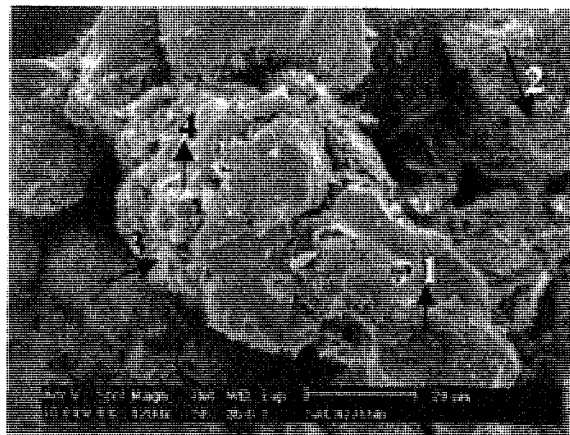
Analyses, wt %:	Na ₂ O	SiO ₂
1	6.7	93.7
2	8.9	91.1
3	47.5	52.5
4	14.7	85.3

Figure 6.11 Micrograph of SEM secondary electron images of SAC mixture exposed to nitrogen atmosphere at 650°C for (a) 45 seconds, (b) 5 minutes and (c) 35 minutes.



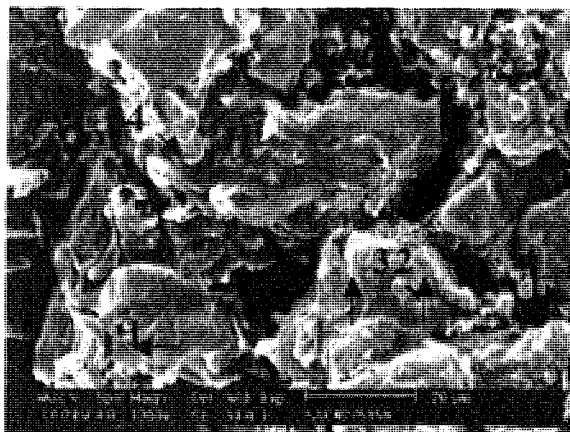
(a)

Analyses, wt %:			Na ₂ O	SiO ₂
1	21.0	79.0		
2	11.3	88.7		
3	10.7	89.3		
4	22.9	77.1		



(b)

Analyses, wt %:			Na ₂ O	SiO ₂
1	19.4	80.6		
2	33.0	67.0		
3	57.4	42.6		
4	23.5	76.5		



(c)

Analyses, wt %:			Na ₂ O	SiO ₂
1	12.3	87.7		
2	25.1	74.9		
3	4.0	96.0		
4	29.4	70.6		

Figure 6.12 Micrographs of SEM secondary electron images of SAC mixture exposed to nitrogen atmosphere at 750°C for (a) 45 seconds, (b) 5 minutes and (c) 35 minutes.

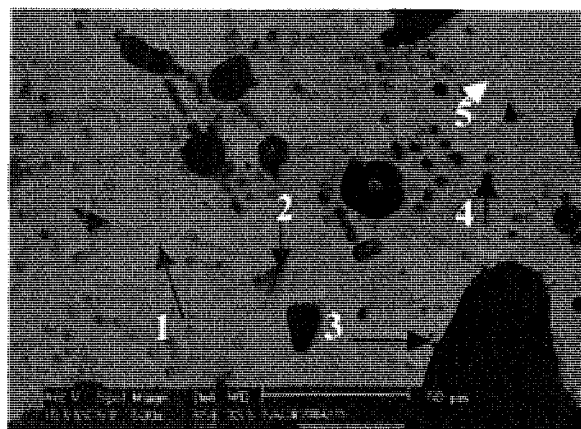
Images of samples exposed to carbon dioxide at 750°C are shown in Figure 6.15. There is a definite formation of joints between the silica grains as clearly shown in Figure 6.15(c),

with the composition indicated to be close to that of lowest temperature eutectic in the sodium oxide-silica system.

Both the surface and cross-section images of the reaction products exposed to 850°C evidently show the formation of glass. The analysis of the glass, as shown in Figure 6.16(b) is different from the composition of sodium disilicate. Once again this suggests that silica dissolves in sodium disilicate formed after the initial reaction. The kinetics of silica solubility would be dependent on the reaction temperature and consequently on the viscosity of the melt.

6.3.3.3 Effect of steam atmosphere

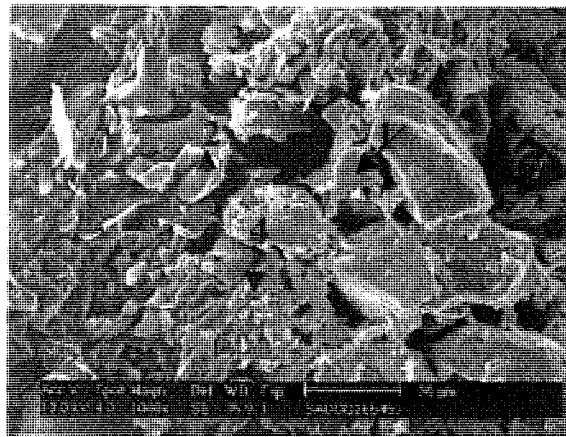
Microscopic analyses of fused material seen in SAC samples exposed to steam atmosphere show a varying degree of reaction between sodium carbonate and silica at 650°C, 750°C and 850°C. This is shown in the cross-sectional backscattered images of these samples in Figures 6.17 through 6.19.



Analyses, wt %:	Na ₂ O	SiO ₂
1	15.9	84.1
2	15.5	84.5
3	16.9	83.1
4	16.6	83.4
5	0.0	100.0

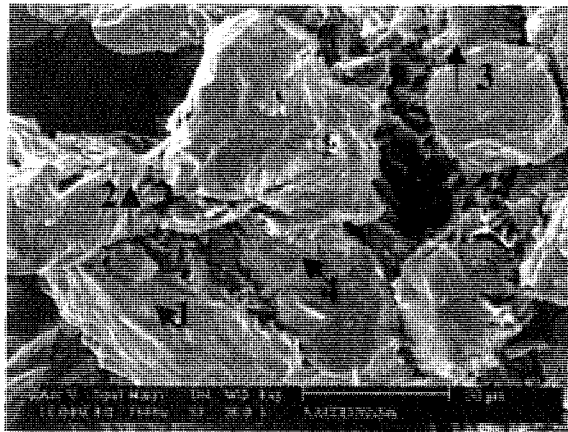
Figure 6.13 Micrograph of a SEM backscattered image of SAC sample exposed to nitrogen atmosphere at 850°C for 35 minutes.

The areas of sodium diffusing into the silica grains are well documented already for 650°C temperature reaction conditions, as shown in Figure 6.17. A number of joints are formed between the silica grains and these joints are low sodium content silicates.



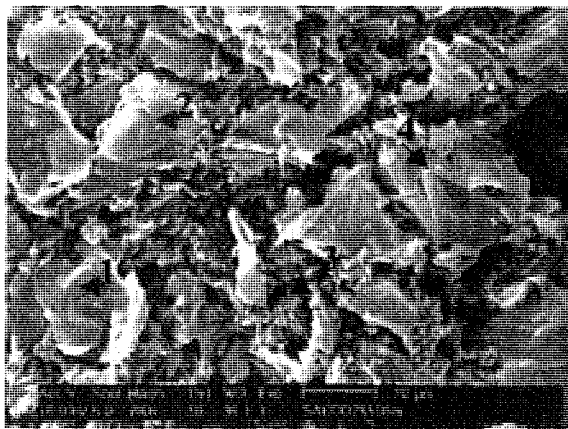
(a)

Analyses, wt %:			Na ₂ O	SiO ₂
1	0.0	100.0		
2	5.7	25.7		
3	25.7	74.3		
4	3.1	96.9		



(b)

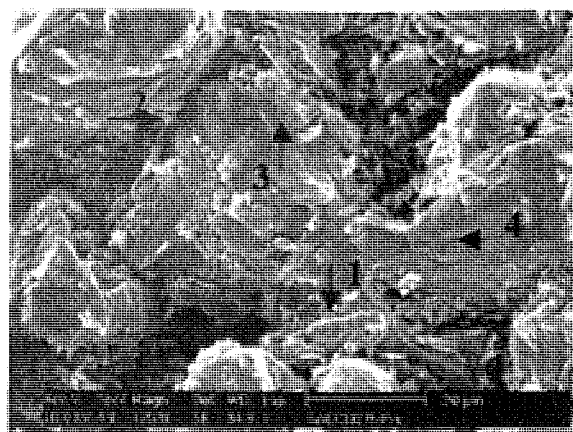
Analyses, wt %:			Na ₂ O	SiO ₂
1	9.1	90.9		
2	12.4	87.9		
3	51.9	48.1		
4	4.0	96.0		



(c)

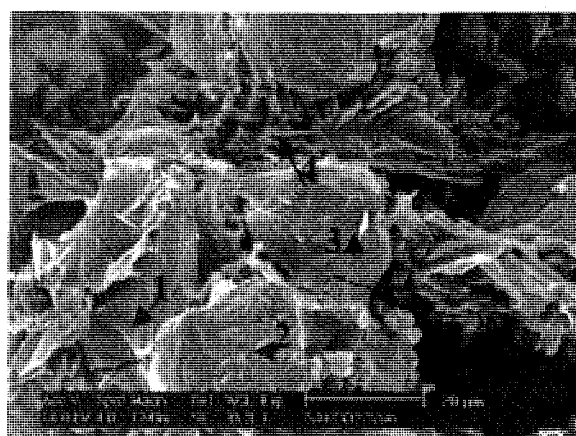
Analyses, wt %:			Na ₂ O	SiO ₂
1	21.5	78.5		
2	14.0	86.0		
3	62.0	38.0		
4	10.6	89.4		

Figure 6.14 Micrograph of SEM secondary electron images of SAC sample exposed to carbon dioxide atmosphere at 650°C for (a) 45 seconds, (b) 5 minutes and (c) 35 minutes.



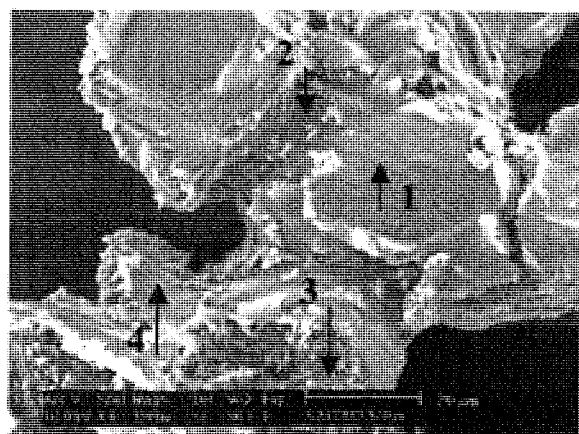
(a)

Analyses, wt %:	Na ₂ O	SiO ₂
1	10.0	90.0
2	8.0	92.0
3	6.8	96.2
4	12.5	87.5



(b)

Analyses, wt %:	Na ₂ O	SiO ₂
1	15.0	85.0
2	11.2	88.8
3	13.9	86.1
4	44.4	55.6



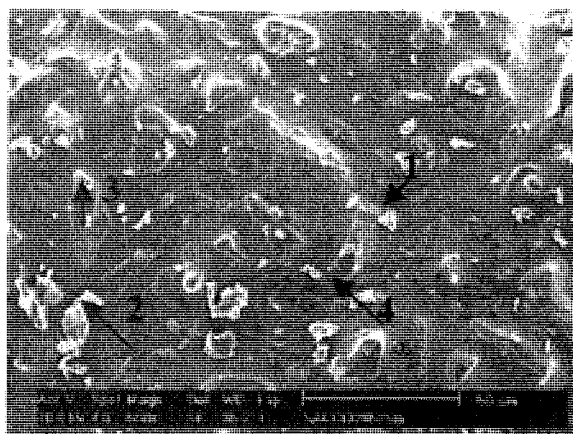
(c)

Analyses, wt %:	Na ₂ O	SiO ₂
1	11.6	88.4
2	20.4	79.6
3	16.5	83.5
4	48.3	51.7

Figure 6.15 Micrograph of SEM secondary electron images of SAC sample exposed to carbon dioxide atmosphere at 750°C for (a) 45 seconds, (b) 5 minutes and (c) 35 minutes.

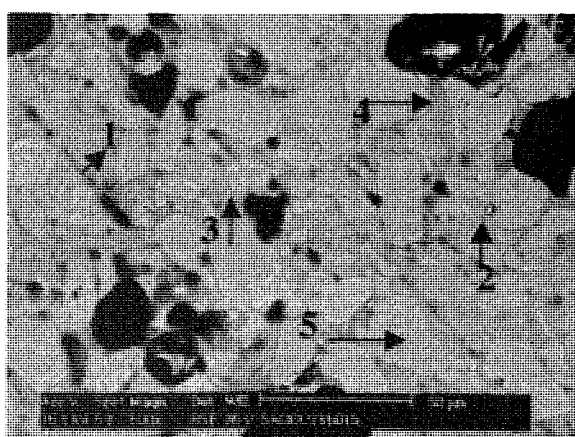
It has also been shown that at 650°C, there is still un-reacted sodium carbonate in the mixture after 15 minutes of reaction.

Images of the samples from 750°C reaction conditions shown in Figure 6.18 show that the SAC mixture became very consolidated. Large agglomerates have formed with silica particles joint by silicate glass. The composition of the formed glass was higher in silica than the composition of sodium disilicate.



(a)

Analyses, wt %:		
	Na ₂ O	SiO ₂
1	8.6	91.4
2	2.2	97.8
3	5.8	94.2
4	8.5	91.5



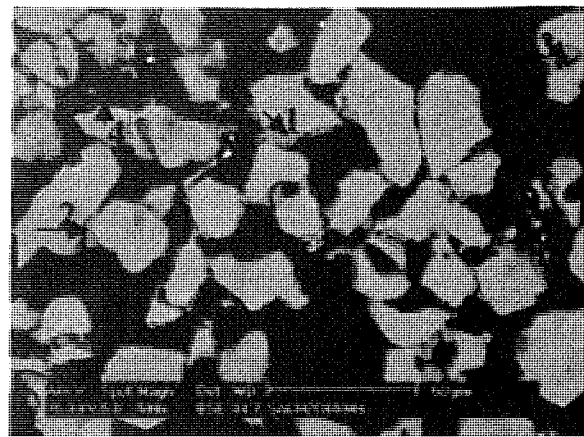
(b)

Analyses, wt %:		
	Na ₂ O	SiO ₂
1	14.5	85.5
2	12.8	87.2
3	14.3	85.7
4	13.9	86.1
5	0.0	100.0

Figure 6.16 Micrograph of SEM (a) secondary electron image of SAC sample exposed to carbon dioxide atmosphere at 850°C for 35 minutes and (b) of backscattered electron image of a cross section of a 15 minutes sample.

When comparing the amount of melt in images for 15 minutes reaction time at 850°C for steam and for carbon dioxide atmosphere conditions, as shown respectively in Figures 6.19 and Figure 6.16, it is clear that a steam atmosphere results in the formation of significantly more glass melt. On average, analyses of the glass melt formed during reactions under steam conditions show more sodium in the final product sample than in carbon dioxide sample. Additionally, comparing the same image from steam conditions with an image in

Figure 6.13 from exposure for 35 minutes at 850°C to nitrogen atmosphere, steam conditions result in more glass melt at much shorter reaction time.



(a)

Analyses, wt %:	Na ₂ O	SiO ₂
1	6.3	93.7
2	6.1	93.9
3	9.2	90.8
4	42.0	58.0

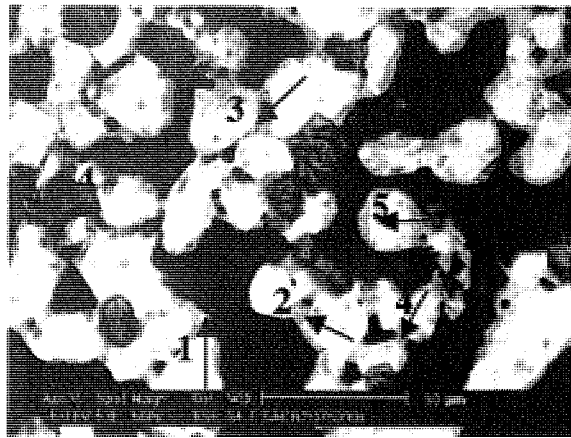


(b)

Analyses, wt %:	Na ₂ O	SiO ₂
1	82.4	17.1
2	5.0	95.0
3	15.6	84.4
4	9.3	90.7

Figure 6.17 Micrographs of SEM backscattered images of SAC mixture exposed to steam atmosphere at 650°C for (a) 90 seconds and (b) 15 minutes.

The assessment of analyses of fused material in samples from rising temperature and reaction time conditions shows that there was a steady increase in concentration of sodium in the silicate melts initially formed around silica grains and finally forming molten matrixes. At the lower 650°C temperature after short reaction time, the sodium oxide content was below 10% wt. At 750°C for longer reaction time it reached the level higher of more than 20% wt. Such a level of sodium concentration is also characteristic for samples from 850°C reaction conditions. The lower value of sodium in the fused material, in comparison with 34% sodium content in sodium disilicate could be caused by silica being dissolved in the formed silicate.



(a)

Analyses, wt %:		
	Na ₂ O	SiO ₂
1	13.1	86.9
2	9.4	90.6
3	8.4	91.6
4	12.4	87.4
5	8.4	91.6



(b)

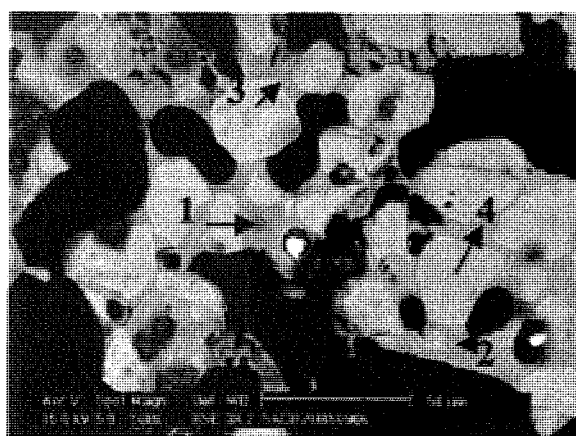
Analyses, wt %:		
	Na ₂ O	SiO ₂
1	11.5	88.8
2	22.4	77.6
3	15.6	84.4
4	9.3	90.7

Figure 6.18 Micrographs of SEM backscattered images of SAC sample exposed to steam atmosphere at 750°C for (a) 90 seconds and (b) 15 minutes.

The results of SEM analyses of the composition of silicates formed in SAC mixtures exposed to steam, carbon dioxide and nitrogen atmospheres, do not correspond to that of the composition of sodium disilicate. However, it is expected that silica dissolves in the formed silicates and increases the silica values in the SEM analyses. Thermodynamic predictions for equilibrium conditions for coal gasification conditions, imply that all silica would dissolve in the formed silicates at temperatures as low as 650°C. Water leaching of the same samples, as shown in previous Sections, showed the ratio between sodium and silica in the leachates approximated that of sodium disilicate. The leaching process of the SAC post-reaction mixtures will result in the leaching of only the silicate structure in which silica was dissolved.

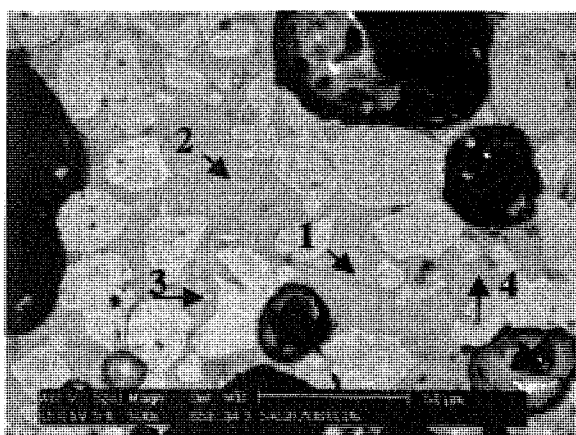
The solubility of silica in the formed silicates would result in an increase in the mass of liquid or fused glass material formed during reaction of sodium carbonate with silica. SEM analyses showed lower sodium content in the fused silicate mass than that from water

leaching analyses. From the solubility analyses, it can be calculated that approximately 17% of the total mass of the initial mixture becomes a liquid phase at 850°C. Microscopic analyses suggest that the mass of silicate formed is greater than this amount. Considering that sodium oxide content is lower in silicates observed under SEM, sometimes up to nearly a half of that analysed by solubility in water, it can be approximated that 35% of the total SAC reaction mixture could be in the liquid phase at this reaction condition. This depends on the kinetics of silica solubility in the formed silicates. The kinetics of the reactions was not taken into account in the thermodynamic calculations for the equilibrium compositions. Further to this, equilibrium is not reached in the experiments reported here.



Analyses, wt %:	Na ₂ O	SiO ₂
1	24.8	75.2
2	14.0	86.0
3	16.2	83.8
4	14.4	85.6

(a)



Analyses, wt %:	Na ₂ O	SiO ₂
1	11.2	88.8
2	16.2	83.8
3	13.5	86.5
4	12.6	87.4

(b)

Figure 6.19 Micrographs of SEM backscattered images of SAC sample exposed to steam atmosphere at 850°C for (a) 90 seconds and (b) 15 minutes.

Consequently, the solubility of silica in silicates will influence the amount of liquid phase formed during fluidised bed gasification of coal containing organically-bound sodium and silica. There could be a much larger mass of liquid phase than the amount of silicates

expected from the amount of sodium present in coal and assumed likely to form sodium disilicate with silica.

6.4 PYROLYSIS AND GASIFICATION OF COAL CONTAINING SILICA AND ORGANIC SODIUM

Samples of prepared NAIS coal containing on dry basis 0.7% of organically-bound sodium and 9.2% silica were used in pyrolysis and gasification experiments. Coal was separately pyrolysed in nitrogen or gasified with carbon dioxide or steam. The experiment conditions are presented in Table 3.7 and are the same as for the SAC sodium and silica mineral mixture samples. Similarly, reaction products between silica and sodium present in NAIS formed chars were examined by conducting solubility tests in water and by examination with SEM and XRD techniques.

Sodium introduced into the NAIS coal was chemically attached to coal functional (mainly carboxylic) groups. It was expected that the sodium would be well dispersed throughout the volume of the formed chars. This sodium, as shown in Chapter 5, during a coal heating process will be transformed into sodium carbonate. This form of sodium is soluble in cold water. However, due to the nature of char it may not leach easily into the cold water and may take several steps to completely leach all of the sodium from the formed char.

Consequently, sodium, which would have not reacted with silica and remained in the char, could be leached into the same water solution as sodium reacting with silica and forming silicates at the surface of silica grains present in char. Because of this, to accurately assess the formation of any reaction products between sodium and silica, any changes in the solubility of silica itself will have to be examined and assessed properly. The solubility of silica is therefore viewed as a way to assess the likely reactions between sodium salts and silica happening during the process of pyrolysis or gasification of coal. The formation of various silicates will result in silica becoming soluble in cold, hot or superheated water.

6.4.1 Chemical Analyses of Char

The results of solubility of silica in NAIS coal chars obtained during pyrolysis in nitrogen and during gasification with steam and carbon dioxide are presented and discussed in the following sections. The results are presented in Table 6.3 and show the content of silica

soluble in cold water, hot water and in water superheated to 120°C as part of the remaining char. The results shown in Table 6.3 also include the change in mass of pyrolysed or gasified coal, to show how much of the residue char has formed from the initial coal mass. This data allows for comparison of gasification rates of coal in steam and in carbon dioxide and shows how much volatile matter leaves coal during pyrolysis in various process conditions.

6.4.1.1 Results for pyrolysis char

The pyrolysis of NA1S coal in a nitrogen atmosphere resulted in very little reaction between silica and sodium for all three reaction temperatures of 650°C, 750°C and 850°C. No soluble silica was detected in the cold water leachate. This suggests no formation of metasilicate Na_2SiO_3 . It appears there has been no solid-state reaction between the grains of silica dispersed in the coal and sodium liberated from char during coal pyrolysis into sodium carbonate.

The values for silica analysed in hot water leachates for all pyrolysis chars as shown in the Table 6.3, are very low and suggest minimal formation of any silicates. Silica analysed in hot water leachates could represent sodium disilicate $\text{Na}_2\text{Si}_2\text{O}_5$ and could also be coming from silicates containing some more silica than in disilicate. At the level of silica solubility in hot water of 0.1% weight of dry pyrolysis char, this corresponds to approximately 0.65% of the total silica present in coal.

Similar silica solubility results have been obtained from leaching the chars for 4 hours in water superheated to 120°C, with soluble silica reaching approximately 1% of the total silica after pyrolysis for 35 minutes at 850°C. These results suggest the formation of silicates with silica contents much higher than in sodium disilicate $\text{Na}_2\text{Si}_2\text{O}_5$.

Table 6.3 Results of solubility in water of silica present in residue char after pyrolysis in nitrogen and gasification in steam and carbon dioxide of NAIS coal containing on dry basis 0.7% of organically-bound sodium and 9.2% of silica.

Atmosphere	Steam		Carbon dioxide		Nitrogen		Steam	Carbon dioxide	Nitrogen
	Cold	Hot	Cold	Hot	Cold	Hot			
Leaching water	120°C		120°C		120°C		Char residue, % wt d.b.		
Temperature, 650°C	4hrs		4hrs		4hrs				
Time, min	Soluble silica in char, % wt. d.b.								
0.45	0.00	0.13	0.00	0.00	0.00	0.00	0.00	0.00	0.00
1.5	0.00	0.17	0.00	0.00	0.13	0.09	0.09	0.09	0.09
5	0.00	0.28	0.00	0.11	0.11	0.19	0.13	0.13	0.13
15	0.28	0.39	0.00	0.11	0.19	0.15	0.11	0.11	0.17
35	0.24	0.41	0.00	0.11	0.24	0.15	0.11	0.11	0.17
Temperature, 750°C	Soluble silica in char, % wt. d.b.								
Time, min									
0.45	0.00	0.15	0.00	0.11	0.15	0.15	0.09	0.17	0.17
1.5	0.00	0.28	0.00	0.13	0.19	0.19	0.09	0.19	0.19
5	0.00	0.32	0.00	0.11	0.19	0.19	0.11	0.19	0.19
15	0.00	0.56	0.00	0.13	0.15	0.15	0.09	0.17	0.17
35	0.00	0.54	0.00	0.15	0.15	0.15	0.11	0.19	0.19
Temperature, 850°C	Soluble silica in char, % wt. d.b.								
Time, min									
0.45	0.00	0.17	0.00	0.04	0.04	0.04	0.11	0.04	0.04
1.5	0.00	0.30	0.00	0.13	0.17	0.17	0.11	0.13	0.13
5	0.00	0.47	0.00	0.15	0.17	0.17	0.09	0.19	0.19
15	0.00	0.88	0.00	0.30	0.30	0.30	0.11	0.21	0.21
35	0.00	1.74	0.00	0.96	0.75	0.75	0.13	0.24	0.24
							Char residue, % wt d.b.		
	60.01	59.99	60.01	59.99	60.01	59.99	60.01	59.99	60.01
	55.78	55.02	55.78	55.02	55.78	55.02	55.78	55.02	55.78
	52.52	52.61	52.52	52.61	52.52	52.61	52.52	52.61	52.52
	50.66	51.71	50.66	51.71	50.66	51.71	50.66	51.71	50.66
	50.14	50.56	50.14	50.56	50.14	50.56	50.14	50.56	50.14
							Char residue, % wt d.b.		
	54.67	52.11	54.67	52.11	54.67	52.11	54.67	52.11	54.67
	50.18	50.37	50.18	50.37	50.18	50.37	50.18	50.37	50.18
	46.73	48.21	46.73	48.21	46.73	48.21	46.73	48.21	46.73
	42.99	43.90	42.99	43.90	42.99	43.90	42.99	43.90	42.99
	41.06	41.73	41.06	41.73	41.06	41.73	41.06	41.73	41.06
							Char residue, % wt d.b.		
	48.07	49.63	48.07	49.63	48.07	49.63	48.07	49.63	48.07
	44.84	47.44	44.84	47.44	44.84	47.44	44.84	47.44	44.84
	38.46	41.98	38.46	41.98	38.46	41.98	38.46	41.98	38.46
	27.74	31.79	27.74	31.79	27.74	31.79	27.74	31.79	27.74
	16.23	20.01	16.23	20.01	16.23	20.01	16.23	20.01	16.23

The results for silica solubility obtained for pyrolysis chars also show little reaction between sodium carbonate formed during pyrolysis and the silica grains of NA1S coal. As in the post-volatilisation char, there is no further char density reduction, where this reduction would allow easier access for sodium to silica grains, and therefore no sodium carbonate movement for reaction with silica. Consequently, during pyrolysis sodium reacts with closely positioned silica grains and all pyrolysis results for silicates formation are very similar. The very low level of formation of silicates during coal pyrolysis is also confirmed by SEM analyses.

6.4.1.2 Results for gasification with carbon dioxide

The gasification of NA1S coal with carbon dioxide results in low levels of formation of soluble silicates at 650°C and 750°C, as presented in Table 6.3. No silica is detected in the cold water leachate solutions. The levels of silicates soluble in hot and superheated water correspond to less than 1% of the total silica present in coal. Very little char gasification is measured and therefore results are similar to those observed during pyrolysis.

However, gasification at 850°C results in significantly higher levels of silica soluble in hot water. A six-fold increase is recorded for the hot water soluble silica and over three times the increase in the level of silica soluble in superheated water for the char gasified for 35 minutes. These results are no surprise as the char residue is 20% when compared with pyrolysis char residue of 47.5%. As suggested in the previous section, a reduction of char volume results in a closer contact between sodium carbonate and silica grains.

The silica soluble in hot and superheated water represents sodium disilicate $\text{Na}_2\text{Si}_2\text{O}_5$ and silicates with higher silica content. All these silicates exist in a liquid state above the 789°C eutectic point. However, the viscosity and consequently the ability of these silicates to cause agglomeration will depend on the silica content and temperature conditions. According to Falcone (1986) and Hlavac (1985), silicates with higher silica content have higher viscosity than the silicates with lower silica content.

The results for silica soluble in hot and superheated water were at similar levels, with results for the superheated water leaching being slightly higher for most of the results for gasification in carbon dioxide. This could be interpreted that at all gasification and also

during pyrolysis conditions, the diffusion of sodium oxide into the silica volume during reaction between silica and sodium carbonate is somewhat faster than the supply rate of sodium carbonate to the silica surface. When the sodium carbonate availability for reaction with silica increases with higher carbon conversion rates, the increased availability and concentration of sodium carbonate near silica grains results in the formation of silicates such as sodium disilicate and other soluble hot water silicates. These silicates contain less silica and more sodium than the silicates soluble in superheated water.

Leaching from char of un-reacted sodium carbonate results in alkaline solutions and as a consequence, silica dissolves in such a solution. This especially happens while digesting coal char in superheated water. Therefore, it is believed that a significant part of the silica found in these leachates could be due to leaching by the formed alkaline solutions.

After gasification at 850°C, approximately 2% of the total silica in NAIS char is present in the form of silicates soluble in hot water. In char, these silicates would be in a liquid form. The formation of these silicates at higher gasification temperature may result in greater tendency for the coal ash to agglomerate.

6.4.1.3 Results for gasification with steam

The gasification of NAIS coal in steam results in the formation of significantly more sodium silicates than gasification in carbon dioxide, as presented in Table 6.3. Some silica is soluble in cold water after gasification in steam for longer times at 650°C. The results suggest that at 650°C, a reaction between silica and sodium carbonate leads to the formation of metasilicate Na_2SiO_3 . There is also formation at 650°C of silicates soluble in hot water. The levels of silica soluble in hot water were much higher than the results obtained for gasification in carbon dioxide atmosphere.

At 750°C, the solubility of silica in hot water is three to four times higher when compared with results for gasification of NAIS coal in carbon dioxide. As shown in Table 6.3, after 35 minutes of gasification in steam at 750°C, silica soluble in hot water consists of more than 0.5% of char, while for carbon dioxide gasification the value being only 0.15%. The char residue for both atmospheres was approximately 41% of the initial coal mass.

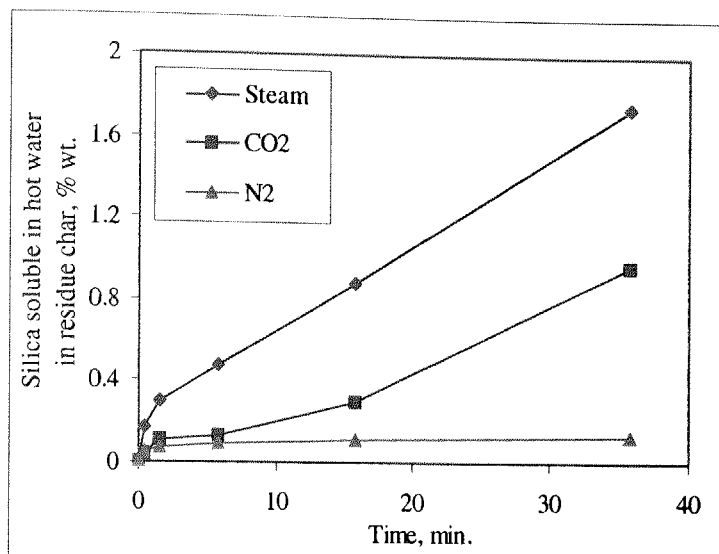


Figure 6.20 Content of silica soluble in hot water present in the residue char of NAIS coal pyrolysed in nitrogen atmosphere or gasified with steam or with carbon dioxide at 850°C presented as function of reaction time.

Gasification with steam at 850°C results in much higher formation of silicates than in chars gasified with carbon dioxide as shown in Figure 6.20. After 35 minutes of gasification in steam, the silica soluble in hot water was 1.74% and leaching for 4 hours in superheated water yielded 0.94% of the char residue mass. When combined, this is nearly two times more than after gasification of NAIS coal in carbon dioxide. At shorter gasification times, these values for steam are more than double carbon dioxide gasification values.

The fact that during gasification with steam at 850°C, up to 5.5% of the total silica present in NAIS coal reacts into soluble silicates as shown in Table 6.4, compares well with results obtained for SAC sodium and silica mixtures. Exposure to steam atmosphere at 850°C of SAC mixture results in approximately 15% of the total silica becoming soluble in water and accounts for approximately 12% of the total SAC post-reaction mass.

The comparison between NAIS coal and SAC mixture results can be made on the basis that some losses of sodium were recorded during coal gasification. During gasification of NAIS coal, similar to the results for gasification of NA1 coal, which contained only sodium and no silica, sodium loss was recorded as shown later in Section 6.3.2.4. Some 44% of the total sodium evaporated from NAIS coal char gasified for 35 minutes at 850°C and this fact substantially reduces the amount of sodium for reaction with silica. However, if the sodium is available for reaction with silica, the amount of soluble silica is nearly 10%

of the char mass. Additionally, in the case of NAIS coal char, there still is some un-reacted sodium dispersed within the char at the end of the gasification experiment, as char carbon conversion reached only 66% for the 35 minutes gasification experiment. The content of soluble silica in char could have then increased to 12% or more and thus in the similar level as that measured for SAC mixtures.

Additionally, SEM results confirm this conclusion as the concentration of sodium and silica in the silicates, which form within the char and form glass melt joining the silica grains, is very similar to the results observed after examination of the SAC mixture results.

The above results also lead to the conclusion that because of sodium evaporation, gasification of coal at high temperatures reduces the possibility of silicate formation.

Table 6.4. Results of solubility of silica present in residue chars after gasification at various conditions in steam and in carbon dioxide of NAIS coal containing on dry basis 0.7% weight of organically-bound sodium and 9.2% of silica.

Gasification atmosphere	Temp.	Time	SiO ₂ content in coal	Char remaining	SiO ₂		Total SiO ₂ present in char	SiO ₂ soluble in hot water as part of total SiO ₂ present in char	Total soluble SiO ₂ as part of total SiO ₂ present in char
					soluble in hot water	soluble in super-heated water			
	°C	min.	%	%	%	%	%	%	%
Steam	650	35	9.2	50.1	0.41	0.34	18.3	2.23	4.09
Steam	750	15	9.2	43.0	0.56	0.32	21.4	2.62	4.11
Steam	750	35	9.2	41.1	0.54	0.45	22.4	2.41	4.42
Steam	850	5	9.2	38.5	0.47	0.49	23.9	1.96	4.01
Steam	850	15	9.2	27.7	0.88	0.79	33.2	2.65	5.04
Steam	850	35	9.2	16.2	1.74	1.39	56.7	3.07	5.52
CO ₂	750	35	9.2	41.7	0.15	0.15	22.0	0.68	1.36
CO ₂	850	15	9.2	31.8	0.30	0.30	28.9	1.04	2.07
CO ₂	850	35	9.2	20.0	0.96	0.75	46.0	2.09	3.72

Once again, the transformation of original silica into silica soluble in hot water suggests the formation of sodium disilicate or silicates containing more silica and less sodium such as corresponding to the composition of the 789°C eutectic between sodium disilicate Na₂Si₂O₅ and silica. All these silicates would be in a liquid state at 850°C. Viscosity of

these silicates, and their ability to cause agglomeration, will depend on silica content and the temperature conditions.

It can be concluded that during gasification of coal with steam more liquid silicates are formed than during gasification with carbon dioxide. Similar observation has been for SAC mixtures exposed to steam or carbon dioxide. The reason behind this phenomenon is very likely to be the same: that sodium carbonate melts in steam at a temperature much lower than its standard melting temperature of 851°C. The lower melting temperature for sodium carbonate in steam will result in a liquid-solid phase reaction between sodium carbonate and silica taking place at much lower temperature than in carbon dioxide.

The practical consequence for gasification process is clear. If steam is used for coal gasification in a fluidised bed process, this will result in the formation of liquid phases at lower temperatures and increase the tendency for the coal ash to agglomerate. SEM images shown in subsequent sections show that during gasification with steam of NAIS coal silicates, which formed, were fused and able to cement silica grains together.

6.4.1.4 Sodium volatilisation during gasification

The fact that some of the sodium present in NAIS coal reacts with silica is reflected in silica becoming soluble in water. The rest of the sodium originally present in coal in the organically-bound form will remain in the char or evaporate. It has been shown in Chapter 5, that nearly a half of the organically-bound sodium originally present in coal evaporates from the char gasified for long periods at 850°C with steam or with carbon dioxide.

During gasification of NAIS coal with steam as shown in Figure 6.21, losses of sodium increase with temperature and are much higher at 850°C than at 750°C. At 850°C sodium losses reached more than 40 % of the initial sodium content. Similar results are recorded for NA1 coal. Sodium losses from NAIS coal char for gasification with carbon dioxide are at similar levels as with steam, as shown in Figure 6.22.

These results show that the presence of silica does not significantly reduce volatilisation of sodium from coal char during gasification in steam.

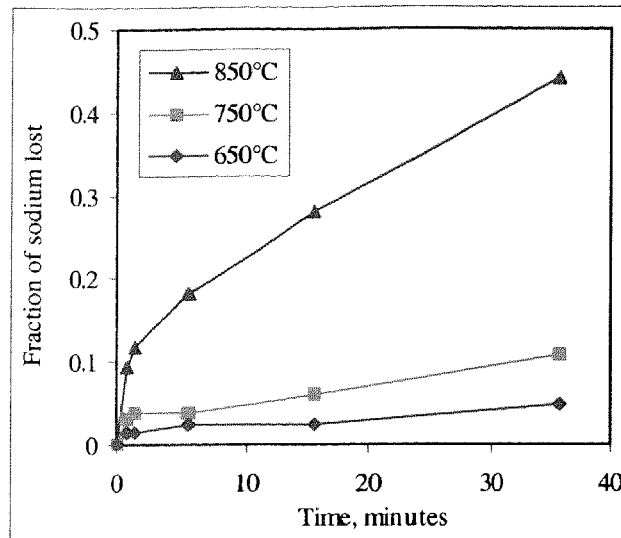


Figure 6.21 Fraction of sodium lost during gasification in steam at 650°C, 750°C and 850°C of NAIS coal containing 0.7% wt. of organically-bound sodium and 9.2% of silica, presented as function of reaction time.

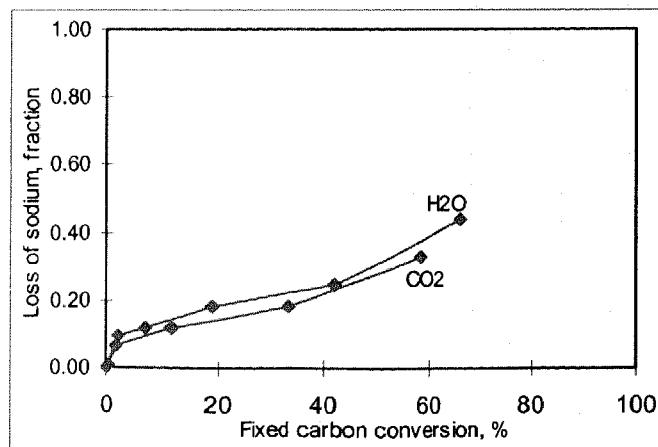


Figure 6.22 Sodium volatilisation as a function of carbon conversion during carbon dioxide and steam gasification at 850°C of NAIS coal containing 0.7% wt. of organically-bound sodium and 9.2% of silica.

As sodium carbonate is distributed at the molecular level within the char and silica is present in micron size particles, the contact between them is restricted. Consequently, most of the sodium carbonate exists freely within the char and may react with char to result in the formation of free metallic sodium, which will evaporate from the char.

6.4.2 Microscopic examination of char

A number of NAIS coal pyrolysis and gasification char samples were examined with SEM for formation of silicates. Analyses of water leachates were used as a guide for sample selection. Backscattered electron images of examined samples were also recorded.

6.4.2.1 Silicate formation during coal pyrolysis

Cross-sections of NAIS coal char samples pyrolysed in nitrogen at 750°C and at 850°C are presented in Figure 6.23 to show even distribution of silica particles in char (white spots in the images) and to show that those chars appear to have similar porosity. The residue char values for both temperature conditions are very similar, as shown in Table 6.3.

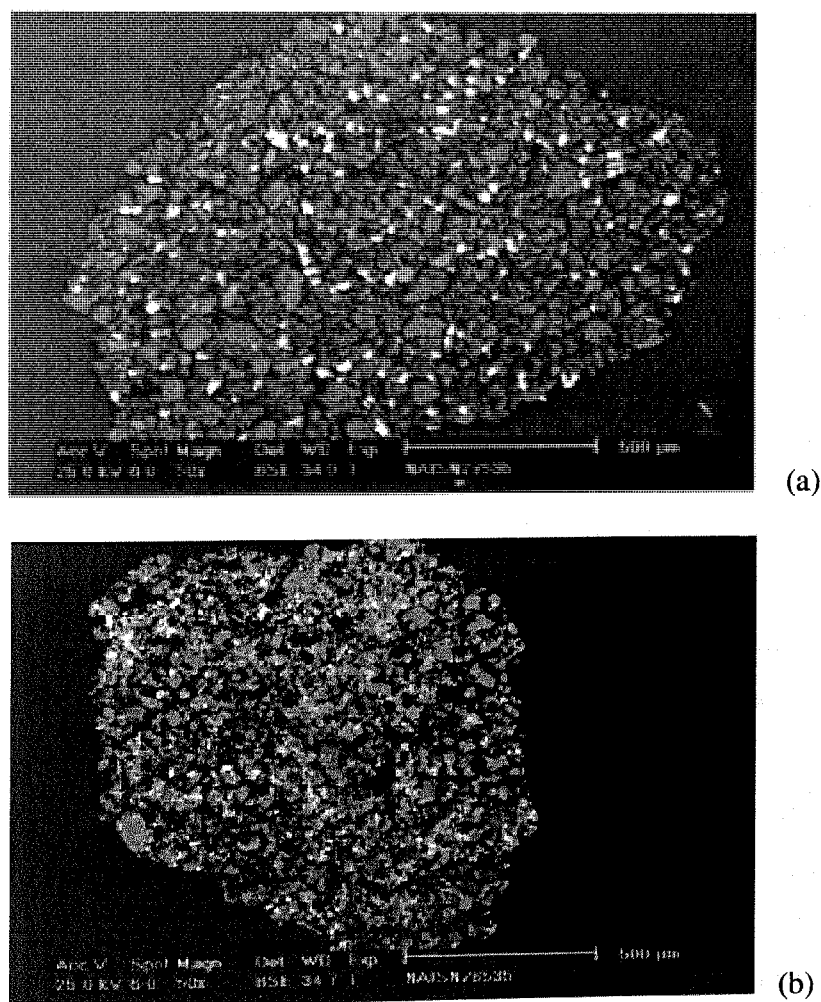


Figure 6.23 Micrograph of SEM backscattered electron images of a 50x magnification of cross section of NAIS coal 35 minutes pyrolysis char from (a) 750°C and (b) 850°C pyrolysis conditions.

The results of silicate formation at the silica grain surface as observed in SEM images shown in Figure 6.24 for the char samples are also similar. It appears that the silica grains hardly reacted with sodium present in the char. There are no definite layers of silicates surrounding silica grains for either 750°C or 850°C samples.

Silicates seem to form a vague, 1 to 2 micron thick build-up in some areas on the surface of silica grains. The joints between silica grains, such as in Spot 2 in Figure 6.24, seem to be formed. The silicates in these joints do not have the appearance of a fused phase, while those observed in images of SAC mixture exposed to nitrogen atmosphere at 850°C appear very fused.

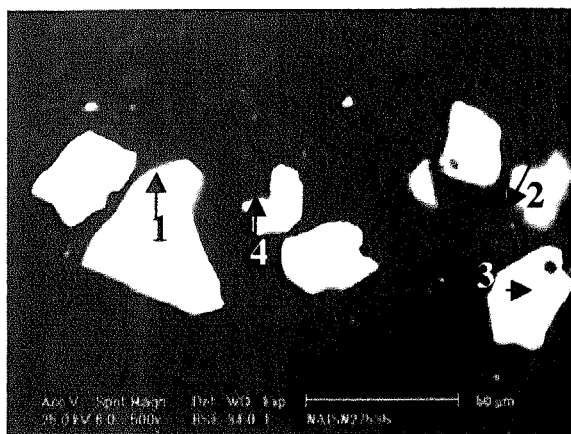
The results of microscopic examination confirm the low level of formation of silicates in pyrolysis char, as suggested by results of char water leachate analysis. The formation of silicates on the surface of the silica particles is established as occurring throughout the char particle, thus suggesting that coal ash formation, although at really microscopic scale, does occur during coal pyrolysis. The concentration of silica in these silicates shown in the images is far higher and sodium far lower, than that corresponding to sodium disilicate composition.

However, as said earlier, during char water leaching the sodium remaining within the char structure is leached out and increases the pH of the leaching solution. Consequently, this increase in pH would cause leaching of more silica than that corresponding only to sodium disilicate. Therefore, analysis given by the leaching of coal chars may show higher concentration of soluble silica than that expected for a given leaching process conditions.

6.4.2.2 Silicate formation during gasification with carbon dioxide

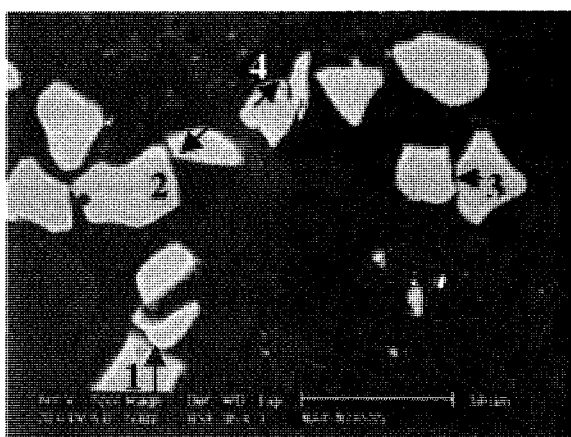
Cross-sections of NA1S coal char samples gasified in carbon dioxide for 35 minutes at 750°C and at 850°C are presented in Figure 6.25. Gasification with carbon dioxide at 750°C shows that there hardly any reaction between silica and sodium present in the char. No formation of a silicate layer around the silica grains is observed. The sodium oxide content in the thin joints developing between and silica grains does not exceed 3%, as shown in Figure 6.25a.

The results for 750°C gasification char are very similar to the results for pyrolysis chars, as there is low carbon conversion at these gasification conditions and therefore limited increase in concentrations within the char of sodium carbonate available for reaction with silica.



(a)

Analyses, wt %: Na ₂ O			SiO ₂
1	2.4	97.6	
2	1.6	98.4	
3	0.0	100.0	
4	3.5	96.5	



(b)

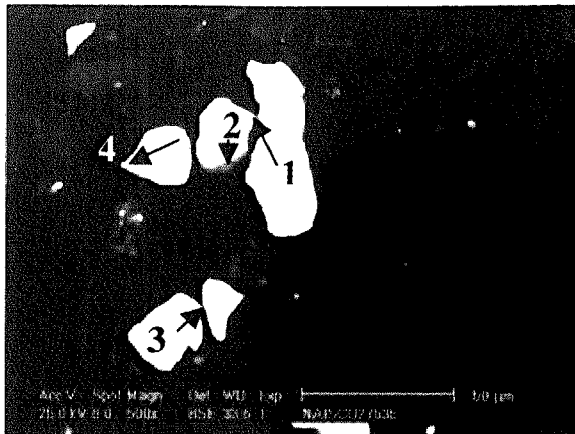
Analyses, wt %: Na ₂ O			SiO ₂
1	1.7	98.3	
2	2.5	97.5	
3	3.3	96.7	
4	1.6	98.6	

Figure 6.24 Micrograph of SEM backscattered electron images of cross-section of NAIS coal pyrolyses char sample exposed for 35 minutes to nitrogen atmosphere (a) at 750°C and (b) at 850°C showing formation of silicate joints between silica particles and formation of silicate layers on the surface of silica particles.

The sample of char gasified at 850°C shown in Figure 6.25(b), shows silica grain clusters inside the char samples and the formation of silicate joints between individual silica grains. The concentration of sodium in the fused silicates did not exceed 5% of the total silicate mass. These joints are shown to be just a few microns thick and appear to be fused. The development of these joints between silica particles is of great importance from the point of view of the formation of ash and potential agglomeration during coal gasification.

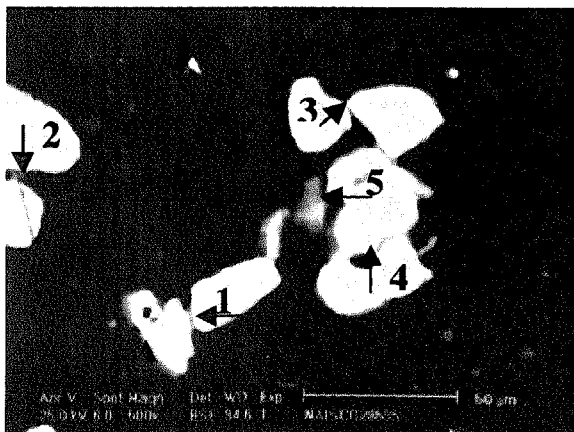
The fact that the fused joints between silica particles have less than 5% sodium shows that very little sodium is required to diffuse into the silica to form molten glass silicates. As

stated previously in the sections relating to SAC mixtures and referring to the phase diagram between sodium oxide and silica, the liquid silicates may exist in a two-component system at 789°C, with the temperature of the lowest-melting eutectic point between these two oxides. The composition of these liquid silicates may vary in a wide range from that of sodium disilicate to a silicate containing even 99.9% of silica and only 0.1% of sodium oxide.



(a)

Analyses, wt %:		
	Na ₂ O	SiO ₂
1	1.1	98.9
2	1.9	98.1
3	2.7	97.3
4	1.0	99.0



(b)

Analyses, wt %:		
	Na ₂ O	SiO ₂
1	1.7	98.3
2	2.5	97.5
3	3.3	96.7
4	1.6	98.6
5	2.6	97.6

Figure 6.25 Micrograph of SEM backscattered electron images of cross-section of NAIS coal gasification char samples gasified for 35 minutes with carbon dioxide (a) at 750°C and (b) at 850°C showing silicate joints between silica grains.

A liquid-solid phase reaction between sodium carbonate and silica leading to the formation of liquid silicates is expected to take place during gasification with carbon dioxide at approximately 850°C, as sodium carbonate melts at 851°C. The wetting of silica grains by the carbonate will increase the contact surface between these two reactants and may lead to a higher reaction rate than if the reaction is between two solid phases. However, with

limited sodium carbonate supply due to its dispersion throughout the char, the lower content silicates form under carbon dioxide gasification conditions.

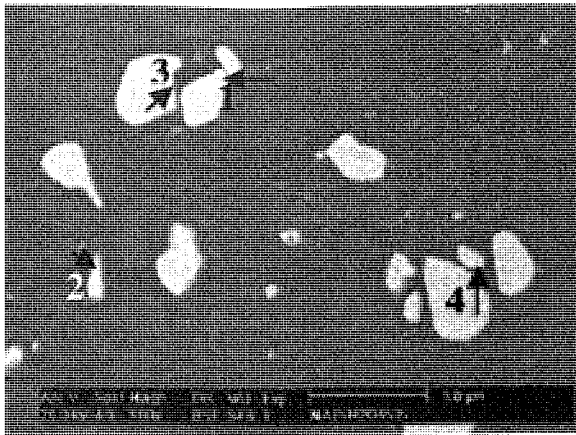
6.4.2.3 Silicate formation during gasification with steam

SEM images of the cross-section of NAIS coal char particles gasified with steam are presented in Figures 6.26 through to 6.29. Gasification at 650°C does not seem to result in formation of fused silicates on the silica grains, although thin layers of silicates still form as shown in Figure 6.26. These thin silicate layers contain sodium concentrations below 3% and are similar to those observed in images for char pyrolysis at 750°C and 850°C and char gasified with carbon dioxide at 750°C.

Char from gasification of NAIS coal with steam at 750°C and 850°C show significant formation of fused glass silicates throughout the particle. Clear borders between silica grains and silicate rims or silicate glass melts are shown in images of NAIS chars in Figures 6.27 through 6.29. The un-reacted core of silica grains can be easily recognized in the micrographs.

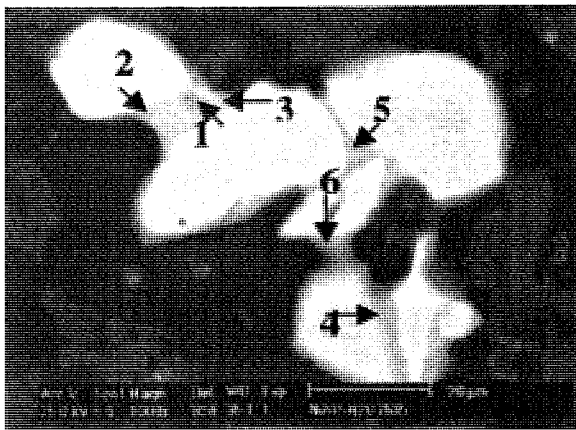
An image of NAIS char after gasification at 750°C shown in Figure 6.27 shows the definite formation of fused glass silicate joints between silica grains. This is a result of the fact that sodium carbonate melts at a lower temperature in steam. Consequently, the liquid-solid phase reaction, between sodium and silica, results in the formation of liquid phase silicate well below the lowest melting eutectic in the sodium oxide-silica system.

Sodium concentration in the silicates varied from between 1% and 6% by weight. The thickness of the silicate joints appears not to exceed 5 microns. In one of these neck joints, the concentration of sodium at a distance less than 1 micron from the silica particle surface is below 2%, as indicated by Spot 2 and Spot 3 in Figure 6.27. While at a distance of approximately 2 microns from the surface of each joined particle it is at 3.4%, as indicated by Spot 1. The difference in sodium concentration suggests the gradual diffusion of sodium oxide into the silica. It also shows that at the point of connection of the two particles, the viscosity of the silicate melt in the centre of the joint will be different than at the surface of silica particle. The higher concentration of sodium in the formed silicates reduces the silicate glass viscosity and allows for easier joint formation between the silica particles



Analyses, wt %: Na ₂ O			SiO ₂
1	0.9		99.1
2	2.1		97.9
3	2.8		97.2
4	3.1		96.9

Figure 6.26 Micrograph of SEM backscattered electron image of a cross-section of NAIS coal char sample after gasification with steam for 35 minutes at 650°C showing signs of silicate formation on the surface of silica grains.



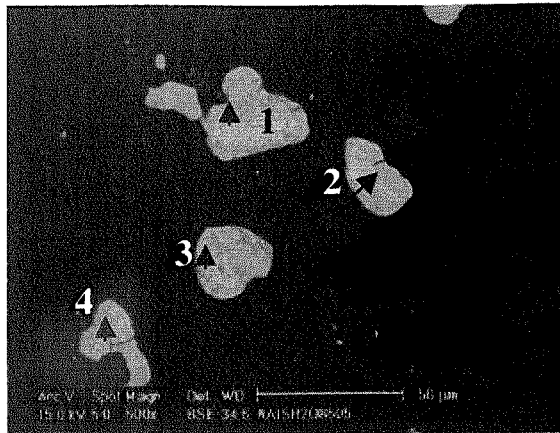
Analyses, wt %: Na ₂ O			SiO ₂
1	3.4		96.7
2	1.2		98.8
3	1.9		98.1
4	3.6		96.6
5	4.6		95.6
6	5.8		94.2

Figure 6.27 Micrograph of SEM backscattered electron image of a cross-section of NAIS coal char sample after gasification in steam for 35 minutes at 750°C showing silicate glass joints between silica grains.

The cross-sectional image of char gasified with steam at 850°C evidently shows the formation of glass silicates coating the silica particles after only 5 minutes of gasification. Analysis of the glass, as shown in Figure 6.28, show a sodium content of up to 7.5%, which is higher than that found for the silicates in the 750°C char.

The presence of sodium-rich silicates is definitely observed in char gasified with steam for 35 minutes at 850°C, as shown in Figure 6.29. This Figure shows that silica particles are not just joined by silicate necks but that the particles are totally embedded in a fused matrix containing approximately 14% sodium oxide. It is believed the formation of silicates with

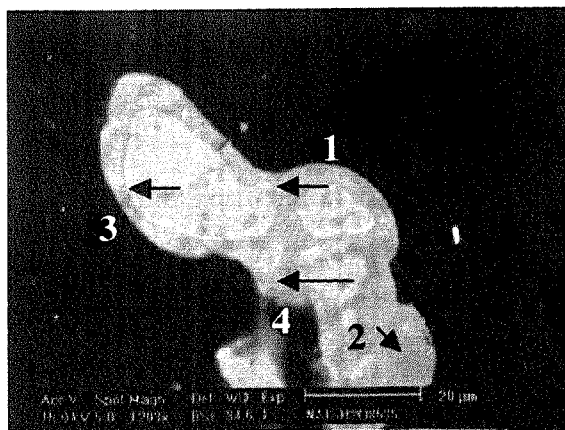
higher concentrations of sodium is a result of the availability of more sodium due to the higher rates of char gasification with steam than with carbon dioxide.



Analyses, wt %:	Na ₂ O	SiO ₂
1	7.5	92.5
2	5.7	94.3
3	7.4	92.6
4	6.8	93.2

Figure 6.28 Micrograph of SEM backscattered electron image of 1000x magnification of a cross-section of NAIS coal char sample from gasification in steam for 5 minutes at 850°C showing silicate rims around silica grains and glass joints between silica grains.

Figure 6.28 shows that some of the silica particles are less than 20 microns in size, while the original silica particles in NAIS coal are in the range of 25 to 32 microns. This reduction of size suggests that silica may have dissolved in the formed silicates.



Analyses, wt %:	Na ₂ O	SiO ₂
1	14.4	85.6
2	14.6	85.4
3	13.2	86.8
4	13.6	86.4

Figure 6.29 Micrograph of SEM backscattered electron image of 1000x magnification of a cross-section of NAIS coal char sample after gasification in steam for 35 minutes at 850°C showing silicate glass joining silica grains.

Dissolution of silica in the formed liquid silicates reduces the concentration of sodium in the melt. Considering this possible dilution effect by the silica dissolving in the formed liquid silicates, it can be inferred that the initial composition of these silicates could be higher and approaching that of sodium disilicate, formation of which has been predicted by

thermodynamic calculations. However, thermodynamic prediction that all silica is to be in a liquid form is definitely not confirmed by these experimental results.

As stated earlier, the thermodynamic predictions do not take into account kinetics of the reaction and only give predictions for equilibrium conditions. Such equilibrium conditions are unlikely to have been reached in the experimental conditions used.

The SEM results for the coal char gasified with steam can be considered in a good agreement with the results of SEM examination of post-reaction SAC mixtures. The SAC mixtures exposed at 850°C in nitrogen, carbon dioxide or to steam (Figures 6.13, 6.17, 6.19, respectively) and also to steam at 750°C (Figure 6.18), show a similar level of concentration for sodium in the formed silicate melts as that observed for silicates formed in char gasified with steam at 850°C.

It may be concluded that gasification with steam results in a liquid-solid phase reaction between sodium carbonate and silica to form fused silicates at a temperature at least 100°C lower than during gasification with carbon dioxide. The same reaction for SAC mixtures results in a 200°C difference. This difference in temperature for silicates formation in mixture and coal can be related to the structural difference being a close contact between sodium carbonate and silica in the SAC mixture, while for the char such intimate contact does not occur.

Results from gasification of coal in steam lead to some practical considerations. As gasification in steam of NAIS coal resulted in 20% residue char, that char contained some 50% of solids and only 10% of the initial organic material. Inside that char silica grains agglomerated as they were joined by silicate matrix, as shown in Figure 6.29. Such agglomerates may not be liberated or exposed to char surface until late into char conversion or if char is fragmented. If a full-scale fluidised bed gasifier plant was then operated at conditions with limited char conversion, this could result in reducing a risk of agglomerates formation within the gasifier. The remaining char could be burnt in a combustion process to recover the energy contained in remained char.

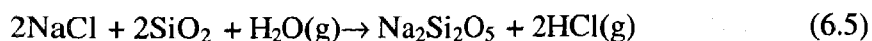
6.5 SILICA AND SODIUM CHLORIDE MIXTURE

This section will report on findings from investigations into the products of reaction between sodium chloride and silica in SNC prepared mixture exposed in the temperature range of between 650°C to 850°C to steam atmosphere. The following sections after this will report on pyrolysis and gasification of synthetic NC1S coal containing controlled quantities of silica and sodium chloride as described in Section 4.2.3.

The results of thermodynamic calculations in Chapter 3 showed that gasification with steam of coal containing silica and sodium chloride would at equilibrium conditions result in almost total transformation of sodium into liquid sodium disilicate. The gasification of with carbon dioxide would result in 50 to 60% of the sodium forming silicates.

The SNC mixture reflected other sodium form present in coal and was used in experiments as an indicator of what products may be expected when coal containing silica and sodium chloride is gasified. The prepared SNC mixture contained 23.5% sodium as sodium chloride. Details of composition are shown in Table 3.6.

For the temperature conditions prevailing in a fluidised bed gasifier, no reaction between sodium chloride and silica is expected if no steam is present in the atmosphere. The reaction between silica and sodium chloride to form a silicate, such as sodium disilicate, both oxygen (to form sodium oxide) and hydrogen (to form hydrogen chloride) are needed in accordance with proposed mechanism of reaction 6.5:



The exposure of SNC mixture to a carbon dioxide atmosphere at 850°C resulted in the melting and partial evaporation of sodium chloride, while silica grains remained, as expected, unaltered. Therefore following results deal only with reaction products between sodium chloride and silica exposed to high temperatures in a steam atmosphere.

6.5.1 Formation of Silicates in Steam Atmosphere

The reaction between sodium chloride vapours and silica at high (above 1000°C) temperatures in steam were already considered decades ago as a base for producing

hydrogen chloride and sodium silicate (Iler and Tauch, 1941). However, for the lower temperature range below the sodium chloride melting point of 801°C, little attention has been given to such a reaction.

Small quantities of prepared silica and sodium chloride SNC mixture were exposed to steam in the temperature range of 650°C to 850°C. Residues were subjected to the same water leaching procedure as SAC mixture samples and NAIS coal char samples.

The results of the water leaching process show no solubility of silica in cold water, allowing the conclusion that no sodium metasilicate formed. The solubility results in cold water for sodium and chlorine are not presented here, as soluble silica is considered the measure of the extent of reaction rather than the remaining part of sodium chloride used in the SNC mixture. It was evident from analyses that sodium chloride, which did not react with silica, partly remained in the residue material and partly evaporated. Most of sodium chloride remained after exposure of mixture at 650°C, while after longer reaction time at 850°C some sodium chloride evaporated from samples.

The solubility in hot water of both sodium and silica are shown in Figure 6.30. There is a steady increase in the sodium soluble in hot water after exposure of SNC mixture at 750°C and 850°C, but little solubility for the 650°C samples.

The increasing solubility of sodium in hot water is clearly confirmed by the trend in results of the solubility of silica in hot water, as shown in Figure 6.30a and Figure 6.30b, respectively. There is no soluble silica in 650°C samples and in short reaction times for both 750°C and 850°C conditions. This shows that the reaction between silica and sodium chloride is a slow process.

Silica reacted with sodium chloride at 750°C, a temperature well below the sodium chloride melting point of 801°C, with even more silica reacting at 850°C. Almost 8% of the residue at 850°C after 35 minutes of reaction was silica soluble in hot water suggesting the formation of sodium disilicate or silicates of similar composition. Assuming that silica forms sodium disilicate, calculation of the value for sodium equivalent to that of silica results in a sodium value of 3.1%, corresponding closely to the value of 3.25% for sodium

presented in Figure 6.30a. The values for other reaction times are similarly close. These results suggest that the reaction of sodium chloride with silica in a steam atmosphere resulted in the formation of sodium disilicate.

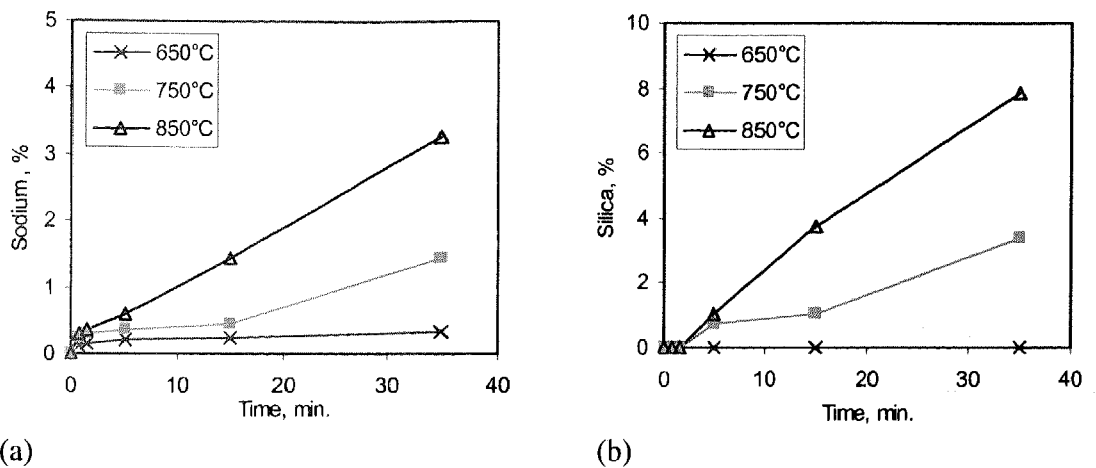


Figure 6.30 Solubility in hot water of (a) sodium and (b) silica as part of a sample of SNC mixture exposed to atmosphere of steam at 650°C, 750°C and 850°C and presented as a function of reaction time.

Solubility in superheated water of both silica and particularly sodium was insignificant in comparison with their solubility values in hot water. These results suggest a low level of sodium diffusion into the silica beyond sodium disilicate layer formed on the silica particles.

Table 6.5 Silica soluble in hot water after exposure of SNC silica and sodium chloride mixture and SAC silica and sodium acetate mixture to steam atmosphere at temperature range of 650°C to 850°C.

Time, minutes	Soluble silica as part of total SiO ₂ , %					
	SNC			SAC		
	650°C	750°C	850°C	650°C	750°C	850°C
0.75	0.0	0.0	0.0	0.9	4.9	9.0
1.5	0.0	0.0	0.0	1.4	6.1	10.4
5	0.0	1.8	2.5	2.3	7.1	12.4
15	0.0	2.6	8.8	3.1	7.9	12.9
35	0.0	8.2	17.7	3.5	11.0	14.7

A comparison of results for silicate formation during exposure to steam of SAC and SNC mixtures is presented in Table 6.5. The reactions for the SAC mixtures were instant, particularly at 750°C and 850°C, while the reaction between sodium chloride and silica in the SNC mixture were much slower as less soluble silica is in the reaction products. The

hot water soluble silicate content in the SNC mixture was much lower than for all SAC mixtures except for the relatively comparable results at the longer reaction times at 850°C.

The above result suggests the conclusion that the reaction of sodium chloride with silica in steam is not an instantaneous reaction and is a slower reaction than between silica and sodium carbonate. However, both reactions appear to result in the formation of sodium disilicate soluble in hot water.

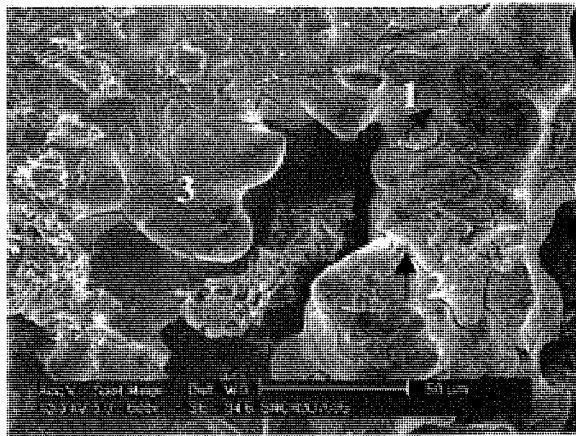
6.5.2 Microscopic examination

Selected samples of SNC mixtures exposed to steam were examined by SEM analysis. Silicate formations around the silica grains were analysed, with mostly backscattered electron images recorded. The analyses of randomly chosen spots of interest show weight per cent content of component analysed and are expressed on an oxide basis for silica and sodium, other than sodium equivalent to the analysed chlorine. The value of analysed chlorine and equivalent sodium are combined and shown as sodium chloride content.

There is no evidence in microscopic examination of any reaction between silica and sodium chloride at 650°C. In the preceding section it was shown that leaching analyses also found no silicate formation at that temperature.

The results of microscopic examination of SNC mixture exposed to steam at 750°C are shown in Figure 6.31, surface morphology in (a) and cross-section image in (b). The surface image clearly shows that the sample is fused and analysis of this surface indicates a significant portion of this fused material is sodium chloride.

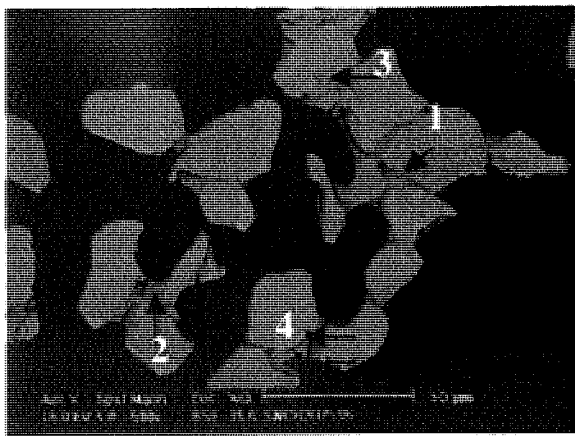
Cross-section analysis shown in Figure 6.31(b) reveals the formation of silicates on the surface of silica grains and joints between them. Un-reacted cores of silica grains can be easily recognized in the micrograph and borders between silica grains and glass joint are clearly shown in these images. The concentrations of sodium in the silicate joints appear higher than the values analysed by the leaching technique. There was some un-reacted sodium chloride analysed in these silicate joints.



(a)

Analyses, wt %:

	Na ₂ O	SiO ₂	NaCl
1	12.8	75.3	11.9
2	14.8	80.6	4.6
3	4.3	94.6	1.1



(b)

Analyses, wt %:

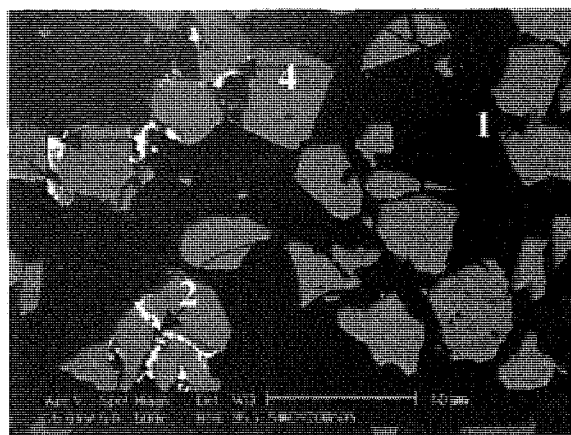
	Na ₂ O	SiO ₂	NaCl
1	9.7	85.7	4.6
2	5.8	93.6	0.6
3	6.9	90.7	2.4
4	7.0	92.3	0.7

Figure 6.31 Micrographs of SEM (a) secondary electron image and (b) of backscattered electron image of a cross section of SNC sample exposed to steam atmosphere at 750°C for 35 minutes.

These micrographs show a very important feature: that at temperatures as low as 750°C, sodium chloride and silica form fused material, which can cement silica particles together.

Backscattered cross sectional images for 850°C samples are presented in Figure 6.32 and show that the formation of silicates in the reaction between silica and sodium chloride was a slow process.

Images of the 5 minutes exposure sample clearly show thin layers of sodium chloride (a) or sodium silicates (b) joining together silica particles. These results confirm results of the low level of silicate formation obtained by the leaching analyses.



(a)

Analyses, wt %:

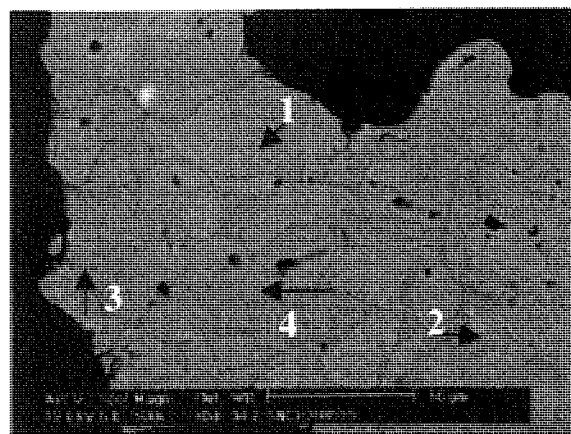
	Na ₂ O	SiO ₂	NaCl
1	11.5	84.0	4.5
2	8.8	35.9	55.3
3	1.3	6.9	91.8
4	9.1	71.0	19.9



(b)

Analyses, wt %:

	Na ₂ O	SiO ₂	NaCl
1	7.1	87.6	5.3
2	7.5	89.8	2.7
3	6.3	92.1	1.6
4	7.3	87.3	5.5



(c)

Analyses, wt %:

	Na ₂ O	SiO ₂	NaCl
1	11.2	86.4	2.4
2	13.2	84.4	2.4
3	10.2	88.2	1.6
4	12.8	85.4	1.8

Figure 6.32 Micrographs of SEM backscattered electron images of cross sections of SNC samples exposed to steam atmosphere at 850°C for (a, b) 5 minutes and (c) 35 minutes.

Prolonged reaction at 850°C resulted in the formation of large areas of fused matrix embedding the silica particles, as shown in Figure 6.32c. The concentration of sodium in this matrix is detected at 12% wt., which is higher than after only 5 minutes of reaction.

These concentrations of sodium compare well with the results from the leaching assays and also with results for SAC mixture exposed to similar conditions.

The general conclusion from the results of exposure of sodium chloride and silica mixture to steam at temperatures characteristic of operating conditions of a fluidised bed gasifier is that the formation of silicates will take place and these silicates show the same characteristics as the silicates formed in the reaction between silica and sodium carbonate.

6.6 PYROLYSIS AND GASIFICATION OF COAL CONTAINING SILICA AND SODIUM CHLORIDE

NC1S coal sample containing sodium in the form of sodium chloride and silica was specially prepared for use in pyrolysis and gasification experiments. The coal contained on a dry basis 0.85% of sodium and 9.6% silica. Samples of this coal were pyrolysed and gasified at the same conditions as NA1S coal. Parameters of these experiments are presented in Table 3.7.

The assessment of the reaction products between silica and sodium chloride after pyrolysis and gasification of NC1S coal was performed on the chars by assaying the solubility in water of silica. Results of the product solubility are related to the formation of soluble silicates in reaction of silica with sodium chloride in the SNC mixture. Examination of char samples to assess extent of silicate formations using electron microscopy was also carried out.

Sodium, which did not react with silica and remained in the char, would leach into the same water solution as sodium that reacted with the silica. Therefore, to independently assess the formation of any reaction products between sodium and silica, any change in the solubility of silica were considered as a measure of the extent of the reaction.

No silica was found in cold water leachates of NC1S coal chars obtained during pyrolysis in nitrogen or during gasification with steam or carbon dioxide. This result obviously suggests no formation of sodium metasilicate.

The results for silica solubility in hot water only for the 850°C experiments are presented in Table 6.6. The results shown in this table also include results of the mass change of pyrolysed or gasified coal. Values for soluble silica at 650°C and 750°C for carbon dioxide and nitrogen atmospheres were not included owing to the very low values obtained for 850°C conditions.

Table 6.6 Results of solubility in hot water of silica present in residue char after pyrolysis in nitrogen and gasification with steam and with carbon dioxide of NC1S coal containing on dry basis 0.85% of organically-bound sodium and 9.6% of silica.

Atmosphere	Steam	Steam	Steam	Nitrogen	Carbon dioxide	Steam	Steam	Steam	Nitrogen	Carbon dioxide
Temperature °C	650	750	850	850	850	650	750	850	850	850
Time, min	Silica soluble in hot water, % wt					Char remaining, % wt				
0.45	0	0	0.03	0.06	0.05	58.19	57.07	48.46	48.62	48.12
1.5	0	0.04	0.06	0.07	0.06	54.00	53.37	44.25	46.78	44.96
5.75	0.06	0.11	0.17	0.06	0.09	51.68	50.71	36.92	46.73	40.90
15.75	0.11	0.15	0.18	0.07	0.12	49.19	49.39	28.81	45.34	30.04
35.75	0.13	0.24	0.33	0.06	0.16	49.17	47.87	18.80	45.58	20.25

6.6.1 Pyrolysis in nitrogen

Pyrolysis of NC1S coal in nitrogen atmosphere at 850°C resulted in basically very little reaction between silica and sodium chloride present in the coal. Only approximately 0.25% of the total silica became soluble in hot water giving very low concentration of silicates in the pyrolysis char. The formation of silicates is expected only if steam is present in the reaction environment. Steam would evolve from coal during early stages of heating due to evaporation of moisture. However, this steam would not participate in the reaction between silica and sodium chloride as in the reported experimental conditions, as it would leave the reaction zone before particle reached the necessary reaction temperature.

The fact that some silica in NC1S pyrolysis chars was found as soluble in hot water was a result, as shown in Chapter 5, of a fact that sodium chloride present in coal may react with the coal and sodium carbonate may form. It is the subsequent reaction between this carbonate and silica leading to the formation of the silicates.

6.6.2 Gasification with carbon dioxide

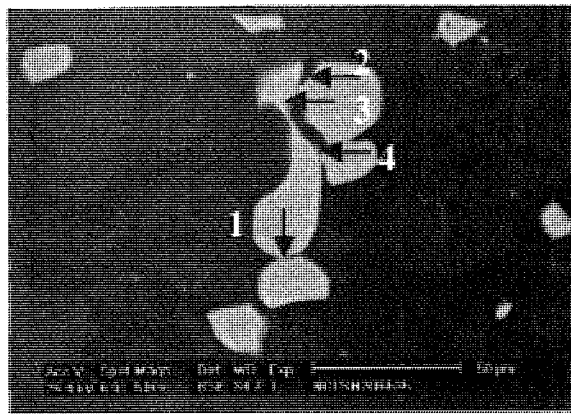
Gasification of NC1S coal in carbon dioxide atmosphere resulted in the transformation of some silica into silica soluble in hot water only at 850°C. This result suggests reaction between silica and sodium originally present in coal as sodium chloride. Approximately 0.35% of the total silica was soluble in hot water. As stated previously, the formation of silicates during gasification of NC1S coal would only be expected if steam was present in reaction environment (Reaction 6.5). The reaction between carbon dioxide and hydrogen evolving from coal during gasification may result in the formation of some steam and methane as products, but such reactions should be considered only for pressurised gasification. Otherwise, the explanation for the reaction between sodium and silica could be considered the same as in the case for the pyrolysis process, that reaction of sodium chloride with coal results in formation of sodium carbonate, which further reacts with silica.

6.6.3 Gasification with steam

Gasification of NC1S coal with steam resulted in transformation of measurable silica into silica soluble in hot water. As shown in Table 6.6, 0.33% of the residual char, equivalent to approximately 0.7% of the total silica became soluble in hot water after gasification in steam at 850°C. This and other values were significantly lower than expected from results obtained for SNC sodium chloride and silica mixture.

The likely explanation for the case of the SNC mixture is the concentration of sodium was a few folds higher than in the gasified NC1S coal. Consequently, due to the higher dispersion of sodium chloride in the char and slower reaction between sodium chloride and silica than between sodium carbonate and silica, the overall conversion of silica was less.

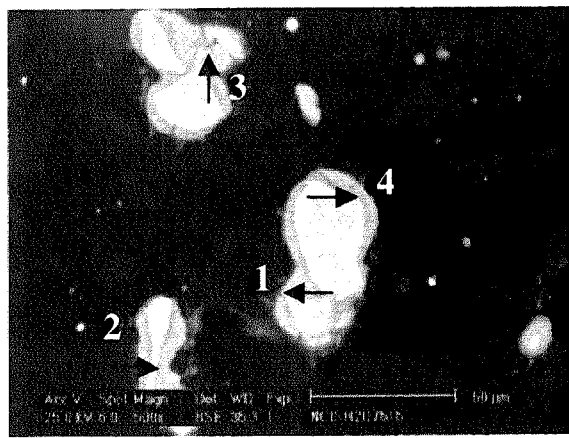
The conclusion drawn from silica solubility results is that sodium silicates do form during coal gasification with steam in reaction between silica and sodium present in coal as sodium chloride. However, the rate of this reaction is substantially lower than between silica and sodium present in coal as organically-bound sodium.



(a)

Analyses, wt %:

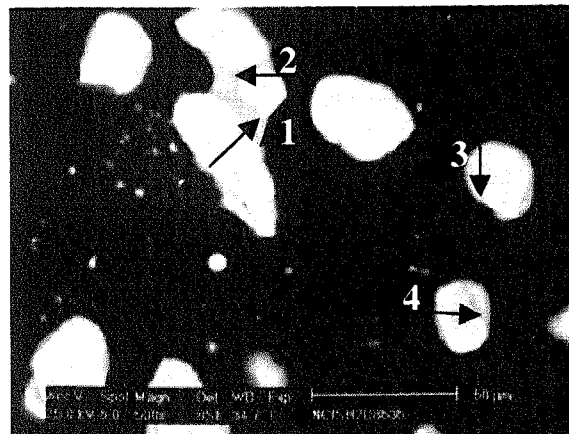
	Na ₂ O	SiO ₂	NaCl
1	1.0	99.0	0.1
2	0.1	99.2	0.8
3	1.0	98.2	0.7
4	0.0	100.0	0.0



(b)

Analyses, wt %:

	Na ₂ O	SiO ₂	NaCl
1	5.2	92.7	2.2
2	1.3	96.4	2.3
3	3.8	95.6	0.4
4	4.6	92.7	2.7



(c)

Analyses, wt %:

	Na ₂ O	SiO ₂	NaCl
1	5.0	95.0	0.0
2	3.3	96.7	0.0
3	7.8	92.2	0.0
4	5.3	94.5	0.1

Figure 6.33 Micrographs of SEM backscattered electron images of cross section of NC1S coal char samples exposed to steam atmosphere for 35 minutes (a) at 650°C, (b) at 750°C and (c) at 850°C.

The above statement finds its confirmation in results from electron microscopic examination of the char samples. Figure 6.33 presents images of magnified cross-sections of NC1S coal char samples gasified in steam at 650°C, 750°C and 850°C. Evidently no reaction between silica and sodium chloride can be assumed for 650°C conditions. Some

reaction leading to the formation of silicates on the surface of silica grains can be observed for the 750°C gasification conditions. The sodium level in these silicates averages between 3 to 4% weight. Silicates formed within the char at 850°C are yet higher in sodium, which approximates to between 5 and 6% weight. This level of concentration is less than a half of that found in silicates formed in NA1S coal char. The viscosity of these NC1S coal silicates can therefore, due to the higher silica content, be expected to be higher than of silicates formed in coal, where silica reacts with sodium carbonate.

6.7 SUMMARY

The following section presents the major conclusions from the experiments with silica and sodium salt mixtures and from the pyrolysis and gasification experiments of specially prepared coals.

6.7.1 Reactions between silica and organic sodium in mineral mixture

1. Solubility results show that sodium disilicate $\text{Na}_2\text{Si}_2\text{O}_5$ is the major reaction product formed at 850°C under all three atmospheres. At 650°C sodium metasilicate Na_2SiO_3 formed under carbon dioxide and nitrogen atmosphere conditions. No particular influence of either nitrogen or carbon dioxide atmosphere on the formation of metasilicate can be concluded, as the rate of formation of this silicate was similar under both gas environments.
2. Microscopy examination results showed that under steam conditions, extensive formation of liquid silicates occurs at temperature as low as 750°C. Similar results for experiments conducted in carbon dioxide or nitrogen atmospheres, however, are obtained at a temperature of 850°C.
3. Steam reduces the melting temperature of sodium carbonate and consequently temperature of formation of liquid sodium disilicate $\text{Na}_2\text{Si}_2\text{O}_5$, which formed in a direct reaction between liquid sodium carbonate and solid silica. Under steam, sodium disilicate was present already at 650°C.

4. Silica dissolves in the formed liquid silicates and increases the total mass of fused silicate glass. Approximately 35% of the mass of SAC reaction mixture could be in the liquid phase under steam conditions.
5. The instantaneous formation of liquid sodium silicates at 750°C in steam, or at 850°C under carbon dioxide or nitrogen atmosphere, should be considered more important than the actual concentration of sodium and silica in the formed silicates. These silicates could be a potential source for bed agglomeration and defluidisation during fluidised bed gasification of coal.
6. The fact that analyses from SEM don't match exactly chemical analyses of silicates in water leachates results from silica dissolution in the formed silicates.
7. Formation of sodium disilicate predicted by thermodynamic calculations has been confirmed by the experimental analyses. Equilibrium composition predicted by thermodynamic calculations with all silica present in liquid phase was not reached for any experimental conditions
8. After examining the SAC mixtures, it can be expected that in coal containing sodium and silica there may be a variety of compositions of silicate melt at the silica grain surface.

6.7.2 Pyrolysis and gasification of coal containing organically-bound sodium and silica

1. Thermodynamic predictions on liquid silicate formation during gasification of coal containing silica and organically-bound sodium in the temperature range of 650°C to 850°C have been only confirmed by results of experiments qualitatively and for the higher temperatures. Gasification of coal at 650°C with steam or with carbon dioxide does not result in the formation of liquid silicates.
2. Pyrolysis of coal results in a very low level of formation of silicates, as implied by results of char water leachate analysis and confirmed by the results of microscopic examination. No fused silicates have been identified in any of the pyrolysis char.

3. Fused glass silicate joints formed between individual silica grains inside char gasified in carbon dioxide at 850°C.
4. Gasification with steam resulted in formation of fused glass silicate joints between silica grains already at 750°C. Gasification of coal with steam results than in the formation of liquid phase silicates at temperature at least 100°C lower than gasification with carbon dioxide.
5. The composition of liquid silicates formed during gasification of coal with steam at 850°C was found to approach that predicted by thermodynamic calculations. Short periods of gasification in steam at 850°C resulted in the formation of liquid silicates with sodium oxide concentration exceeding that found in silicates formed under longer periods of gasification with carbon dioxide at 850°C.
6. The formation of ash in coal char during gasification takes place within the whole volume of char particles as formation of silicates around silica particles is established as taking place everywhere within char particles. Liquid silicates create neck joints between the silica particles or form a fused matrix in which silica particles are embedded. The formation of so formed agglomerates of silica particles occurs throughout the whole volume of the char particle.
7. It is inferred that during gasification with steam at 750°C a liquid-solid phase reaction between sodium carbonate and silica leads to the formation of liquid silicates. This is as a result of a fact that in a steam atmosphere, sodium carbonate melts at a temperature substantially lower than the standard melting point temperature. The melting temperature of sodium carbonate in a given gasifier environment will be depend on the steam mass fraction in such environment.
8. It is also inferred that dissolution of silica in the formed silicates increases the total mass of the formed liquid glass phase and reduces concentration of sodium in that phase. Thermodynamic prediction of all silica being in a liquid form is definitely not confirmed by experimental results.

9. The results on formation of silicates during gasification of tested coal are considered as being in a good agreement with the results of microscopic examination of post-reaction SAC mixtures.
10. The presence of silica does not significantly reduce volatilisation of sodium from coal char during gasification with steam or with carbon dioxide, as nearly 40% of sodium may evaporate during gasification.
11. Gasification of coal at 850°C will result in the formation of liquid silicates regardless of the gasification environment. The presence of steam in the gasifier atmosphere will reduce the temperature of formation of silicates and therefore increase tendency for coal ash to agglomerate.
12. The formation of liquid silicates during gasification of coal containing silica and organically-bound sodium may result in the agglomeration of coal ash and may influence gasifier bed operation.

6.7.3 Reactions between sodium chloride and silica

1. Reaction between mixed sodium chloride and silica can only take place if steam is present in the reaction environment.
2. Sodium chloride and silica react and form fused silicates in steam at 750°C, which is below sodium chloride melting point.
3. The reaction between sodium chloride and silica during gasification in steam at 850°C results in the formation of sodium disilicate, similar to the reaction between silica and sodium carbonate, but reaction rate is a substantially lower than for reaction between silica and sodium carbonate.
4. It may be inferred that during gasification or pyrolysis of coal, sodium chloride present in coal will react with coal and sodium carbonate may form. This sodium carbonate in turn will react with silica present in coal to form sodium silicates.

Chapter 7**REACTIONS OF SODIUM WITH KAOLIN DURING GASIFICATION AND PYROLYSIS OF COAL - EXPERIMENTAL RESULTS****7.1 INTRODUCTION AND OBJECTIVES**

This Chapter will report the results of reactions between sodium compounds and kaolin during the pyrolysis and gasification of coal under conditions similar to those existing in a typical atmospheric fluidised bed gasifier. When sodium and kaolin react under such conditions, they form aluminosilicates. The formation of these products is very beneficial for the stable operation of a gasifier, as aluminosilicates remain in the solid state under typical temperatures of operation for a gasifier and may help prevent the creation of silicates, which can be responsible for bed agglomeration and/or bed defluidisation.

The objective of this Chapter is to provide experimental validation to predictions presented in Chapter 3 on the formation of solid sodium aluminosilicates such as nepheline $\text{Na}_2\text{O} \cdot \text{Al}_2\text{O}_3 \cdot 2\text{SiO}_2$ or liquid albite $\text{Na}_2\text{O} \cdot \text{Al}_2\text{O}_3 \cdot 6\text{SiO}_2$ under coal gasification conditions.

In this chapter experimental results are presented and discussed for specially prepared mixtures of:

- 1) Sodium salts with kaolin and
- 2) Coal samples containing sodium salts and kaolin

Both sample mixtures were exposed to the same experimental temperature and atmospheric conditions. Understanding the reactions occurring during heating of mixtures

of just sodium salts and kaolin without the complications of carbon based gasification reactions will help to examine the process of mineral transformations and form a basis for the assessment of products of reaction between sodium and kaolin during coal pyrolysis and gasification.

7.2 KAOLIN AND ITS THERMAL TRANSFORMATION

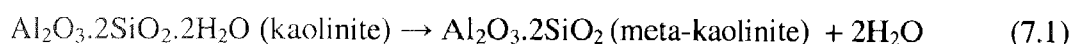
Kaolin, a common clay mineral often present in coal, can react with sodium present in coal to form products melting at significantly higher temperatures than sodium silicates or sodium sulphate. These products are sodium aluminosilicates such as nepheline $\text{Na}_2\text{O} \cdot \text{Al}_2\text{O}_3 \cdot 2\text{SiO}_2$ or albite $\text{Na}_2\text{O} \cdot \text{Al}_2\text{O}_3 \cdot 6\text{SiO}_2$. Formation of such products has been predicted for gasification conditions by thermodynamic equilibrium calculations as presented in Chapter 3.

Kaolin was used by many researchers in crucible experiments to identify interactions of the inorganic constituents in coal at high temperature in studies reflecting combustion conditions. Reactions of kaolin with sodium salts have been shown by Falcone and Schobert (1986), Warne (1983), Nelson and Leslie (1965), Brinsmead and Kear (1956) and others. Nelson and Leslie (1965) report reaction of kaolin and sodium sulphate at 600°C. Falcone and Schobert (1986) showed that when kaolin is mixed with sodium acetate they reacted at 750°C. Wall et al. (1975) report on using kaolin clay in a fluidised bed combustor burning sludge and operated at 740°C to eliminate sodium salts from gas stream. They report formation of nepheline in the combustor. Lindner et al. (1988) established that addition of kaolin clay to coal helps to control fouling when burning high-sodium high-sulphur content Lochiel coal.

The term kaolin is used for a group of clay minerals represented by the formula $\text{Al}_2\text{O}_3 \cdot 2\text{SiO}_2 \cdot 2\text{H}_2\text{O}$, of which kaolinite is the principal constituent and most common mineral (Hlavac, 1983). Kaolinite belongs, from the point of view of its structure, to two-layer structure silicates. Its structure is based on SiO_4 tetrahedra hexagonal array of silica sheets and one octahedral sheet of the hydroxyl ions dominated by gibbsite type composition $(\text{OH})_6\text{-Al}_4\text{-(OH)}_2\text{O}_4$ forming a base for the mid-structure layer according to Deer et al. (1965) and Holdridge and Vaughan (1957). Kaolinite forms plates 0.1 to 3 micrometers in size of about 0.05 of micrometer in thickness (Hlavac, 1983). Kaolin used

in current work was of very finely divided crystalline structure, giving well-defined XRD patterns. Particle size was lower than 10 micron.

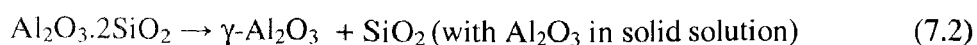
On heating, kaolinite loses the combined water (reaction 7.1) in a temperature range of between 500°C - 600°C and decomposes (Holdridge and Vaughan, 1957). According to Grimshaw (1971), the rapid decomposition – dehydroxylation of kaolinite occurs at 585°C and kaolinite loses hydration water and transforms into a non-crystalline state. The product is commonly called meta-kaolinite according to Eitel (1954), Grofcsik (1961) or meta-kaolin according to Brindley (1951) and Grim (1968).



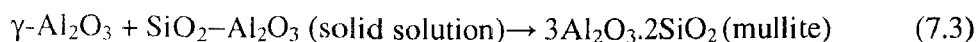
Dehydrated kaolinite according to Grim (1968) and Holdridge and Vaughan (1957) retains minor amounts of hydroxyl water even if heated up to 930°C. Identification of meta-kaolinite from the XRD patterns is difficult due to its poor crystalline, or amorphous structure. Holdridge and Vaughan (1957) show that meta-kaolinite may not be strictly amorphous and may still retain some degree of order and it is not a simple mixture of alumina and amorphous silica. It has been shown by Brindley (1951) and Grim (1968) that hexagonal shape of kaolinite persists far above the dehydration temperature of kaolinite. Eitel (1965) reports that in the temperature range from 600°C to 850°C tetrahedral layer of kaolinite is preserved, as most of hydroxyl ion layer is lost. This causes voids in meta-kaolinite structure, which for example could be filled by alkali ions.

Meta-kaolinite decomposes on further heating; aluminium oxide $\gamma\text{-Al}_2\text{O}_3$ appears above 800°C, together with cristabollite- SiO_2 . Above approximately 900°C, mullite- $3\text{Al}_2\text{O}_3 \cdot 2\text{SiO}_2$ forms (Holdridge and Vaughan, 1957). Grim (1968) reports that formation of mullite is retarded by presence of alkali ions. Bridley (1951) suggests that reactions of meta-kaolinite leading to formation of $\gamma\text{-Al}_2\text{O}_3$ and mullite could be expressed as follows:

At 850°C to 1050°C:



At 900°C and above:



7.3 KAOLIN AND ORGANIC SODIUM MIXTURE

This part reports on the results of investigations into products of reaction between kaolin and sodium acetate mixed together into KAC mixture. This mixture was exposed in a series of experiments under nitrogen, carbon dioxide or steam atmospheres to the temperature range of between 650°C to 850°C. Details are shown in Table 4.7.

In these experiments with kaolin and sodium acetate KAC mixture, it was expected that sodium would react with kaolinite or its decomposition products. Sodium acetate, as reported in Chapter 6, would be transformed upon heating into sodium carbonate and it was considered that sodium carbonate would be the form of sodium to participate in any reaction with kaolinite or its transformation products.

7.3.1 Mineralogical analysis

The high-temperature exposure of kaolin was carried out to identify kaolin breakdown products and to establish a reference base for product solubility and reaction product mineralogy for kaolin – sodium salt mixtures and prepared special coal samples. Mineralogical results of X-ray diffraction analysis are presented in Table 7.1, together with results for some of KAC mixture samples.

7.3.1.1 Products of thermal decomposition of kaolin

Kaolin contained kaolinite as the principal mineral, and quartz and mica have been identified at trace level. Exposure of kaolin to elevated temperature resulted in disappearance of kaolinite structure and dominant amorphous material was identified, with preservation of traces of quartz and mica. A broad peak obtained in all XRD patterns of samples reported in Table 7.1 was indicative of an amorphous material dominating the samples. It is expected that this broad peak was reflecting the presence of meta-kaolinite.

7.3.1.2 Results for carbon dioxide atmosphere experiments

Exposure of KAC mixture to experiment temperatures resulted in formation of nepheline, a sodium aluminosilicate, which melts at 1270°C. There was a steady increase in the amount of nepheline in KAC mixture exposed to carbon dioxide, from trace levels at 650°C to a co-dominant level at 850°C. These results suggest a slower reaction at lower temperatures between kaolinite, or rather meta-kaolinite, as shown in reaction (7.4) and sodium

carbonate and they also suggest that it is a solid-solid reaction below 850°C and a solid-liquid reaction at 850°C. The sodium carbonate melting point is 851°C.

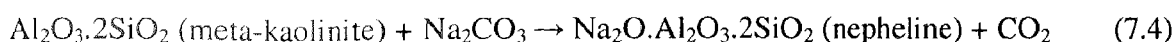


Table 7.1 X-ray diffraction analysis of samples of kaolin and kaolin and sodium acetate KAC mixture exposed to carbon dioxide or steam atmosphere at temperature of 650°C to 850°C.

Sample	Atmo-sphere	Time, min.	Temp. °C	Mineralogical Composition*			
				Dominant**	Co-dominant	Minor	Trace
Kaolin	CO ₂	-	-	kaolinite			quartz, mica
Kaolin	CO ₂	15	650	amorphous material			quartz, mica
Kaolin	CO ₂	15	750	amorphous material			quartz, mica
Kaolin	CO ₂	15	850	amorphous material			quartz, mica
KAC	CO ₂	35	650	amorphous material			nepheline, quartz
KAC	CO ₂	35	750	amorphous material		nepheline	quartz
KAC	CO ₂	35	850		nepheline, amorphous material		quartz
KAC	Steam	35	650	amorphous material		nepheline, paragonite	quartz
KAC	Steam	35	750	amorphous material		carnegietite, paragonite	quartz
KAC	Steam	35	850	amorphous material		nepheline, zeolite, carnegietite, paragonite	quartz

* The phases identified were: nepheline ($\text{Na}_2\text{O} \cdot \text{Al}_2\text{O}_3 \cdot 2\text{SiO}_2$), carnegietite ($\text{Na}_2\text{O} \cdot \text{Al}_2\text{O}_3 \cdot 2\text{SiO}_2$), sodium aluminium silicates: ICDD card 46-470 - dehydrated paragonite structure $\text{Na}_2\text{O} \cdot 3\text{Al}_2\text{O}_3 \cdot 6\text{SiO}_2$, ICDD card 42-217 – unknown zeolite structure $\text{Na}_6(\text{AlSiO}_4)_6$, quartz (SiO_2), mica ($\text{K}_2\text{O} \cdot 3\text{Al}_2\text{O}_3 \cdot 6\text{SiO}_2 \cdot 2\text{H}_2\text{O}$).

** Dominant (>60%), co-dominant (sum of phases >60%), minor (5-20%), trace (<5%).

XRD analysis did not show the presence of albite $\text{Na}_2\text{O} \cdot \text{Al}_2\text{O}_3 \cdot 6\text{SiO}_2$. Thermodynamic calculations have predicted that 20% of the total sodium would form liquid albite.

7.3.1.2 Results for steam atmosphere experiments

In steam, the KAC sample formed nepheline together with other mineral structures of the same chemical formula $\text{Na}_2\text{O} \cdot \text{Al}_2\text{O}_3 \cdot 2\text{SiO}_2$ or slightly differing sodium aluminium silicates. At 650°C two sodium aluminosilicates were identified as minor phases: nepheline and a structure reflecting XRD pattern of dehydrated paragonite, $\text{Na}_2\text{O} \cdot 3\text{Al}_2\text{O}_3 \cdot 6\text{SiO}_2$. This structure contains one third of the sodium present in nepheline. At the same conditions in carbon dioxide atmosphere, nepheline was detected only at trace levels.

At 750°C there was also formation as minor phases of nepheline polymorph form carnegietite and again formation of paragonite. In nepheline the sodium cation is octahedrally coordinated, whereas in carnegietite the sodium cation is tetrahedrally coordinated (Falcone and Schubert, 1986). Falcone and Schubert (1986) also reported the formation of carnegietite at the same temperature for a sodium acetate and kaolin mixture, but in air environment.

Reactions between kaolin and sodium carbonate at 850°C resulted in the formation of all those forms of sodium aluminosilicate ($\text{Na}_2\text{O} \cdot \text{Al}_2\text{O}_3 \cdot 2\text{SiO}_2$), with nepheline as a minor phase, together with some formation of a zeolite structure. It appears that in a steam environment, the formed aluminosilicate $\text{Na}_2\text{O} \cdot \text{Al}_2\text{O}_3 \cdot 2\text{SiO}_2$ preferably crystallises into carnegietite structure rather than nepheline structure. Steam also promotes structures such as paragonite with sodium to aluminium or sodium to silica ratio of one third of that in nepheline.

It is apparent that phases other than nepheline and carnegietite were possibly present in the examined samples. Identification of any phase in the XRD patterns of KAC samples exposed to steam was not an easy task. The presence however, of a structure identified as dehydrated paragonite – a sodium based mica mineral - still shows reaction of sodium carbonate with the same proportion of aluminium to silica oxide structure of meta-kaolinite, as found in the nepheline. A structure identified in the XRD patterns and attributed to a zeolite also has the same chemical ratio of oxides as in nepheline. All these results indicate a definite reaction between sodium and kaolinite at temperature as low as 650°C, but somehow diversifying into different crystal structures. When a steam environment was used in the experiments, these hydrothermal conditions may reflect conditions of formation of these minerals in nature, and thus explain the variety of structures identified.

Results of XRD analysis for KAC mixtures exposed to steam did not show presence of any albite $\text{Na}_2\text{O} \cdot \text{Al}_2\text{O}_3 \cdot 6\text{SiO}_2$ and showed much more formation of $\text{Na}_2\text{O} \cdot \text{Al}_2\text{O}_3 \cdot 2\text{SiO}_2$ sodium aluminium silicate than in carbon dioxide atmosphere. This can be related to lower melting temperature of sodium carbonate in steam, as discussed in Chapter 6, and consequently liquid-solid reaction between sodium carbonate and kaolin can commence at lower temperatures of at least 750°C.

For both, the steam and carbon dioxide atmospheres, the results show that the original kaolinite elemental hexagonal structure can be preserved in the final nepheline, which also represents hexagonal crystal structure. These results suggest that reaction between sodium carbonate and meta-kaolinite may be that of interstitial in-filling of sodium oxide into the structure of dehydrated kaolinite, increasing with temperature due to reordering of the collapsed clay structure.

Traces of quartz were identified in the original kaolin sample, and also in kaolin and KAC thermally treated samples. It is therefore concluded, as the quartz level was the same in all samples shown in Table 7.1, that the quartz identified in thermally treated KAC samples would originate from kaolin, and not be a product of its thermal breakdown.

7.3.2 Chemical analyses of reaction products

Chemical analysis for sodium, silicon and aluminium was carried out on acid and water leachates on number of kaolin and KAC mixture samples exposed to elevated temperature of carried out experiments.

7.3.2.1 Solubility of kaolinite and its transformation products

Kaolinite and its thermal transformation products, together with possible products of reaction with sodium, are insoluble in water, but some may be soluble in acids, as presented in Table 7.2.

Table 7.2 Solubility in acids of kaolin and its breakdown and reaction with sodium products (Dean, 1985).

Name	Formula	Solubility
Kaolinite	$\text{Al}_2\text{O}_3 \cdot 2\text{SiO}_2 \cdot 2\text{H}_2\text{O}$	Insoluble in acid
Meta-kaolinite	$\text{Al}_2\text{O}_3 \cdot 2\text{SiO}_2$	Soluble in acid
Mullite	$3\text{Al}_2\text{O}_3 \cdot 2\text{SiO}_2$	Insoluble in acid (except HF)
Aluminium oxide	Al_2O_3	Very slightly soluble in acid
Albite	$\text{Na}_2\text{O} \cdot \text{Al}_2\text{O}_3 \cdot 6\text{SiO}_2$	Soluble in HCl only
Nepheline	$\text{Na}_2\text{O} \cdot \text{Al}_2\text{O}_3 \cdot 2\text{SiO}_2$	Soluble in acid

Kaolinite is not soluble in acid, however kaolinite thermal breakdown product meta-kaolinite shows significant solubility in diluted hydrochloric acid according to Insley and Ewell (1935). Out of total aluminium present in the kaolin, nearly 70% becomes acid

soluble when in the form of meta-kaolinite. Grim (1968) reports, that 100% of aluminium in kaolinite heated to 800°C becomes soluble in sulphuric acid and that solubility reduces above that temperature. These solubility tendencies may play an important role in assessment of reactions between sodium salts and kaolin.

Assessment of the results for solubility of aluminium in kaolinite thermal transformation products presented in Table 7.3 shows that these products were different for mixtures of kaolin with sodium or for kaolinite itself. Pure kaolinite transformation products showed a drop of solubility of aluminium in acid as temperature increased. As meta-kaolinite is an initial product of thermal decomposition of kaolin, at 650°C solubility of aluminium was highest; three quarters of total aluminium became soluble in diluted sulphuric acid. As the temperature increased to 850°C, this solubility dropped to near 40%, as other insoluble products, aluminium oxide and mullite may have formed. These results correspond to those reported by Grim (1968) and Insley and Ewell (1935). XRD analysis however did not show the presence of these insoluble minerals.

Table 7.3 Solubility of aluminium in sulphuric acid in samples of pure kaolin and kaolin mixed with sodium acetate into KAC mixture exposed respectively to carbon dioxide and to steam for 15 minutes at elevated temperatures.

Temperature, °C	Acid soluble Aluminium content, %		Part of original aluminium, %	
	Kaolin	KAC	Kaolin	KAC
20	0.18	0.12	0.93	0.62
650	16.7	19.4	74.3	75.3
750	14.5	16.6	64.5	75.1
850	8.6	16.4	37.8	74.4

Solubility of aluminium in KAC mixtures remained steady as reaction temperature was increased. This leads to a conclusion that the products resulting from kaolin mixtures were, particularly at 850°C, chemically different from pure kaolinite transformation products. It can be assumed that products such as nepheline formed under those conditions. These solubility tests confirm the formation of nepheline chemical structure, as it dissolved in the sulphuric acid used in this analysis, rather than the formation of sodium aluminosilicate, albite, an insoluble in sulphuric acid aluminosilicate.

The solubility tests in sulphuric acid and mineralogical analyses results show that the reaction of kaolinite with sodium carbonate leads principally to formation of a melting at

high temperature $\text{Na}_2\text{O} \cdot \text{Al}_2\text{O}_3 \cdot 2\text{SiO}_2$ sodium aluminosilicate nepheline or its polymorph carnegietite.

7.3.2.2 Solubility of reaction products

Samples of KAC mixture exposed to all experiment conditions and under all three atmospheres were subjected to stage leaching in water. This was to evaluate solubility in water of sodium present in mixture samples after exposure to high temperatures and on this basis evaluate formation of silicates and aluminosilicates.

7.3.2.2.1 Solubility in cold water

Sodium present in KAC mixture was fully soluble in cold water and any reduction of this solubility could be considered as a measure of extent of reaction between sodium and kaolin and formation of insoluble aluminosilicates.

Results of analysis of leaching solutions showed that after exposure of KAC mixtures at high temperatures, solubility in cold water of the sodium present in the KAC mixture has been substantially reduced. These results are shown graphically in Figure 7.1, and present sodium remaining in form soluble in cold water, as fraction of total initial sodium. The remaining sodium reacted with kaolin to form insoluble sodium aluminosilicate mineral nepheline, and other aluminosilicates, the formation of which has been shown by mineralogical and acid solubility analysis.

From the results shown in Figure 7.1 it is clear that less un-reacted sodium remained in samples exposed to steam, than to either, nitrogen or carbon dioxide atmosphere. In steam, approximately 95% of sodium reacted with kaolinite after 90 seconds of KAC mixture being exposed to 650°C or 750°C. At 850°C this value increased to 97% of total sodium. These results clearly show that reaction of kaolin and sodium carbonate in steam atmosphere is almost immediate at a temperature as low as 650°C.

In both, nitrogen and carbon dioxide, approximately 10 to 15% of sodium did not react with kaolinite at 650°C or 750°C. The values are higher for carbon dioxide, which suggest that under a carbon dioxide atmosphere, slightly less sodium reacted with kaolinite. It could be that the reaction of kaolin with sodium carbonate in carbon dioxide was impaired

by the presence of this atmosphere, as one of the products of reaction of the sodium carbonate and kaolin would be carbon dioxide. However, as the reactants were both in the condensed phase, the carbon dioxide partial pressure has only limited influence on the reaction outcome. At 850°C, approximately 8% of the total sodium remained soluble in cold water after exposure to a nitrogen atmosphere and 5% after exposure to a carbon dioxide.

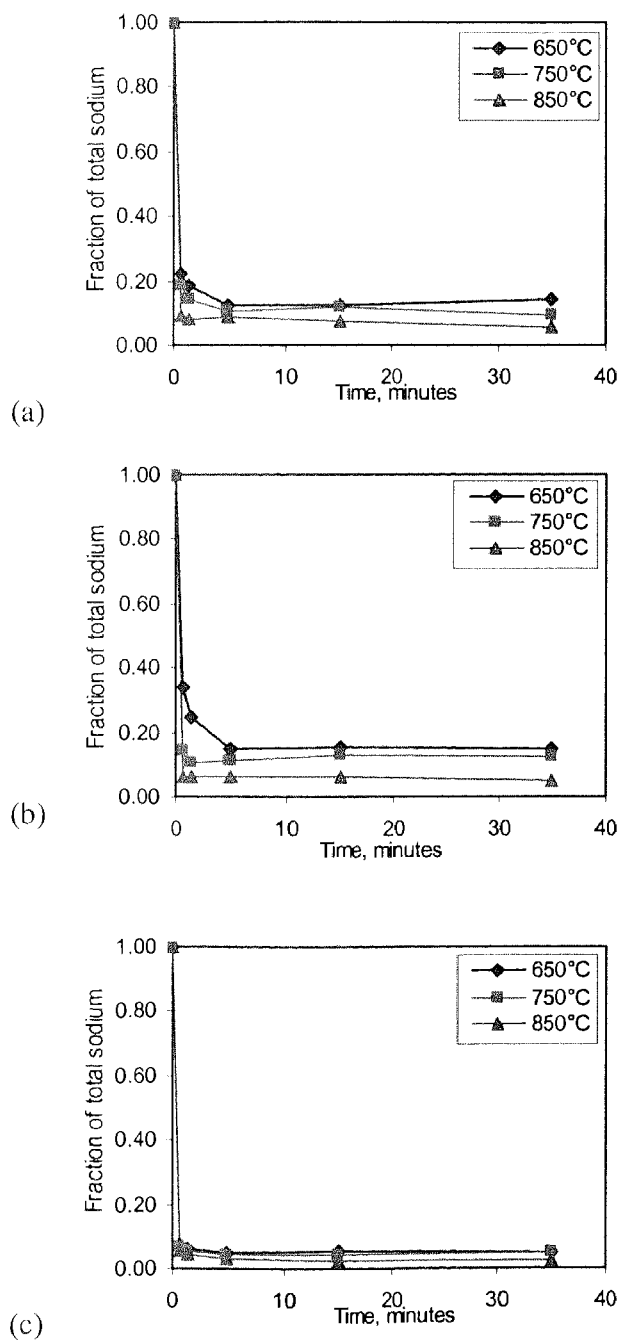


Figure 7.1 Solubility in cold water of sodium present in KAC mixture exposed to atmosphere of (a) nitrogen, (b) carbon dioxide and (c) steam at 650°C, 750°C and 850°C, shown as part of total initial sodium, and presented as a function of reaction time.

In summary, sodium cold water leaching results show that in a steam atmosphere, reactions between sodium carbonate and kaolinite are faster, particularly at lower examined temperature range than in either carbon dioxide or nitrogen atmosphere.

7.3.2.2.2 Solubility in hot water

After leaching in cold water of the un-reacted sodium, leaching of KAC samples in hot water and in superheated water followed, in order to assess how stable and developed were structures of the formed sodium aluminosilicates. Results of leaching analysis are presented in Figure 7.2. Mineralogical analysis indicated well-developed structures formed in a steam atmosphere, but less so in a carbon dioxide atmosphere. Analysis of hot water and superheated water leachate solutions also allowed for an assessment of formation of any sodium silicates from the quartz present in kaolin, or possible kaolin decomposition products.

Results for 650°C experiments show, that nearly 40% of the initial total KAC sodium was leached from the structures formed under both, carbon dioxide and nitrogen atmospheres. At 750°C, this value dropped to approximately 25% for carbon dioxide atmosphere and was approximately 30% for nitrogen conditions. These results clearly show that the reactions between sodium carbonate and kaolinite resulted in structures in which sodium did not penetrate too deep into the kaolinite structure and therefore, a fair part of it could be leached out in a prolonged water leaching process.

Under steam conditions at 650°C, only 20% of the total sodium present initially in the mixture could be leached out from formed structures. At 750°C this value was even lower. Exposure of KAC mixture to carbon dioxide at 850°C resulted in just less than 20% of initial sodium being leached out from formed structures, while exposure to nitrogen gave results of approximately 25%. A steam atmosphere resulted in less than 15% of this sodium form being leached out by the hot and superheated water.

When assessing combined results for all leaching analysis it appears that between 15% and 25% of total sodium was leached out as un-reacted sodium and from structures formed under steam, while under carbon dioxide and nitrogen atmospheres, these values varied between only 50% and 25%, respectively, in the temperature range of 650°C to 850°C.

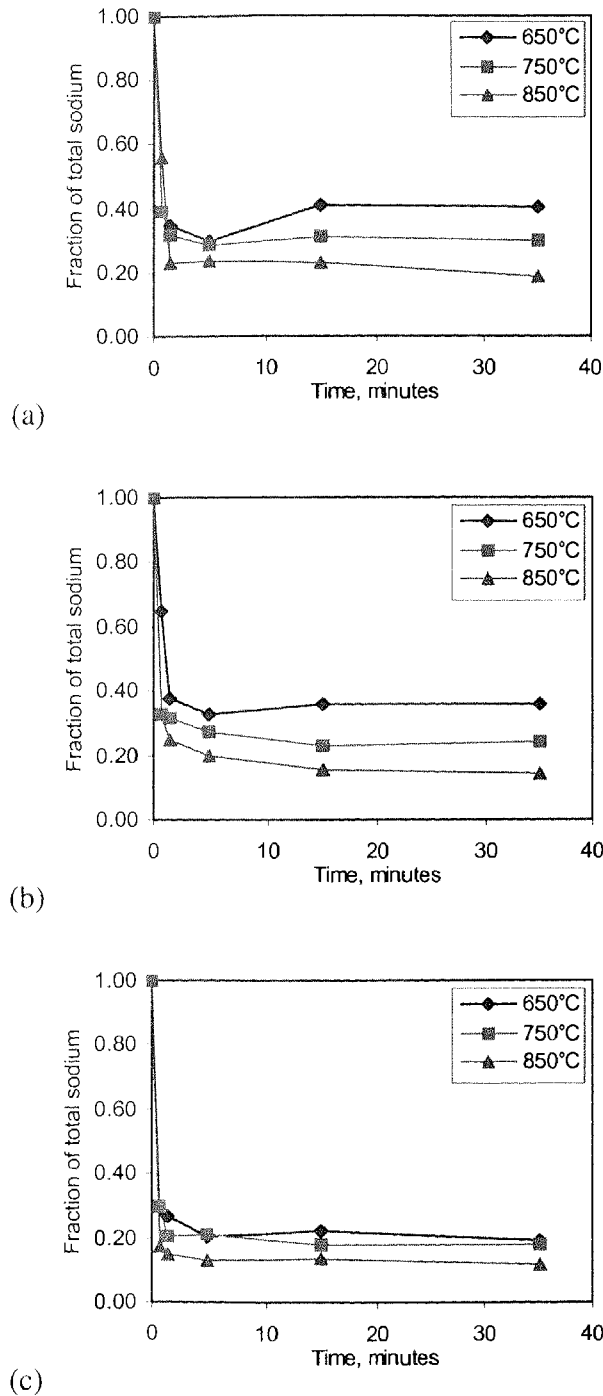


Figure 7.2 Combined sodium soluble in hot and in superheated water as part of total initial sodium of KAC mixture exposed to atmosphere of (a) nitrogen, (b) carbon dioxide and (c) steam at 650°C, 750°C and 850°C and presented as a function of reaction time.

As it has been shown in Chapter 5 and 6, sodium carbonate melts in a steam environment at much lower temperatures than its standard melting point of 851°C. Therefore, it is expected that under steam at 750°C, and may be partly at 650°C, the sodium carbonate-

kaolin reaction is a liquid-solid reaction. However, in nitrogen or carbon dioxide atmosphere, that reaction would be a solid-state reaction below 850°C.

At 850°C under all three atmospheres, the sodium carbonate-kaolin reaction would be a liquid-solid reaction. It is however expected that under steam conditions, the viscosity of sodium carbonate would be lower than under carbon dioxide or nitrogen. Therefore, the penetration of sodium carbonate into the kaolin structure and the wetting of kaolin flakes would be easier and faster in steam, than in the other two atmospheres. This obviously results in a faster reaction rate in steam, as has been shown by all solubility and mineralogical results. The solubility results show that even at 650°C, which is a low temperature from coal gasification or combustion point of view, reaction between sodium carbonate and kaolin is essentially an immediate process under steam, and an efficient reaction in a carbon dioxide or nitrogen atmosphere.

In summary, the reaction between kaolin and organically-bound sodium present in the coal will be more effective under steam conditions than under nitrogen or carbon dioxide conditions.

7.3.2.3 Formation of sodium silicates

As quartz was present in original kaolin, that quartz, as shown in the previous Chapter, may react with sodium carbonate. However, there was no soluble silica analysed in either the cold or hot water leachates of the KAC mixtures after exposure to steam, carbon dioxide or nitrogen atmospheres. Results for leaching in superheated water for 4 hours can be considered as negligible as the values of silica were generally below 1% of the mass of total sample for all three atmospheres, as shown for steam experiments in Table 7.4. There was also no soluble aluminium analysed in any of the leachates.

Table 7.4 Solubility in superheated water of silica present in samples of KAC mixtures exposed to steam at elevated temperatures.

Reaction time, minutes	Soluble silica as part of total sample, %		
	650°C	750°C	850°C
0.75	0.96	0.71	0.19
1.5	0.99	0.39	0.08
5	0.77	0.36	0.11
15	0.73	0.19	0.06
35	0.51	0.19	0.14

Silica solubility was very low and the amount of soluble silica reduced with temperature and also with time. This could be evidence of a much faster a reaction of sodium carbonate with kaolin than with silica.

Lower values of soluble silica for longer reaction times may reflect reduced amounts of leached sodium in respective samples and the lower pH of the solutions. Alkaline solutions would dissolve silica, and solubility of the examined samples could therefore be as a result of analytical procedures, rather than of the experimental process. There was no measurement of pH values carried out for the KAC leaching solutions, but results for some of NAIS samples, from which more sodium was leached at lower reaction temperatures showed declining pH values from 8 to below 6.

On the basis of these values, it can be concluded that no sodium silicates formed during exposure of KAC mixtures to high temperatures in atmospheres of steam, carbon dioxide or nitrogen. The results for solubility of silica however indicate that further research into reaction between sodium carbonate and mixtures of kaolin and silica would be of value.

7.3.3 Microscopic examination

Electron microscopic SEM examinations of post-reaction KAC mixtures were carried out for all tested atmospheres and temperatures. Attention was on sample morphology and comparison of that morphology with silicates formed in SAC mixtures. The cross sections of a number of samples were also examined, with the backscattered electron images recorded. Micrographs of samples only exposed to steam have been chosen for presentation here, as this is sufficiently representative of results obtained for the electron microscopic examinations.

Surface morphologies of KAC mixture samples exposed to steam atmosphere at 650°C, 750°C and 850°C for 35 minutes are presented in Figures 7.3. All examined samples after experiments were soft and partly fluffy in their appearance. This has been also shown in these microscopic images. There was no apparent change in morphology of samples shown in Figure 7.3 with the increase in reaction temperature. Some consolidation appears to be in samples exposed to 750°C and 850°C in comparison with 650°C sample.

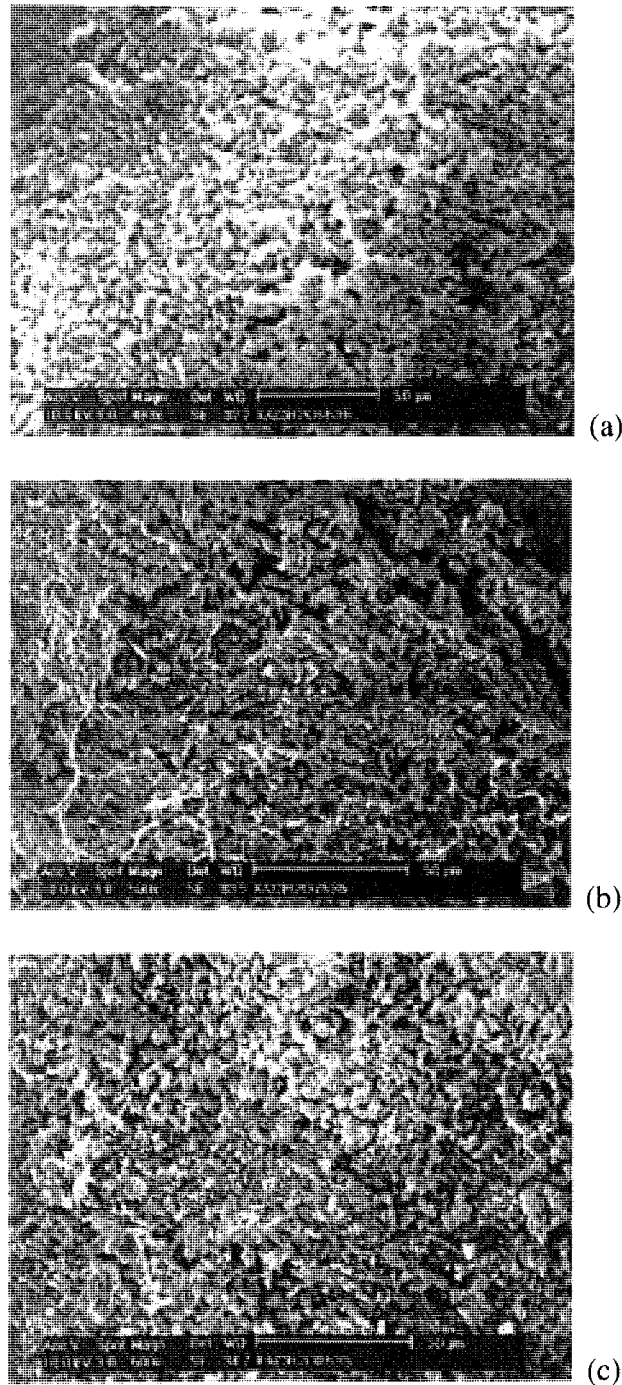


Figure 7.3 Morphology of KAC mixture exposed to steam atmosphere at (a) 650°C, (b) 750°C and (c) 850°C for 35 minutes.

Silicates formed from SAC mixtures, as shown in Figures 6.12 through 6.18 were forming fused glass. There was no evidence of any fused material present in any of the examined KAC samples. If sodium silicates were formed, it would be reasonable to expect the presence of some fused material, but no such evidence of this was established. It can be therefore concluded from these examinations, that products of reaction between sodium

carbonate and kaolin within KAC mixtures, for experiment conditions to which they were exposed, were dry and showed no signs of fusion.

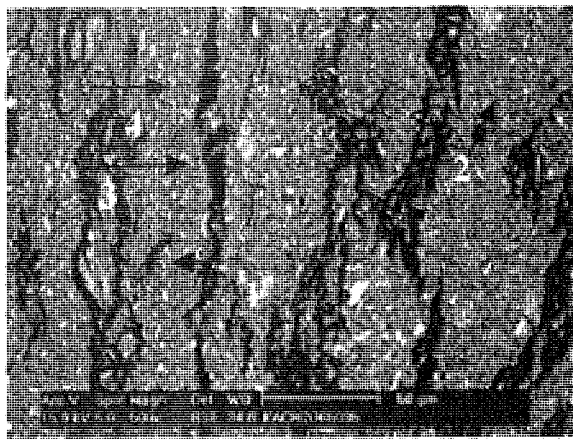
Back-scattered SEM images of cross-sections of KAC mixtures exposed to steam atmosphere at 650°C, 750°C and 850°C for 35 minutes are presented in Figures 7.4. Analyses for sodium, silicon and aluminium of chosen spots are expressed on oxide basis and are included in that Figure. It was found that sodium content in formed aluminosilicates increased with increasing reaction temperature.

The compositions shown in Figures 7.4 did not reach the values for nepheline composition, but an increase of sodium content with increase of temperature from 650°C to 750°C is clearly noticeable. It has been shown in previous Section 7.3.1 that nepheline has formed as a basic mineral from reactions within KAC mixture. The ideal composition of nepheline $\text{Na}_2\text{O} \cdot \text{Al}_2\text{O}_3 \cdot 2\text{SiO}_2$ is 21.9 % for Na_2O , 35.9% for Al_2O_3 and 42.3% weight for SiO_2 .

Also it can be noticed that there was no significant increase of sodium in the formed aluminosilicates as temperature increased from 750°C to 850°C. This would suggest that reaction rates for both temperatures were similar. That would be a result of sodium carbonate becoming liquid below 750°C and therefore giving the same product which otherwise would be expected at 850°C reaction conditions, as standard sodium carbonate melting point is 851°C.

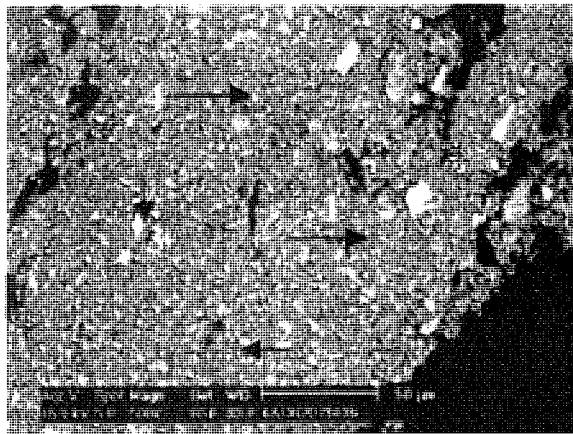
Reaction of sodium carbonate with kaolin, whether at 650°C or at 850°C, leads to formation of aluminosilicate material, which appears dry and does not undergo fusion in the reaction environment. This is regardless whether the reaction was a liquid-solid reaction, as in a steam atmosphere in the given temperature range, or whether it was solid-solid reaction. This observation may have its consequences during coal utilization, including gasification process.

From results presented here it can be than expected that during gasification of coal containing organically-bound sodium and kaolin, there should be formation of dry aluminosilicates, principally nepheline, and this should help to avoid the formation of liquid silicates and the problems associated with agglomeration and potentially defluidisation of a fluidised bed material.



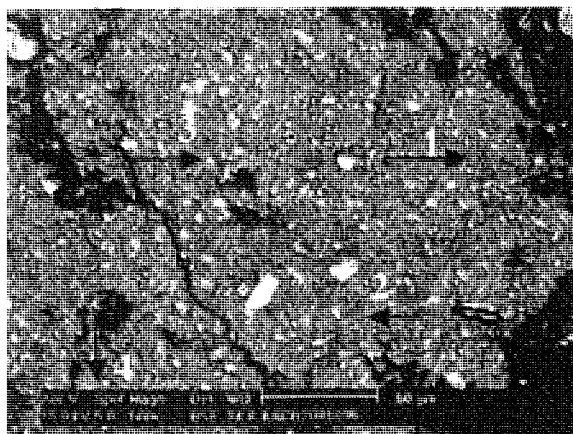
(b)

Analyses, wt. %:	Na ₂ O	Al ₂ O ₃	SiO ₂
1	4.4	39.9	55.7
2	3.9	39.4	56.7
3	0.5	37.3	62.2
4	3.7	40.5	55.8



(b)

Analyses, wt. %:	Na ₂ O	Al ₂ O ₃	SiO ₂
1	14.5	35.9	49.5
2	8.6	38.4	53.0
3	2.9	41.1	56.0
4	12.3	36.7	51.0



(b)

Analyses, wt. %:	Na ₂ O	Al ₂ O ₃	SiO ₂
1	6.7	38.6	54.8
2	3.8	40.1	56.1
3	11.9	38.9	51.2
4	12.8	38.7	48.5

Figure 7.4 Micrographs of SEM back-scattered electron images of KAC mixture exposed to steam atmosphere at (a) 650°C, (b) 750°C and (c) 850°C for 35 minutes.

7.4 PYROLYSIS AND GASIFICATION OF COAL CONTAINING KAOLIN AND ORGANIC SODIUM

The specially prepared coal sample NA1K contained 0.76% organically-bound sodium and some 10% kaolin. This coal was used to investigate reactions between that sodium and kaolin during gasification and pyrolysis of coal. Experiments were conducted at the same conditions as those for KAC mixtures: gasification with carbon dioxide and with steam at 650°C to 850°C and pyrolysis in nitrogen at the same temperature range.

From KAC results, it has been inferred that below 850°C sodium carbonate-kaolin reaction in nitrogen or carbon dioxide atmosphere is a solid state reaction, and in steam this reaction is a liquid-solid state reaction between 750°C and 850°C and probably at 650°C. Guided by those results a careful consideration was given to ways how the best to assess possible sodium and kaolin reactions within the char during gasification and pyrolysis experiments.

Interpretation of char leaching results was difficult. If sodium was leached from the char it would come from both un-reacted sodium and could be leached from aluminosilicates formed within char. The leaching of chars with acid and analysing for sodium and aluminium would then not help to assess extent of aluminosilicate formation. Aluminium from both nepheline and meta-kaolinite would dissolve in the acid, thus it would not be possible to distinguish between the two forms from which aluminium came into solution. It would be impossible to assign the contribution from each source. Staged water leaching was then considered the appropriate method to determine sodium solubility, as the unleached portion of original sodium could be considered as that which reacted with kaolinite and formed aluminosilicates.

7.4.1 Chemical Analyses of Char

Samples of chars from both gasification and pyrolysis at 650°C and 750°C, temperatures, at which it was believed the solid-state reactions between sodium carbonate and kaolin were happening, were chosen for the most detailed leaching analyses process. Sodium was analysed in leachates obtained by leaching char in cold water, hot water and series of 4, 16 and 44 hours leaching in superheated water at 120°C. Results of the leaching tests are presented in Table 7.5.

Sodium analysed in cold water leaching solution for all char samples accounted for only 10% to 15% of the total leached sodium. Hot water and superheated water leaching of NA1K chars on average resulted in leaching of approximately 20% of total leached sodium per leaching step. All these sodium solubility results for NA1K chars are very similar to those for the examined KAC mixtures shown in preceding sections.

In Table 7.5 are also included some cold water leaching results for chars from gasification of NA1S coal, which contained organically-bound sodium and silica. For NA1S chars, more sodium was leached into the cold water for longer reaction times and sodium leached into the cold water represented 50-60% of total sodium.

The results for both 650°C and 750°C experiments are similar and show that as pyrolysis and gasification temperature and reaction time increased, less un-reacted sodium was leached from the NA1K chars, as more of sodium carbonate would have reacted with kaolin. It thus shows that during pyrolysis and gasification in carbon dioxide of coal, kaolin reacts with sodium carbonate at temperature of 650°C, which is 200°C lower than sodium carbonate melting point.

From these sodium-leaching results, it can be concluded that most of the sodium leached from the char had to be leached from the formed aluminosilicate structures (sodium in hot and superheated water) rather than from the char itself (sodium in cold and hot water). It can again be inferred from these results, that sodium carbonate reaction with kaolin would be a solid-state reaction during pyrolysis or gasification with carbon dioxide at 650°C or 750°C.

Presented in the next Chapter are results for the char conversion and catalytic effect of sodium during coal gasification. Char conversion for all NA1K gasification tests were much lower than for NA1 coal, suggesting that the catalytic effect of sodium has been reduced as sodium readily reacted with kaolin, resulting in lower char conversions.

Further assessment of sodium reaction with kaolin can be made on the basis of results of how much of the total sodium present in NA1K coal was leached in the staged-leaching from those examined gasification and pyrolysis chars. The results of such calculations are presented in Table 7.6 and show that generally 60% to 70% of the total sodium was

leached in the staged-leaching, with the remaining left behind believed to be in the formed aluminosilicates. On the basis of results presented in Chapter 5 it has been assumed that there was no sodium loss due to vaporisation.

Table 7.5 Sodium content in char samples of NAIK and NAIS coals gasified with carbon dioxide and pyrolysed in nitrogen, established after leaching the chars in cold water, hot water and in sequences of leaching in water superheated to 120°C.

(a) gasification and pyrolysis at 650°C

Water leaching process	Coal NAIK	Sodium content in coal char, %											
		Gasification in carbon dioxide						Pyrolysis in nitrogen					
		NAIK					NAIS	NAIK					NAIS
		Reaction time, minutes						Reaction time, minutes					
		0.75	1.5	5	15	35	5	0.75	1.5	5	15	35	5
Cold Water	0.17	0.20	0.09	0.08	0.11	0.12	0.45	0.22	0.12	0.09	0.08	0.14	0.22
Hot Water	0.22	0.35	0.23	0.19	0.20	0.21	0.23	0.43	0.27	0.21	0.22	0.21	0.41
4 hrs @120°C	0.24	0.32	0.23	0.19	0.20	0.22	0.16	0.43	0.27	0.20	0.22	0.22	0.20
16 hrs @120°C	0.07	0.24	0.16	0.26	0.26	0.30	n/a*	0.14	0.29	0.28	0.28	0.23	n/a
44 hrs @120°C	0.06	0.09	0.15	0.19	0.12	0.22	n/a	0.05	0.20	0.21	0.25	0.21	n/a

(b) gasification and pyrolysis at 750°C

Water leaching process	Coal NAIK	Sodium content in coal char, %											
		Gasification in carbon dioxide						Pyrolysis in nitrogen					
		NAIK					NAIS	NAIK					NAIS
		Reaction time, minutes						Reaction time, minutes					
		0.75	1.5	5	15	35	5	0.75	1.5	5	15	35	5
Cold Water	0.17	0.20	0.09	0.08	0.11	0.12	0.66	0.22	0.12	0.09	0.08	0.14	0.44
Hot water	0.22	0.35	0.23	0.19	0.20	0.21	0.23	0.43	0.27	0.21	0.22	0.21	0.26
4 hrs @120°C	0.24	0.32	0.23	0.19	0.20	0.22	0.14	0.43	0.27	0.20	0.22	0.22	0.16
16 hrs @120°C	0.07	0.24	0.16	0.26	0.26	0.30	n/a	0.14	0.29	0.28	0.28	0.23	n/a
44 hrs @120°C	0.06	0.09	0.15	0.19	0.12	0.22	n/a	0.05	0.20	0.21	0.25	0.21	n/a

* n/a – not assayed

Considering, that leaching of NAIK chars for much longer periods in superheated water leaches out more sodium, the results in Table 7.6 would be lower if that additional leaching period did not take place. Therefore all those results presented for gasification and pyrolysis of NAIK coal are considered to be in very good agreement with results for KAC mixtures presented in preceding sections. Having such a good agreement between these results for corresponding NAIK coal and KAC mixtures, the assessment of other NAIK gasified samples was carried out with electron microscopy SEM technique.

Table 7.6 Results of leaching in cold water, hot water and for 64 hours in water superheated to 120°C of char samples of NA1K coal gasified with carbon dioxide and pyrolysed in nitrogen at 650°C and 750°C showing sodium leached from char as part of the initial sodium present in coal.

Reaction time, minutes	Sodium leached from char in stage leaching as part of initial sodium present in coal, %			
	Gasification in carbon dioxide		Pyrolysis in nitrogen.	
	650°C	750°C	650°C	750°C
0.7	100	74	94	61
1.5	66	71	81	62
5	66	66	69	58
15	64	62	73	61
35	69	59	70	59

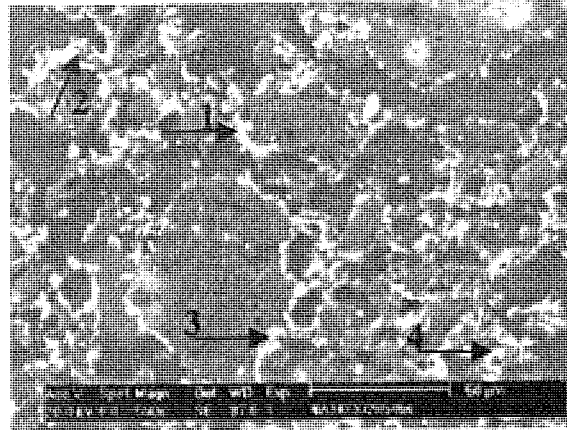
Presented here results for NA1K coal chars and KAC mixtures show that during pyrolysis, at temperature as low as 650°C, between 50% to 85% of organically-bound sodium present in coal can react with kaolin and form aluminosilicates. Finding an efficient way of introducing kaolin into a coal structure could allow minimise problems associated with coal ash agglomeration, due to formation of sulphates during combustion, or, due to formation of silicates during gasification. This knowledge of reactions involving sodium and kaolin at lower temperatures would also be very important for a pyrolysis/mild gasification process preceding coal combustion or gasification process, such as APFBC process.

7.4.2 Microscopic examination of char

Electron microscopic SEM examinations of NA1K coal chars from gasification and pyrolysis at all tested temperatures were carried out for the examination of the formation of any aluminosilicates in coal char. Cross sections of number of samples were examined and backscattered electron images were recorded. The coal ash material based on kaolin introduced to coal was examined for sodium, silicon and aluminium.

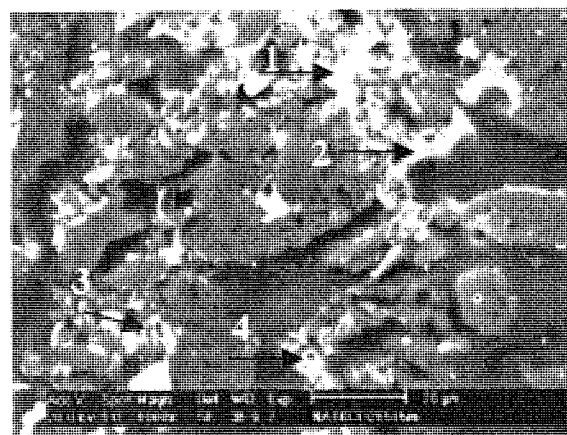
All examined samples showed uniform ash distribution throughout the char reflecting the good distribution of kaolin in the prepared coal samples. There was little consolidation of the formed aluminosilicates. Selected images of cross-sections of chars gasified at 850°C in carbon dioxide are presented in Figure 7.5. These images show the changing content of sodium in the formed aluminosilicates with reaction time.

The concentration of sodium in the formed aluminosilicates for the 45 seconds sample, was found on average to be 9.6% and not much less than the average value of 10.6% shown in the analysis for much longer gasification times.



Analyses, wt. %:	Na ₂ O	Al ₂ O ₃	SiO ₂
1	7.7	35.2	57.1
2	9.3	39.2	51.5
3	12.0	25.2	63.8
4	9.6	36.5	53.9

(a)



Analyses, wt. %:	Na ₂ O	Al ₂ O ₃	SiO ₂
1	9.8	37.9	52.3
2	11.3	36.9	51.8
3	10.1	29.8	60.1
4	11.3	27.6	61.1

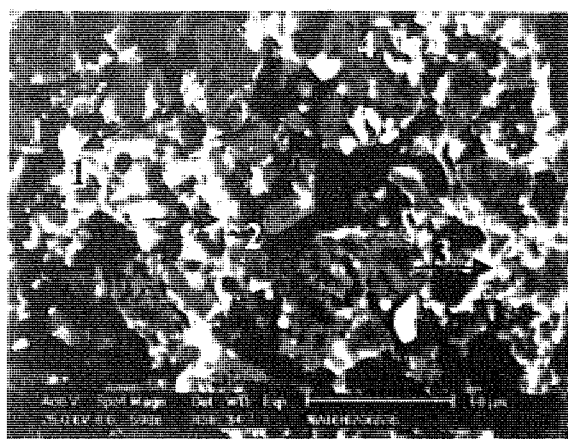
(b)

Figure 7.5 Micrographs of SEM back-scattered electron images of char of NAIK coal gasified with carbon dioxide for (a) 45 seconds and (b) for 15 minutes at 850°C.

Examples of the cross-sections of NAIK char samples gasified with steam for 35 minutes are presented in Figure 7.6. Sodium content in the formed aluminosilicates for the 650°C sample was lower than in 750°C and 850°C samples, which were found to be equivalent. This suggests the exhaustion of sodium for formation of aluminosilicates by 750°C. The average sodium concentration in aluminosilicates in the 750°C and 850°C steam gasification chars was at 11.5%, higher than for the 850°C carbon dioxide gasification char sample.

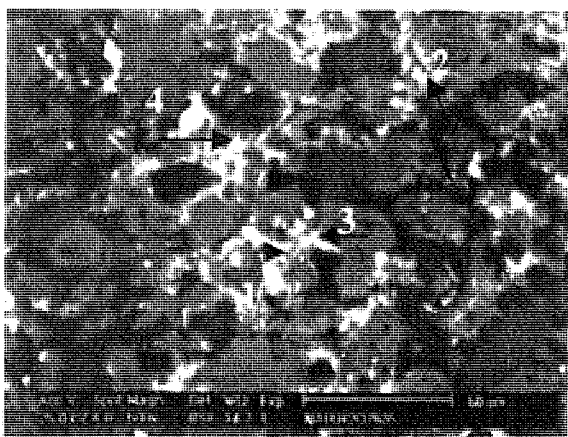
Concentrations of sodium in steam gasification chars as shown in Figure 7.6 are very similar to the values of sodium analysed in corresponding KAC samples (Figure 7.4).

Similarly, as for the results for KAC mixture, NAIK char results also do not reflect stoichiometric concentration of sodium in the nepheline.



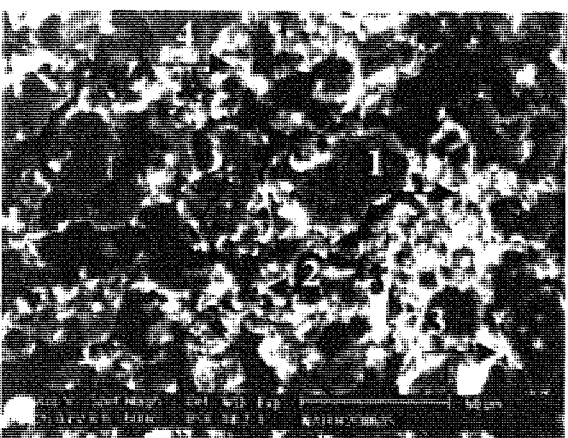
Analyses, wt. %:	Na ₂ O	Al ₂ O ₃	SiO ₂
1	6.5	34.1	59.4
2	9.1	34.8	56.1
3	9.6	33.6	56.8
2	10.9	30.5	58.6

(a)



Analyses, wt. %:	Na ₂ O	Al ₂ O ₃	SiO ₂
1	11.4	35.0	53.3
2	11.8	35.7	52.5
3	10.7	35.0	54.3
4	8.5	35.5	56.1

(b)



Analyses, wt. %:	Na ₂ O	Al ₂ O ₃	SiO ₂
1	9.6	36.1	54.3
2	13.6	36.4	50.1
3	10.6	35.2	54.0
4	11.4	35.3	53.3

(c)

Figure 7.6 Micrographs of SEM back-scattered electron images of char of NAIK coal gasified in steam for 35 minutes at (a) 650°C, (b) 750°C and (c) 850°C.

No evidence of any of fused material was present in the examined gasification chars. This proves, further to the solubility results, that there has been no formation of sodium silicates during gasification of NAIK coal.

7.4.3 Mineralogical examination

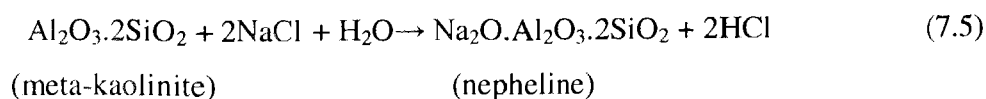
Structures of formed aluminosilicates were insufficiently developed to give XRD diffraction patterns in mineralogical analyses. Traces of aluminosilicate carnegietite were found in the 15minute 850°C steam gasification char sample. Corresponding carbon dioxide gasification and nitrogen pyrolysis chars samples did not show the presence of sodium aluminosilicate minerals.

7.5 KAOLIN AND SODIUM CHLORIDE MIXTURE

Experiments for kaolin and sodium chloride KNC mixtures were carried out in the same temperature range of 650°C to 850°C as the experiments for KAC mixture and NAIK coal.

Thermodynamic predictions presented in Chapter 3 for equilibrium conditions for gasification and pyrolysis of coal containing sodium chloride and kaolin have not been as uniform as for coal containing kaolin and organically-bound sodium. They showed that in the above temperature range solid aluminosilicate $\text{Na}_2\text{O} \cdot \text{Al}_2\text{O}_3 \cdot 2\text{SiO}_2$, which could crystallise as nepheline, should form in steam environment together with some liquid albite (20% of total sodium). During gasification in carbon dioxide nepheline amount would reduce and gaseous sodium chloride content would increase with increasing process temperature. Pyrolysis in nitrogen would result in formation of similar amount of liquid albite, as to be formed during gasification, and the rest would remain as sodium chloride. No nepheline supposed to form from sodium chloride and kaolin during pyrolysis.

Sodium chloride can be expected to react with kaolinite, or its decomposition product in presence of steam in accordance with the following reaction:



chloride and kaolin in nitrogen or carbon dioxide environment would have low yield. This is reflected in result shown in Figure 7.7.

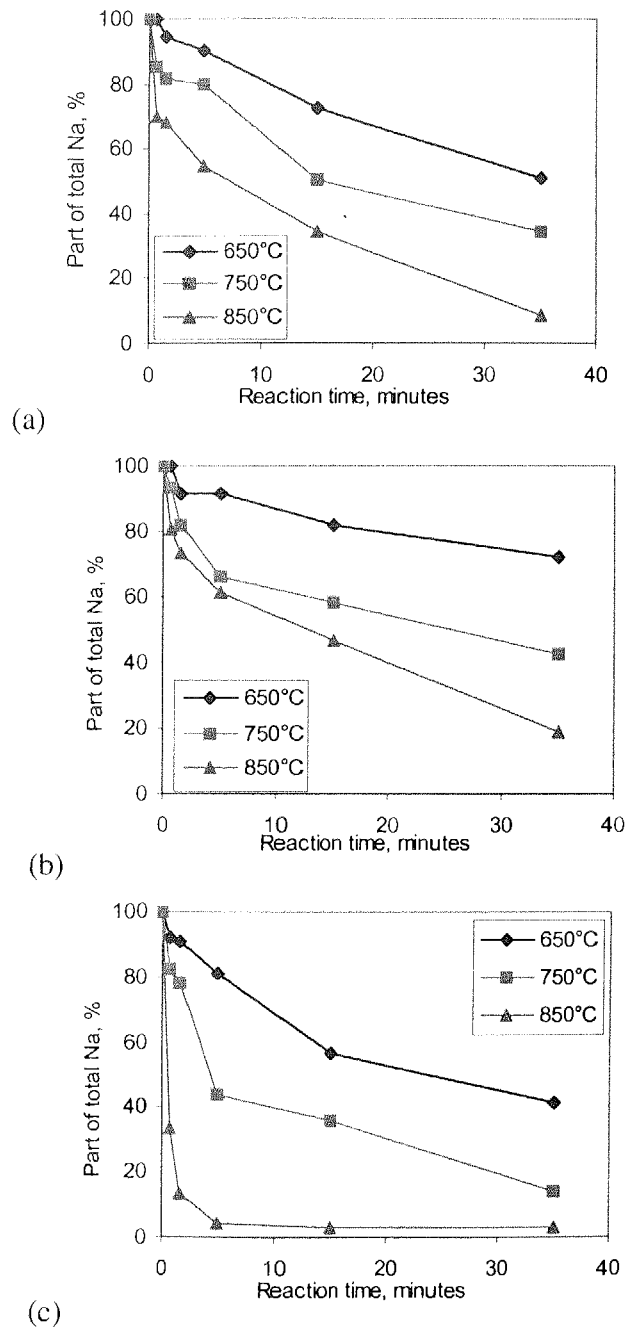


Figure 7.7 Combined sodium soluble in cold, hot and superheated water as part of total initial sodium present in KNC mixture exposed at 650°C, 750°C and 850°C to (a) carbon dioxide, (b) nitrogen and (c) steam atmosphere presented as a function of reaction time.

The results in Figure 7.7 show a steady reduction of soluble sodium in post-reaction KNC mixtures as reaction time increased. This steady reduction is characteristic for all of the results, with the exception for 850°C steam results. The 850°C steam results were very similar to the results for KAC mixtures (Figure 7.1 and 7.2), which showed not much

change in sodium solubility after short reaction times for all experimental temperatures and environments. That was a result of a fast reaction between sodium carbonate and kaolinite.

The KNC mixture results show that reaction between sodium chloride and kaolinite is a slow process, particularly in dry gas atmosphere. But also in steam, at temperatures below sodium chloride melting point, the reaction between sodium chloride and kaolinite is a slow process. Partial evaporation of sodium chloride from KNC mixtures can be expected, although according to Jackson (1963) at atmospheric pressure sodium chloride partial vapour pressure at 750°C would be only 0.2 torr and 1 torr at 850°C.

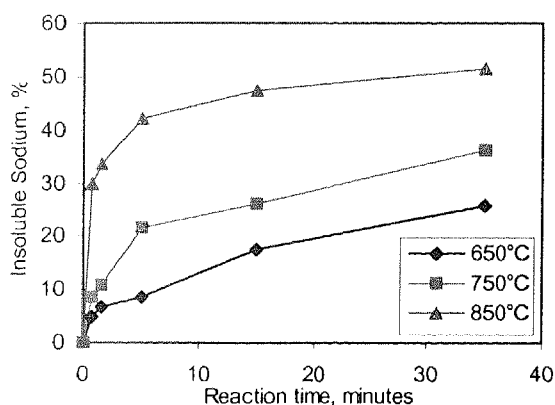


Figure 7.8 Insoluble sodium as part of total initial sodium present in KNC mixture exposed to steam at 650°C, 750°C and 850°C and presented as a function of reaction time.

At 850°C reaction between sodium chloride and kaolin would be a liquid-solid reaction, and much faster than at 750°C. The results for steam environment particularly show a fast disappearance of soluble sodium, resulting in formation of insoluble aluminosilicates. Figure 7.8 shows, that for steam experiments, up to 50% of sodium was found in post-leaching KNC mixture residue as insoluble sodium. When combining the results in Figure 7.8 and in Figure 7.7(c), it shows that up to 45% of sodium chloride, considering there was no analytical or experimental error, could have evaporated in steam atmosphere from KNC mixture during longer exposure times at 850°C.

Evaporation of sodium chloride from KNC mixture would be higher in steam than in nitrogen, and again higher in nitrogen than in carbon dioxide atmospheres as sodium

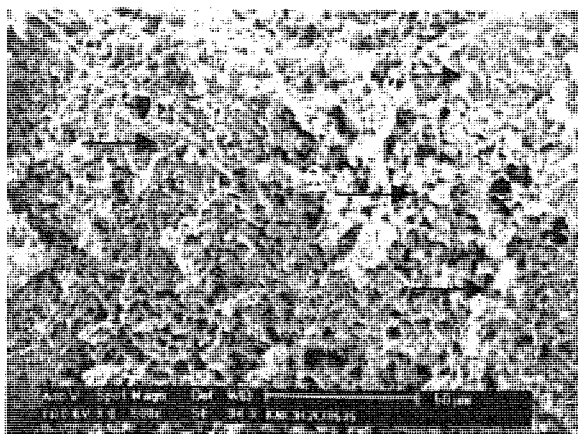
chloride vapours were diffusing into a higher molecular weight gas. The results presented in Figure 7.7 seem to support this conclusion.

The results for KNC mixtures showed that a reaction between sodium chloride and kaolinite resulted in formation of insoluble aluminosilicates already at 650°C. But reactions at 850°C were faster as more than half of sodium reacted into insoluble aluminosilicates. These results are similar to the results quoted above from Botting's et al. (1989) work.

Analytical results for silica do not indicate any formation of sodium silicates within KNC mixtures in steam atmosphere.

7.5.2 Microscopic examination

Electron microscopic SEM examinations were carried out on KNC mixtures exposed at 850°C to all test atmospheres to examine morphology of samples and carry elemental analysis. All examined samples were soft, showed no fusion, although became consolidated. Example micrograph of 850°C sample exposed to steam has been shown below in Figure 7.9. Analysis of sample surface shows almost no presence of sodium chloride and level of sodium oxide concentration in formed aluminosilicates similar to equivalent KAC and NAIK samples.



Analyses, wt. %:	NaCl	Na ₂ O	Al ₂ O ₃	SiO ₂
1	0.4	12.8	40.6	46.2
2	0.0	12.2	38.9	48.9
3	0.2	14.2	38.2	47.4
4	0.2	9.1	40.7	50.0

Figure 7.9 Morphology of KNC mixture exposed to steam atmosphere at 850°C for 35 minutes.

Spot random surface analyses of other examined samples showed significant residue of sodium chloride in shorter reaction time samples. But as average results presented in Table 7.5 show, with an increase of reaction time the concentration of sodium chloride has been

reduced, and that of sodium reacting into aluminosilicates have increased. Long exposure time samples, particularly steam sample, showed almost total disappearance of sodium chloride. These results are in a very good agreement with solubility results and confirm reaction of sodium chloride with kaolin in all atmospheres.

Table 7.7 Results of SEM-EDAX analysis of sodium chloride and kaolin KNC mixture exposed to carbon dioxide, nitrogen and steam atmosphere at 850°C.

Reaction time, minutes	Average concentration in spot analyses, % wt.			
	NaCl	Na ₂ O	Al ₂ O ₃	SiO ₂
Carbon dioxide atmosphere				
0.75	26.1	10.9	27.1	35.9
5	9.7	7.7	35.5	47.1
35	1.2	6.1	40.3	52.3
Nitrogen atmosphere				
1.5	34.8	11.8	23.1	30.3
5	10.4	6.7	35.5	47.4
35	2.4	4.1	39.3	54.2
Steam atmosphere				
35	0.2	12.1	39.7	48.2

Concentration of sodium chloride in any spot analysis was derived from elemental analysis of that spot and any sodium present was first attributed to the presence of chlorine in the same spot, and then shown as sodium chloride, with remainder of sodium attributed to sodium oxide participating in formation of aluminosilicates.

7.5.3 Mineralogical examination

Mineralogical results of X-ray diffraction analysis for chosen KNC mixture samples from experiments at 850°C, identified sodium aluminosilicates carnegietite and paragonite in 35 minutes steam sample. No sodium chloride has been identified in that sample. These results do not exclude formation of aluminosilicates in other conditions, as they may have not developed crystal structure, which would be detected by used technique.

As it has been found earlier for KAC mixtures, it appears that sodium aluminosilicates formed in steam environment from sodium chloride and kaolin crystallise into carnegietite rather than nepheline structure and into paragonite structures.

7.6 PYROLYSIS AND GASIFICATION OF COAL CONTAINING KAOLIN AND SODIUM CHLORIDE

A specially prepared NC1K coal sample containing 10% kaolin and 1.1% sodium as sodium chloride was used in gasification in carbon dioxide or steam and in pyrolysis in

nitrogen experiments conducted at 650°C to 850°C to investigate reaction between sodium chloride and kaolin, taking place within coal char.

From KNC results it has been concluded that sodium chloride-kaolin reaction is a solid state reaction below sodium chloride melting point of 801°C and liquid-solid reactions at 850°C regardless the atmosphere, in which experiments were conducted.

In Chapter 5 in Section 5.4.1 were presented results on volatilisation of sodium and chlorine from coal. Those results showed that during gasification and pyrolysis at 850°C losses of sodium from coal were at 40% to 50% lower than losses of chlorine, which could be higher than 90%.

7.6.1 Chemical Analyses of Char

Guided by the results of reaction between sodium chloride and kaolin for KNC mixture, an emphasis was on the steam gasification char samples and concentration of soluble sodium in those chars. Analyses of staged water leachates of NC1K coal char samples obtained during gasification with steam were carried out for sodium to assess its retention in the char. Results of steam char leaching, which include cold, hot and superheated water leaching, are presented in Figure 7.10. These results show, that during gasification with steam at 850°C less than 40% of the initial sodium was leached out in stage water leaching.

In Chapter 5 Figure 5.9 showed sodium losses during gasification of NC1 coal, which contained similar level of sodium chloride as the NC1K coal. The proportion of sodium, which was retained in that NC1 char, when looking to it as complementing the lost sodium, was higher, than the proportion of sodium leached from NC1K chars from steam gasification. Assuming that the same proportion of sodium volatilised from either char, comparison of results for sodium retained shows that for NC1K steam chars for longer reaction times at all experiment temperatures up to 20% of sodium would react into aluminosilicates. That part of sodium was not leached from the char. If any of sodium was leached from the formed aluminosilicates, as it was shown for KAC samples, the amount of formed aluminosilicates would be yet higher.

Distribution of kaolin and sodium chloride throughout the char would limit such intimate contact between them as in KNC mixture. Therefore finding, that at least 20% of the total

initial sodium forms aluminosilicates in reaction with kaolin corresponds well to results for KNC mixture, which were approximately twice higher. It also definitely shows that kaolin can absorb not only sodium originally organically-bound to coal structure but also it can react inside the char with sodium chloride. This could prevent sodium chloride from reaction with silica during gasification of coal containing all those minerals.

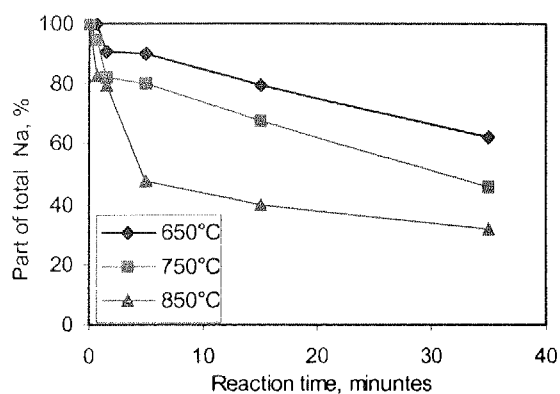


Figure 7.10 Combined sodium soluble in cold, hot and superheated water as part of total initial sodium present in NC1K coal gasified with steam at 650°C, 750°C and 850°C presented as a function of reaction time.

The water solubility results seem to confirm formation of aluminosilicates with up to 20% of sodium engaged into such forms. But these results are far from thermodynamic predictions for equilibrium conditions, which suggest that almost all of the sodium under steam conditions would form aluminosilicates, mostly of nepheline composition. The predictions were not realised in the practical conducted experiments.

7.6.2 Mineralogical examination

Results of XRD mineralogical analysis showed the presence of aluminosilicate $\text{Na}_2\text{O} \cdot \text{Al}_2\text{O}_3 \cdot 2\text{SiO}_2$ in its mineralogical form of nepheline as a trace phase and in the form of carnegietite as the minor phase in the 15 minutes, 850°C steam gasification char sample.

There were again no indications of any presence in any sample of albite $\text{Na}_2\text{O} \cdot \text{Al}_2\text{O}_3 \cdot 6\text{SiO}_2$.

7.6.3 Microscopic examination

SEM examinations of NC1K coal gasification and pyrolysis chars were carried out to establish formation of any aluminosilicates within coal char. Cross sections of number of

samples were examined and back-scattered electron images were recorded. The ash material formed within char was based on kaolin introduced to coal; it was examined for sodium, chlorine, silicon and aluminium.

Representative cross-section images of 850°C pyrolysed and carbon dioxide gasified chars are presented in Figure 7.11. Chars from gasification with steam at 750°C and 850°C are shown in Figure 7.12. Micrographs in Figure 7.11(a) and Figure 7.11(b) clearly show that there was no formation of ash on the char surface either during pyrolysis or during gasification. These, and all other micrographs shown in this work, show that during gasification or pyrolysis, ash had formed uniformly within the whole volume of char particles.

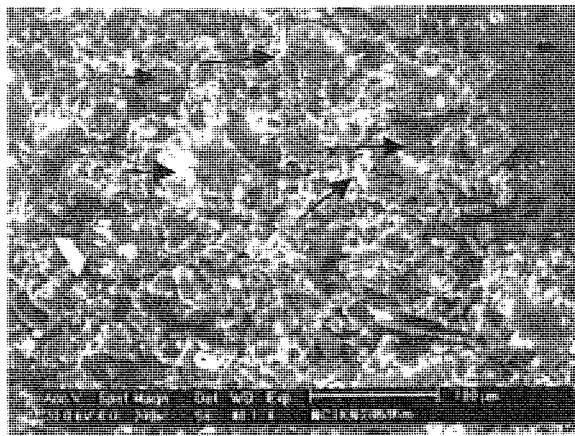
Pyrolysis char still shows a fair content of sodium chloride within the carbonaceous matter of the char, while in the ash only a residue amount of sodium chloride is present. Concentration of sodium in NC1K coal samples gasified with carbon dioxide was at similar level as in pyrolysed char. On average there was a residue of 2% of sodium chloride in the ash. Sodium oxide constituted approximately 5% of the mass of formed aluminosilicates.

These results suggest a low reaction yield between sodium chloride and kaolin during pyrolysis or gasification in carbon dioxide. This would be due to the low concentration of water able to participate in the reaction between kaolin and sodium chloride in accordance with proposed reaction scheme (Reaction 7.6).

Similar results for pyrolysis and gasification in carbon dioxide suggest the formation of the same type of products. The thermodynamic prediction for the formation of nepheline during gasification in carbon dioxide and not during pyrolysis was not confirmed as it formed in both atmospheres.

Char gasified in steam at 750°C as shown in Figures 7.12(a) showed the same level of sodium concentrations in the formed aluminosilicates as for char gasified in carbon dioxide at 850°C. Char from steam gasification at 850°C showed on average 9% sodium oxide concentration in aluminosilicates, nearly double of that under gasification conditions in carbon dioxide. These sodium values for NC1K chars gasified in steam are lower than the

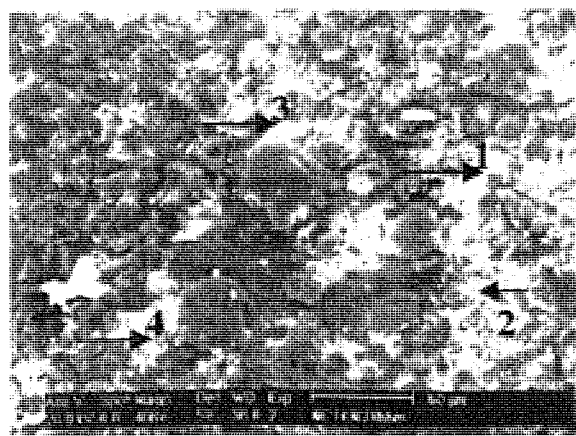
values of sodium analysed in corresponding KNC samples. They were also lower than in NAIK samples, in which on average sodium oxide was 11.3% of aluminosilicates mass.



Analyses, wt. %:	NaCl	Na ₂ O	Al ₂ O ₃	SiO ₂
1	14.8	14.6	35.4	35.2
2	2.3	6.1	35.0	56.7
3	2.8	7.0	36.9	53.3
4	34.6	15.0	33.7	16.7
5	0.0	18.5	37.2	44.3



Analyses, wt. %:	NaCl	Na ₂ O	Al ₂ O ₃	SiO ₂
1	1.8	4.4	39.5	54.3
2	2.7	5.5	33.1	58.7
3	1.6	5.2	33.9	59.3
4	8.3	8.1	32.7	51.4
5	8.0	4.4	26.7	60.8

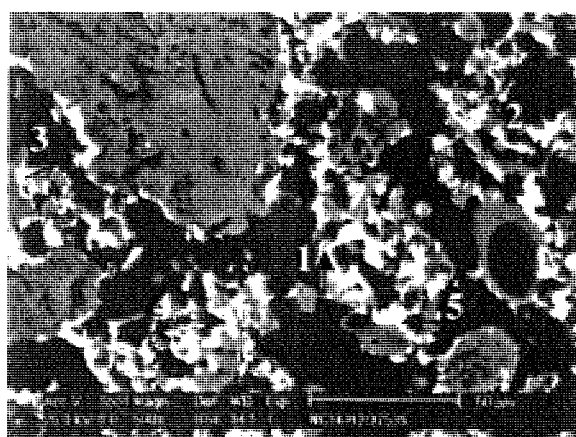


Analyses, wt. %:	NaCl	Na ₂ O	Al ₂ O ₃	SiO ₂
1	1.7	4.1	38.9	55.3
2	2.3	4.0	38.8	54.9
3	2.4	5.1	32.9	59.6
4	1.2	5.2	33.6	60.0

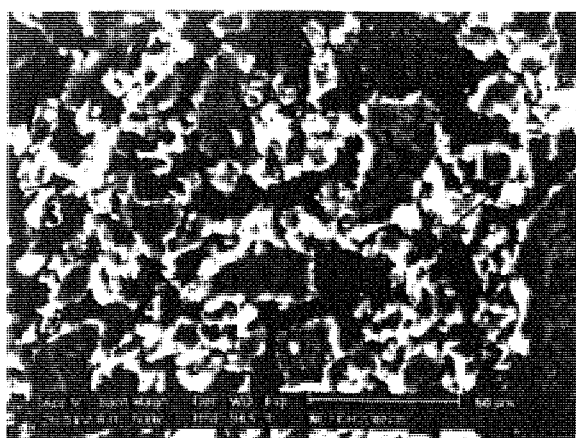
Figure 7.11 Micrographs of SEM back-scattered electron images of char of NC1K coal (a) pyrolysed in nitrogen and (b) and (c) gasified with carbon dioxide at 850°C for 35 minutes. Images in (a) and (b) show the edges of char particles, while (c) shows inside of char grain.

Concentrations of sodium in aluminosilicates analysed in NC1K chars shown in Figures 7.11 and 7.12, and also earlier in KNC mixtures (Table 7.7 and Figure 7.9), are lower than in aluminosilicate $\text{Na}_2\text{O} \cdot \text{Al}_2\text{O}_3 \cdot 2\text{SiO}_2$ (21.9% wt.), an ideal composition of sodium nepheline. However, they resemble somewhat the composition of that aluminosilicate predicted by thermodynamic calculation to form during gasification with steam.

The SEM-EDAX analysis results are far from the composition of albite $\text{Na}_2\text{O} \cdot \text{Al}_2\text{O}_3 \cdot 6\text{SiO}_2$, where Na_2O represents 11.8%, Al_2O_3 19.5% and SiO_2 68.7% weight of an ideal stoichiometric composition. Thermodynamic calculations predicted formation of liquid albite during pyrolysis and gasification of NC1K coal. No fused phases in NC1K chars or KNC samples examined under SEM could be seen.



Analyses, wt. %:	NaCl	Na ₂ O	Al ₂ O ₃	SiO ₂
1	0.0	5.5	35.9	58.6
2	2.3	0.0	34.9	62.8
3	1.6	4.6	35.2	58.7
4	0.0	6.4	35.5	58.1
5	2.7	4.7	36.3	56.3



Analyses, wt. %:	NaCl	Na ₂ O	Al ₂ O ₃	SiO ₂
1	1.6	10.4	34.0	54.0
2	2.3	8.9	39.8	49.0
3	2.1	9.8	30.5	57.7
4	1.4	5.9	33.2	59.5
5	2.0	6.9	33.3	57.8

Figure 7.12 Micrographs of SEM back-scattered electron images of char of NC1K coal gasified with steam at (a) 750°C and (b) 850°C for 35 minutes.

The formation of one molecule of albite requires an additional four molecules of silica as compared with molecule of nepheline. As it has been shown earlier, in the temperature range of 650°C to 850°C, kaolin forms meta-kaolinite $\text{Al}_2\text{O}_3 \cdot 2\text{SiO}_2$ and there would form no free silica to join into the formation of albite. Therefore, it can be concluded that the formation of albite structure as a product of thermal decomposition of kaolin does not occur in the temperature range of 650°C to 850°C. Consequently, in any environment, as long as there is oxygen to form sodium oxide, or the sodium oxide comes from a source such as sodium carbonate, this sodium oxide along with meta-kaolinite will form a structure in which the aluminium oxide to silica molar ratio is one to two; the same as in meta-kaolinite. Such was the case for all the sodium aluminosilicates minerals identified by XRD in kaolin mixtures with sodium carbonate and with sodium chloride, whether on their own or in coal being exposed to temperature range of 650°C to 850°C.

The above discussion illustrates the limitations of applying thermodynamic calculations to situations where given mineralogy of components in a practical system is not exactly copied in thermodynamic calculations by taking into account elemental or molecular composition of a system.

From all the results analysed, it leads to the conclusion that in principle, the same type of sodium aluminosilicate ($\text{Na}_2\text{O} \cdot \text{Al}_2\text{O}_3 \cdot 2\text{SiO}_2$) is formed during pyrolysis and gasification of coal regardless whether the reaction is between sodium chloride and kaolin or between sodium carbonate and kaolin. The yields and thus reaction rates were higher under steam gasification conditions, while under pyrolysis or gasification in carbon dioxide, less sodium reacted into aluminosilicates. The formation of $\text{Na}_2\text{O} \cdot 3\text{Al}_2\text{O}_3 \cdot 6\text{SiO}_2$ paragonite structure has been also confirmed under steam gasification conditions.

Results for NC1K coal are very similar to the results for KNC mixtures. This is similarly the case for results between the NAIK coal and KAC mixture. The chemistry of reactions and the products formed is the same in the mixtures as is in coal chars. The initial reactants: sodium chloride or sodium carbonate and kaolin were more dispersed in coal samples than in the mixtures and had a reduced contact surface area. These factors had an effect on reaction rates, but not on the type of products formed.

7.7 SUMMARY

The following conclusions are drawn from the pyrolysis and gasification of NA1K coal containing kaolin and organically-bound sodium and of KAC mixtures of kaolin and organically-bound sodium exposed to nitrogen, carbon dioxide and steam in the temperature range between 650°C to 850°C.

1. Kaolinite, $\text{Al}_2\text{O}_3 \cdot 2\text{SiO}_2 \cdot 2\text{H}_2\text{O}$, the principal mineral of kaolin, undergoes thermal decomposition to meta-kaolinite $\text{Al}_2\text{O}_3 \cdot 2\text{SiO}_2$ with the preservation of its hexagonal crystal structure.
2. Sodium carbonate formed from organically-bound sodium reacts with meta-kaolinite and interstitial in-filling of sodium oxide into the structure of dehydrated kaolinite takes place. This results principally in preservation of meta-kaolinite hexagonal crystal structure in the formation of a high melting point sodium aluminosilicate $\text{Na}_2\text{O} \cdot \text{Al}_2\text{O}_3 \cdot 2\text{SiO}_2$ nepheline, or its polymorph carnegietite. Increasing the process temperature increases the reaction rate.
3. Gasification under steam conditions of coal containing kaolin and organically-bound sodium results in the formation of more sodium aluminosilicate $\text{Na}_2\text{O} \cdot \text{Al}_2\text{O}_3 \cdot 2\text{SiO}_2$ than under gasification with carbon dioxide or pyrolysis in nitrogen atmosphere.
4. In a steam atmosphere, the liquid-solid reaction between sodium carbonate and kaolin can commence at temperatures below the reference melting point of sodium carbonate of 851°C. It is inferred that in steam, this liquid-solid reaction takes place at 750°C, and probably at 650°C, i.e. steam lowers the sodium carbonate melting point. In a nitrogen or carbon dioxide atmosphere, the reaction between sodium carbonate and kaolin below 850°C is a solid-state reaction, while at 850°C it is a liquid-solid reaction.
5. The results of analyses show that even at 650°C, which is a low temperature from coal gasification or combustion point of view, the sodium carbonate and kaolin reaction is rapid under steam, and occurs more slowly carbon dioxide or nitrogen.

6. Reaction between kaolin and organically-bound sodium present in the coal will be more effective, whether at 650°C or at 850°C, under gasification with steam than under gasification with carbon dioxide. This reaction leads to the formation of aluminosilicate material, which appears dry and does not undergo fusion in the reaction environment. This is regardless whether this is a liquid-solid or solid-solid reaction.
7. No sodium silicates formed during exposure to high temperatures of kaolin and organically-bound sodium mixtures, or during the pyrolysis or gasification of coal containing such components. No evidence of any fused silicate material was established. However, research into reactions between sodium carbonate and mixtures of kaolin and silica would be of value.
8. All results presented for gasification and pyrolysis of NAIK coal are in good agreement with results for kaolin and organically-bound sodium (sodium acetate) KAC mixtures.
9. The above observations may have their consequences during coal utilization, including the gasification process. The formation of dry aluminosilicates, principally nepheline, will help avoid the formation of liquid silicates or sulphates and the problems associated with agglomeration and potentially defluidisation of a fluidised bed process.
10. Finding an efficient way of introducing kaolin into a coal structure could reduce problems associated with coal ash agglomeration, due to formation of sulphates during combustion, or, due to formation of silicates during gasification. Also this knowledge of reactions involving sodium and kaolin at lower temperatures would be very important for a pyrolysis/mild gasification process preceding coal combustion or gasification process, such as APFBC process.

The following major conclusions are drawn from pyrolysis and gasification of NC1K coal containing kaolin and sodium chloride and of KNC mixtures of kaolin and sodium chloride exposed to nitrogen, carbon dioxide and steam in the temperature range between 650°C to 850°C.

1. Sodium chloride reacts with kaolin to form the same solid aluminosilicate $\text{Na}_2\text{O} \cdot \text{Al}_2\text{O}_3 \cdot 2\text{SiO}_2$ as during the reaction between sodium carbonate and kaolin. Sodium aluminosilicate $\text{Na}_2\text{O} \cdot \text{Al}_2\text{O}_3 \cdot 2\text{SiO}_2$ has been identified as the principal form of sodium in coal char obtained during steam gasification.
2. The KNC mixture results show that the reaction between sodium chloride and kaolinite resulting in the formation of insoluble aluminosilicates is a slow process, particularly in dry gas atmosphere, but increases with temperature and time. A solid-state reaction takes place at 650°C and 750°C under gasification and pyrolysis conditions.
3. In a steam atmosphere at 850°C , up to 50% of sodium may form insoluble aluminosilicate in a liquid-solid reaction between sodium chloride and kaolin. At temperatures below the sodium chloride melting point of 801°C , the reaction between sodium chloride and kaolinite is a slow solid-state reaction process.
4. Up to 45% of sodium chloride may be vaporised in a steam atmosphere for the KNC mixture during long exposure times at 850°C . A higher vaporisation rate of sodium chloride was found under steam than in nitrogen or carbon dioxide atmospheres, as sodium chloride vapours were diffusing into a lower molecular weight gas.
5. There was no formation during gasification or pyrolysis of coal containing sodium chloride and kaolin of liquid sodium aluminosilicate albite $\text{Na}_2\text{O} \cdot \text{Al}_2\text{O}_3 \cdot 6\text{SiO}_2$. The formation of liquid albite was predicted by thermodynamic calculations.
6. During gasification with steam at least 20% of sodium present in coal as sodium chloride reacted into insoluble aluminosilicates. This result corresponds well with results from experiments with sodium chloride and kaolin mixture.
7. Analytical results do not indicate any formation of sodium silicates within KNC mixtures for a steam atmosphere.

Chapter 8

GASIFICATION KINETICS

8.1 INTRODUCTION

This chapter examines kinetics of gasification, catalytic activity of sodium and the influence of silica and kaolin on the gasification of low-rank coal with steam and with carbon dioxide.

The activation energy for gasification with steam or with carbon dioxide of coal containing various forms of sodium and containing silica or kaolin will be presented.

8.2 MECHANISM OF CATALYTIC GASIFICATION

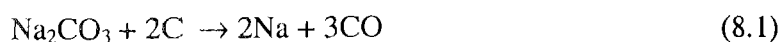
Low-rank coals have a high proportion of macropores, contain high concentration of oxygen-containing functional groups, to which exchangeable metal cations, such as sodium, are attached. Therefore these exchangeable metal cations are highly dispersed within the coal structure. These ions, particularly alkali and alkaline earth cations, act as the catalysts for the gasification reactions. If they are removed from the coal structure, the low-rank coals have reactivity similar to high-rank coals.

The reactivity of lignites such as Lochiel coal is strongly influenced by the presence of catalyst species. It has been widely shown that sodium amongst other alkali and alkali earth metals is a leading catalyst (McKee et al., 1983, 1985; Mims and Pabst, 1983; Kikuchi et al., 1983; McKee, 1983; Sams et al., 1985; Spiro et al., 1983; Suzuki et al.;

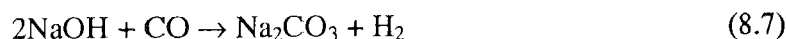
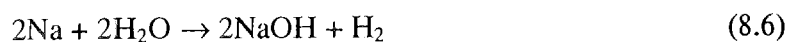
1989, Takarada et al., 1986, 1987, 1991; Yamashita et al., 1991; Matsukata et al., 1992; Ye, 1994; Meijer et al., 1994;).

It is suggested that sodium-catalysed char gasification reactions with carbon dioxide or steam may involve for sodium carbonate and sodium hydroxide as a part of a possible catalytic mechanism (Mims and Pabst, 1983; Kikuchi et al., 1983; McKee, 1983; Wigmans et al., 1983; Suzuki et al., 1989) in accordance with the following reactions:

for Na_2CO_3 :



for steam:



During gasification, Na-O-C bonds in sodium carbonate will be broken in the initial stage of gasification, after which sodium becomes active in a redox cycle. This will involve reduction of sodium carbonate to sodium oxide or to metallic sodium with the release of carbon monoxide.

8.2.1 Catalytic effect of sodium on coal gasification

The results on catalytic effects of sodium on gasification process presented in the literature suggest transformations and various forms of sodium during gasification. Consequently, formation of sodium metal or hydroxide, may lead to the volatilisation of elemental sodium vapour, as shown in Chapter 5. Reactions with coal mineral matter such as silica or clay may also involve the liberated sodium oxide or hydroxide. McKee et al. (1983) report that the catalytic activity of alkali suffered a progressive loss during steam gasification of coal due to reaction of the alkali with mineral matter present in the coal. Ye (1994) studied kinetics of gasification with steam and carbon dioxide of Bowmans coal, a coal very similar in type to Lochiel coal used in the present study. Ye (1994) also investigated catalytic effects of organically-bound sodium and calcium on Bowmans coal gasification

rate and concluded that catalysts increase coal gasification rate several times. Other factors to influence coal reactivity such as porosity and surface area were found by Ye (1994) to be less important in determining the coal gasification reactivity.

Mass balance data collected during experiments has allowed for the assessment of the influence of sodium, silica and kaolin on the rate of coal gasification with steam and carbon dioxide. Examples for carbon conversion as function of time for various studied coals are presented in Figure 8.1 through 8.3. For coal containing only near 1% of organically-bound sodium, the NAI coal, char carbon conversion for gasification with steam was double that of gasification with carbon dioxide and approximately six times higher than carbon conversion of acid washed coal, as shown in Figure 8.1

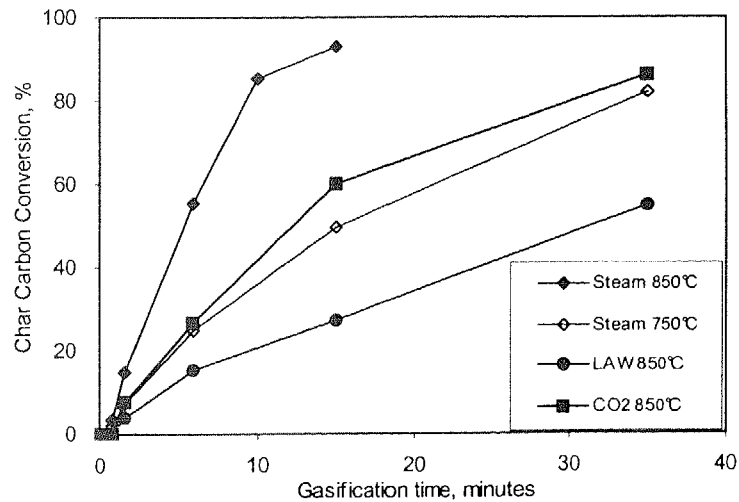


Figure 8.1 Catalytic effect of sodium on char carbon conversion during gasification with steam and with carbon dioxide at 750°C and at 850°C of coal containing 1% organically-bound sodium (NAI coal). LAW designates sodium-free acid-washed low-mineral Lochiel coal used in preparation of NAI coal.

These results show then strong influence of sodium on the gasification rate of coal. Conversion of char, and thus reaction rates, decreased slightly as reaction time increased for the samples studied.

That strong influence of sodium on the gasification rate of coal can be significantly reduced by the presence of silica or kaolin. Results presented in Figure 8.2 show significant drop in char conversion for coals containing organically-bound sodium and containing also silica or kaolin. The NAI coal shows 50% conversion at 850°C after 5

minutes of gasification with steam. The same conversion for NA1K coal containing similar quantity of organically-bound sodium and some 10% kaolin is achieved after 35 minutes and for NA1S coal containing 10% silica after approximately 30 minutes.

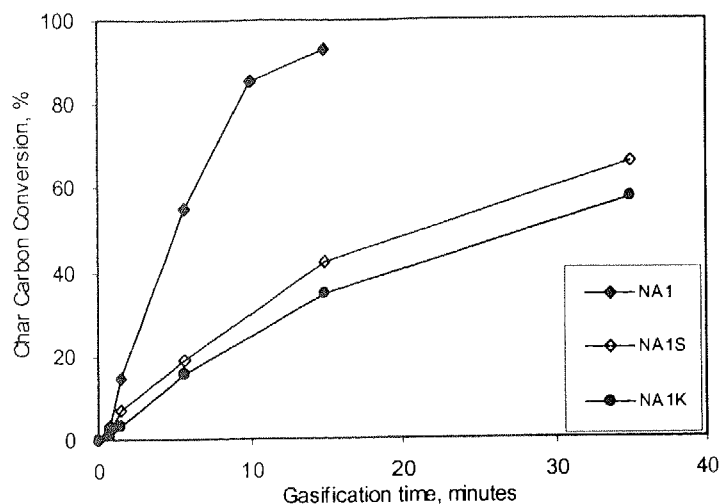


Figure 8.2 Char carbon conversion during gasification with steam at 850°C of NA1 coal containing 1% of organically-bound sodium, NA1S coal containing 1% organically-bound sodium and 10% silica and NA1K coal containing 1% organically-bound sodium and 10% kaolin.

These results clearly show that the presence of silica or kaolin in coal will, due to their reactions with sodium, significantly reduce char conversion and thus the rate of char gasification. Formation of silicates, as shown in Chapter 6, and of aluminosilicates, as shown in Chapter 7, results then in sodium species, which do not offer the same catalytic effect on char gasification as organically-bound sodium. Kaolin appears to be a greater inhibitor of sodium catalytic effect than silica.

Sodium present in coal in the form of sodium chloride does not offer the same catalytic effect as organically-bound sodium. When comparing results for gasification of NA1 coal, as shown in Figure 8.1, with results for NC1 coal, the coal containing sodium chloride, presented in Figure 8.3, it becomes clear that much longer gasification time is need for coal with sodium chloride to achieve the same carbon conversion as for coal containing equal amount of organically-bound sodium.

High char conversion for NC1 coal was achieved after almost three and a half times longer gasification time in comparison with char conversion results for NA1 coal. Catalytic activity of sodium present in coal as sodium chloride can be explained on the basis that

part of that sodium is transformed, through reactions with coal hydrogen, into organically-bound form and consequently, during pyrolysis or gasification, forms sodium carbonate, which is believed to take part in catalytic gasification of coal. It has been shown in Chapter 5 that sodium carbonate was present in pyrolysis and gasification chars of coal originally containing only sodium chloride.

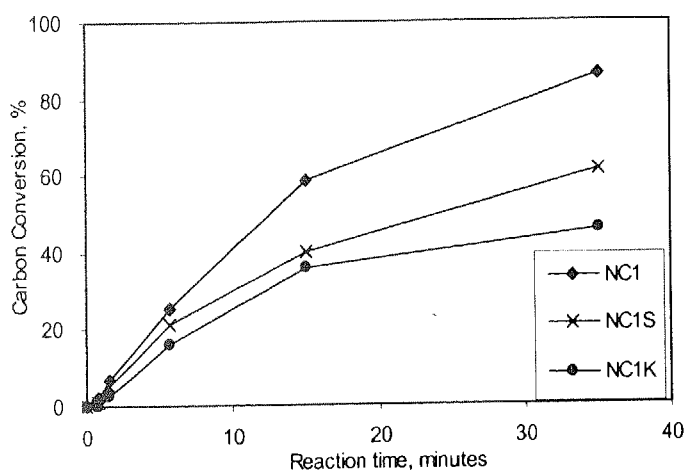


Figure 8.3 Fixed carbon conversion as a function of time during gasification with steam at 850°C of NC1 coal containing sodium chloride, NC1S coal containing sodium chloride and silica and NC1K coal containing sodium chloride and kaolin.

The presence of silica and of kaolin in coal containing sodium chloride will also result in the reduction of sodium catalytic ability and, consequently, of char conversion. Results in Figure 8.3 show, as it has been the case with organically-bound sodium, that kaolin reduces this ability more than silica.

8.3 GASIFICATION KINETICS OF COAL

The experimental work, as presented in Chapter 4, was designed to obtain data for both, pyrolysis and gasification, the two consecutive steps in a process of gasification of coal. Pyrolysis is a fast process, but gasification of char is a much slower process. Kinetic studies on the gasification of the char with agents such as steam and carbon dioxide are of great significance and importance.

In numerous studies reported in the literature on the gasification and kinetics of post-pyrolysis coal char, various theoretical solutions and models have been developed to describe the gasification process (Kwon et al., 1988; Shufen and Ruizheng, 1994; Ye,

1994; Poeze and Zhang, 1996;). Amongst the many models, the most often used for validation is the *Shrinking-core* model or the *Homogeneous* model. The Shrinking-core model considers that the reaction will occur at the external surface of char particle, and as reaction progresses, an ash layer is formed on the surface, leaving a shrinking un-reacted core. The Homogeneous model assumes uniform solid-gas reaction throughout the volume of char particle with constant particle diameter and decreasing density.

Application of a mathematical model to the gasification process may allow determination of the rate of reaction and hence activation energy. Ye (1994) reported that the gasification rate of Bowmans coal was independent of particle size and that up to 850°C gasification followed the Homogeneous model with carbon dioxide or steam gasification being controlled by kinetics of the chemical reaction. Above 850°C diffusion rate and chemical reaction are combined in controlling gasification process.

Examination with SEM of many char particles from experiments conducted in this work did not indicate any evidence of ash formation on the char surface. Char particles contained ash uniformly distributed within the whole volume. Although it was not a particular aim of the investigation, attention was always paid to the porosity of formed chars. It has been noted that with increased temperature and reaction time, macropores of char particles increased.

On the basis of those observations and the results reported by Ye (1994), it was considered that the Homogeneous model would be more suitable to define the rate-controlling factor for char gasification. The Homogeneous model was thus chosen to describe the gasification reaction and to assess reaction rates of gasification and to help in the determination of coal activation energies for those reactions. The principal equation for the Homogeneous model according to Levenspiel (1979) for uniform reaction throughout char particle for the relationship between carbon conversion and reaction time is

$$\frac{dX}{dt} = k(1 - X) \quad (8.8)$$

or in a logarithmic form

$$-\ln(1 - X) = kt \quad (8.9)$$

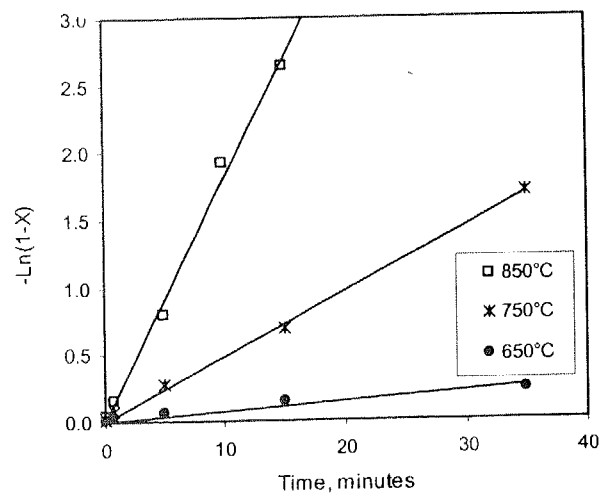
where:

k - first-order reaction rate constant, min^{-1} ,

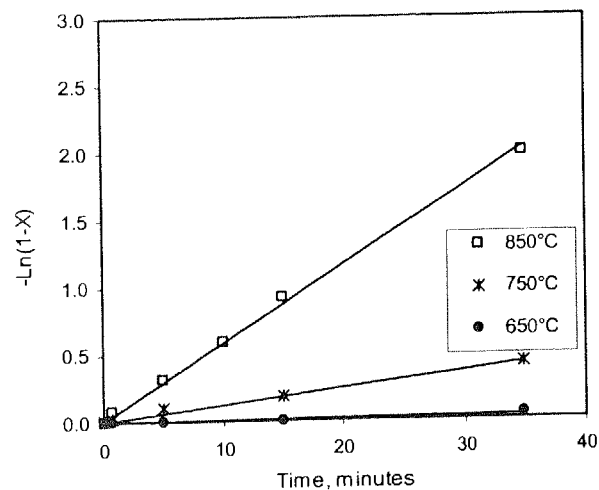
t - reaction time, minutes

X - fractional conversion of solid reactant, (carbon char).

The carbon conversion data shown in the previous section can then be plotted for this logarithmic equation and rate constant for gasification reactions can be found from linear fits. An example presented in Figures 8.4 shows the relations between carbon conversion and time for C-steam and C-CO₂ reactions.



(a)



(b)

Figure 8.4 Char carbon conversion data plotted for different temperatures according to Homogenous model for gasification with (a) steam and (b) carbon dioxide of coal containing 1% of organically-bound sodium (NA1 coal).

The correlation coefficient, r^2 , signifying the relative statistical best fit of the data with the Homogenous model equation was in most cases greater than 0.99 for data shown in Figure 8.4, and for other coals results not presented graphically here, with exception for data for 650°C reactions when this coefficient values were greater than 0.85. It comes as no surprise as char conversion at that temperature was very low, particularly for the shorter reaction times and in the vicinity of experimental error.

Rates of gasification of the NA1 coal char for C-steam and C-CO₂ reaction are then presented in Table 8.1. For the temperature range of 650°C to 850°C steam gasification has been found nearly 3 to 8 times faster than gasification with carbon dioxide. An increase in gasification temperature increases C-CO₂ reaction rate more than the C-steam reaction. These results show also that the carbon gasification reaction is sensitive to temperature variations, which suggests that the chemical reaction rate is the controlling step. It can therefore be said, that under experimental conditions for coal gasification in the fixed bed, the external and internal diffusion effects were negligible and chemical reaction was the rate-controlling step.

Table 8.1 Reactivity values for gasification in steam and in carbon dioxide of NA1 coal.

Temperature:	650°C	750°C	850°C
$k_{\text{Steam}}, \text{min}^{-1}$	0.0071	0.0484	0.180
$k_{\text{CO}_2}, \text{min}^{-1}$	0.00093	0.0121	0.0579
$k_{\text{Steam}} / k_{\text{CO}_2}$	7.6	4.0	3.1

The determination of the reaction rate constant k then allows for the evaluation of the coal activation energy in accordance with Arrhenius equation:

$$k = k_0 \exp(-E_a/RT) \quad (8.10)$$

or

$$\ln k = \ln A - E_a/RT \quad (8.11)$$

where: E_a is coal activation energy.

For the same NA1 coal containing only organically-bound sodium Arrhenius plots are presented in Figure 8.5 showing the dependence of the carbon gasification rate on temperature.

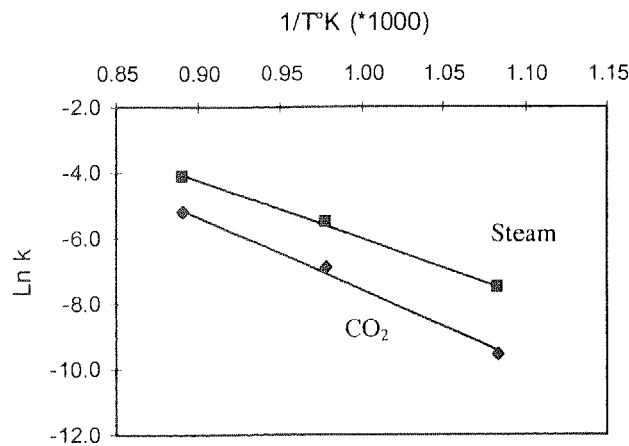


Figure 8.5 Arrhenius plot of reaction rate constants on gasification with steam and carbon dioxide of NAI coal containing 1% of organically-bound sodium.

Rate of gasification can then be explained by the activation energy E_a of reaction. The lower the activation energy, the higher is the gasification rate. The activation energy E_a values are thus the slope of the line fitting the experimental data according to Equation 8.10. The activation energy values for all the coals used in the experiments are tabulated below in Table 8.2, and for ease of comparison are also presented in Figure 8.6.

Table 8.2 Activation energy for gasification reactions with steam or with carbon dioxide of coal containing controlled form and amount of sodium and silica or kaolin and prepared from acid-washed low-mineral Lochiel coal.

	Coal	NAI	NAIS	NAIK	NCI	NCIS	NCIK
Gasification in Steam	E_a , kJ/mol	148.1	161.6	162.4	230.0	236.7	232.3
Gasification in Carbon dioxide	E_a , kJ/mol	187.3	200.1	195.8	242.5	246.8	242.6

The above results show that not only reactivity of coal but also activation energy is affected by

- 1) the presence of sodium in the coal,
- 2) the form of sodium present and
- 3) the presence of minerals that interact with sodium.

Coal containing organically-bound sodium shows activation energy for the gasification reaction with carbon dioxide as approximately 25% higher than for gasification with steam. However, for coal impregnated with sodium chloride, the activation energies

increase substantially and are in much more narrow range. Both silica and kaolin significantly impact on the activation energy for both gasification reactions for coal containing organically-bound sodium and to a much lesser extent on coal containing sodium chloride. This appears to be associated with the catalytic activity of the particular form of sodium and its reactions with silica and kaolin resulting in formation of silicates and aluminosilicates.

Low-rank coals typically have higher levels of alkali or alkali earth elements present. These elements catalyse coal gasification, increase coal reactivity and rates of reaction. Low-rank coals activation energies are in the range 92 to 135 kJ/mol, while for high rank coals, which have low reactivity, activation energies are relatively high, for given example coals in range from 219 to 233 kJ/mol (Poeze and Zhang, 1996).

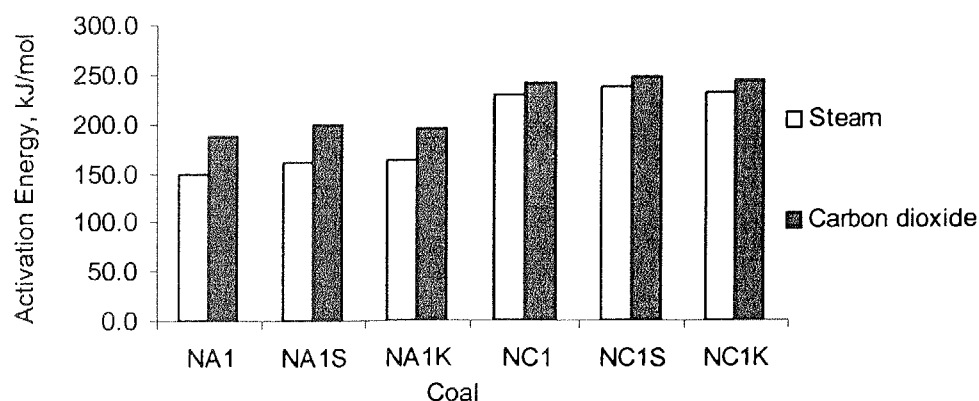


Figure 8.6 Activation energy for gasification reactions with steam or with carbon dioxide of coal containing controlled form and amount of sodium with silica or kaolin, as prepared from acid-washed low-mineral Lochiel coal.

Table 8.3 presents, for comparison, the results of current work and of other researchers studying gasification kinetics of Australian lignites. Ye (1994) conducted gasification experiments in a fluidised single-particle bed. Poeze and Zhang (1996) used thermogravimetric equipment in their work. The Bowmans coal used by Ye (1994) contained on average (dry basis) 0.7% calcium and 1.35% sodium, of which nearly 60% could be considered as being in the form of sodium chloride.

Taking into account that calcium is considered a stronger catalyst than sodium the results of current work compare well with both Ye (1994) and Poeze and Zhang (1996) results,

confirming that the experimental method chosen for investigation of gasification of coal was appropriate. Further, results for NC1 coal and NC1S and NC1K coals, which were impregnated with sodium chloride, were in a narrow range of between 230 to 247 kJ/mol for both steam and carbon dioxide reactions, both of which compare favourably with Poeze and Zhang (1996) results of 252 kJ/mol for demineralized Lochiel coal.

Table 8.3 Activation energies for gasification reactions with steam or with carbon dioxide for South Australian coals as reported in literature in comparison with current work.

Work by	Coal	Sodium form/sodium, calcium concentration	Gasification Atmosphere	Activation energy, kJ/mol
Ye, 1994	Bowmans, R.O.M.	0.7% Ca 1.35% Na	Steam	131
Poeze and Zhang, 1996	Lochiel, R.O.M.	0.82% Ca 0.6% Na	Carbon dioxide	114
Poeze and Zhang, 1996	Lochiel, demineralised	0% Na	Carbon dioxide	252
Poeze and Zhang, 1996	Lochiel, impregnated with Na ₂ CO ₃	5% Na ₂ CO ₃	Carbon dioxide	115
Current study	NA1	Organically-bound sodium, 0.9% wt.	Steam	148
Current study	NA1	Organically-bound sodium, 0.9% wt.	Carbon dioxide	187

8.4 SUMMARY

This chapter examines kinetics of gasification, catalytic activity of sodium and the influence of silica and kaolin on the gasification of coal with steam and with carbon dioxide. The activation energy for gasification with steam or with carbon dioxide of coal containing various forms of sodium and containing silica or kaolin are reported at atmospheric pressure and at temperatures between 650 and 850°C. The coal gasification rate at a given temperature was modelled by the “homogeneous” kinetic model. This model assumes that the overall rate of gasification is independent of particle size and while the reaction progresses the particle size remains constant, while density decreases.

From the results obtained in this work on the kinetics of the gasification reaction of coal, the following conclusions can be made:

1. Gasification with steam of coal containing organically-bound sodium requires considerably lower activation energy than gasification with carbon dioxide.
2. The steam coal gasification reaction rate at 850°C for coal containing organically-bound sodium was found to be three times faster than for corresponding gasification in a carbon dioxide atmosphere.
3. Activation energy is associated with the catalytic activity of sodium present in the coal.
4. If sodium is present in the form of sodium chloride, activation energies increase substantially over organically-bound form of sodium, as sodium catalytic activity is substantially reduced.
5. Both silica and kaolin significantly impact the activation energies for the coal gasification reactions with steam and carbon dioxide. Such an impact is lower for coal containing sodium in the form of sodium chloride.
6. Both kinetic and catalytic data obtained in this work compare well with data published in the literature, thus confirming that the experimental method chosen for this investigation into the gasification of coal was appropriate.

Chapter 9

GENERAL DISCUSSION

9.1 INTRODUCTION

The work presented in this study has been directed towards achieving a better understanding of the behaviour of low-rank coal inorganic matter, principally the interactions of organically-bound sodium and sodium chloride with silica and kaolin, under conditions representative of a fluidised bed gasification system.

An evaluation of the experimental data obtained from the coal pyrolysis and gasification experiments presented in Chapters 5, 6, 7 and 8 is featured in this chapter. Comparison of a selection of the results from the current study with results studies from the literature is also presented to confirm the validity of the data.

9.2 SODIUM TRANSFORMATIONS

Initial experiments were devoted to establishing the fate of sodium in coal in conditions reflecting fluidised bed gasifier conditions, its transformation from original forms to products, which could or would not participate in reactions with coal minerals such as silica or kaolin. Literature reports were clear on defining sodium carbonate as the form of sodium into which sodium originally present as organically-bound transforms during coal pyrolysis (Murray, 1973; Yamashita et al., 1991). As pyrolysis of coal is the initial process which coal undergoes when exposed to high temperatures this would be also a first

significant process for coal undergoing gasification. Those reports were clearly specific for coals containing low levels of sulphur in them.

Reports for coals with high sulphur content (Manzoori, 1990) on the basis of theoretical evaluations suggested that sodium sulphide might be a product of sodium transformations during pyrolysis. The same was predicted from thermodynamic calculations carried out in this work, as shown in Chapter 4. Examination of pyrolysis and gasification chars by analysing with FT-IR the presence of carbon dioxide in the gases evolved after treating the char with acid, allowed defining sodium carbonate as the form into which organically-bound sodium was transformed. Other analyses especially directed to establish presence of sodium sulphides or sulphates gave definite answer that there was no formation of such forms of sodium in pyrolysis or gasification chars. Telfer (1999) in her recently published thesis arrived at the same conclusion while studying sulphur forms and their transformations during pyrolysis of high-sulphur low-rank coals.

The results of those analyses to establish the forms of organically-bound sodium in post-pyrolysis char of high-sulphur coal showed that it was the same as in chars originating from low-sulphur low-rank coals. Organically-bound sodium at elevated temperature breaks away from coal carboxylic groups and forms sodium carbonate. This finding that sodium carbonate is the principal form of transformed sodium is important for investigation of reactions between sodium present in coal and silicon minerals, silica or kaolin.

9.2.1 Vaporisation of Sodium

Both pyrolysis and gasification of coal resulted in sodium losses from char. This was found for both forms of sodium. The losses of organically-bound sodium were higher during gasification. They were higher when coal was gasified with carbon dioxide than with steam and increased with time and with temperature. Sodium vaporisation from coal gasified at 850°C with carbon dioxide reached 57% after 35 minutes. This result compares well, as presented in Table 5.2, with result of 80% sodium loss during gasification for 1 hour at 840°C with carbon dioxide of Yallourn coal of 0.3% wt d.b sulphur content impregnated with 5% of sodium carbonate as reported by Takarada et al., 1995. The same researchers report for the same coal 35% loss of sodium also at 840°C during 1 hour-long pyrolysis in

nitrogen. The result was similar to the present work of 19% for 35 minutes pyrolysis in nitrogen at 850°C.

Investigations into transformations of sodium were directed also towards transformations during pyrolysis and gasification of sodium chloride present in coal. Particular care was exercised when preparing synthetic coal samples impregnated with sodium chloride to make sure that the sodium was not organically-bound to coal structure. It was achieved by ensuring acidic pH of coal water paste during coal preparation. Sodium chloride was distributed in that coal physically at molecular level, but not chemically through reaction with coal.

On heating, both during pyrolysis and gasification, it was found that there was a disproportionate release of chlorine and sodium from char. Release of both elements increased with increase of temperature and initially with time. At the highest experiment temperature of 850°C 70% of chlorine was lost from coal char after 1.5 minute of pyrolysis or gasification. The comparable result of 62% chlorine loss at 830°C has been reported by Manzoori and Agarwal (1992) from pyrolysis experiments of fluidising 5.5 to 9 mm diameter single coal particles. For the same time at 770°C, Manzoori and Agarwal (1992) reported 56 % chlorine loss, while in this work at 750°C 50% chlorine loss was recorded. Sodium volatilisation amounted in the current work to 20% at 850°C and some 10% at 750°C, while Manzoori and Agarwal (1992) report 27% loss at 830 °C and 19% at 770°C. Both sets of results seem to compare reasonably well considering differences in techniques and quantities of coal used in experiments. Manzoori and Agarwal (1992) used low-mineral Lochiel coal in their experiments, the same coal used for preparation of synthetic coals used in this work.

Generally by 850°C chlorine release was 80% complete after 5 minutes of pyrolysis or gasification and near completion after 35 minutes. However, during gasification with steam, more chlorine left the char than during gasification with carbon dioxide. Pyrolysis or gasification reaction times greater than 5 minutes resulted in sodium losses from char approaching half of the value measured for chlorine. This was generally true for all three experimental temperatures investigated of 650, 750 and 850°C.

Evaluation of sodium and chlorine loss results for both pyrolysis and gasification leads to the conclusion that both elements were released partly in the form of sodium chloride and part of chlorine left char as hydrogen chloride. Examination of char samples for any sodium compounds showed that sodium carbonate was present in both pyrolysis and gasification chars. It was concluded that on heating, sodium chloride reacted with coal structure by chlorine engaging with coal hydrogen, including hydrogen from coal carboxylic groups in protonated (acid) form, to form hydrogen chloride.

No other forms of sodium were identified, but it could be assumed that they led to metallic form of sodium, which would be a form in which sodium could easily vaporise from char and be another reason for observing sodium release from coal char during pyrolysis and gasification. If sodium were vaporising from char in this form, then there would be a lower level of direct vaporisation of sodium chloride.

The published results of Takarada et al. (1995) and Manzoori and Agarwal (1992) thus support the findings of this investigation.

9.3 REACTIONS OF SODIUM WITH SILICA

After establishing sodium transformation products, investigations concentrated on the influence of process environment and temperature conditions on reactions of sodium with silica. Literature sources are limited for the reactions of sodium with silica in coal in the temperature range tested in this work. The product of reaction at high temperatures between sodium carbonate and silica is basically silicate glass, which can form a eutectic 73% mole of silica melting at 789°C. A temperature appropriate for operation of a fluidised bed gasifier would be 800 to 900°C and it can be expected that the glass silicates would form at 850°C in reaction of molten sodium carbonate and solid silica. Liquid silicates will form and consequently may be a source of agglomeration of coal ash.

Thermodynamic predictions presented in Chapter 3 showed that in pure steam sodium carbonate will melt at 800°C. Examined literature sources (Song and Kim, 1993; Huttinger and Mingos, 1985) say that steam reduces the standard 851°C melting temperature of sodium carbonate. It could be estimated from Figure 6.1, which incorporates literature data, that in pure steam sodium carbonate melts at approximately 700°C. Such high

reduction of sodium carbonate melting point reduces obviously temperature, at which it will react efficiently with silica in a liquid-solid reaction with a consequence of forming liquid silicates at temperature level substantially lower than those for efficient gasification of coal.

It was shown in Chapter 6 that if silica reacts with organically-bound sodium in any of the tested atmospheres of nitrogen, carbon dioxide or steam, liquid silicates will form at 850°C. The rate of reaction in steam was found to be substantially faster than in carbon dioxide or in nitrogen. However it was also shown that as much liquid silicates form during gasification of coal containing organically-bound sodium with steam at 750°C as when coal is gasified with carbon dioxide at 850°C. The same resulted from experiments with sodium-silica mixtures. This was obviously a consequence of the reduced temperature of melting of sodium carbonate.

Microscopic images in Figure 6.26 show evidence of formation of silicate joints between silica particles, and consequent agglomeration of such particles, inside the char gasified with steam at 750°C, with analysis showing only 2-6% sodium oxide content in these silicates. Looking for comparison of results from gasification with carbon dioxide, the image of char from gasification at 850°C in Figure 6.24(b) clearly shows, despite 100°C higher process temperature, a lesser development of silicate joints between silica particles and yet with lower, 2-3% sodium oxide content.

Both images show significantly lower sodium content in silicates, than for predicted sodium disilicate, but these silicates, with their as low as only 2% of sodium oxide content, have created joints for silica particle inside char. Dynamic conditions of a fluidised bed gasifier will influence the effects of the rheological properties of these silicates, which in turn will influence the process of sintering of ash particles and of formation of agglomerates. Increasing the sodium content in silicates, as happens if gasification of coal is carried out in steam, will according to Falcone (1989), decrease viscosity and surface tension of formed silicates and at the same time will increase their sintering rate. This in turn will enhance agglomeration of gasifier bed material. And therefore, as steam reduces the temperature at which liquid silicates will form, it reduces the temperature at which sintering of ash and agglomeration may commence. Falcone (1989) further states that the reducing atmosphere of a gasifier decreases the viscosity of slag, which will include

silicates. Therefore, the potential for further sintering will be greater for silicates formed under an atmosphere, which contains steam. This may potentially result in significantly higher agglomeration of coal ash in a fluidised bed gasifier at temperature conditions considerably below the temperature conditions at which high char conversion rate would be accepted.

Theoretical predictions for equilibrium in a sodium-silica system during gasification showed that organically-bound sodium and silica present in coal will form only liquid silicates and that all silica will dissolve in those silicates, being principally sodium disilicate. Experimental evidence seems to confirm the fact that part of silica dissolved in the formed sodium disilicate but to far less an extent than predicted. Yet this was established for mineral product mixtures and for gasification with steam at temperature of 850°C, while the predictions were for total solubility of silica during both pyrolysis and gasification at temperature as low as 650°C. Such a significant discrepancy between the results may result from the kinetics of the solubility process, which according to Eitel (1965) is very slow at lower temperatures, and also from limitations on thermodynamic data for silica polymerisation and assumptions of phase activity introduced in calculations (Harb et al., 1993).

Formation of silicates in coal containing sodium chloride has been predicted for coal gasification with carbon dioxide and with steam. However negligible quantities of any silicates were formed during gasification with carbon dioxide, as it is clear that for balance of components of chemical reaction between sodium chloride and silica steam is needed for such reaction to occur. As shown in studies of transformations of sodium chloride during gasification, some sodium carbonate may form during such a process. It is reasonable to expect then, that sodium in such form reacted with silica during gasification with carbon dioxide and formed some silicates, the presence of which was established by solubility analysis.

Silicates formed from silica and sodium chloride during gasification with steam, but at a slower rate than those formed from organically-bound sodium and silica, showing for 850°C gasification conditions higher sodium content silicates than those formed under steam gasification at 750°C. Figure 6.32 provides clear evidence of formation inside the

char of silicate rims around silica grains and of silica particles being joint by silicates into agglomerates.

Evidence of formation inside the char of agglomerates based on silicate matrix and containing several silica particles provides clear proof to the fact that gasification of coal results in formation of ash uniformly throughout char particles and that reactions of gasification also take place thoroughly within particle volume.

The results of this work lead also to a clear confirmation of sodium catalytic activity during the process of coal gasification. They also show that the organically-bound sodium has been found to be a much better catalyst than sodium in the form of sodium chloride. As a measure of that activity, activation energies presented in Table 8.2 show that a coal containing sodium as sodium chloride requires 55% higher activation energy for gasification reaction with steam than the 148 kJ/mol required for coal containing organically-bound sodium.

The presence of silica in coal and its reactions with sodium reduced conversion of char carbon during gasification with steam by more than half, as was shown in Figure 8.2. Silica by its reactions with sodium reduced the catalytic activity of sodium and as a consequence increased the activation energy for gasification reactions of coal. A near 10% increase in activation energy was measured.

9.4 REACTIONS OF SODIUM WITH KAOLIN

Similar reduction of sodium catalytic activity and consequently reduction in conversion of carbon and increase of activation energies for gasification reactions was observed in experiments with coal containing equal forms and quantities of sodium and containing kaolin instead of silica. But the difference in the products of reaction between sodium and kaolin is of considerable importance.

Instead of liquid silicates causing sintering of silica grains at temperature considered probably too low from the point of view of process of gasification of coal, reactions of kaolin and sodium resulted in the formation of dry aluminosilicates even at a temperature of 850°C. Aluminosilicate nepheline, melting above 1250°C, was found as principal

product of reaction. Thermodynamic predictions were for formation of solid nepheline and also for liquid phase of aluminosilicate albite. No fused phases were established in samples examined with microscope. Kaolin has therefore been recognised as a possible inhibitor of reactions of sodium with silica.

It has been experimentally established that reaction between organically-bound sodium and kaolin takes place at temperature as low as 650°C during pyrolysis of coal and during gasification, with at least 50% of sodium reacting with kaolin. Reaction of kaolin with sodium under steam gasification conditions was much more efficient than in carbon dioxide. Literature reports (Falcone and Schobert, 1986) indicate reaction between sodium and kaolin at a temperature of 750°C.

Kaolin hexagonal structure (Deer et al., 1965) on heating transforms into meta-kaolinite with the preservation of its hexagonal crystal structure according to Holdridge and Vaughan (1957). It is inferred that this structure reacts with sodium carbonate (formed from organically-bound sodium) to form nepheline, which also represents the hexagonal structure (Deer et al., 1965); also, that this is a reaction of interstitial filling of sodium oxide into the structure of dehydrated kaolinite.

Sodium chloride also reacted with kaolin to form sodium aluminosilicate nepheline, but at a slower rate than for reactions of kaolin with organically-bound sodium, and again with steam a rate much higher than in carbon dioxide. That is obvious, as again for balance of components of chemical reaction between sodium chloride and kaolin steam is needed to supply hydrogen and oxygen for the formation of hydrogen chloride and sodium oxide, respectively. Increasing the process temperature increased the reaction rate.

Gasification experiments with coal containing sodium and kaolin showed that reactions of sodium with kaolin will produce a solid product of reaction below temperatures at which reasonable rate of reaction between sodium and silica can be expected. Hence, kaolin present in coal will prevent reactions of sodium with silica to form liquid silicates. This may have an important effect on coal ash behaviour during coal gasification as well as during combustion.

9.5 IMPLICATIONS FOR AGGLOMERATION

The results of this work have shown that the inherent sodium and silica in coal can interact during conditions characteristic of a fluidised bed gasifier FBG to produce liquid silicates, which can cause ash agglomeration and potentially result in defluidisation of the bed. The presence of steam will promote the formation of silicates and reduce the limiting temperature of their formation by at least 100°C. The formation of silicates will be more pronounced for coal containing more organically-bound sodium. If coal contains silicon in association with aluminium in mineral kaolin, it has been shown that solid aluminosilicates will form in the reaction between sodium and kaolin.

The formation of dry aluminosilicates, principally nepheline, will help avoid the formation of liquid silicates, or sulphates during combustion, and be a contributing source of avoiding problems associated with agglomeration and potentially defluidisation of a fluidised bed process.

Finding an efficient way of introducing kaolin into the coal structure could reduce problems associated with coal ash agglomeration, due to formation of sulphates during combustion, or, due to formation of silicates during gasification. Also the knowledge of reactions involving sodium and kaolin at lower temperatures would be very important for a pyrolysis/mild gasification process preceding coal combustion or gasification process, such as in the APFBC process

Conducting such a pyrolysis/mild gasification process would minimise the quantity of vaporised sodium in its metallic or chloride form. The volatilisation of sodium chloride or hydrogen chloride will lead to extensive deposition of chlorides in the cooler parts of gasifier plant.

Reactions between sodium and silica in steam significantly reduce the temperature at which liquid silicates are present. The extent of silicate formation is expected to increase with coal particle size due to the increase of gasification time of such particles.

However, a compromise may well need to be found in avoiding the formation of silicates by using kaolin to react with sodium, as carbon reactivity (conversion) may be reduced by

such reactions due to the loss of the sodium catalytic effect. The char reactivity is significantly higher for coal if sodium is present in organically-bound form.

Sodium present in coal can react with kaolin during pyrolysis at temperatures below those typical of FBG or FBC operation. This finding may assist ways of preventing sodium reacting with sulphur and consequent formation of sodium sulphates responsible for agglomeration and defluidisation of FBC beds.

Chapter 10

CONCLUSIONS AND RECOMMENDATIONS

10.1 CONCLUSIONS

Transformations of sodium, reactions between sodium and silica and between sodium and kaolin present in high-sulphur lignite coal were studied under pyrolysis and gasification conditions, for temperatures between 650-850°C, characteristic of a fluidised bed gasifier. The following conclusions are drawn from the results of the work presented in this thesis:

10.1.1 Thermodynamic Studies

Thermodynamic calculations based on Gibbs free energy minimisation for formation of possible sodium and silica reaction products to establish equilibrium composition for given gasification or pyrolysis conditions were conducted. The following are conclusions from results of these calculations:

- Significant influence of gasification atmosphere on transformation of organically-bound sodium has been predicted. Pyrolysis is predicted to result in solid sodium sulphide, while gasification with steam or carbon dioxide results in condensed sodium carbonate.
- Liquid silicates, dominated by sodium disilicate, were predicted to form in each atmosphere from reactions between organically-bound sodium and silica at a temperature as low as 650°C. All the silica was predicted to be dissolved in the

silicates. Reactions of sodium chloride in steam with silica are also predicted to result in silicate-silica melt at 650°C.

- Solid sodium aluminosilicate, nepheline, is predicted to dominate products of reactions between organically-bound sodium and kaolin in each atmosphere. Liquid sodium aluminosilicate, albite, is predicted to contain nearly a third of all sodium.
- Steam exerts the most suppressive effect on sodium chloride vaporisation in its reaction with silica and on formation of liquid phase aluminosilicates in reaction with kaolin.
- Reaction products between sodium chloride and silica or kaolin will depend on gaseous atmosphere.
- Metallic sodium vapour is predicted to form at higher temperatures in nitrogen from organically-bound sodium.

10.1.2 Transformations of Sodium

The following conclusions deal with the physico-chemical transformations of sodium.

- Sodium release was observed during pyrolysis in nitrogen and during gasification with carbon dioxide or steam of coal containing sodium organically-bound to coal carboxylic groups. Sodium volatilisation increased with temperature and time.
- Significantly higher sodium vaporisation was observed during gasification with carbon dioxide or steam than during pyrolysis. For similar carbon conversion, sodium vaporisation was higher during gasification with carbon dioxide than with steam, particularly at 850°C.
- Sodium carbonate forms in char as the principal form of sodium during both pyrolysis and gasification of coal containing organically-bound sodium.
- Sodium sulphide does not form from organically-bound sodium during pyrolysis or during gasification of high-sulphur lignite coal under the conditions tested. Neither sodium sulphide nor sodium hydroxide was identified in pyrolysis or gasification char of coal containing sodium chloride.
- The release of both sodium and chlorine from coal containing sodium chloride is disproportionate. Almost all of the chlorine was released during gasification and pyrolysis at 850°C. The release of sodium was nearly a half of that of chlorine and inferred to be in the form of sodium chloride vapour.

- Sodium chloride reacts with hydrogen present in coal/char and chlorine is released in the form of hydrogen chloride. The identification of sodium carbonate in pyrolysis char confirms the reaction of sodium chloride with hydrogen from the coal carboxylic acid groups.
- The physical status of the char pores and accessibility of sodium, not its actual chemical form(s), can be considered a limiting factor on sodium reactions with coal mineral inclusions such as silica or kaolin.
- Reaction of sodium chloride with free carboxylic acid groups present in ROM coal could enhance formation of ash agglomerates during coal gasification.

10.1.3 Reactions of Sodium with Silica during Gasification of Coal

The following conclusions are drawn from pyrolysis and gasification experiments with specially prepared coals, which contained controlled quantities of silica and forms of sodium.

10.1.3.1 Reactions of silica and organically-bound sodium

- Thermodynamic predictions on liquid silicate formation during gasification of coal containing silica and organically-bound sodium have been only confirmed by results of experiments qualitatively and for the higher temperatures.
- Pyrolysis of coal results in a very low level of formation of silicates, as implied by results of char water leachate analysis and confirmed by the results of microscopic examination. No fused silicates have been identified in any of the pyrolysis char.
- Gasification with steam at 750°C showed the formation of fused glass silicate joints between silica grains. Coal gasification with steam results in the formation of liquid phase silicates at a temperature at least 100°C lower than the corresponding gasification with carbon dioxide as fused glass silicate joints formed between individual silica grains inside char gasified in carbon dioxide at 850°C.
- The composition of liquid silicates formed during gasification of coal with steam at 850°C was found to approach that predicted by thermodynamic calculations. Short gasification times in steam at 850°C resulted in the formation of liquid silicates with sodium oxide concentration exceeding that found in silicates formed under long time gasification with carbon dioxide at 850°C.
- The gasification of coal at 650°C with steam or with carbon dioxide does not result in the formation of liquid silicates as predicted by thermodynamic calculations.

- The formation of ash in coal char during gasification takes place within the whole volume of char particles as formation of silicates around silica particles is established as taking place everywhere within char particles. Liquid silicates create neck joints between the silica particles or form a fused matrix in which silica particles are embedded. The formation of agglomerates of silica particles occurs throughout the whole volume of the char particle.
- It is inferred that during gasification with steam at 750°C a liquid-solid phase reaction between sodium carbonate and silica leads to the formation of liquid silicates. This is as a result of a fact that in a steam atmosphere, sodium carbonate melts at a temperature substantially lower than the standard melting point. The melting temperature of sodium carbonate in a given gasifier environment will be dependent on the steam mass fraction in such environment.
- It is also inferred that dissolution of silica in the formed silicates increases the total mass of the formed liquid glass phase and reduces concentration of sodium in that phase. Thermodynamic prediction of all silica being in a liquid form has not been confirmed by experimental results.
- The results on the formation of silicates during gasification of the tested coal are considered as being in good agreement with the results of examination of post-reaction residues of sodium acetate and silica mixtures.
- The presence of silica does not significantly reduce volatilisation of sodium from coal char during gasification with steam or with carbon dioxide, as nearly 40% of sodium may evaporate during gasification.
- Gasification at 850°C of coal containing silica and organically-bound sodium will result in the formation in liquid-solid phase reaction of liquid silicates regardless of the gasification environment. However the presence of steam in the gasifier atmosphere will reduce the temperature of formation of silicates and therefore increase the tendency for coal ash to agglomerate and influence operation of a fluidised bed gasifier.

10.1.3.2 Reactions between sodium chloride and silica

- The reaction between sodium chloride and silica in fluidised bed gasification can only take place if steam is present in the reaction environment. The reaction is not instantaneous, and is substantially slower than reaction between silica and sodium

carbonate. Formed silicates may have similar characteristics to those formed in reaction between silica and sodium carbonate.

- Sodium chloride and silica react to form fused silicates during gasification with steam at a temperature of 750°C, which is below the sodium chloride melting point. Reaction at 850°C results in the formation of liquid silicates with sodium content lower than in silicates formed in the reaction between silica and sodium carbonate.
- It has been inferred that during gasification or pyrolysis of coal, sodium chloride present in coal will react with coal and sodium carbonate forms. The sodium carbonate in turn will react with silica present in the coal to form sodium silicates.

10.1.4 Reactions of Sodium with Kaolin during Gasification of Coal

The following conclusions are drawn from the pyrolysis and gasification experiments with specially prepared coals, which contained controlled quantities of kaolin and forms of sodium:

10.1.4.1 Reactions of kaolin and organically-bound sodium

- Kaolinite, $\text{Al}_2\text{O}_3 \cdot 2\text{SiO}_2 \cdot 2\text{H}_2\text{O}$, the principal mineral of kaolin, undergoes thermal decomposition to meta-kaolinite $\text{Al}_2\text{O}_3 \cdot 2\text{SiO}_2$ with the preservation of its hexagonal crystal structure.
- Sodium carbonate formed from organically-bound sodium reacts with meta-kaolinite and it is inferred that interstitial in-filling of sodium oxide into the structure of dehydrated kaolinite takes place. This results principally in the preservation of meta-kaolinite hexagonal crystal structure in the formation of a high melting point sodium aluminosilicate $\text{Na}_2\text{O} \cdot \text{Al}_2\text{O}_3 \cdot 2\text{SiO}_2$, nepheline, or its polymorph carnegietite. Increasing the process temperature increases the reaction rate.
- The results of analyses showed that at 650°C sodium carbonate and kaolin reaction was essentially an immediate process under steam, and an efficient reaction in a carbon dioxide or nitrogen atmosphere. Similarly the reaction between kaolin and organically-bound sodium present in coal will be more effective, whether at 650°C or at 850°C, under gasification with steam than with carbon dioxide.
- In a nitrogen or carbon dioxide atmosphere, the reaction between sodium carbonate and kaolin below 850°C is a solid-state reaction, while at 850°C it is a liquid-solid

reaction. In a steam atmosphere, the liquid-solid reaction between sodium carbonate and kaolin can commence below 750°C.

- There was no evidence for the formation of fused aluminosilicate albite nor fused sodium silicates formed during the pyrolysis or gasification of coal containing organically-bound sodium and kaolin.
- Gasification with steam of coal containing kaolin and organically-bound sodium results in the formation of more sodium aluminosilicate $\text{Na}_2\text{O} \cdot \text{Al}_2\text{O}_3 \cdot 2\text{SiO}_2$ than under gasification with carbon dioxide or pyrolysis in nitrogen.
- All results for gasification and pyrolysis of coal containing kaolin and organically-bound sodium are in good agreement with results for post-reaction products of kaolin and sodium acetate mixture.

10.1.4.2 Reactions of kaolin and sodium chloride

- Sodium chloride reacts with kaolin to form the same solid aluminosilicate $\text{Na}_2\text{O} \cdot \text{Al}_2\text{O}_3 \cdot 2\text{SiO}_2$ as during the reaction between sodium carbonate and kaolin. Sodium aluminosilicate $\text{Na}_2\text{O} \cdot \text{Al}_2\text{O}_3 \cdot 2\text{SiO}_2$ has been identified as the principal form of sodium in coal char obtained during steam gasification.
- During gasification with steam at least 20% of sodium present in coal as sodium chloride reacted into insoluble aluminosilicates at all experiment temperatures. This result corresponds well with results from experiments with sodium chloride and kaolin mixture.
- There was no formation of liquid sodium aluminosilicate $\text{Na}_2\text{O} \cdot \text{Al}_2\text{O}_3 \cdot 6\text{SiO}_2$, albite, during gasification or pyrolysis of coal containing sodium chloride and kaolin as predicted by thermodynamic calculations. No formation of sodium silicates was established.

10.1.5 Kinetics of Coal Gasification

From the results obtained in this work on the kinetics of the gasification reaction of coal, the following conclusions can be made:

- The gasification with steam of coal containing organically-bound sodium requires considerably lower activation energy than gasification with carbon dioxide.

- The steam coal gasification reaction rate at 850°C for coal containing organically-bound sodium was found to be three times faster than for corresponding gasification in a carbon dioxide atmosphere.
- Coal activation energy is associated with the catalytic activity of sodium present in the coal. For sodium in coal present in the form of sodium chloride, activation energies increase substantially over organically-bound form of sodium.
- Both silica and kaolin significantly impact the activation energies for the coal gasification reactions with steam and carbon dioxide. Such an impact is lower for coal containing sodium in the form of sodium chloride.
- Both kinetic and catalytic data obtained in this work compare well with data published in the literature.

10.2 RECOMMENDATIONS FOR FUTURE WORK

The results presented here are a contribution to improved knowledge in the area of reactions of sodium with silicon minerals during FBG of high-sulphur, high-sodium low-rank coal. Further work to extend this knowledge is suggested, particularly in the following areas:

- As has been shown in this study reactions of kaolin with sodium result in formation of solid aluminosilicates under FBG conditions. In order to optimise the operating conditions for a FBG system and prevent formation of liquid silicates, ways of efficient introduction of kaolin should be determined.
- The reactions of sodium with both kaolin and silica should be further investigated to determine silica : kaolin ratio on reaction products with various forms of sodium during coal gasification. The effects of temperature and the presence of steam should be investigated. The physical properties of product sodium aluminosilicates should be studied to ascertain how they influence agglomeration and defluidisation.
- The work presented shows formation of fused silicates and their agglomerates deep inside coal particles. Studies could be directed towards determination of a safe cut-off point to carbon conversion before full liberation of the formed ash.
- To extend fundamental knowledge on behaviour of sodium and reactions between sodium and silicon minerals in conditions of FBG it is recommended that a

laboratory study be carried out for systems similar to those in this study exposed to an atmosphere of carbon monoxide.

- Alkali earth elements often present in coal are calcium and magnesium. Experiments should be carried to investigate their effect on the reactions of sodium with silica and kaolin.
- A general model could be developed to quantify the influence of coal properties and gasification conditions on formation of aluminosilicates and silicates.

BIBLIOGRAPHY

Allan, R.J., "Sodium removal from Wakefield Coal" AMDEL Report, p. 1408, July (1981a).

Allan, R.J., "Sodium removal from Wakefield Coal: Stage II" AMDEL Report, p. 1435 (1981b).

Arastoopour, H., Hariri, M. H., Rehmat, A., "Agglomeration in a fluidized bed with a central jet", Fluidization VI, Banff, pp. 563- 570, (1989).

Atogi, O.M., Altenkirch, R.A. and Midkiff, K.C., "Distribution of sulphur in one-dimensional pulverized-coal flames", *Fuel*, 65, pp. 1663-1669 (1986).

Attar, A., "Chemistry, thermodynamics and kinetics of reactions of sulphur in coal-gas reactions: A Review", *Fuel*, 57, pp. 201-210 (1978).

Bachovin, D.M., Alvin, M.A., DeZubay, E.A. and Mulik, P.R., "A study of high temperature removal of alkali in a pressurized gasification system", Final report for U.S. Department of Energy under Contract No.: DE-AC21-83MC20050, by Westinghouse Research and Development Center, Pittsburgh, Pennsylvania, October (1986).

Basu, P., "A study of agglomeration of coal ash in fluidized beds", *The Canadian Journal of Chemical Engineering*, 60, pp. 791-795 (1982).

Beer, J.M., Sarofim, A.F., Barta, L.E., "From properties of coal mineral matter to deposition tendencies of fly ash - a modelling route", *Journal of the Institute of Energy*, 65, pp. 55-62, March (1992).

Bellin, A., Bruck, U. and Schrader, L., "Report on the results of the HTW-pilot plant gasification tests with Bowmans coal", Rheinbraun AG, Report to Department of Mines and Energy, Adelaide, South Australia, April (1987).

- Benson, S.A. and Nowok, J.W., "Gasification ash and slag: Slag properties and ash deposition," Proc. 10. Annual gasification and gas stream cleanup system contractors' review meeting, Morgantown, WV (USA), Ed. Kothari, V.P. and Beeson, J.L., II: pp. 415-424 (1990).
- Bjorkman, E. and Stromberg, B., "Release of Chlorine from Biomass at Pyrolysis and Gasification Conditions," *Energy and Fuels*, 11, pp. 1026-1032 (1997).
- Boll, R.H., and Patel, H.C., "The role of chemical thermodynamics in analysing gas-side problems in boilers", *Transactions of the ASME, Journal of Engineering for Power, Series A*, 83(4), pp. 451-467 (1961).
- Botting, A.J., Hodges, N.J., Richards, D.G. and Wood, F.O., "The influence of mineral interactions upon the behaviour of sodium during combustion," in Proc. Intern. Coal Science Conference, Tokyo, pp. 63-66 (1989).
- Brindley, G. W., In "X-Ray identification and crystal structures of clay minerals", Edited by Brindley, Chapter II, pp.33-75, Mineralogical Society (Clay Minerals Group), London (1951).
- Brinsmead, K.H. and Kear, R.W., "Behaviour of sodium chloride during the combustion of carbon", *Fuel*, 35, pp. 84-91 (1956).
- Brockway, D.J. and Borsaru, R.M., "Ion concentration profiles in Victorian brown coals", Proc. 1985 Int. Conf. Coal Science, Sydney, pp. 593-596 (1985).
- Brockway, D.J., Ottrey, A.L. and Higgins, R.S., "Inorganic constituents" in "The science of Victorian brown coal", R.A. Durie (Ed.), Butterworth, Heinemann, pp. 597-650 (1991).
- Bryers, R.W. and Walchuck, O.R., "Operating experience with a pilot scale combustion facility used for studying slagging and fouling characteristics of coal. Part II - Experimental results.", Third Engineering Conference On Slagging and Fouling Due to Impurities in Combustion Gases. Colorado (1984).

Calkins, W.H., "The chemical forms of sulphur in coal: a review", *Fuel*, 73, 4, pp. 475-484 (1994).

Carthy, R. H., Mason, D. M., Babu, S. P., "Fundamental studies on mineral matter behaviour in ash-agglomerating coal gasifiers", presented at The Third Pittsburgh Coal Conference, pp. 717-729, Sept. 8-12 (1986).

Chou, C.-L., "Distribution and forms of chlorine in Illinois Basin coals," in *Coal Science and Technology*, Vol. 17, Ed., J.Stringer and D.D.Banerjee, Elsevier, New York, pp.11-29 (1991).

Cleyle, P.J., Caley, W.F., Stewart, I. and Whiteway, S.G., "Decomposition of pyrite and trapping of sulphur in a coal matrix during pyrolysis of coal", *Fuel*, 63, pp.1579-1582 (1984).

Davidson, J.F., "Fluidised combustion of solids, gases and mixtures thereof", *Proceedings Engineering Foundation Conference: Fluidization VII*, Eds. O.E.Potter and D.J. Nicklin, pp. 3-14 (1992).

Davidson, J.F., Clift, R. and Harrison, D., (Editors), *Fluidization*, 2nd Edition, *Academic Press*, (1985).

Davies, C.E., Dawson, S.G.B., Fielders, R.B., "An investigation of thermal agglomeration in fluidized beds", *Fluidisation VI*, Banff, (1989).

Daybell, G.N., "The relationship between sodium and chlorine in some British coals.", *Journal Institute of Fuel*, 40, 312 (1967).

Dean, J.A., (Ed.), "Lange's handbook of chemistry - 13th Edition", *McGraw Hill Book Co.* (1985).

Deer, W. A., Howie, R. A. and Zussman, J., "Rock-Forming Minerals" Vol.3, Sheet Silicates, Longmans, (1965).

Deer, W.A., Howie, R.A. Zussman, J., "An introduction to the rock-forming minerals", 2nd edition, Longman, London, (1992).

Domazitis, G., "The chemistry of formation of ash during combustion of brown coal - Part I." State Electricity Commission of Victoria, Research and Development Department, Brown Coal Research Division, Report No. SO/85/91, Project No. 262 (1985).

Douchanov, D. and Angelova, G., "Effect of catalysis and inlet gas on coal gasification", *Fuel*, 62, pp.231-233 (1983).

Douchanov, D., Dolachka, P. and Razvigorova, M., "Interaction of mineral matter of coal with additives during gasification", (Bulgarian Academy of Sciences, Sofia (Bulgaria). Inst. Of Organic Chemistry) *Doklady Bolgorskoj Akademii Nauk*; 45, pp. 17-20 (1992).

Dunderdale, J., Durie, R.A., Mulcahy, M.F.R. and Schafer, H.N.S., "Studies relating to the behaviour of sodium during the combustion of solid fuels", *The Mechanism of Corrosion by Fuel Impurities*, Butterworth, London 139 (1963).

Durie, R.A., "The inorganic constituents in Australian coals. III. Morwell and Yallourn brown coals", *Fuel*, 40, 407 (1961).

Durie, R.A. and Swaine, D.J., "Inorganic constituents in coal", *Coal Research in CSIRO*, 45, pp. 9-19 (1971).

Edgecombe, L.J., "State of combination of chlorine in coal. I- Extraction of coal with water.", *Fuel*, 35, 8 (1956).

Edger, T.F. and Kaiser, W.R., "Resources, properties and utilization of Texas lignite: A Review", in *The Chemistry of Low Rank Coals*, Schobert, H.H. Ed. ACS Symposium Series 264, American Chemical Society, Washington D.C. (1984).

Eitel, W., "The physical chemistry of the silicates", The University of Chicago Press, Chicago, Illinois, (1954).

Eitel, W., *Silicate Science*, Vol. 2; Glasses, Enamels, Slags. Academic Press (1965).

Eitel, W., *Silicate Science*, Vol. 4; Glasses, Enamels, Slags. Academic Press (1966).

Ershov, Yu.B., Meshcheryakov, V.G., and Enyakin, Yu.P., "Formation of hydrogen chloride in the pulverised coal flame when burning coal with a high chlorine content," *Thermal Engineering*, 39, (7), 394 (1992).

Falcone, S., "Ash and slag characterization," *Proc. 9. Annual gasification and gas stream cleanup system contractor's review meeting, Morgantown, WV (USA)* Report no. DOE/MC/10637-89, pp. 230-240 (1989).

Falcone, S.K. and Schobert, H.H., "Mineral transformations during ashing of selected low rank coals", ACS Symposium Series 301, American Chemical Society, Washington D.C. (1986).

Federer, J.I. and Lauf, R.J., "Crystallization behaviour of coal gasification ash," *Nuclear and Chemical Waste Management*, 5, pp. 221-229 (1985).

Frederick, W.J., Huppa, M., Stengberg, J. and Hernberg, R., "Optical pyrometric measurement of surface temperature during black liquor char burning and gasification", *Fuel*, 73, pp. 1889-1893 (1994).

Gale, J.J., Laughlin, K.M. and Lane, G.J., "Modification of a fluidized-bed coal-gasification process to improve carbon conversion" *Journal of the Institute of Energy*, 64, pp. 143-150 September (1991).

Gibb, W.H. and Angus, J.G., "The release of potassium from coal during bomb combustion", *J. Inst. Energy*, 53, pp. 149-157 (1983).

Gluckman, M.J., Yerushalmi, J. and Squires, A.M., "Defluidization characteristics of sticky or agglomerating beds", *Proc. Inter. Fluidization Conf., California, U.S.A.*, 395 (1976).

Gluskoter, H.J. and Rees, O.H., "Chlorine in Illinois coals", Illinois Geological Survey Circ. p. 372 (1964).

Gluskoter, H.J., "An introduction to the occurrence of mineral matter in coal", International Conf. on Ash Deposits and Corrosion from Impurities in Combustion Gases, Engineering Foundation, pp. 3-19 (1977).

Godel, A.A., Rev. Gen. Therm., 5, 349 (1966).

Gow, A.S. and Phillips, J., "Microcalorimetric study of oxygen adsorption on catalytically promoted gasification chars: mechanistic evidence for alkali- and alkaline-earth-metal carbonate catalyzed reactions", *Energy and Fuels*, 6, pp. 526-532 (1992).

Grim, R. E., "Clay mineralogy", 2nd edition, McGraw-Hill Book Company, New York, (1968).

Grimshaw, R. W., "The chemistry and physics of clays and allied ceramic materials" 4th edition, Ernest Benn Limited, London (1971).

Grofcsik, J., "Mullite, Its structure, formation and significance", Publishing House of the Hungarian Academy of Science, Budapest (1961).

Gryglewicz, G. and Jasienko, S., "The behaviour of sulphur forms during pyrolysis of low-rank coal", *Fuel*, 71, pp. 1225-1229 (1992).

Gururajan, V.S. Agarwal, P.K. and Agnew, J.B., "Mathematical modelling of fluidized bed coal gasifiers", *University of Adelaide, Department of Chem. Eng.* Internal Report, October (1991).

Hale, G.L., Levasseur, A.A., Tyler, A.L. and Hensel, R.P., "The alkali metals in coal: A study of their nature and their impact on ash fouling", Coal Technology in '80; 3rd International Coal Utilization Exhibition and Conference, Houston, Texas, November 18-20, (1980).

Halstead, W.D. and Raask, E., "The behaviour of sulphur and chlorine compounds in pulverised-coal-fired boilers", *Journal of Institute of Fuel*, 42 pp. 344-349 (1969).

Harb, J.N., Munson, C.L. and Richards, G.H., "Use of equilibrium calculations to predict the behaviour of coal ash in combustion systems," *Energy and Fuels*, 7, pp. 208-214 (1993).

Harrington, R. V., Hutchins, J. R. and Sherman, J. D., "The kinetics and mechanisms of subliquidus alkali carbonate-silica reactions", in *Advances in Glass Technology*, Plenum Press, NY, (1963).

Hayhurst, A.N. and Tucker, R.F., "The reductive regeneration of sulphated limestone for flue-gas desulphurisation: Thermodynamic consideration of converting calcium sulphate to calcium oxide", *Journal of the Institute of Energy*, 64, pp. 212-229, December (1991).

Hendrickson, J.B., Cram, D.J. and Hammond, G.S., "Organic Chemistry", 3rd edition, McGraw-Hill Book Co., New York, (1972).

Heng, S., Thomas, S., Perry, G.J. and Allardice, D.J., "Forms of chlorine in Victorian brown coals", In proceedings: The Australian Institute of Energy, 6th Australian Coal Science Conference, pp. 198-205, Newcastle, 17-19 October (1995).

Highsmith, J.R., Soelberg, N.R., Hedman, P.O., Smoot, D.L. and Blackham, A.U., "Entrained flow gasification of coal. 2. Fate of nitrogen and sulphur pollutants as assessed from local measurements", *Fuel*, 64, pp.782-788 (1985).

Hinckley, C.C., Smith, G.V., Twardowska, H., Saporoschenko, M., Shiley, R.H. and Griffen, R.A., "Mossbauer studies of iron in Lurgi gasification ashes and power plant fly and bottom ash:", *Fuel*, 59, 161 (1980).

Hlavac, J., "The Technology of Glass and Ceramics", Elsevier Scientific Publishing Co., (1983).

Hodges, N.J., Landner, W.D. and Marti, T.G., "Chlorine in coal: A review of its origin and mode of occurrence", *Journal of the Institute of Energy*, pp. 158-169, September (1983).

Hodges, N.J. and Richards, D.G., "The fate of sulphur, sodium, potassium, calcium and magnesium during fluidised bed combustion of coal", *Fuel*, 68, pp. 440-445 (1989).

Holdridge, D. A. and Vaughan, F., In "The differential thermal investigations of clays", (MacKenzie, ed.) Chapter IV, pp. 98-113, Mineralogical Society (Clay Minerals Group) London, (1957).

Hrma, P., Reaction between Sodium Carbonate and Silica Sand at 874 °C <T<1022 °C, *J. Am. Ceram. Soc.*, 68 [6] pp. 337-341 (1985).

Hsieh, C.R. and Roberts, F.T., "A laboratory study of agglomeration in coal gasification", *Preprints American Chemical Society*, 30(3), pp.468-479 (1985).

Huffman, G.P. and Huggins, F.E., "Mossbauer studies of coal and coke: quantitative phase identification and direct determination of pyritic and iron sulphide sulphur content", *Fuel*, 57, pp. 592-603 (1978).

Huffman, G.P. and Huggins, F.E., "Reactions and transformations of coal mineral matter at elevated temperatures," American Chemical Society Symposium Series, No. 266, pp.100-113, (1986).

Huffman, G.P., Huggins, F.E. and Dunmyre, G.R., "Investigation of the high-temperature behaviour of coal ash in reducing and oxidizing atmospheres", *Fuel*, 60, pp. 585-597 (1981).

Huffman, G.P., Huggins, F.E., Levasseur, A.A., Durant, J.F., Lytle, F.W., Greegor, R.B. and Mehta, A., "Investigation of atomic structures of calcium in ash and deposits produced during the combustion of lignite and bituminous coal", *Fuel*, 68, pp. 238-242, (1989).

Huffman, G.P., Huggins, F.E., Shah, N. and Shah, A., "Behaviour of basic elements during coal combustion", *Prog. Energy Combust. Sci.* 16, pp. 243-251 (1990).

Huggins, F.E., Kosmack, D.A. and Huffman, G.P., "Correlation between ash-fusion temperatures and ternary equilibrium phase diagrams", *Fuel*, 60, 577 (1981).

Huggins, F.E., Huffman, G.P., Shah, N., Jenkins, R.G., Lytle, F.W., and Greeger, R.B., "Further EXAFS examination of the state of calcium in pyrolysed char", *Fuel*, 67, pp. 938-941 (1988a).

Huggins, F.E., Shah, N., Huffman, G.P., Lytle, F.W., Greeger, R.B. and Jenkins, R.G., "*In situ* XAFS investigation of Ca and K catalytic species during pyrolysis and gasification of lignite chars", *Fuel*, 67, pp. 1662-1667 (1988b).

Huhn, F., Klein, J. and Jüntgen, H., "Investigation on the alkali-catalysed steam gasification of coal: kinetics and interactions of alkali catalyst with carbon," *Fuel*, 62, pp. 196-199 (1983).

Hupa, M., Skrifvars, B-J. and Moilanaen, A., "Measuring the sintering tendency of ash by a laboratory method," *Journal of the Institute of Energy*, pp. 131-137, September (1989).

Huttinger, K. J. and Minges, R., "Catalytic water vapour gasification of carbon. Importance of melting and wetting behaviour of the 'catalyst'." , *Fuel*, 64, 491 (1985).

Ibarra, J.V., Palacios, J.M. and de Andres, A.M., "Analysis of coal and char ashes and their ability for sulphur retention", *Fuel*, 68, pp. 861-857 (1989).

Insley, H. and Ewell, R. H., "Thermal behaviour of kaolin minerals", *J. Res. Nat. Bur. Std.*, 14, pp. 615-627 (1935).

Iler, H. K. and Tauch, K. J., "Sodium silicate and hydrochloric acid from sand, salt and steam", *Trans. American Institute of Chemical Engineers*, V 37, pp.853-877 (1941).

Jackson, P.J., "The physicochemical behaviour of alkali--metal compounds in fireside boiler deposits.", *The Mechanism of Corrosion by Fuel Impurities*, Butterworth, London 484 (1963).

- Jensen, K.F., Bartok, W. And Freund, H., "A pore diffusion model of char gasification with simultaneous sulphur capture," *American Chemical Society Symposium Series* No 196, pp. 335-346 (1982).
- Jia, L., Becker, H.A. and Code R.K., "Devolatilization and char burning of coal particle in a fluid bed combustor", *The Canadian Journal of Chemical Engineering*, 71, pp.10-19 (1993).
- John, R.C., "Slag, gas, and deposit thermochemistry in a coal gasifier," *Journal of Electrochemical Society*, 133, 1, pp. 205-211 (1986).
- Jung, B. and Schobert, H.H., "Viscous sintering of coal ashes. 1. Relationships of sinter point and sinter strength to particle size and composition," *Energy and Fuels*, 5, pp. 555-561 (1991).
- Jung, B. and Schobert, H.H., "Viscous sintering of coal ashes. 2. Sintering behaviour at short residence times in a drop tube furnace," *Energy and Fuels*, 6, pp. 59-68 (1992a).
- Jung, B. and Schobert, H.H., "Improved prediction of coal slag viscosity by thermodynamic modelling of liquid-phase composition," *Energy and Fuels*, 6, pp. 387-398 (1992b).
- Kapteijn, F., Jurriaans, J. and Moulijn, A., "Formation of intercalate-like structures by heat treatment of K_2CO_3 -carbon in an inert atmosphere", *Fuel*, 62, pp.249-251 (1983).
- Karner, F.R., Benson, S.A., Schobert, H.H. and Roaldson, R.G., "Geochemical variation of inorganic constituents in a North Dakota lignite", American Chemical Society, pp. 175 (1984).
- Kemezys, M. and Taylor, G.H., "Occurrence and distribution of minerals in some Australian coals", *Journal of the Institute of Fuel*, 37, pp. 389-397 (1964).

Khan, R.M. and Williford, C., "A novel technique for direct measurement of ash fusion and sintering behaviour at elevated temperature and pressure," Proc. Coal Science Conference, Tokyo, pp. 385-388 (1989).

Kikuchi, E. Adachi, H., Momoki, T., Hirose, M. and Morita, Y., "Support alkali catalysts for steam gasification of carbonaceous residues from petroleum", *Fuel*, 62, pp. 226-230 (1983).

Kojima, T. and Tanaka, K., in Proceedings, International Conference on Coal Science, Tokyo, 1989, p. 469, (1989).

Kojima, T., Ohtani, T., Shimuzu, T., Furusawa, T., "Effect of coal ash properties and burning temperature on behaviour of minerals with vitrification and sintering of ash", *Fuel Processing Technology*, 36, pp.129-135 (1993).

Kosminski, A. and Manzoori, A.R., "Inorganic matter behaviour in the gasification of South Australian coals for combined cycle power generation", Technical Services Department, The Electricity Trust of South Australia, Report submitted to S.A.N.R.A.C., September (1990).

Koyama, S., Miyadera, H., Nogita, S., Hishinuma, Y. and Tamura, Z., "Effect of temperature on coal gasification near the ash melting point," Eighteens Intersociety Energy Conversion Engineering Conference, pp. 455-457 (1983).

Kurkela, E., Staahiberg, P., Mujtahedi, W., and Niemen, M., "The first PFB gasification experiments at the Otaniemi PFBC/G test rig", in Karkonen, M (ed.), Seminar on low-grade fuels, Helsinki (Finland), June 1989, p. 353-363 (1990).

Kwon, T.W., Kim, S.D. and Fung, D.P.C., "Reaction kinetics of char-CO₂ gasification", *Fuel*, Vol. 67, pp. 530-535 (1988).

Lang, R.J., "Anion effects in alkali-catalysed steam gasification", *Fuel*, 65, 1324 (1986)

-
- Langston, B.G. and Stephens, F.M., "Self-agglomerating fluidized-bed reduction" *Journal of Metals*, pp. 312-316, April (1960).
- Laughlin K. and Reed G., "Behaviour of coal ash in a Pressurised Fluidised Bed Gasifiers", 1991 International Conference on Coal Science, Newcastle upon Tyne, September 1991, 396-399 (1991).
- Laughlin K. and Reed G., "Coal ash behaviour during Pressurised Fluidised Bed Gasification", 7th International Conference on Coal Science, Banff, AB (Canada), pp. 27-30, September (1993).
- Lee, S.H.D. and Carls, E.L., "Measurement of sodium and potassium vapours in pressurised fluidised-bed combustion of Beulah lignite", *Journal of the Institute of Energy*, 63, pp. 203-210, December (1990).
- Lee, S.H.D. and Johnson, I., "Removal of gaseous alkali metal compounds from hot flue gas by particulate sorbents", *Journal of Engineering for Power*, 102, 397-402, April (1980).
- Lee, S.H.D., Henry, R.F. and Myles, K.M., "Removal of alkali vapours by a fixed granular-bed sorbents using activated bauxite as a sorbent", *CON-8503513*, Argonne National Laboratory, Argonne, Il, USA (1985).
- Lee, S.H.D., Teats, F.G., Swift, W.M. and Banerjee D.D., "Measurement of alkali-vapour emission from pressurised fluidised-bed combustion of Illinois coals", Proceedings, International Conference on Fluidized Bed Combustion 1993, ed. Lynn N. Rubow, pp. 1359-1368 (1993).
- Levenspiel, O., "Chemical reaction engineering", John Willey and Son, Inc. New York, (1979).
- Levin, E.M., Robbins, C.R. and M^cMurdie, M.F., "Phase diagrams for ceramists", The American Chemical Society, Ohio USA, 4th Edition (1979).
-

Li, J. and van Heiningen, A.R.P., "Sodium emission during pyrolysis and gasification of black liquor char", *Tappi Journal*, pp. 213-219, December (1990).

Lindner, E.R., "A study of sodium-ash reactions during the combustion of pulverised coal", *PhD Thesis, The University of Adelaide*, (1988)

Lindner, E.R., Kosminski, A., Taylor, C. and Williams, R.G., "Effects of additives on fouling behaviour characteristics of South Australia brown coals", In Proc. Mineral matter and ash deposition from coal," Ed. Bryers, R.W. and Vorres, K.S., Engineering Foundation Conference, Santa Barbara, pp.331-345 (1988).

Linjewile, T.M., Hull, A.S. and Agarwal, P.K., "Optical probe measurements of the temperature of burning particles in fluidized beds", *Fuel*, 73, pp. 1880-1888 (1994).

Lloyd, W.G., Riley, J.T., Risen, M.A., Gilleland, S.R. and Tibbitts, R.L., "Estimation of ash fusion temperatures," *Journal of Coal Quality*, 12, 1, pp. 30-36 (1993).

Luthra, K.L. and LeBlanc, Jr., O.H., "Adsorption of NaCl and KCl on Al₂O₃ at 800-900°C", American Chemical Society, *Journal of Physical Chemistry*, 88, 1896-1901 (1984).

Ma, R.P., Felder, R.M. and Ferrell, J.K., "Evolution of Hydrogen Sulfide in a Fluidized Bed Coal Gasification", *Ind. Eng. Chem. Res.*, 28, pp. 27-33 (1989).

Mann, M.D., Galbreath, K.C. and Kalmanovitch, D.P., "The role of ash chemistry and operating parameters on ash agglomeration and deposition in FBC system", in Proc. of The Eng. Found. Conf. on Inorganic Transformations and Ash Deposition during Combustion (1992).

Manzoori, A.R., "Role of the inorganic matter in agglomeration and defluidization during the CFBC of low-rank coals", *PhD Thesis, The University of Adelaide*, (1990).

Manzoori, A.R. and Agarwal, P.K., "Agglomeration and defluidization under simulated circulating fluidized-bed combustion conditions", *Fuel*, 73, pp. 563-568 (1994).

-
- Manzoori, A.R. and Agarwal, P.K., "The fate of organically bound inorganic elements and sodium chloride during fluidized bed combustion of high sodium, high sulphur low rank coals", *Fuel*, 71, pp. 513-522 (1992).
- Marinov, V., Marinov, S.P., Lazarov, L., Stefanova, M., "Ash agglomeration during fluidized bed gasification of high sulphur content lignites," *Fuel Processing Technology*, 31, pp. 181-191 (1992).
- Martinez-Tarazona, M.R., Martinez-Alonso, A. and Tascon, J.M.D., "Interactions between carboxyl groups and inorganic elements in Spanish brown coals", *Fuel*, 69, pp. 362-367 (1990a).
- Martinez-Tarazona, M.R., Palacios, J.M., Martinez-Alonso, A. and Tascon, J.M.D., "The characterization of organomineral components of low-rank coals," *Fuel Processing Technology*, 25, pp.81-87 (1990b).
- Mason, D.M., "The behaviour of iron-sulphur species in fluidized-bed gasification on coal," *Fuel Processing Technology*, 30, pp. 215-226 (1992).
- Mason, D.M. and Patel, J.G., "Chemistry of ash agglomeration in the U-GAS® process," *Fuel Processing Technology*, 3, pp. 181-206 (1980).
- Mason, D.M., Rehmat, A., and Tsao, K.C., "Chemistry of ash deposits in the U-GAS process" *Proc. Engineering Foundation Conference* (1982).
- Matl, K. and Tomkow, K., in "Wegiel brunatny", Ed. A. Bolewski, *Wydawnictwa Geologiczne, Warszawa* (in Polish) (1981) .
- Matsukata, M., Kikuchi, E. and Morita, Y., "Migration of alkali and alkaline earth elements into carbon black," *Fuel*, 71, pp. 705-707 (1992).
- McCarthy, G.J., "Qualitative X-ray phase analysis of lignite gasification ash. Illustration of a strategy for analysis of very complex solids." *Powder Diffraction*, V.1, No 1, March (1986).
-

McKee, D.V., "Mechanisms of the alkali metal catalysed gasification of carbon" *Fuel*, 62, pp. 170-175 (1983).

McKee, D.W., Spiro, C.L., Kosky, P.G. and Lamby, E.J., "Catalysis of coal char gasification by alkali metals salts", *Fuel*, 62, pp. 217-220 (1983).

McKee, D.W., Spiro, C.L., Kosky, P.G. and Lamby, E.J., "Eutectic salt catalysts for graphite and coal char gasification," *Fuel*, 64, pp. 805-809 (1985).

Merry, J.M., Chen, J.L. and Kearns, D.L., "Fluidization technology", McGraw Hill, 3, 423, (1975).

Mims, C.A. and Pabst, J.K., "Role of surface complexes in alkali-catalysed carbon gasification", *Fuel*, 52, pp. 176-179 (1983).

Mitchell, R.M. and Gluskoter, H.J., "Mineralogy of ash of some American coals: Variations with temperature and source", *Fuel*, 55, pp. 90-96 (1976).

Moilanen, A., "Behaviour of peat ash in gasification", in proceedings of International Conference on Peat Production and Use, Finland, 11-15 June 1990, pp.309-315, (1990).

Moilanen, A., Kline, S., Carty, R. and Mason, D., "The effect of ash viscosity on the sintering of peat fly-ash", *Journal of the Institute of Energy*, 64, pp. 21-25, March (1991).

Moilanen, A., Skrifvars, B-J. and Hupa, M., "The effect of temperature, chemical composition and gas atmosphere on sintering of peat fly ash," Proc. Coal Science Conference, Tokyo, pp. 397-400 (1989).

Mojtahedi, W. and Backman, R., "Release of alkali metals in pressurised fluidised-bed combustion and gasification of peat", *Ed. Technical Research Centre of Finland (VTT) Publication No 53*, 48 p. March (1989a).

Mojtahedi, W. and Backman, R., "The fate of sodium and potassium in the pressurised fluidised-bed combustion and gasification of peat", *Journal of the Institute of Energy*, pp. 189-196, December (1989b).

Mojtahedi, W., Kurkela, E. and Nieminen, M., "Release of alkali metals in PFB gasification of peat", *Journal of the Institute of Energy*, pp. 95-100, September (1989).

Morgan, M.E., Jenkins, R.G. and Walker, P.L., "Inorganic constituents in American lignites", *Fuel*, 60, pp. 189-193 (1981).

Mraw, S.C., De Neufville, J.P., Freund, H., Baset, Z., Gorbaty, M.L. and Wright, F.J., "The science of mineral matter in coal", in *Coal Science*, Ed: Gorbaty, M.L., Larssen, J.W. and Wender, I., Academic Press, pp.2-64 (1983).

Muchmore, C.B., Hippo, E.J., Chen, H.L., Joslin, J.L. Jr., Wang, L., Hughes, A., Sivanandan, S., Daman, E. and Banerjee, D.D., "Distribution of sodium, potassium and chlorine between solid and vapour phases under coal gasification conditions", in *Coal science*, Editors; J.A. Pajares and J.M.D. Tascon, Elsevier, pp. 819-822 (1995).

Mulholland, J.A.; Sarofim, A.F.; Sosothikul, P.; Lafleur, A.L.; "Effects of organic chlorine on the composition and carbon number distribution of pyrolysis tars", *Combustion and Flame*, 92, pp. 161-177 (1993).

Murray, J.B., "The state of combination of the inorganic ash-forming constituents of Yallourn brown coal." State Electricity Commission of Victoria, Planning and Investigations Department, Scientific Division, Miscellaneous Report No. Mr-145 (1968).

Murray, J.B., "The state of combination of the major inorganic ash-forming constituents of Yallourn North Extension brown coal." State Electricity Commission of Victoria, Report No. 224, Feb. (1971).

Murray, J.B. "Changes in state of combination of inorganic constituents during carbonization of Victorian brown coal", *Fuel*, 52, pp. 105-111 (1973).

Murray, J.B. and Bonafede, G., "The state of combination of the major inorganic ash-forming constituents in additional coal samples from the Loy Yang Field", State Electricity Commission of Victoria, Report No. 249, Jan. (1972).

Nelson, W., and Lisle, B.S., "High temperature external corrosion on coal-fired boilers: Siliceous inhibitors," *Journal of Institute of Fuel*, 38, pp.179-186 (1965).

Nichols, K.M., Hedman, P.O., Smoot, L.D. and Blackham, A.U., "Fate of coal-sulphur in a laboratory-scale coal gasifier", *Fuel*, 68, pp. 243-247 (1989).

Niles, W.D. and Siegmund, C.W., "Reaction between fuel ash components and additive combinations. The mechanism of corrosion by fuel impurities", Ed. Johnson and Littler, Butterworths, pp. 332-346 (1963).

Nowok, J.W., Bieber, J.A., Benson, S.A. and Jones, M.L., "Physicochemical effects influencing the measurements of interfacial surface tension of coal ashes", *Fuel*, 70, pp.951-956 (1991).

Nowok, J.W., Benson, S.A. and Kalmanovitch, D.P., "Sintering, crystallization and mechanical properties of selected coal ashes", in Proc. 6th International Coal Conference, Pittsburgh pp. 90-99 (1989).

Oakey, J.E. Minchener, A.J., Hodges, N.J., "The use of high-chlorine coals un industrial boilers", *Journal of the Institute of Energy*, 64, 3-11, March (1991).

Ogunsola, O.I., "Thermal upgrading effect on oxygen distribution in lignite," *Fuel Processing Technology*, 34, pp. 73-81 (1993).

Otake, Y. and Walker, P.L. Jr., "Pyrolysis of demineralised and cation loaded lignites," *Fuel*, 72, pp. 139-149 (1993).

Pang, Y., Sathe, C. and Li, C-Z., "Volatilisation of alkali and alkaline earth metals during the pyrolysis of Loy Yang coal", in *Proc. AIE 8th Australian Coal Science Conference*, December (1999).

Parikh, N. M., *Journal of American Ceramic Society*, **41**, pp.18-22 (1958).

Pearce, M.L. and Beisler, J.F., "Miscibility gap in the system sodium oxide-silica-sodium sulphate at 1200°C", *Journal of the American Ceramic Society*, **48**, (1), 40 (1965).

Pearce, W.C. and Hill, J.W.F., "The mode of occurrence and combustion characteristics of chlorine in British coals," *Prog. Energy Combust. Sci.* **12**, pp. 117-162 (1986).

Pooze, A. Private communication to the author (2000).

Poeze, A. and Zhang, D.-K., "The effect of conversion level on gasification kinetics of a low-rank coal", in Proc. Third Annual Conference Cooperative Research Centre for New Technologies from Low-rank Coal, Adelaide, June 1996, pp. 49-54 (1996).

Price, T.D., Smoot, L.D. and Hedman, P.O., "Measurement of nitrogen and sulphur pollutants in an entrained-bed gasifier", *Ind. Eng. Chem. Fundam.*, **22**, pp.110-116 (1983).

Punjak, W.A., Uberoi, M., and Shadman, F., "High-temperature adsorption of alkali vapours on solid sorbents", *AIChE Journal*, **35**, No 7, 1186-1194 (1989).

Punjak, W.A. and Shadman, F., "Aluminosilicate sorbents for controlling of alkali vapours during coal combustion and gasification", *Energy and Fuels*, **2**, 702 (1988).

Quann, R.J. and Sarofim, A.F., "A scanning electron microscopy study of the transformations of organically bound metals during lignite combustion", *Fuel*, **65**, pp.40-46 (1986).

Raask, E., *Mineral Impurities in Coal Combustion*. Hemisphere Publishing Corp. (1985).

Radovic, L.R., Walker, P.L., Jr. and Jenkins, R.G., "Effect of lignite pyrolysis conditions on calcium oxide dispersion and subsequent char reactivity" *Fuel*, **62**, pp. 209-212 (1983).

Readett, D.J., "Beneficiation of Wakefield lignite: With particular reference to the reduction of the sodium content", South Australian Institute of Technology, Feb. (1983).

Readett, D.J., "Beneficiation of Wakefield lignite: With particular reference to the reduction of the sodium content. Stage 2, Parts 1", South Australian Institute of Technology, March/July (1984).

Readett, D.J. and Quast, K., "Minerals and inorganics associated with South Australian lignites - Stage 1", South Australian Institute of Technology, Report to S.E.N.R.A.C. December (1986).

Readett, D.J. and Quast, K., "Minerals and inorganics associated with South Australian lignites - Final report", South Australian Institute of Technology, Report to S.E.N.R.A.C. December (1987).

Rehmat, A., Abbasian, J., Kothari, M., Hariri, H. and Arastoopour, H., "Agglomeration in fluidized bed using multiple jet streams", Institute of Gasifier Technology, Chicago, Illinois, USA, paper prepared for presentation at Engineering Foundation Conference: Fluidization VII, Broadbeach, Australia, May 3-8 (1992).

Riley, R.K. and Judd, M.R., "The measurement of char-steam gasification kinetics for the design of a fluidised bed coal gasifier which contains a draft tube", *Chem. Eng. Comm.* 62, pp. 151-161 (1987).

Sams, D.A., Talverdian, T. and Shadman, F., "Kinetics of catalyst loss during potassium catalysed CO₂ gasification of carbon", *Fuel*, 64, pp. 1208-1214 (1985).

Sathe, C., "Fates and roles of cations during the pyrolysis of low-rank coals", Report No 98026 to Cooperative Research Centre for New technologies For Power Generation From Low-Rank Coal, December (1998).

Scandrett, L.A. and Clift, R., "The thermodynamics of alkali removal from coal-derived gases", *Journal of the Institute of Energy*, pp. 391-397, December (1984)

Schafer, H.N.S., "Carboxyl groups and ion exchange in low-rank coals" *Fuel*, 49, pp. 197-213 (1970).

Schafer, H.N.S., "Pyrolysis of brown coals. 1. Decomposition of acidic groups in coals containing carboxyl groups in the acid and cation forms," *Fuel*, 58, pp. 667-672 (1979a).

Schafer, H.N.S., "Pyrolysis of brown coals. 1. Decomposition of acidic groups on heating in the range 100-900°C", *Fuel*, 58, pp. 673-679 (1979b).

Schobert, H.H., "Lignites of North America", *Coal Sci. and Tech.*, 23, (1995).

Shakaryan, R.Y., Katsovsky, M.Y. and Grigoryants, R.R., "A mathematical model of the process of low-grade fuel gasification in pressurised circulating fluidized bed", In Proceedings VTT Symposium on Low-Grade Fuels. Part 2. Vol. 2, Helsinki, pp. 341-352 (1989).

Shao, D., Hutchinson, H.C. and Pan, W.-P., "Behaviour of chlorine during coal pyrolysis," *Energy and Fuels*, 8, pp. 399-401 (1994).

Shufen, Li. and Ruizheng, Sn., "Kinetic studies of a lignite char pressurized gasification with CO₂ and steam", *Fuel*, 73, pp. 413-415 (1994).

Simons, G.A., "The role of pore structure in coal pyrolysis and gasification", *Prog. Energy Combust. Sci.*, 9, pp. 269-290, (1984).

Singh, K.P., "Models for prediction of total and carboxyl acidity of low rank coals," *Fuel Processing Technology*, 32, pp. 181-190 (1992).

Skrifvars, B.J., Hupa, M., Backman, R., Hiltunen, M., "Sintering mechanisms of FBC ashes". *Fuel*, 73, 171, (1994).

Sondreal, E.A., Gronhovd, H., Tufte, P.H. and Beckering, W., "Ash fouling studies of low-rank Western U.S. coals", International Conf. on Ash Deposits and Corrosion from Impurities in Combustion Gases, New England College (1977).

Song, B.H. and Kim, S.D., "Catalytic activity of alkali and iron salt mixtures for steam-char gasification", *Fuel*, 72, pp. 797-803 (1993).

Spiro, C.L., McKee, D.W., Kosky, P.G., Lamby, E.J. and Maylotte, D.H., "Significant parameters in the catalysed CO₂ gasification of coal chars", *Fuel*, 62, pp.323-330 (1983).

Spiro, G.L., Chen, C.C., Kimura, S.G., Lavign, R.G. and Schields, P.W., "Deposit remediation in coal-fired gas turbines through the use of additives," *Prog. Energy Combust. Sci.* 16, pp. 213-220 (1990).

Srinivasachar, S. and Boni, A., "A kinetic model for pyrite transformations in a combustion environment", *Fuel*, 68, pp. 829-836 (1989).

Srinivasachar, S., Helble, J., and Boni, A.A., "Mineral behaviour during coal combustion. I. Pyrite transformations", *Prog. Energy Combust. Sci.*, 16, pp. 281-291 (1990).

Stallmann, J.J. and Neavel, R.C., "Technique for measuring the temperature of agglomeration of coal ash" *Fuel*, 59, pp. 584-586 (1980).

Steadman, E.N., and Nowok, J.W., "Gasification ash and slag," Eds: Venkataraman, V.K., Rath, L.K., Martin, J.W., Bedick, R.C.,: *Proc. 11. Annual gasification and gas stream cleanup system contractor's review meeting, Morgantown, WV (USA), 13-15 Aug 1991*, Report no. DOE/METC-91/6123-Vol.1, pp. 159-167 (1991).

Sugawara, K., Tozuka, Y., Sugawara, T., and Nishiyama, Y., "Effect of heating rate and temperature on pyrolysis desulphurisation of a bituminous coal", *Fuel Processing Technology*, 37, pp. 73-85 (1994).

Suzuki, T., Inoue, K., and Watanabe, Y., "Steam pulsed gasification of Na₂CO₃ or Fe(NO₃)₃ loaded Yallourn coal char", *Fuel*, 68, pp. 626-630 (1989).

Takarada, T., Ishikawa, H., Abe, H. and Nakaike, Y., "Alkali volatilisation during pyrolysis and gasification of coal", in *Coal Science*, Pajares, J.A. and Tascon, J.M.D. Eds.; Elsevier: Amsterdam, pp. 687-690 (1995).

Takarada, T., Nabatame, T., Ohtsuka, Y. and Tomita, A., "Preparation of active catalyst from alkali chlorides for the steam gasification of coal" In *Coal Science and Technology*, Moulijn, J. A., Nater, K.A., Chermin, H.A.G.,Eds.; Elsevier: Amsterdam, 11, pp. 547-550 (1987).

Takarada, T., Ogiwara, M., Kumori, U., and Kato, K., "Gasification of coal with K-exchanged brown coal prepared from potassium chloride" International Conference on Coal Science, University of Newcastle-upon-Tyne (1991).

Takarada, T., Tamai, Y. and Tomita, A., "Effectiveness of K_2CO_3 and Ni catalysts in steam gasification", *Fuel*, 65, pp. 679-683 (1986).

Takarada, T., Ishikawa, H., Abe, H. and Nakaike, Y., "Alkali volatilisation during pyrolysis and gasification of coal", in *Coal Science*, Pajares, J.A. and Tascon, J.M.D. Eds.; Elsevier: Amsterdam, pp. 687-690 (1995).

Telfer, M., "Sulphur transformations during pyrolysis of low-rank coals and characterisation of Ca-based sorbents", *PhD Thesis, The University of Adelaide* (1999).

Thambimuthu, K.V. and Clift, R., "Ash filtration and agglomeration in fluidized beds," *Proceed. Intern. Conf. On Fluidization: Fluidization VI, Banff*, pp. 547-554 (1989).

Tsao, K.C., Tabrizi, H., Rehmat, A. and Mason, D.M., "Coal-ash agglomeration mechanism in a high temperature cyclone," *ASME Annual Meeting* (1982).

Tsuji, T., Shibata, K., Yamaguchi, K., and Uemaki, O., in *Proceedings, International Conference on Coal Science, Tokyo, 1989*, pp. 457-460 (1989).

Turnbull, A.G. and Wadsley, M.W., "The CSIRO-MONASH Thermochemistry System Version: 1.00 IBM-PC DOS system." CSIRO Division of Minerals (1992).

Uberoi, M., Punjak, W.A., and Shadman, F., "The kinetics and mechanism of alkali removal from flue gases by solid sorbents", *Progress in Energy and Combustion Science*, 16, 205-211 (1990).

Vora, M.K., Mason, D.M., Rehmat. A. And Sandstrom, W.A., "Ash agglomerates from coal," *Energy Communications*, 6(3), pp. 195-210 (1980).

Wall, C.J., Graves, J.T. and Roberts, E.J., "How to burn salty sludges," *Chemical Engineering*, pp. 77-82, April (1975).

Wall, T.F., Lowe, A., Wibberley, L.J. and Stewart, I.McC., "Mineral matter in coal and the thermal performance of large boilers", *Prog. Energy Combust. Sci.*, 5, pp. 1-29 (1979).

Warne, S.S.J., "Coal mineral reactions", Lecture Notes, Department of Geology, University of Newcastle (1983).

Watkinson. A.P., Cheng. G. and Prakash, C.B., "Comparison of coal gasification in fluidized and spouted beds", *The Canadian Journal of Chemical Engineering*, 61, pp.468-474 (1983).

Watt, J.D. and Federay, F., "The flow properties of slags from the ashes of British coals: Part1. Viscosity of homogeneous liquid slags in relation to slag composition", *Journal of the Institute of Energy*, pp. 99-103, March (1969).

Wibberley, L.J. and Wall, T.F., "Alkali-ash reactions and deposit formation in pulverised-coal-fired boilers: the thermodynamic aspects involving silica, sodium, sulphur and chlorine", *Fuel*, 6, 87-92, (1982).

Wigmans, T., van Doorn, J., and Moulijn, J.A., "Temperature-programmed desorption study of Na₂CO₃-containing activated carbon", *Fuel*, 62, pp.190-195 (1983).

Yamashita, H., Yoshida, S. and Tomita, A., "Local structures of metals dispersed in coal. 3. NaCl K-edge XANES studies on the structure of sodium gasification catalyst", *Ind. Eng. Chem. Res.*, 30, pp. 1651-1955 (1991).

Yan, H-M., Heindreich, C. and Zhang, D-K., "Mathematical modelling of a bubbling fluidised-bed coal gasifier and the significance of 'net flow'", *Fuel*, 77, pp. 1067-1079 (1998).

Ye, D. P., "Gasification of South Australian lignite", *PhD thesis, Department of Chemical Engineering, The University of Adelaide*, March (1994).

Yerushalmi, J., Gluckman, M.J. and Graff, R.A., "Fluidization technology", McGraw Hill, 2, 423, (1976).

Zygarlicke, C.J., Steadman, E.N. and Benson, S.A., "Studies of transformations of inorganic constituents in a Texas lignite during combustion", *Prog. Energy Combust. Sci.*, 16, pp. 195-204 (1990).